

# Radiolabeled Gastrins in CCK2R-Positive Tumor Targeting – Toward Improved Diagnostic Efficacy Via In Situ Enzyme-Inhibition Approaches

Aikaterini Kaloudi



**Radiolabeled Gastrins in CCK2R-Positive  
Tumor Targeting – Toward Improved  
Diagnostic Efficacy Via In Situ  
Enzyme-Inhibition Approaches**

**Aikaterini Kaloudi**

Radiolabeled gastrins in CCK2R-positive tumor targeting –  
Toward improved diagnostic efficacy via in situ enzyme-inhibition approaches

Copyright 2016 © Aikaterini Kaloudi  
ISBN: 978-94-028-0179-8

Design and layout: Legatron Electronic Publishing, Rotterdam  
Printing: Ipskamp Printing, Enschede

No part of this thesis may be reproduced, stored in a retrieval system or transmitted in any form or by any means without permission from the author or, when appropriate, from the publishers of the publications.

**Radiolabeled gastrins in CCK2R-positive tumor targeting –  
Toward improved diagnostic efficacy via in situ  
enzyme-inhibition approaches**

Radioactieve gastrines voor CCK2R-positieve tumoren –  
naar verbeterde diagnostiek door in situ enzymremming

Proefschrift

ter verkrijgen van de graad van doctor  
aan de Erasmus Universiteit Rotterdam

op gezag van rector magnificus

Prof.dr. H.A.P. Pols

en volgens besluit van College voor Promoties.

De openbare verdediging zal plaatsvinden op  
dinsdag 5 juli 2016 om 15.30 uur

door

**Aikaterini Kaloudi**

geboren te Marousi Attikis, Griekenland

## PROMOTIECOMMISSIE

**Promotor:** Prof.dr. M. de Jong

**Overige leden:** Prof.dr. O.C. Boerman  
Prof.dr. R.P. Peeters  
Prof.dr. H.T. Wolterbeek

**Co-promotors:** Dr. T. Maina-Nock  
Dr. B. A. Nock

# Contents

<b>Chapter 1</b>	General Introduction and Outline of the Thesis	<b>7</b>
<b>Chapter 2</b>	Radiolabeled Gastrin/CCK Analogs in Tumor Diagnosis – Towards Higher Stability and Improved Tumor Targeting <i>Q. J. Nucl. Med. Mol. Imaging 59 (3):287-302, 2015</i>	<b>31</b>
<b>Chapter 3</b>	In Vivo Inhibition of Neutral Endopeptidase Enhances the Diagnostic Potential of Truncated Gastrin <sup>111</sup> In-Radioligands <i>Nucl. Med. Biol. 42(11):824-32, 2015</i>	<b>55</b>
<b>Chapter 4</b>	Improving the in Vivo Profile of Minigastrin Radiotracers – A Comparative Study Involving the Neutral Endopeptidase Inhibitor Phosphoramidon <i>Cancer Biother. Radiopharm. 31(1):20-8, 2016</i>	<b>75</b>
<b>Chapter 5</b>	Impact of Clinically Tested NEP/ACE Inhibitors on Tumor Uptake of [ <sup>111</sup> In-DOTA]MG11 – First Estimates for Clinical Translation <i>EJNMMI Res. 6(1):15, 2016</i>	<b>93</b>
<b>Chapter 6</b>	<sup>99m</sup> Tc-Labeled Gastrins of Varying Peptide Chain Length: Distinct Impact of NEP/ACE-Inhibition on Stability and Tumor Uptake in Mice <i>Nucl. Med. Biol. 43:347-354, 2016</i>	<b>109</b>
<b>Chapter 7</b>	Summary and Concluding Remarks	<b>127</b>
	Samenvatting	<b>135</b>
	Acknowledgements	<b>139</b>
	Curriculum Vitae	<b>141</b>
	List of Publications	<b>143</b>
	PhD Portfolio	<b>145</b>





# CHAPTER

# 1

## General Introduction and Outline of the Thesis

## GENERAL INTRODUCTION

Cancer is the biggest cause of mortality worldwide with approximately 8.2 million deaths from cancer in 2012. According to the reports of the World Health Organization (WHO), cancer cases worldwide are predicted to rise by 75% and reach close to 25 million over the next two decades. Globally, lung cancer is the most common cancer and cause of cancer-related mortality in men, while in women the most frequent cancer and cause of cancer-related death is breast cancer [1]. Thyroid cancer is the most common endocrine cancer and is one of the few cancers that have increased in incidence rates over recent years [2]. Amongst thyroid cancers, medullary thyroid carcinoma (MTC) is the third most usual, it accounts for 3-4% of all such tumors [3].

Despite the increase of cancer incidents, the mortality has significantly decreased mainly due to continuous advances in cancer prevention, (early) diagnosis, staging, and treatment. In the field of diagnosis and staging, oncologic imaging has undergone remarkable progress as it has shifted from anatomic and spatial 2D and 3D images to molecular, functional, biological and genetic imaging. Cancer biomarkers can be used to screen asymptomatic individuals in the general population, to assist in early and specific diagnosis in suspect cases, to select patients who may benefit from specific treatments, to predict prognosis and response to therapy, and finally to monitor patients after therapy [4].

## DIAGNOSIS AND THERAPY OF CANCER IN NUCLEAR MEDICINE

Molecular imaging is a promising field that aims to combine information on patient-specific and disease-specific molecular events with anatomical imaging readouts. Molecular imaging differs from traditional imaging in that often probes are used to determine the expression of molecular biomarkers at various stages of disease [5].

Nuclear molecular imaging records radiation emitting from within the body rather than radiation that is generated by external sources, like X-rays in computed tomography (CT) or radiography. Nuclear imaging modalities, which include single photon-emission computed tomography (SPECT) and positron emission tomography (PET) imaging, involve a pharmaceutical labeled with a radionuclide, which is the source for detection that stimulates the production of an image of functional processes in the body. These techniques have the advantages of high intrinsic sensitivity, low toxicity and unlimited depth penetration, however, the spatial resolution of these approaches is inferior to that of CT or magnetic resonance imaging (MRI) [6].

### SPECT

In SPECT imaging  $\gamma$ -emitting radionuclides are the source of detection by the cameras, which detect the light energy and convert it into electrical signals for image reconstruction. The gamma camera was first developed by Hal Anger in the 1950s and consists of a collimator, a scintillation crystal, a photomultiplier tube array and a computer system (Figure 1) [7]. The collimator is usually made of lead and it contains many tiny holes. Only gamma rays that travel in parallel to the axes of the holes enter the collimator and can be detected. The detector consists of scintillation crystals, which produce scintillation photons as a result of gamma radiation. The photons are subsequently converted into electric current, amplified by the photomultiplier tubes and processed by a computer system to reconstruct the image.

Optimal performance of SPECT is obtained when using radionuclides with energies between 100-250 keV. The most commonly applied  $\gamma$ -emitting radionuclide in SPECT imaging is  $^{99m}\text{Tc}$  (Table 1), other frequently used radionuclides are listed in the Table as well. The ideal half-life and the wide availability of  $^{99m}\text{Tc}$  via commercial  $^{99}\text{Mo}/^{99m}\text{Tc}$  generators in combination with the commercial freeze-dried kits containing the radiopharmaceutical precursor, facilitate the in situ preparation of the radiopharmaceutical in SPECT imaging centers [8]. SPECT is less expensive than PET, however, its sensitivity is suboptimal, because of the collimators that allow only a small percentage of photons to reach the detector [9]. Finally, this method is lacking the ability to provide anatomical information. This problem can be overcome by the use of hybrid SPECT/CT and SPECT/MRI systems, which combine in one image the functional information of SPECT with the anatomical data of CT or MRI using the same device [10].

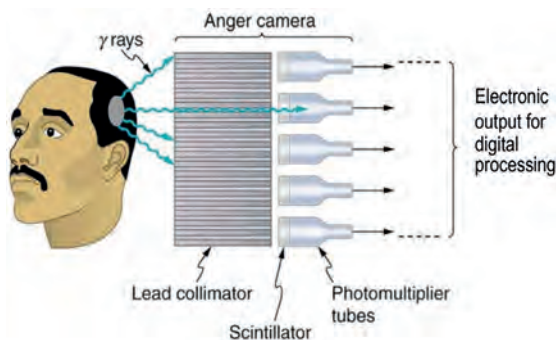


Figure 1.1 | Diagrammatic representation of an Anger gamma camera (adapted from 11).

## PET

PET is based on radiotracers labeled with positron ( $\beta^+$ ) emitting radionuclides. A positron ejected by a radionuclide travels a very short distance in a tissue, during which it loses its kinetic energy and finally interacts with an electron to produce two annihilation photons of 511 keV, moving in approximately opposite directions (Figure 2). The PET scanner detects this pair of annihilation photons almost simultaneously and after mathematical processing of many of such detections, visualization of the PET tracer distribution is generated. In most PET scanners the detectors are arranged in rings that completely surround the patient. The detectors consist of scintillation crystals coupled to photomultiplier tubes. In contrast to SPECT, PET doesn't need collimators for the selection of photons, hence it is more sensitive [12,13].

The most commonly used positron emitting radionuclides in PET are listed in Table 1, most of them are characterized by a very short half-life. Accordingly, PET radiotracers must be synthesized and the image must be achieved within a time frame compatible with the radionuclide half-life. Therefore, most PET tracers must be produced in close proximity to the PET imaging facility. As compared to SPECT, PET has higher sensitivity, resolution and quantitative potential. Moreover, unlike SPECT, PET cannot image multiple probes simultaneously as all PET radionuclides result in two  $\gamma$ -rays of the same energy. Therefore, to investigate multiple molecular events, molecular probes are usually injected separately, allowing for the decay of one radionuclide prior to administration of the other [9]. Finally, the multimodal imaging of PET/CT and PET/MRI provides anatomical and functional information with great accuracy and detail [14,15].

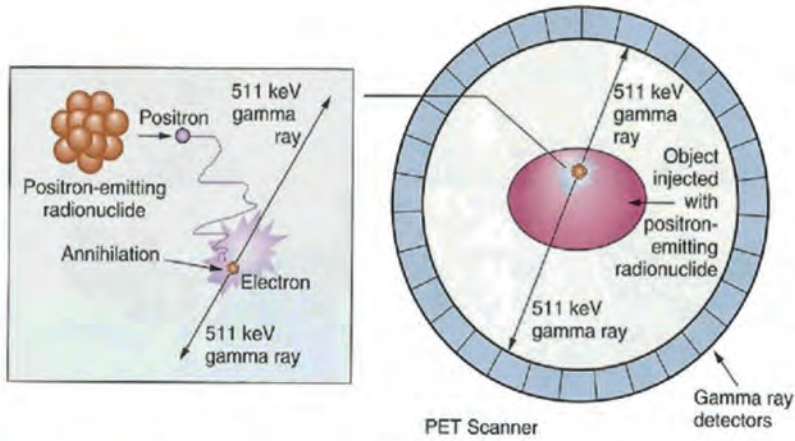


Figure 2 | Schematic representation of basic physics of PET (adapted from 16).

Table 1 | Characteristics of main radionuclides for PET or SPECT imaging and radionuclide therapy.

Modality	Radionuclide	Half-Life	Decay mode (%)	$E_{\gamma}/E_{\beta}/E_{\alpha}$ (keV)	Production
SPECT	$^{99m}\text{Tc}$	6.02 h	$\gamma$ , IT (100%)	141	$^{99}\text{Mo}/^{99m}\text{Tc}$ Generator
	$^{111}\text{In}$	67.2 h	Auger $e^{-}$ , EC (100%)	172, 247	Cyclotron
	$^{67}\text{Ga}$	78.1 h	$\gamma$ , EC (100%)	91, 93, 185, 296, 388	Cyclotron
PET	$^{11}\text{C}$	20.3 min	$\beta^{+}$ (100%)	326	Cyclotron
	$^{13}\text{N}$	9.97 min	$\beta^{+}$ (100%)	432	Cyclotron
	$^{15}\text{O}$	2.03 min	$\beta^{+}$ (100%)	650	Cyclotron
	$^{18}\text{F}$	109.8 min	$\beta^{+}$ (97%), EC (3%)	202	Cyclotron
	$^{68}\text{Ga}$	67.8 min	$\beta^{+}$ (90%), EC (10%)	820, 1895	$^{68}\text{Ge}/^{68}\text{Ga}$ Generator
	$^{64}\text{Cu}$	12.7 h	$\beta^{+}$ (18%), $\beta^{-}$ (39%), EC (43%)	653	Reactor
Therapy	$^{89}\text{Zr}$	78.4 h	$\beta^{+}$ (23%), EC (77%)	396	Cyclotron
	$^{177}\text{Lu}$	6.7 d	$\beta^{-}$ (79%), $\gamma$ (21%)	174, 249, 385, 497	Reactor
	$^{90}\text{Y}$	64.1 h	$\beta^{-}$ (100%)	2270	$^{90}\text{Sr}/^{90}\text{Y}$ Generator
	$^{213}\text{Bi}$	45.6 min	$\beta^{-}$ (97.8%), $\alpha$ (2.2%)	5500, 5900 8320	$^{225}\text{Ac}/^{213}\text{Bi}$ Generator
	$^{67}\text{Cu}$	61.8 h	$\beta^{-}$ (100%)	570	Accelerator

EC= electron capture, IT= internal transmission,  $E_{\gamma}$  = photon energy,  $E_{\beta}$  =  $\beta$  energy  $E_{\alpha}$  =  $\alpha$  energy

### Targeted Radionuclide Therapy

Targeted radionuclide therapy applies molecules labeled with a therapeutic radionuclide to deliver a cytotoxic load of radiation to diseased sites. The radionuclides used for therapy include  $\beta^{-}$  or  $\alpha$  particle, or Auger electron emitters. Each type of these particles has different effective range of energy deposition and linear energy transfer (LET) properties, which are essential factors for choosing the most suitable radionuclide depending on the size and the stage of the tumor. Low

energy  $\beta^-$  (i.e.  $^{177}\text{Lu}$ ),  $\alpha$  (i.e.  $^{213}\text{Bi}$ ) and Auger electron (i.e.  $^{111}\text{In}$ ) emitters are preferred for small and medium size lesions, because of their ability to produce high tumoricidal activity in a short range, causing less damage to surrounding healthy tissues. On the other hand, medium and high energy  $\beta^-$  emitters (i.e.  $^{90}\text{Y}$ ) are probably more efficient for eradicating larger lesions because of their ability to destroy also cancer cells that are not directly targeted (cross-fire effect) [17,18]. To increase the therapeutic impact, application of “radionuclide cocktails” has been proposed and applied to simultaneously assault tumors with a broad size range. Thus, combination of low with medium or high energy particle emitters can simultaneously eradicate micro-metastases and bulky tumors [19].

## RADIOPHARMACEUTICALS FOR MOLECULAR TARGETING OF TUMORS

In the early 1900s, the German Nobel Prize winner Paul Ehrlich introduced the concept of “magic bullet”, an ideal drug able to selectively target a disease. Such an approach could be applied for countless diseases, including cancer [20]. In the early 1950s this idea was first explored with an antibody conjugated to a radionuclide. The first radiopharmaceutical for targeted diagnosis and therapy of thyroid diseases was  $^{131}\text{I-Nal}$ , which selectively targets the sodium iodide symporter. It was introduced in 1942 for therapy of hyperthyroidism and is still the treatment of choice for thyroid cancers and hyperthyroidism [21]. Furthermore,  $^{99\text{m}}\text{TcO}_4^-$ , which targets the sodium iodide symporter as well, is one of the first radiopharmaceuticals used for thyroid imaging. In fact,  $^{99\text{m}}\text{TcO}_4^-$  is preferred for diagnostic imaging over  $^{131}\text{I-Nal}$  because of the availability and cost effectiveness of  $^{99\text{m}}\text{Tc}$ , the short imaging times and the low radiation dose [22].

### Preclinical evaluation of novel radiopharmaceuticals

The development of a novel radiopharmaceutical in oncology is a long lasting, complex and expensive process. Radiotracers are first assessed *in vitro* for target affinity and specificity, uptake and impact on cellular responses. Given that the new radiopharmaceutical needs to be delivered at the target intact, metabolic stability should be high and should be tested preferably *in vivo*. Animal studies are performed to determine the efficacy and biosafety of a new radiopharmaceutical. In general, rodents and mainly mice are used for such purposes because of their size, their short gestation and life period and their low cost [23]. Experimental tumors developed in animal models constitute a major preclinical tool to evaluate targeting efficacy and pharmacokinetics. Biodistribution studies are important in determining whether binding of the radiopharmaceutical is target-specific and if there is an optimal target-to-background ratio. Toxicology and biodistribution studies verify if the radiopharmaceutical is safe at doses corresponding to those administered to patients. Initial dosimetry studies are performed in animals over a number of time points depending on the biological and physical half-life of the radiotracer. The radioactivity in tumor, blood, urine and tissues, expressed as a percentage of injected radioactivity per gram, is determined to enable calculation of the predicted human radiation dose to each tissue. The dose to critical organs, especially excretory organs such as the kidneys and liver, can limit the amount of radioactivity that can be injected in human studies and therefore has the potential to limit the success of the tracer [24].

Despite the extensive preclinical evaluation of new radiopharmaceuticals, only a small percentage of the most promising tracers are tested clinically and an even smaller number are able to enter the market. Translational barriers can be assigned to significant differences in size and physiology between mice and men potentially inducing diverse biodistribution patterns [25]. In addition, some targets may have different tissue distribution or may not be highly conserved in the two species. Therefore, the choice of a relevant experimental tumor model, preferably originating from human, as well as the accurate design, execution and evaluation of the experiment are critical parameters for the applicability of preclinical data to the clinic [26].

### The target

Nowadays a wide range of molecular targets is considered when developing radiopharmaceuticals for imaging and therapy. The targets are situated either inside the cell (DNA, mRNA, enzymes or proteins) or on the cell membrane, the latter being the preferred target. Such targets situated on the cell membrane include antigens, peptide receptors, symporters, and other proteins that are easily accessible by the radiopharmaceutical. For example, sodium iodide symporters are intrinsic membrane proteins of the sodium-dependent transporter family, expressed in thyroid follicular cells and allow for imaging as well as therapy of differentiated thyroid carcinomas and their metastases [27]. Tumor associated antigens include glycoproteins, carbohydrates and growth factor receptors [28].

Of great clinical relevance are G-protein coupled receptors (GPCRs), which consist of a single polypeptide chain with seven transmembrane domains. The extracellular domain contains the ligand binding site, and the intracellular domain that is linked to G-proteins and arrestin for the activation of a second messenger pathway after internalization upon binding of a receptor agonist (Figure 3) [29]. Upon activation by a ligand, the GPCR adopts an active conformation that promotes the exchange of GDP for GTP on the  $G\alpha$  subunit. This leads to the dissociation of  $G\beta\gamma$ -subunits from  $G\alpha$  and subsequently, the activated G-protein subunits can regulate a variety of downstream effectors such as phospholipases, adenylyl cyclases and ion channels. However, GPCRs can also signal via G-protein-independent mechanisms, such as  $\beta$ -arrestin-mediated signalling via Src and mitogen-activated kinase pathways [30,31]. GPCRs regulate important physiological processes such as neurotransmission and cardiovascular function. The critical role of GPCRs in medicine is highlighted by the fact that at least 30–40% of prescription drugs target these proteins [32]. Such receptors are somatostatin (sst), gastrin releasing peptide (GRP) and cholecystokinin (CCK) receptors, which are overexpressed in many cancer types and thus may serve as targets for radiopharmaceutical imaging and therapy.

The ideal target for a molecular radiopharmaceutical in cancer diagnosis and therapy needs to fulfill certain criteria: i) it should be easily accessible, as for example the peptide receptors located on the cell surface, ii) it should be available in substantial amounts; CCK subtype 2 receptors (CCK2Rs) are overexpressed in MTC, iii) it should be present within the diseased tissue and not in surrounding healthy tissues or radiosensitive tissues, and iv) it should be accessible and highly expressed through the propagation of the disease. For example, in primary MTC somatostatin receptors are expressed in significant amounts, however, their expression is considerably down-regulated in dedifferentiated

and clinically more aggressive forms of the disease. Accordingly, CCK2R scintigraphy and targeted radiotherapy is preferable because of the consistent overexpression of CCK2R throughout all MTC stages [33,34].

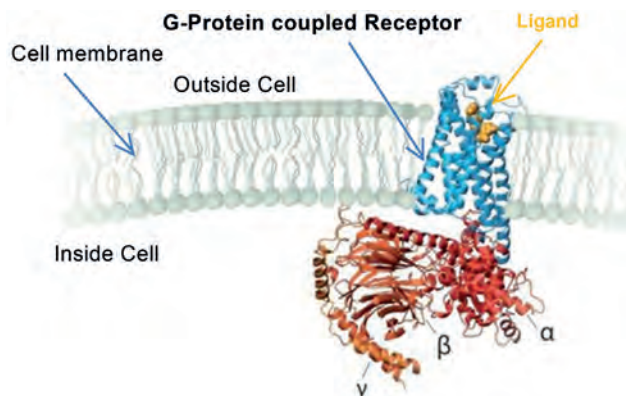


Figure 3 | G-protein coupled receptor (adapted from 35).

### Radiolabeled Antibodies

The use of antibodies as targeting molecules for the delivery of radioisotopes to tumors is an appealing concept that has received widespread attention since the advent of monoclonal antibody (mAb) technology in 1975 from Kohler and Milstein [36]. In the late 1970s antibody-based tumor localization was first clinically achieved with  $^{131}\text{I}$ -labeled IgG for the detection of tumors containing carcinoembryonic antigen (CEA) [37]. This then led to the first radioimmunodetection product in the mid 1990s consisting of a specific anti-CEA MAb fragment (Fab') labeled with  $^{99\text{m}}\text{Tc}$  for colorectal cancer imaging (CEA-Scan<sup>®</sup>) [38]. In the early years of the 21<sup>st</sup> century, the first radiolabeled antibodies were approved for the treatment of non-Hodgkin's lymphoma (NHL). This type of therapy uses an antibody targeted against the antigen CD20, expressed in B-cells, labeled with the beta-emitting radionuclide  $^{90}\text{Y}$  ( $^{90}\text{Y}$ -ibritumomab tiuxetan, Zevalin<sup>®</sup>) or with  $^{131}\text{I}$  ( $^{131}\text{I}$ -tositumomab, Bexxar<sup>®</sup>) [39].

Despite these advances, one of the main drawbacks of radiolabeled antibodies is the potential immune response of the patient. Another major disadvantage is the large size of antibodies (~150 kDa) that leads to slow penetration rates in tumor tissue and slow blood and background clearance. In addition, this long half-life in blood accounts for deposition of unwanted radioactivity doses in the sensitive bone marrow. Aiming to overcome these limiting factors smaller antibody fragments have been developed, such as radiolabeled bivalent F(ab)<sub>2</sub> and monovalent Fab fragments, while recently new entities have been introduced, such as affibodies, diabodies and various minibodies. Generally, radionuclides with short half-lives (e.g.  $^{18}\text{F}$  and  $^{99\text{m}}\text{Tc}$ ) are more suitable for labeling smaller proteins while the radionuclides with longer half-lives (e.g.  $^{177}\text{Lu}$  and  $^{111}\text{In}$ ) better match the relatively long circulation times of antibodies.



Some of these antibody constructs are being considered in pre-targeting strategies that separate tumor targeting from delivery of the radionuclide. Firstly, a modified antibody is administered followed by a sufficient waiting period to ensure high tumor accumulation and clearance from blood. Then, in a second step a radiolabeled compound with high specific binding affinity against the pre-targeting antibody localized on the tumor is administered. Such radiolabeled compounds should exhibit ideal pharmacokinetics with rapid distribution, very low accumulation in healthy tissues, and fast renal blood clearance. One approach for pretargeting has been achieved with bispecific antibodies (bsMAb) that bind both to a target antigen as well as to a radiometal-chelate complex. Another system is the biotin-avidin (or streptavidin) in which avidin or streptavidin conjugated to antibody is targeted first, followed by the administration of radiolabeled biotin [40].

### Radiopeptides

Radiolabeled peptides have become valuable tools for peptide receptor imaging (PRI) and radionuclide therapy (PRRT) of tumors over the last 25 years. The overexpression of different kind of peptide receptors on tumor cells in comparison to normal tissues is one of the main reasons for the increasing interest in developing peptide radiopharmaceuticals (Table 2). Peptides are molecules consisting of a short chain of amino acids (<50) linked together by peptide bonds. Their small size allows for efficient penetration into tumors, rapid pharmacokinetics and clearance from background tissues. Moreover, peptides can be easily synthesized or modified at a low cost and can tolerate rather tough conditions during labeling. Unlike antibodies, peptides have low immunogenicity. However, a major disadvantage of peptides is their rapid degradation by peptidases present in blood and most tissues of the body [41,42].

Peptides are attached by covalent coupling to a bifunctional chelator, usually at their N-terminus, either directly or through a linker (Figure 4). The chelators are essential for stable binding of the radiometal, however, they can also affect the receptor binding and other properties of the end compound. A wide range of bifunctional chelators have been developed, allowing for convenient and rapid radiolabeling of peptides with the suitable radionuclide [43]. During labeling, a minimum possible amount of the peptide conjugate needs to be used in order to avoid saturation of the receptor sites on the tumor, as well as for safety reasons in view of side effects that may be elicited after receptor binding of peptide agonists. Therefore, the radiopeptide must be administered in high specific activity (radioactivity per unit mass of peptide) [44]. The resulting radiolabeled peptide conjugate should have high affinity for the target receptor, be specific for the receptor target evading normal tissues and be sufficiently stable to reach the tumor sites intact for interaction with its cognate receptor. Fast clearance from blood and background will lead to high contrast imaging and higher therapeutic index during therapy. The preferred clearance pathway is through the kidneys into the urine and accordingly hydrophilicity plays an important role. A method to increase the hydrophilicity of radiopeptides is to introduce suitable linkers between the chelator and the peptide [41,42]. Until recently, the preferred radiopeptides for detection and therapy of cancer have been radiolabeled peptide receptor agonists because they internalize after binding to the receptor, permitting the accumulation of radioactivity into tumor cells. However, recent studies have shown that in some cases radiolabeled receptor antagonists display higher tumor uptake and faster

background clearance as compared to agonists. In addition, as they do not elicit second messenger activation, their use is associated with higher biosafety [45,46].

**Table 2 |** Peptide hormones and tumors expressing their cognate receptor. The main receptor types overexpressed in human tumors are marked in bold.

Peptide	Receptor	Tumor Expression
Somatostatin	<i>sst</i> <sub>1</sub> , <b><i>sst</i><sub>2</sub></b> , <i>sst</i> <sub>3</sub> , <i>sst</i> <sub>4</sub> , <i>sst</i> <sub>5</sub>	NET, NHL, melanoma, breast cancer, MTC, SCLC
Bombesin/GRP	BB1R (NMBR), <b>BB2R (GRPR)</b> , BB3R	Prostate cancer, breast cancer, SCLC, colorectal cancer, glioblastoma, gastrinoma, GIST
CCK/gastrin	CCK1R, <b>CCK2R</b>	MTC, SCLC, astrocytoma, stromal ovarian cancer, GIST
Neurotensin	NTSR1, <b>NTSR2</b> , NTSR3	SCLC, ductal exocrine pancreatic carcinoma, Ewing sarcoma, meningioma, astrocytoma
Substance P	<b>NK1R</b> , NK2R, NK3R	Glioblastoma, astrocytoma, SCLC, MTC, breast cancer
LHRH	<b>LHRHR</b>	Breast cancer, prostate cancer
NPY	<b>NPY1R</b> , <b>NPY2R</b> , NPY4, NPY5	Breast cancer, renal cell carcinomas, ovarian adenocarcinomas, neuroblastomas, nephroblastomas, paragangliomas, GIST
VIP	<b>VPAC1R</b> , <b>VPAC2R</b>	SCLC, colorectal cancer, breast cancer, gastrinomas, prostate cancer
α-MSH	<b>MC1-5R</b>	Melanoma

NET= neuroendocrine tumor, NHL= non-Hodgkin's lymphoma, MTC= medullary thyroid carcinoma, SCLC= small cell lung cancer, GRP= gastrin releasing peptide, GIST= gastrointestinal stromal tumors, LHRH= luteinizing hormone-releasing hormone, NPY= neuropeptide Y, VIP= vasoactive intestinal peptide, α-MSH= α-melanocyte-stimulating hormone.

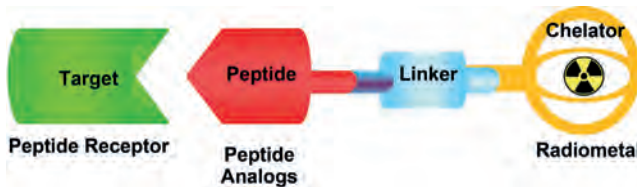


**Figure 4 |** Representation of a radiolabeled peptide consisting of the metallic radionuclide, the chelator, the linker and the peptide part, which recognizes the receptor-target on the tumor.

The first radiolabeled peptide that was approved by the Food and Drug Administration (FDA) and was successfully applied in diagnostic imaging of neuroendocrine tumors (NET) expressing the somatostatin subtype 2 (*sst*<sub>2</sub>) receptors is OctreoScan® (Figure 5 A). It consists of the cyclic octapeptide somatostatin analog, octreotide, coupled at its N-terminus to the open chain chelator DTPA (diethylenetriaminepentaacetic acid) and labeled with the diagnostic radionuclide <sup>111</sup>In ([<sup>111</sup>In-DTPA<sup>0</sup>]octreotide) [47]. Later on, modified somatostatin analogs were introduced to improve the affinity for *sst*<sub>2</sub> receptor, such as [Tyr<sup>3</sup>]octreotide (TOC) and [Tyr<sup>3</sup>]octreotate (TATE); in the latter the

C-terminal threoninol of octreotide has been replaced by threonine (Figure 5 B). These analogs were coupled with a different chelator, such as DOTA (1,4,7,10-tetraazacyclododecane-1,4,7,10-tetraacetic acid) to ensure a more stable binding of various bivalent or trivalent radiometals, like  $^{68}\text{Ga}$  attractive for imaging (Figure 6) or  $^{90}\text{Y}$  and  $^{177}\text{Lu}$  in theranostic approaches (Figure 7) [48-51]. For theranostic applications the peptide used in diagnostic imaging mimics as closely as possible the peptide that is used for therapy.

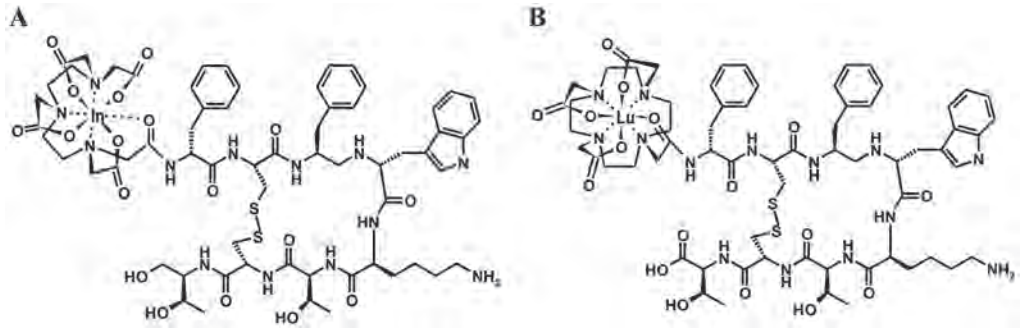
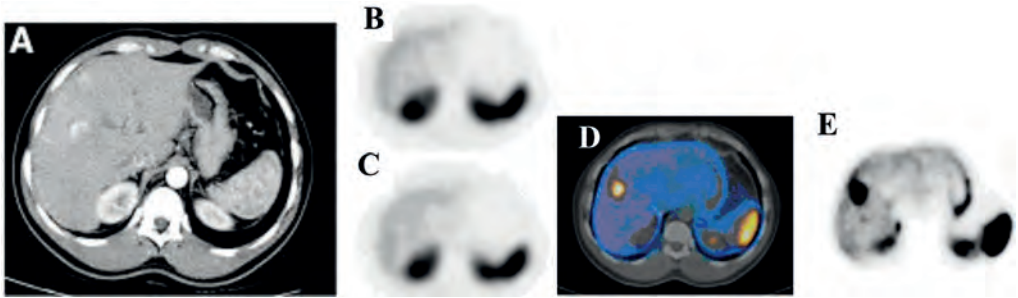
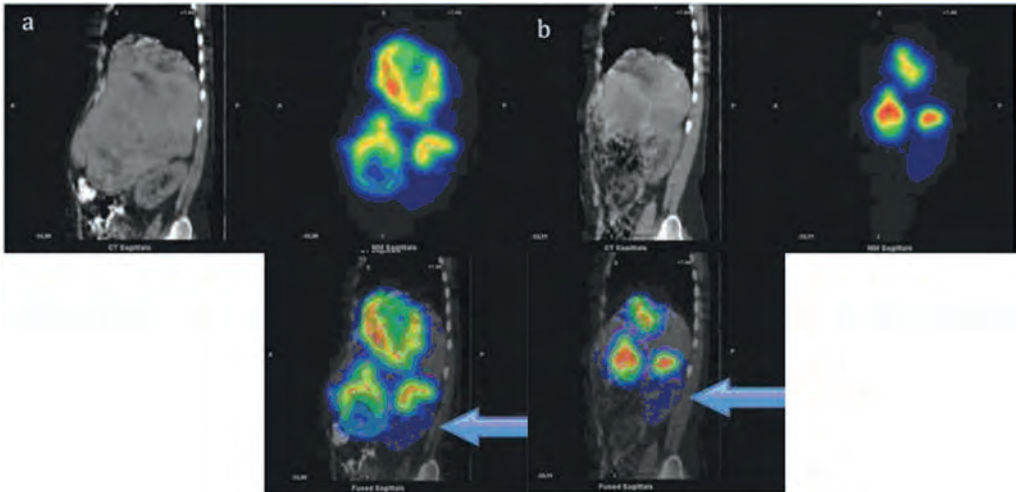


Figure 5 | Structure of A) [ $^{111}\text{In}$ -DTPA] $^0$ octreotide (OctreoScan $^{\text{®}}$ ) and B) [ $^{177}\text{Lu}$ -DOTA]TATE.

PRRT started initially using high doses of OctreoScan $^{\text{®}}$ , however, partial remissions were rare and severe toxicities were observed due to the high doses [52,53]. The next generation of PRRT used peptides radiolabeled with  $\beta$ -emitting radionuclides. Different phase 1 and phase 2 PRRT trials have been performed using DOTATOC labeled with  $^{90}\text{Y}$  [54-57]. Moreover,  $^{177}\text{Lu}$ -based PRRT has been introduced into clinical practice with DOTATATE. Both radiopeptides showed impressive results in terms of tumor regression, however renal toxicity is a limiting factor that can be minimized using proper kidney protection methods [58-61]. Recently, a first-in-human experience with  $^{213}\text{Bi}$ -DOTATOC targeted alpha therapy in patients pre-treated with beta emitters was reported. This type of therapy was able to induce long-lasting anti-tumour responses in contrast to beta radiation. In addition, the renal and haematological toxicity remained within the acceptable range, opening a new route in therapeutic nuclear medicine [62]. Finally, a pilot clinical study of a  $^{177}\text{Lu}$ -labeled  $\text{sst}_2$ -receptor antagonist showed promising results and proved that treatment of NETs with radiolabeled  $\text{sst}_2$ -antagonists is clinically feasible and may have a significant impact on PRRT [63].



**Figure 6** | Images of a 42 year-old man with intermediate grade metastatic midgut NET. **A)** Arterial-phase CT at level of splenic hilum shows 2 arterially enhancing liver metastases. **B** and **C)** Axial [<sup>111</sup>In-DTPA]octreotide SPECT at level of spleen shows no discernable liver lesions. **D)** Axial <sup>68</sup>Ga-DOTATATE PET/CT shows large metastatic liver deposit. **E)** Axial <sup>68</sup>Ga-DOTATATE PET shows large metastatic liver deposit (adapted from 50).



**Figure 7** | SPECT-CT images of a NET patient with a large liver metastasis, 24 hrs after treatment with <sup>177</sup>Lu-DOTATATE. **A)** Cycle 1, May 2010 **b)** cycle 7, August 2011. Left upper panel in each image: attenuation correction CT, right upper panel attenuation corrected SPECT, lower panel in each image fused SPECT-CT. Note the volume reduction of the liver along with the tumour burden on sagittal views at start of PRRT and during the final treatment cycle. The right kidney, dislocated at start of PRRT, had returned back to its normal anatomical place by cycle 7 (arrow) (adapted from 51).

### Metallic radionuclides in oncology

There is a wide range of metallic radionuclides available for application either in diagnostic imaging or in radionuclide therapy. The design of the radiopharmaceutical is related with some characteristics of the radiometals: i) physical half-life, ii) decay mode, iii) energy of emission, iv) cost,

v) availability, vi) chemical purity and vii) specific activity. As discussed earlier, positron emitting (e.g.  $^{68}\text{Ga}$ ) or gamma emitting (e.g.  $^{99\text{m}}\text{Tc}$ ,  $^{111}\text{In}$ ,  $^{67}\text{Ga}$ ) radionuclides are employed for PET or SPECT imaging, respectively, while  $\alpha$  (e.g.  $^{213}\text{Bi}$ ) or  $\beta^-$  (e.g.  $^{177}\text{Lu}$ ,  $^{90}\text{Y}$ ) or Auger electron (e.g.  $^{111}\text{In}$ ) emitters are considered for radionuclide therapy (Table 1) [17].

The metastable radionuclide ***Technetium-99m*** ( $^{99\text{m}}\text{Tc}$ ) is widely used in diagnostic imaging since 1960 mainly because of its physical properties and its convenient availability via the inexpensive commercial  $^{99}\text{Mo}/^{99\text{m}}\text{Tc}$  generator (Figure 8) [64]. The physical half-life of  $^{99\text{m}}\text{Tc}$  is 6.03 h, which is well suited for radiopharmaceutical preparation, collection of images and low radiation exposure of patients and personnel. The energy of the emitted photon of 140 keV is sufficient to penetrate the biological tissues and is most effectively absorbed in the thallium-doped NaI crystals employed in most SPECT cameras.  $^{99\text{m}}\text{Tc}$  is produced from the parent radionuclide  $^{99}\text{Mo}$  ( $t_{1/2} = 2.78$  days) in the  $^{99}\text{Mo}/^{99\text{m}}\text{Tc}$  generator in the form of  $\text{Na}^{99\text{m}}\text{TcO}_4$ , however it is never carrier free as  $\sim 13\%$  of  $^{99}\text{Mo}$  decays directly to the long-lived  $\beta^-$  emitter  $^{99\text{g}}\text{Tc}$  ( $t_{1/2} = 2.12 \times 10^5$  years). In general, the concentration of technetium ( $^{99\text{m}}\text{Tc} + ^{99\text{g}}\text{Tc}$ ) in the eluate is in the range of  $10^{-8} - 10^{-7}$  M thus, the  $^{99\text{m}}\text{Tc}$  radiopharmaceutical is administered in very low concentrations [65]. Another breakthrough that has further promoted the widespread use of  $^{99\text{m}}\text{Tc}$  is the availability of commercial kits of the radiopharmaceutical precursor (non-radioactive freeze dried kits) that can be stored for long periods and simplify the preparation of  $^{99\text{m}}\text{Tc}$ -based radiopharmaceuticals [66].

$^{99\text{m}}\text{Tc}$  is not appropriate for radionuclide therapy, however, there are two radioisotopes of Rhenium (which is a chemical surrogate of Tc), ***Rhenium-186*** ( $^{186}\text{Re}$ ) and ***Rhenium-188*** ( $^{188}\text{Re}$ ) that are used in therapy. Rhenium-186 is reactor produced and contains carrier  $^{185}\text{Re}$ , while  $^{188}\text{Re}$  is carrier free and is obtained from  $^{188}\text{W}/^{188}\text{Re}$  generator. The half-life of  $^{186}\text{Re}$  is 3.7 days and of  $^{188}\text{Re}$  is 17 h and they both emit  $\beta^-$  and also  $\gamma$  rays allowing for theranostic applications. Rhenium-188 has a 2fold higher  $\beta^-$  energy ( $E_{\text{max}} = 2.12$  MeV) and thus longer range in tissues (maximum  $\sim 11$  mm), as compared to  $^{186}\text{Re}$  ( $E_{\text{max}} = 1.07$  MeV, maximum particle range  $\sim 4.5$  mm), and is more useful for treating larger tumors [67].

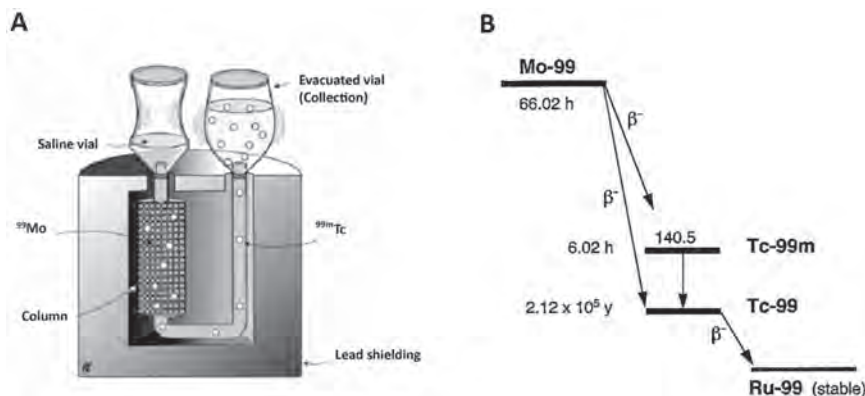


Figure 8 | **A**) Representation of a  $^{99}\text{Mo}/^{99\text{m}}\text{Tc}$  generator (adapted from 68) and **B**) the decay scheme of  $^{99}\text{Mo}$  (adapted from 69).

**Indium-111** ( $^{111}\text{In}$ ) is a frequently used radionuclide in the field of diagnostic nuclear medicine with a half-life of 68 h. It decays by electron capture to give excited states of  $^{111}\text{Cd}$  and high intensity and low energy gamma rays (171 and 245 keV) are emitted. There is also some internal conversion generating Auger electrons in the range of 19–23 keV, which are suitable for therapeutic applications. It is produced by proton bombardment of  $^{111}\text{Cd}$  in a medium energy cyclotron [70].

**Gallium-68** is produced from a  $^{68}\text{Ge}/^{68}\text{Ga}$  generator, which can be used for 1–2 years, allowing for PET imaging at facilities without on-site cyclotron. It decays by positron emission and hence 511 keV annihilation radiation [71]. Gallium-68 has a short half-life of 68 min which is practically inconvenient for preclinical studies and thus  $^{67}\text{Ga}$  is frequently used as a surrogate [72,73]. **Gallium-67** has a half-life of 78 h and is produced by the proton irradiation of a  $^{68}\text{Zn}$  target. It decays by electron capture with 10 gamma emissions ranging from 90–400 keV and there is also accompanying Auger electron emission (7.2–9.7 keV) [70].

**Lutetium-177** ( $^{177}\text{Lu}$ ), which has a half-life of 6.7 days, is a radiolanthanide attractive for radiotherapeutic applications. It emits medium energy  $\beta^-$  with maximum energy 0.497 MeV. In addition,  $^{177}\text{Lu}$  emits accompanying low energy gamma rays of 208 and 113 keV with 11% and 6.4% abundance, respectively, which are suitable for scintigraphic imaging, thereby providing a theranostic opportunity for the use of this radionuclide [74]. Lutetium-177 has a maximum particle range of ~2–4 mm, which makes it a more favorable radionuclide for radiotherapy of smaller lesions. High specific activity  $^{177}\text{Lu}$  can be produced by high flux nuclear reactor by direct neutron irradiation of isotopically enriched  $^{176}\text{Lu}$  or by neutron activation of  $^{176}\text{Yb}$  and its further chemical separation [75].

**Yttrium-90** ( $^{90}\text{Y}$ ) is a generator-produced radionuclide, resulting from the  $\beta$  decay of  $^{90}\text{Sr}$  and is currently used as a therapeutic radionuclide in nuclear medicine. It decays with the high energy  $\beta^-$  ( $E_{\text{max}} = 2.28$  MeV, 100% abundance) to form  $^{90}\text{Zr}$  and has a maximum particle range of ~10 mm and is thus suitable for treatment of larger tumors. It has a half-life of 2.7 days, which is short enough to achieve a critical dose rate and at the same time is long enough to allow the radiopharmaceutical to be manufactured, transported and delivered for clinical use. The specific activity for  $^{90}\text{Y}$  is very high (49 mCi/nmol), and is well suited for the development of receptor-based therapeutic radiopharmaceuticals. For quantitative imaging, the corresponding  $^{111}\text{In}$ - or  $^{68}\text{Ga}$ -labeled compound is often used as a surrogate to determine the biodistribution characteristics and radiation dosimetry of the  $^{90}\text{Y}$ - radiopharmaceutical [71,76].

Peptide receptor targeted alpha therapy has been recently introduced in clinical practice with the use of **Bismuth-213** ( $^{213}\text{Bi}$ ), however, other alpha emitting radionuclides such as **Actinium-225** ( $^{225}\text{Ac}$ ) and **Astatine-211** ( $^{211}\text{At}$ ) are also very promising. Alpha particles are positively charged helium nuclei with a shorter range (50–80  $\mu\text{m}$ ) and higher energy (5000–8000 keV) than  $\beta$  particles. The short range of alpha particles allows for optimal treatment of micrometastases and also limits damage to normal tissues.  $^{213}\text{Bi}$  decays to stable  $^{209}\text{Bi}$  by emitting an  $\alpha$  particle and two  $\beta^-$  particles. The short half-life of  $^{213}\text{Bi}$  ( $t_{1/2} = 45.6$  min) raises logistical difficulties, while the  $^{225}\text{Ac}/^{213}\text{Bi}$  generator which is required for its production is quite expensive and has limited availability [77,78].  $^{225}\text{Ac}$  ( $t_{1/2} = 10$  days) decays to stable  $^{209}\text{Bi}$  through a series of six radionuclides with a total of four  $\alpha$  particles emitted. It can be produced by the natural decay of  $^{233}\text{U}$  or by accelerator-based methods. The possibility of

free daughter radioisotopes in circulation after decay of  $^{225}\text{Ac}$  raises concerns about the potential toxicity of this radionuclide.  $^{211}\text{At}$  ( $t_{1/2} = 7.2$  h) decays to stable  $^{207}\text{Pb}$  through a branched pathway with each branch resulting in the production of an  $\alpha$  particle. It is typically produced in the cyclotron by irradiation of  $^{209}\text{Bi}$ , however, its availability is limited due to the lack of appropriate cyclotrons [69,70,79].

### Bifunctional chelators – coordination chemistry aspects

The use of radiometals for labeling biomolecules generally requires the use of a bifunctional chelator, which has a metal binding moiety function and also possesses a chemically reactive functional group for covalent linkage to a targeting vector. The choice of the bifunctional chelator is determined by the nature and oxidation state of the metallic radionuclide. The ideal chelator should fulfil certain requirements: i) it should form thermodynamically stable and kinetically inert complexes to prevent any ligand exchange reactions or hydrolysis in vivo, ii) it should have rapid complexation kinetics, iii) it should stably bind the radiometal of interest with high specific activity, iv) it should have low cost and v) commercial availability. Bifunctional chelators can have a great impact on several biological parameters of a radiopharmaceutical, such as receptor binding and in vivo profile. The two most important parameters that influence the properties of radiopharmaceuticals are the overall charge and the lipophilicity of the corresponding metal-chelate complex. As discussed earlier, a linker may also be introduced between the chelator and the targeting vector to influence the pharmacokinetic properties of the conjugate. In most cases the bifunctional chelator is attached to the peptide prior to radionuclide labeling, following the so called postlabeling method, which is more practical for routine clinical applications [80,81].

### Bifunctional chelators for $^{99\text{m}}\text{Tc}$

Technetium belongs to the VII group of the periodic table and its oxidation states vary from -1 to +7. In aqueous solution the most stable chemical form is the pertechnetate anion  $^{99\text{m}}\text{TcO}_4^-$  with a +7 oxidation state (Figure 9 A). As  $^{99\text{m}}\text{TcO}_4^-$  is chemically stable and inert, the radiometal can only bind a chelator when reduced to lower oxidation states, with oxidation state V being the most frequent (Figure 9).

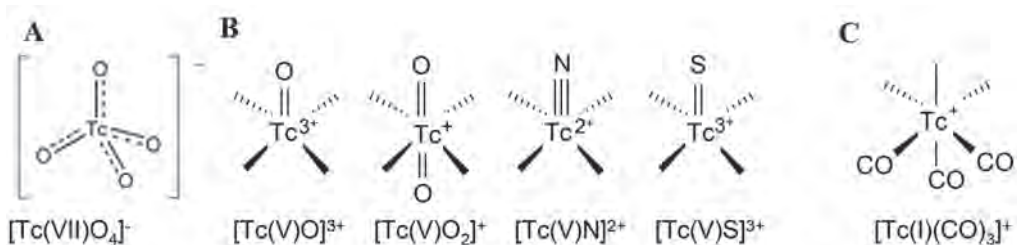


Figure 9 | A) Structure of the pertechnetate anion  $^{99\text{m}}\text{TcO}_4^-$ , B) Cores of Tc(V) and C) the Tc(I)-tricarbonyl core.



### Tc(V)-complexes

The radiopharmaceutical chemistry of Tc(V) is dominated by the  $[Tc(V)=O]^{3+}$  core which is stabilized by a wide range of donor atoms (N, S, O) but has a preference for thiolates. Consequently, several tetradentate chelators, such as  $N_2S_2$ ,  $N_3S$  and numerous examples of tripeptides and tetrapeptides appropriately derivatized to act as bifunctional chelators, have been investigated. The resulting complexes have a square pyramidal configuration [82]. Some of the complexes formed are neutral and lipophilic, hence they undesirably accumulate in the abdomen [83].

The *trans*- $[O=Tc(V)=O]^+$  core forms Tc-complexes with cyclic and open chain tetraamine bifunctional chelators, such as 1,4,8,11-tetraazaundecane ( $N_4$ ) analogs (Figure 10 A) [84]. Labeling of  $N_4$ -coupled peptides with  $^{99m}Tc$  produces complexes with high radiochemical purity and high specific activities ( $\geq 1$  Ci/ $\mu$ mol). Moreover, these chelators form kinetically inert monocationic octahedral dioxometal complexes. The total net charge of 1+ and the presence of two oxygen atoms convey high hydrophilicity, which favours excretion via the kidneys and the urinary system [85]. Many [ $^{99m}Tc-N_4$ ]radiotracers including somatostatin and gastrin have been developed and evaluated pre-clinically and some of those have already been tested in patients with promising results [86-88].

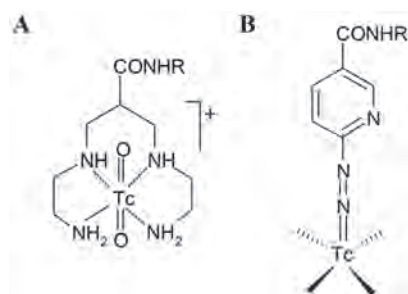


Figure 10 | Structures of A) Tc- $N_4$  complex and B) Tc-HYNIC core.

HYNIC (6-hydrazinopyridine-3-carboxylic acid) is of interest because it strongly binds Tc(V) in the monodentate diazenido unit ( $Tc=N=N-R$ ) and leaves coordination sites on the Tc atom free to be completed by different co-chelators, such as EDDA (ethylenediamine N,N' diacetic acid), that are selected for optimal pharmacokinetics (Figure 10B). However, the  $^{99m}Tc$ -HYNIC based radioligands are poorly characterized at the tracer level, which restricts the potential of clinical application due to the increasing demand of FDA regulators for fully characterized products [89].

### Tc(I) and Tc(III)-complexes

Tc(I) and Tc(III) is stabilized by ligands with  $\pi$ -accepting groups, such as phosphines, isonitriles and carbon monoxide and usually form six-coordinated complexes in an octahedral configuration. The low oxidation state of organometallic Tc(I)-complexes received little attention until the discovery of a very stable, water soluble hexakis-isonitrile complex of the type  $[Tc(CNR)_6]^+$  that is widely used as a myocardial perfusion agent [90]. Later on, in an effort to establish new organometallic precursors for radiopharmaceutical applications, the highly adaptable tricarbonyl Tc core  $[Tc(CO)_3]^+$  was developed



(Figure 9 C) [91]. The use of  $[\text{Tc}(\text{CO})_3]^+$ -core is based on the chemical properties of the precursor complex  $[\text{Tc}(\text{OH})_2(\text{CO})_3]^+$  in which the three water molecules can be easily replaced by chelators having the appropriate set of donor atoms. The popularity of this method is largely based on the availability of a commercial lyophilized kit (IsoLink™), which allowed the easy conversion into the final  $[\text{Tc}(\text{CO})_3]$ -based compounds, after the instant production of the intermediate  $[\text{Tc}(\text{CO})_3(\text{H}_2\text{O})_3]^+$  complex. Bidentate and tridentate chelators can bind rapidly to the  $[\text{Tc}(\text{CO})_3]^+$  core of the precursor at the tracer level, yielding complexes with high specific activity [82,89].

### **Bifunctional chelators for trivalent radiometals**

Most trivalent radiometals  $[\text{M}(\text{III})]$ , such as  $^{111}\text{In}$ ,  $^{67}\text{Ga}$ ,  $^{90}\text{Y}$  and  $^{177}\text{Lu}$  used in nuclear medicine applications require polydentate chelators to efficiently bind the radionuclide and form kinetically inert and in vivo stable complexes. Derivatives of DTPA are used for the fast incorporation of  $^{111}\text{In}$ , as in the case of the first clinically approved radiopharmaceutical OctreoScan® (Figure 11). However, because of in vivo instability DTPA is not suitable for any other radionuclide than  $^{111}\text{In}$ . The most widely used bifunctional chelators are DOTA and its derivatives (Figure 11). The DOTA chelator allows for labeling with various radiometals and forms complexes with high thermodynamic stability and kinetic inertness. For coupling the trivalent radiometals to the peptide, the most common method involves the attachment of the peptide to one of the four carboxylate groups of DOTA to a primary amine group of the peptide. To increase the number of donor atoms available for radiometal binding, DOTA derivatives carrying an extra carboxylate arm in one of the nitrogens have been developed, such as DOTASA (1,4,7,10-tetraazacyclodecane-1-(*R,S*)-succinic acid-4,7,10-triacetic acid) and DOTAGA (1,4,7,10-tetraazacyclodecane-1-glutaric acid-4,7,10-triacetic acid) [75,81].

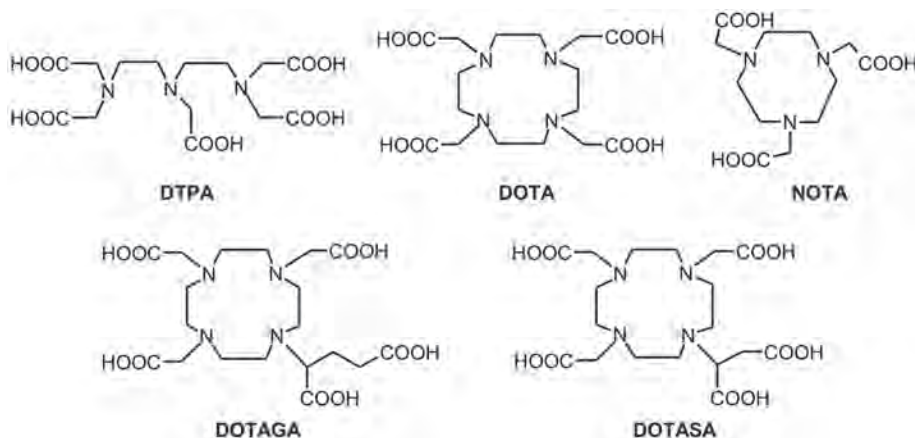


Figure 11 | Structures of DTPA, DOTA, NOTA, DOTAGA and DOTASA chelators.

The DOTA chelator forms complexes with coordination number between 6 and 9. The coordination chemistry of the trivalent radiometals with DOTA differs mainly because of their variable size. Yttrium(III) has an ionic radius of 90-108 pm and is often treated as a “pseudolanthanide” due to its similarity to lanthanides with respect to the cationic charge, ionic radii, and coordination chemistry. Because of its large size, the coordination number for Y(III) and the lanthanides is normally 8 or 9 and are most likely coordinated by the four N and four O atoms within the macrocyclic ring. Indium(III) has a smaller size with an ionic radius of 62–92 pm and its typical coordination number is 7 or 8. The In(III)-DOTA complex adopts a twisted square anti-prismatic geometry in solid state, while in solution the amide oxygen is not coordinated. Gallium(III) is even smaller than In(III) as its ionic radius is 47–62 pm. The complex of Ga(III) with DOTA has a completely different octahedral geometry with coordination number 6 (Figure 12C). Accordingly, Y(III) fits perfectly within the cavity of DOTA, while Ga(III) and In(III) are not ideal to fit because of their smaller size and cavity. Therefore, Ga(III) and In(III) prefer chelators with fewer donor atoms, like NOTA (1,4,7-triazacyclononane-N,N'N''-triacetic acid) (Figure 12) [92,93]. The difference in coordination geometries of the Y(III), In(III), and Ga(III) complexes of the same DOTA peptide can cause differences in the biological behaviour of the respective radiopeptide [94].

The formation rates of the M(III) complexes with macrocyclic ligands, especially with DOTA, are typically slow. To speed up the chelation process, high temperatures are required during the complexation (80–100°C). In addition, pH plays a critical role in the chelation as the rate of complex formation increases with pH. However, when the pH is higher than 6, the lanthanide ions start to form insoluble polyhydroxo complexes, thus the optimal pH for labeling is between 4 and 5 [95].

## OUTLINE OF THE THESIS

A general introduction of the thesis is given in **Chapter 1** and focuses on the molecular imaging techniques (SPECT and PET), on targeted radionuclide therapy and on the radiopharmaceuticals applied. In particular, the target-biomolecules, the vector, the radiometals and the chelating systems used for associating the radiometal to the targeting vector are described.

**Chapter 2** focuses on the physiological role of gastrin and CCK, as well as their role as carriers of radioactivity to CCK2R-expressing tumor sites. A short review on the various gastrin and CCK based radiopeptides proposed for nuclear medicine applications is also provided. The issue of in vivo catabolism of radiolabeled gastrin and CCK analogs mainly by neutral endopeptidase (NEP) is addressed. For enhancing their in vivo stability and tumor uptake coinjection with the NEP inhibitor phosphoramidon (PA) is introduced. First promising results with the rapidly biodegradable [ $^{111}\text{In}$ -DOTA]MG11 are reported.

In **Chapter 3** a series of novel  $^{111}\text{In}$ -labeled analogs of [DOTA]MG11 are introduced. The in vitro profile of new analogs was studied as well as the stability in mouse circulation and the biodistribution in CCK2R-positive tumor bearing mice during in situ NEP inhibition by PA. The minigastrin radiotracer [ $^{111}\text{In}$ -DOTA]MG0, previously reported for good tumor targeting, but unfavourably high kidney retention, was included in the study for comparison.

In **Chapter 4** the efficacy of the novel method of in situ NEP inhibition by PA coinjection is assessed for three  $^{111}\text{In}$ -labeled gastrin radiotracers differing in the (Glu) $^{6-10}$ -chain of native gastrin, previously proven to be critical for metabolic stability, kidney retention and tumor localization. Thus, substitution of (Glu) $^{6-10}$  by (DGlu) $^{6-10}$  was compared versus truncation of the penta-Glu repeat. The need to validate this promising concept in the clinic was highlighted in this study.

In **Chapter 5** the in vivo efficacy of PA vs. clinically tested NEP or/and angiotensin converting enzyme (ACE) inhibitors was compared using [ $^{111}\text{In}$ -DOTA]MG11 as a model radiotracer. Different doses and administration routes were examined in mouse models aiming toward fast translation of this concept in the clinic.

Advances in SPECT imaging combined with the optimal nuclear characteristics of  $^{99\text{m}}\text{Tc}$  and its wide availability have prompted the study described in **Chapter 6**. The aim was first to evaluate the in vitro and in vivo profile of three  $^{99\text{m}}\text{Tc}$ -labeled gastrin analogs with different peptide chain lengths. Moreover, the impact of NEP and/or ACE inhibition on stability, pharmacokinetics and tumor targeting of these radiotracers was investigated.

The thesis concludes with **Chapter 7**, the **Summary** and general **Conclusions Chapter**, where the results of the studies are summarized and discussed further and a future outlook is given.

## REFERENCES

1. Stewart B. World Cancer Report 2014: IARC Nonseries Publication, 2014.
2. Pellegriti G, Frasca F, Regalbuto C, Squatrito S, Vigneri R. Worldwide increasing incidence of thyroid cancer: update on epidemiology and risk factors. *J Cancer Epidemiol* 2013;2013:965212.
3. Ferreira CV, Siqueira DR, Ceolin L, Maia AL. Advanced medullary thyroid cancer: pathophysiology and management. *Cancer Manag Res* 2013;5:57-66.
4. Bhardwaj JR. Recent advances in diagnosis of cancer. *Medical Journal Armed Forces India*;61:112-114.
5. Jaffer FA, Weissleder R. Molecular imaging in the clinical arena. *Jama* 2005;293:855-62.
6. Vallabhajosula S. *Molecular Imaging*: Springer-Verlag Berlin Heidelberg, 2009:372.
7. Anger HO. Scintillation Camera. *Review of Scientific Instruments* 1958;29:27-33.
8. Banerjee S, Pillai MR, Ramamoorthy N. Evolution of Tc-99m in diagnostic radiopharmaceuticals. *Semin Nucl Med* 2001;31:260-77.
9. Rahmim A, Zaidi H. PET versus SPECT: strengths, limitations and challenges. *Nucl Med Commun* 2008;29:193-207.
10. Seo Y, Mari C, Hasegawa BH. Technological development and advances in single-photon emission computed tomography/computed tomography. *Semin Nucl Med* 2008;38:177-98.
11. College Physics: Medical Imaging and Diagnosis, <<http://voer.edu.vn/c/medical-imaging-and-diagnostics/0e60bfc6/b71066ff>>.
12. Nutt R. The History of Positron Emission Tomography. *Molecular Imaging & Biology* 2002;4:11-26.
13. Ganguly B, Mondal N, Nandy M, Roesch F. Some physical aspects of positron annihilation tomography: A critical review. *Journal of radioanalytical and nuclear chemistry* 2009;279:685-698.
14. Townsend DW. Positron emission tomography/computed tomography. *Semin Nucl Med* 2008;38:152-66.
15. Catana C, Procissi D, Wu Y, Judenhofer MS, Qi J, Pichler BJ, et al. Simultaneous in vivo positron emission tomography and magnetic resonance imaging. *Proc Natl Acad Sci U S A* 2008;105:3705-10.
16. Partle R. Nuclear Imaging <<http://www.slideshare.net/Blindsided/nucleaer-imaging>>.
17. Ginj M, Maecke HR. Radiometallo-labeled peptides in tumor diagnosis and therapy. *Met Ions Biol Syst* 2004;42:109-42.
18. Humm JL. Dosimetric aspects of radiolabeled antibodies for tumor therapy. *J Nucl Med* 1986;27:1490-7.
19. Oyen WJ, Bodei L, Giammarile F, Maecke HR, Tennvall J, Luster M, et al. Targeted therapy in nuclear medicine--current status and future prospects. *Ann Oncol* 2007;18:1782-92.
20. Schwartz RS. Paul Ehrlich's magic bullets. *N Engl J Med* 2004;350:1079-80.
21. Hertz S, Roberts A. Radioactive iodine as an indicator in thyroid physiology. V. the use of radioactive iodine in the differential diagnosis of two types of Graves' disease. *J Clin Invest* 1942;21:31-2.
22. Treves S. *Pediatric Nuclear Medicine and Molecular Imaging*: Springer-Verlag New York; 2014.
23. Mather S, Maina T, de Jong M. Animal models for developing radiopharmaceuticals for therapy. In: Baum RP, ed. *Therapeutic nuclear medicine*: Springer, 2012:807-815.
24. Sharma R, Aboagye E. Development of radiotracers for oncology--the interface with pharmacology. *Br J Pharmacol* 2011;163:1565-85.
25. Davies B, Morris T. Physiological parameters in laboratory animals and humans. *Pharm Res* 1993;10:1093-5.
26. de Jong M, Maina T. Of mice and humans: are they the same?--Implications in cancer translational research. *J Nucl Med* 2010;51:501-4.
27. Spitzweg C, Harrington KJ, Pinke LA, Vile RG, Morris JC. Clinical review 132: The sodium iodide symporter and its potential role in cancer therapy. *J Clin Endocrinol Metab* 2001;86:3327-35.
28. Scott AM, Allison JP, Wolchok JD. Monoclonal antibodies in cancer therapy. *Cancer Immun* 2012;12:14.
29. Henderson R, Baldwin JM, Ceska TA, Zemlin F, Beckmann E, Downing KH. Model for the structure of bacteriorhodopsin based on high-resolution electron cryo-microscopy. *J Mol Biol* 1990;213:899-929.

30. Shenoy SK, Lefkowitz RJ. Seven-transmembrane receptor signaling through beta-arrestin. *Sci STKE* 2005;2005:cm10.
31. Tuteja N. Signaling through G protein coupled receptors. *Plant Signal Behav* 2009;4:942-7.
32. Magalhaes AC, Dunn H, Ferguson SS. Regulation of GPCR activity, trafficking and localization by GPCR-interacting proteins. *Br J Pharmacol* 2012;165:1717-36.
33. Behr TM, Gratz S, Markus PM, Dunn RM, Hufner M, Schauer A, et al. Anti-carcinoembryonic antigen antibodies versus somatostatin analogs in the detection of metastatic medullary thyroid carcinoma: are carcinoembryonic antigen and somatostatin receptor expression prognostic factors? *Cancer* 1997;80:2436-57.
34. Reubi JC, Waser B. Unexpected high incidence of cholecystokinin-B/gastrin receptors in human medullary thyroid carcinomas. *Int J Cancer* 1996;67:644-7.
35. Kojić-Prodić B. A century of X-ray crystallography and 2014 international year of X-ray crystallography. *Maced.J.Chem.Chem.Eng.* 2015;34.
36. Kohler G, Milstein C. Continuous cultures of fused cells secreting antibody of predefined specificity. *Nature* 1975;256:495-7.
37. Goldenberg DM, DeLand F, Kim E, Bennett S, Primus FJ, van Nagell JR, Jr., et al. Use of radiolabeled antibodies to carcinoembryonic antigen for the detection and localization of diverse cancers by external photoscanning. *N Engl J Med* 1978;298:1384-6.
38. Goldenberg DM, Juweid M, Dunn RM, Sharkey RM. Cancer imaging with radiolabeled antibodies: new advances with technetium-99m-labeled monoclonal antibody Fab' fragments, especially CEA-Scan and prospects for therapy. *J Nucl Med Technol* 1997;25:18-23; quiz 34.
39. Sharkey RM, Goldenberg DM. Perspectives on cancer therapy with radiolabeled monoclonal antibodies. *J Nucl Med* 2005;46 Suppl 1:115s-27s.
40. Goldenberg DM. Targeted therapy of cancer with radiolabeled antibodies. *J Nucl Med* 2002;43:693-713.
41. Reubi JC. Peptide receptors as molecular targets for cancer diagnosis and therapy. *Endocr Rev* 2003;24:389-427.
42. Fani M, Maecke HR, Okarvi SM. Radiolabeled peptides: valuable tools for the detection and treatment of cancer. *Theranostics* 2012;2:481-501.
43. Liu S. The role of coordination chemistry in the development of target-specific radiopharmaceuticals. *Chem Soc Rev* 2004;33:445-61.
44. Breeman WA, de Jong M, Kwekkeboom DJ, Valkema R, Bakker WH, Kooij PP, et al. Somatostatin receptor-mediated imaging and therapy: basic science, current knowledge, limitations and future perspectives. *Eur J Nucl Med* 2001;28:1421-9.
45. Ginj M, Zhang H, Waser B, Cescato R, Wild D, Wang X, et al. Radiolabeled somatostatin receptor antagonists are preferable to agonists for in vivo peptide receptor targeting of tumors. *Proc Natl Acad Sci U S A* 2006;103:16436-41.
46. Cescato R, Maina T, Nock B, Nikolopoulou A, Charalambidis D, Piccand V, et al. Bombesin receptor antagonists may be preferable to agonists for tumor targeting. *J Nucl Med* 2008;49:318-26.
47. Krenning EP, Bakker WH, Kooij PP, Breeman WA, Oei HY, de Jong M, et al. Somatostatin receptor scintigraphy with indium-111-DTPA-D-Phe-1-octreotide in man: metabolism, dosimetry and comparison with iodine-123-Tyr-3-octreotide. *J Nucl Med* 1992;33:652-8.
48. Henze M, Schuhmacher J, Hipp P, Kowalski J, Becker DW, Doll J, et al. PET imaging of somatostatin receptors using [<sup>68</sup>Ga]DOTA-D-Phe<sup>1</sup>-Tyr<sup>3</sup>-octreotide: first results in patients with meningiomas. *J Nucl Med* 2001;42:1053-6.
49. van Essen M, Sundin A, Krenning EP, Kwekkeboom DJ. Neuroendocrine tumours: the role of imaging for diagnosis and therapy. *Nat Rev Endocrinol* 2014;10:102-14.
50. Srirajskanthan R, Kayani I, Quigley AM, Soh J, Caplin ME, Bomanji J. The role of <sup>68</sup>Ga-DOTATATE PET in patients with neuroendocrine tumors and negative or equivocal findings on <sup>111</sup>In-DTPA-octreotide scintigraphy. *J Nucl Med* 2010;51:875-82.
51. Garske U, Sandstrom M, Johansson S, Granberg D, Lundqvist H, Lubberink M, et al. Lessons on Tumour Response: Imaging during Therapy with (177)Lu-DOTA-octreotate. A Case Report on a Patient with a Large Volume of Poorly Differentiated Neuroendocrine Carcinoma. *Theranostics* 2012;2:459-71.

52. Valkema R, De Jong M, Bakker WH, Breeman WA, Kooij PP, Lugtenburg PJ, et al. Phase I study of peptide receptor radionuclide therapy with [In-DTPA]octreotide: the Rotterdam experience. *Semin Nucl Med* 2002;32:110-22.
53. Anthony LB, Woltering EA, Espenan GD, Cronin MD, Maloney TJ, McCarthy KE. Indium-111-pentetreotide prolongs survival in gastroenteropancreatic malignancies. *Semin Nucl Med* 2002;32:123-32.
54. Imhof A, Brunner P, Marincek N, Briel M, Schindler C, Rasch H, et al. Response, survival, and long-term toxicity after therapy with the radiolabeled somatostatin analogue [<sup>90</sup>Y-DOTA]-TOC in metastasized neuroendocrine cancers. *J Clin Oncol* 2011;29:2416-23.
55. Waldherr C, Pless M, Maecke HR, Schumacher T, Crazzolaro A, Nitzsche EU, et al. Tumor response and clinical benefit in neuroendocrine tumors after 7.4 GBq (90)Y-DOTATOC. *J Nucl Med* 2002;43:610-6.
56. Bodei L, Cremonesi M, Grana C, Rocca P, Bartolomei M, Chinol M, et al. Receptor radionuclide therapy with <sup>90</sup>Y-[DOTA]<sup>0</sup>-Tyr<sup>3</sup>-octreotide (<sup>90</sup>Y-DOTATOC) in neuroendocrine tumours. *Eur J Nucl Med Mol Imaging* 2004;31:1038-46.
57. Valkema R, Pauwels S, Kvols LK, Barone R, Jamar F, Bakker WH, et al. Survival and response after peptide receptor radionuclide therapy with [<sup>90</sup>Y-DOTA<sup>0</sup>,Tyr<sup>3</sup>]octreotide in patients with advanced gastroenteropancreatic neuroendocrine tumors. *Semin Nucl Med* 2006;36:147-56.
58. Kam BL, Teunissen JJ, Krenning EP, de Herder WW, Khan S, van Vliet EI, et al. Lutetium-labelled peptides for therapy of neuroendocrine tumours. *Eur J Nucl Med Mol Imaging* 2012;39 Suppl 1:S103-12.
59. Kwekkeboom DJ, Kam BL, van Essen M, Teunissen JJ, van Eijck CH, Valkema R, et al. Somatostatin-receptor-based imaging and therapy of gastroenteropancreatic neuroendocrine tumors. *Endocr Relat Cancer* 2010;17:R53-73.
60. Vegt E, Wetzels JF, Russel FG, Masereeuw R, Boerman OC, van Eerd JE, et al. Renal uptake of radiolabeled octreotide in human subjects is efficiently inhibited by succinylated gelatin. *J Nucl Med* 2006;47:432-6.
61. Rolleman EJ, Forrer F, Bernard B, Bijster M, Vermeij M, Valkema R, et al. Amifostine protects rat kidneys during peptide receptor radionuclide therapy with [<sup>177</sup>Lu-DOTA<sup>0</sup>,Tyr<sup>3</sup>]octreotate. *Eur J Nucl Med Mol Imaging* 2007;34:763-71.
62. Kratochwil C, Giesel FL, Bruchertseifer F, Mier W, Apostolidis C, Boll R, et al. (2)(1)(3)Bi-DOTATOC receptor-targeted alpha-radionuclide therapy induces remission in neuroendocrine tumours refractory to beta radiation: a first-in-human experience. *Eur J Nucl Med Mol Imaging* 2014;41:2106-19.
63. Wild D, Fani M, Fischer R, Del Pozzo L, Kaul F, Krebs S, et al. Comparison of somatostatin receptor agonist and antagonist for peptide receptor radionuclide therapy: a pilot study. *J Nucl Med* 2014;55:1248-52.
64. R. Dilworth J, J. Parrott S. The biomedical chemistry of technetium and rhenium. *Chemical Society Reviews* 1998;27:43-55.
65. Deutsch E, Heineman WR, Zodda JP, Gilbert TW, Williams CC. Preparation of "no-carrier-added" technetium-99m complexes: Determination of the total technetium content of generator eluents. *The International Journal of Applied Radiation and Isotopes* 1982;33:843-848.
66. Liu S, Edwards DS. <sup>99m</sup>Tc-Labeled Small Peptides as Diagnostic Radiopharmaceuticals. *Chem Rev* 1999;99:2235-68.
67. Reilly RM. *Monoclonal Antibody and Peptide-Targeted Radiotherapy of Cancer*. New York: Wiley; 2010.
68. Isotopes used in SPECT. <<http://oftankonyv.reak.bme.hu/tiki-index.php?page=Isotopes+Used+in+SPECT>>.
69. Steinebach OM, Terpstra BE, Denkova AG, Bode P, H.T. W. Enhancing radioisotope specific activity by Szilard Chalmers reaction. <<http://www.tnw.tudelft.nl/index.php?id=34621&L=1>>.
70. Weiner RE, Thakur ML. *Chemistry of Gallium and Indium Radiopharmaceuticals*, in *Handbook of Radiopharmaceuticals: Radiochemistry and Applications*. Chichester, UK: John Wiley & Sons; 2002.
71. Liu S. Bifunctional coupling agents for radiolabeling of biomolecules and target-specific delivery of metallic radionuclides. *Adv Drug Deliv Rev* 2008;60:1347-70.
72. Smith-Jones PM, Stolz B, Bruns C, Albert R, Reist HW, Fridrich R, et al. Gallium-67/gallium-68-[DFO]-octreotide-a potential radiopharmaceutical for PET imaging of somatostatin receptor-positive tumors: synthesis and radiolabeling in vitro and preliminary in vivo studies. *J Nucl Med* 1994;35:317-25.
73. Eisenwiener KP, Prata MI, Buschmann I, Zhang HW, Santos AC, Wenger S, et al. NODAGATOC, a new chelator-coupled somatostatin analogue labeled with [<sup>67</sup>/68Ga] and [<sup>111</sup>In] for SPECT, PET, and targeted therapeutic applications of somatostatin receptor (hsst2) expressing tumors. *Bioconjug Chem* 2002;13:530-41.
74. Banerjee S, Pillai MR, Knapp FF. Lutetium-177 therapeutic radiopharmaceuticals: linking chemistry, radiochemistry, and practical applications. *Chem Rev* 2015;115:2934-74.

75. Cutler CS, Smith CJ, Ehrhardt GJ, Tyler TT, Jurisson SS, Deutsch E. Current and potential therapeutic uses of lanthanide radioisotopes. *Cancer Biother Radiopharm* 2000;15:531-45.
76. Kunikowska J, Krolicki L, Hubalewska-Dydejczyk A, Mikolajczak R, Sowa-Staszczak A, Pawlak D. Clinical results of radionuclide therapy of neuroendocrine tumours with  $^{90}\text{Y}$ -DOTATATE and tandem  $^{90}\text{Y}/^{177}\text{Lu}$ -DOTATATE: which is a better therapy option? *Eur J Nucl Med Mol Imaging* 2011;38:1788-97.
77. Seidl C. Radioimmunotherapy with alpha-particle-emitting radionuclides. *Immunotherapy* 2014;6:431-58.
78. Zalutsky MR, Pozzi OR. Radioimmunotherapy with alpha-particle emitting radionuclides. *Q J Nucl Med Mol Imaging* 2004;48:289-96.
79. Mulford DA, Scheinberg DA, Jurcic JG. The promise of targeted {alpha}-particle therapy. *J Nucl Med* 2005;46 Suppl 1:199s-204s.
80. Bartholomä MD. Recent developments in the design of bifunctional chelators for metal-based radiopharmaceuticals used in Positron Emission Tomography. *Inorganica Chimica Acta* 2012;389:36-51.
81. Liu S, Edwards DS. Bifunctional Chelators for Therapeutic Lanthanide Radiopharmaceuticals. *Bioconjugate Chemistry* 2001;12:7-34.
82. Bolzati C, Carta D, Salvarese N, Refosco F. Chelating systems for (99m)Tc/(188)Re in the development of radiolabeled peptide pharmaceuticals. *Anticancer Agents Med Chem* 2012;12:428-61.
83. Van de Wiele C, Dumont F, Dierckx RA, Peers SH, Thornback JR, Slegers G, et al. Biodistribution and dosimetry of (99m)Tc-RP527, a gastrin-releasing peptide (GRP) agonist for the visualization of GRP receptor-expressing malignancies. *J Nucl Med* 2001;42:1722-7.
84. Nock B, Maina T. Tetraamine-coupled peptides and resulting (99m)Tc-radioligands: an effective route for receptor-targeted diagnostic imaging of human tumors. *Curr Top Med Chem* 2012;12:2655-67.
85. Kastner ME, Lindsay MJ, Clarke MJ. Synthesis and structure of trans-[O<sub>2</sub>(en)<sup>2</sup>TcV]<sup>+</sup>. *Inorganic Chemistry* 1982;21:2037-2040.
86. Decristoforo C, Maina T, Nock B, Gabriel M, Cordopatis P, Moncayo R.  $^{99\text{m}}\text{Tc}$ -Demotate 1: first data in tumour patients-results of a pilot/phase I study. *Eur J Nucl Med Mol Imaging* 2003;30:1211-9.
87. Gabriel M, Decristoforo C, Maina T, Nock B, vonGuggenberg E, Cordopatis P, et al.  $^{99\text{m}}\text{Tc}$ -N<sub>4</sub>-[Tyr<sup>3</sup>]Octreotate Versus  $^{99\text{m}}\text{Tc}$ -EDDA/HYNIC-[Tyr<sup>3</sup>]Octreotide: an inpatient comparison of two novel Technetium-99m labeled tracers for somatostatin receptor scintigraphy. *Cancer Biother Radiopharm* 2004;19:73-9.
88. Froberg AC, de Jong M, Nock BA, Breeman WA, Erion JL, Maina T, et al. Comparison of three radiolabelled peptide analogues for CCK-2 receptor scintigraphy in medullary thyroid carcinoma. *Eur J Nucl Med Mol Imaging* 2009;36:1265-72.
89. Banerjee SR, Maresca KP, Francesconi L, Valliant J, Babich JW, Zubieta J. New directions in the coordination chemistry of  $^{99\text{m}}\text{Tc}$ : a reflection on technetium core structures and a strategy for new chelate design. *Nucl Med Biol* 2005;32:1-20.
90. Abrams MJ, Davison A, Jones AG, Costello CE, Pang H. Synthesis and characterization of hexakis(alkyl isocyanide) and hexakis(aryl isocyanide) complexes of technetium(I). *Inorganic Chemistry* 1983;22:2798-2800.
91. Alberto R, Schibli R, Egli A, Schubiger AP, Abram U, Kaden TA. A Novel Organometallic Aqua Complex of Technetium for the Labeling of Biomolecules: Synthesis of [ $^{99\text{m}}\text{Tc}(\text{OH})_2(\text{CO})_3$ ]<sup>+</sup> from [ $^{99\text{m}}\text{TcO}_4$ ]<sup>-</sup> in Aqueous Solution and Its Reaction with a Bifunctional Ligand. *Journal of the American Chemical Society* 1998;120:7987-7988.
92. Wadas TJ, Wong EH, Weisman GR, Anderson CJ. Coordinating radiometals of copper, gallium, indium, yttrium, and zirconium for PET and SPECT imaging of disease. *Chem Rev* 2010;110:2858-902.
93. Liu S, Pietryka J, Ellars CE, Edwards DS. Comparison of yttrium and indium complexes of DOTA-BA and DOTA-MBA: models for (90)Y- and (111)In-labeled DOTA-biomolecule conjugates. *Bioconjug Chem* 2002;13:902-13.
94. Heppeler A, Froidevaux S, Mäcke HR, Jermann E, Béhé M, Powell P, et al. Radiometal-Labelled Macrocyclic Chelator-Derivatised Somatostatin Analogue with Superb Tumour-Targeting Properties and Potential for Receptor-Mediated Internal Radiotherapy. *Chemistry – A European Journal* 1999;5:1974-1981.
95. Breeman WA, De Jong M, Visser TJ, Erion JL, Krenning EP. Optimising conditions for radiolabelling of DOTA-peptides with  $^{90}\text{Y}$ ,  $^{111}\text{In}$  and  $^{177}\text{Lu}$  at high specific activities. *Eur J Nucl Med Mol Imaging* 2003;30:917-20.





# CHAPTER

# 2

## Radiolabeled Gastrin/CCK Analogs in Tumor Diagnosis – Towards Higher Stability and Improved Tumor Targeting

Aikaterini Kaloudi<sup>1</sup>, Berthold A. Nock<sup>1</sup>, Eric P. Krenning<sup>2</sup>,  
Theodosia Maina<sup>1</sup>, Marion de Jong<sup>2,3</sup>

<sup>1</sup>Molecular Radiopharmacy, INRASTES, National Center for  
Scientific Research "Demokritos", Athens, Greece

<sup>2</sup>Department of Nuclear Medicine and

<sup>3</sup>Department of Radiology, Erasmus MC,  
Rotterdam, The Netherlands

*Q. J. Nucl. Med. Mol. Imaging* 59 (3):287-302, 2015

## ABSTRACT

Cholecystokinin subtype 2 receptors (CCK2R) are overexpressed in several human cancers, including medullary thyroid carcinoma. Gastrin and cholecystokinin (CCK) peptides that bind with high affinity and specificity to CCK2R can be used as carriers of radioactivity to CCK2R-expressing tumor sites. Several gastrin and CCK related peptides have been proposed for diagnostic imaging and radionuclide therapy of primary and metastatic CCK2R-positive human tumors. Their clinical application has been restricted to a great extent by their fast in vivo degradation that eventually compromises tumor uptake. This problem has been addressed by structural modifications of gastrin and CCK motifs, which, however, often lead to suboptimal pharmacokinetic profiles. A major enzyme implicated in the catabolism of gastrin and CCK based peptides is neutral endopeptidase (NEP), which has very wide distribution in the body. Coinjection of the NEP inhibitor phosphoramidon (PA) with radiolabeled gastrin and other peptide analogs has been recently proposed as a new promising strategy to increase bioavailability and tumor-localization of radiopeptides in tumor sites. Specifically, co-administration of PA with the truncated gastrin analog [<sup>111</sup>In-DOTA]MG11 ([<sup>111</sup>In-DOTA)DGlu<sup>10</sup>]gastrin(10-17)) impressively enhanced the levels of intact radiopeptide in mouse circulation and has led to 8-fold increase of CCK2R-positive tumor uptake in SCID mice. This increase of tumor uptake, visualized also by SPECT/CT imaging, is expected to eventually translate into higher diagnostic sensitivity and improved therapeutic efficacy of radiolabeled gastrin analogs in CCK2R-expressing cancer patients.

*Key words:* radiolabeled gastrin and cholecystokinin, cholecystokinin subtype 2 receptor, tumor targeting, in vivo stability, enzyme inhibition, phosphoramidon

## GENERAL

Many frequently occurring human tumors overexpress receptors that can be targeted by native regulatory peptides, providing the opportunity to use radiolabeled peptide analogs for carrying the preferred radionuclide specifically to the target receptor, located at primary or metastatic tumor sites. A diagnostic radionuclide allows visualization of tumors through the detection of  $\gamma$  photons by positron emission tomography (PET) or single photon emission tomography (SPECT) imaging techniques. On the other hand, a therapeutic radionuclide that emits particle radiation ( $\alpha$ , or  $\beta$  particles, or Auger electrons) allows radiotherapy of cancer [1,2]. The regulatory peptide, which serves as a targeting moiety, is usually coupled at its N-terminus, directly or through a spacer to a suitable chelator, which binds the metallic radionuclide [3]. Radiolabeled somatostatin analogs, like [ $^{111}\text{In}$ -DTPA]octreotide (OctreoScan), have been developed over the last years for diagnostic imaging and radionuclide therapy of tumors overexpressing the somatostatin subtype 2 receptor ( $\text{sst}_2$ ). These analogs have opened new horizons for the development of more peptide radioligands targeting a broader spectrum of cancer types [4]. Gastrin and cholecystokinin (CCK) are regulatory peptides that interact with the cholecystokinin subtype-2 receptor (CCK2R). The CCK2R is overexpressed in many human cancers, such as medullary thyroid carcinoma (MTC), small cell lung cancer and others (*vide infra*) [5]. Accordingly, several radiolabeled gastrin and CCK analogs have been developed for application in the diagnosis and therapy of such cancers.

Radiolabeled peptides should meet some basic criteria to successfully visualize or treat CCK2R-positive human tumors, including low nanomolar receptor affinity, rapid and efficient accumulation in the tumor, low uptake in and rapid clearance from peripheral tissues. To be effective, radiopeptides need to be delivered intact to the target site without being degraded after systemic administration into the organism. Ubiquitous proteolytic enzymes in mammals, however, may assault the radiopeptides, compromising tumor targeting. The main strategy to overcome this handicap inherent to peptide radioligands has involved the chemical modification of lead structures, such as amino acid substitution, cyclization, multimerization, reduction or methylation of biodegradable peptide bonds, to name some of the few. Such structural changes, however, were often at the cost of important pharmacological properties and eventually led to unfavourable pharmacokinetic profile [6]. We have recently proposed a new approach to increase the *in vivo* metabolic stability of radiolabeled peptides, including gastrin and CCK. This method involves the coinjection of the neutral endopeptidase (NEP) inhibitor phosphoramidon (PA). Co-administration of PA led to enhanced *in vivo* radiopeptide stability and amplification of tumor uptake and is expected to strongly improve diagnostic sensitivity and therapeutic efficacy of biodegradable peptide based drugs [7].

## GASTRIN AND CHOLECYSTOKININ

Gastrin was discovered by Edkins in 1905 in extracts of pyloric mucosa of cats, three years after the discovery of the first hormone, secretin, by Bayliss and Starling [8]. At first, Edkins named this hormone gastric secretin, but later he abbreviated it to gastrin. The biological activity of gastrin is the regulation of gastric acid secretion by stomach epithelial cells and the proliferation of the gastric mucosa. It

is produced as preprogastrin by endocrine gastric G cells from the gastric antrum and converted into progastrin after cleavage of the 21 amino acids of the N-terminus [9]. Several posttranslational modifications, including C-terminal amidation, are required to generate the bioactive forms of gastrin, which are gastrin-71, -34, -17 and -14 and all contain a penta-Glu sequence and an identical C-terminus [10-12]. Biological active gastrins also exist in non-sulphated forms. Gastrin-17 (Gastrin I) is the most common (90%) form in human antral G cells, followed by gastrin-34 (5%). However, the distribution of gastrins in peripheral plasma varies because of differences in metabolic stability, favouring the larger gastrin with longer half-life [13].

CCK was found by Ivy in 1928 in extracts of canine duodenal mucosa, as a hormone that regulates gallbladder contraction and evacuation [14]. It is a gut hormone that also controls pancreatic enzyme secretion, hormone secretion and growth and influences intestinal sensitivity and satiety. CCK is produced and secreted by discrete endocrine cells from the small intestinal mucosa as pro-CCK, which is processed by proteolytic cleavages to release bioactive forms of different length (CCK-83, -58, -39, -33, -22, -8) with sulphated or non-sulphated tyrosine at position 7 of the C-terminus [15,16]. CCK peptides are also massively produced in neurons, but neuronal CCK has a minor contribution in plasma CCK, which is responsible for the hormonal effects [17]. CCK-33 and CCK-22 are the predominant forms in the plasma, while CCK-8 is the form most commonly found in vertebrate brains [16].

All of the bioactive forms of CCK contain a five amino acid sequence (Gly-Trp-Met-Asp-Phe-CO-NH<sub>2</sub>) in the C-terminal bioactive region which is identical to that of gastrin (Figure 1 A, B). As a result, CCK and gastrin exert several common biological and pharmacological activities. The biological action of these peptide hormones is elicited after binding to G protein-coupled receptors (GPCRs), named CCK receptors (CCKR), which are situated in the outer membrane of target cells in the central nervous system and in peripheral organs [18].

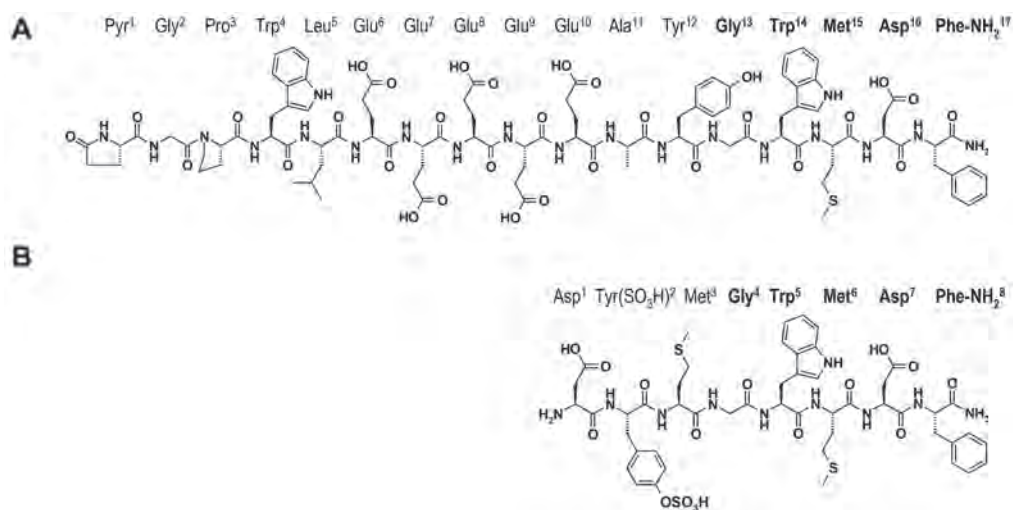


Figure 1 | Chemical structure of A) human Gastrin I and B) sulphated CCK-8.

## CHOLECYSTOKININ RECEPTORS

Two different types of CCK receptors have been identified, the CCK subtype 1 receptor (CCK1R) and the CCK subtype 2 receptor (CCK2R). Formerly, these receptors were known as CCK-A and CCK-B, however based on recommendations of the International Union of the Pharmacology (IUPHAR) committee with regards to receptor nomenclature and drug classification, they were renamed to CCK1R and CCK2R in 1996 [19]. Recently, a third receptor (CCK2i4sv) was discovered in human colorectal cancer cells, which is a splice variant of CCK2R and stimulates cell growth through a gastrin-independent mechanism [20]. All CCK receptors belong to the superfamily of GPCRs, which means that they consist of seven transmembrane domains and activate a second messenger pathway after internalization upon binding of a receptor agonist. CCK1R and CCK2R differ in their relative affinity for the natural ligands, their differential distribution and their molecular structure.

The native ligand with the highest affinity for CCK1R is the sulphated CCK octapeptide CCK-8, while N-terminally extended CCK forms, such as CCK-33, CCK-39 and CCK-58, bind with similar to CCK-8 affinities to CCK1R [21,22]. Sulphation of CCK at position 7 from the C-terminus is critical for binding to CCK1R, as its removal causes a more than 500 fold drop of affinity. Non-sulphated Gastrin I discriminates between the two CCK receptors: it has negligible affinity for CCK1R, but binds CCK2R with similar affinity to the non-selective CCK variants. Therefore, the CCK2R is often called the gastrin receptor [18].

Many studies have been performed to identify the binding mode of gastrin and CCK to their cognate receptors, revealing that a sequence of five amino acids in the second extracellular loop of CCK2R is crucial for high affinity binding of gastrin I and CCK-8 [23]. Within this moiety His<sup>207</sup> has been shown to interact with the aspartic acid of CCK-8 and is essential for recognition [24]. Selectivity of CCK1R for sulphated over non-sulphated CCK involves the Met<sup>195</sup> and Arg<sup>197</sup> residues in the second extracellular loop [25,26]. Several amino acids and vital regions in transmembrane helices IV and VI have been shown to interact with the amidated C-terminal Phe of CCK as well. Binding sites of CCK on CCK1R and CCK2R implicate residues located in homologous regions, however, with slightly distinct positioning within the two receptors [27].

CCK receptors, as most peptide receptors, can rapidly internalize upon binding of a receptor agonist. Many different transduction pathways are activated by these receptors, such as phospholipases/calcium mobilization, protein kinase C activation, adenylyl cyclase and cAMP production [18]. The receptors are naturally expressed in several normal organs and tissues and display a wide variety across the different species. In humans, CCK1R is typically present in the gallbladder, gastric smooth muscles, endocrine pancreas and the peripheral nervous system, while CCK2R is predominantly expressed in the stomach, gut mucosa and the brain (Table 1) [28].

## CCK2R EXPRESSION IN HUMAN TUMORS

The expression of CCK2R has been documented in many human tumor types. In a study performed by Reubi et al., the most frequently CCK2R expressing neoplasms were found to be medullary thyroid

carcinomas – MTC (92%), small cell lung cancers (57%), astrocytomas (65%) and stromal ovarian cancers (100%). Less frequent CCK2R expression was found in several other tumor types, such as gastroenteropancreatic tumors, meningiomas, endometrial and ovarian adenocarcinomas and breast carcinomas. CCK receptors were rarely expressed or not expressed at all in neuroblastomas, schwannomas, glioblastomas, lymphomas, renal cell cancers, prostate carcinomas, hepatocellular carcinomas and neuroendocrine tumors, such as pituitary adenomas, pheochromocytomas, paragangliomas and parathyroid adenomas [29]. Recently, Upp et al. [30] have demonstrated CCK2R expression in colon and gastric cancers, while Reubi et al. [31] have documented high incidence of CCK2Rs (63%) in gastrointestinal stromal tumors in most cases in extremely high density. Earlier studies have shown that small cell lung cancers often express CCK2Rs, whereas non-small cell lung cancers do not [32,33]. The data acquired for exocrine pancreatic carcinomas are more contradictory. CCK1 and CCK2 receptor mRNA was found in most exocrine pancreatic carcinomas, although the receptor protein could not be detected in the tumor cells [34,35].

**Table 1** | CCK1R and CCK2R (over)-expression in human tumors and physiological expression in normal tissues [30-34].

Receptor	Tumor type	Normal tissues
CCK1R	– Gastroenteropancreatic tumors	– Gallbladder
	– Meningiomas	– Endocrine pancreas
	– Leiomyosarcomas	– Gastric smooth muscles
	– Ileal carcinoids	– Peripheral nervous system
	– Bronchial carcinoids	
CCK2R	– Medullary thyroid cancer	– Stomach
	– Small cell lung cancer	– Gut mucosa
	– Stromal ovarian cancer	– Brain
	– Astrocytomas	
	– Gastrointestinal stromal tumors	

Because of the extremely high incidence and density of CCK2R in MTC (Figure 2 A-F) and, as there is currently no good therapy for disseminated MTC, this type of tumor was selected for the development of gastrin and CCK based radioligands. MTC derives from malignant dedifferentiation of the thyroid parafollicular or C cells [36]. These cells produce calcitonin, carcinoembryonic antigen (CEA) and occasionally CA19-9 that can serve as tumor markers. MTC comprises 3 to 12% of all thyroid cancers and among them 60–80% are sporadic cases, whereas 20–40% are associated with distinct familial syndromes. In most patients the disease has already metastasised at the time of diagnosis. Imaging of metastatic MTC with somatostatin receptor scintigraphy is of limited value because of the low expression of somatostatin receptors in dedifferentiated and clinically more aggressive forms of MTC [37]. Similar observations have been reported for the loss of somatostatin receptors in

metastatic small cell lung cancer as well [38]. MTC is unresponsive to radioiodine treatment. Surgery is the primary treatment for MTC and there is a restricted role for external beam radiation and chemotherapy, thus patients with disseminated disease are left with very few therapeutic options [39]. Taking into account all the above, CCK2R is regarded as an attractive target for diagnosis and therapy of MTC patients using CCK2R-selective radiolabeled gastrin and CCK analogs.

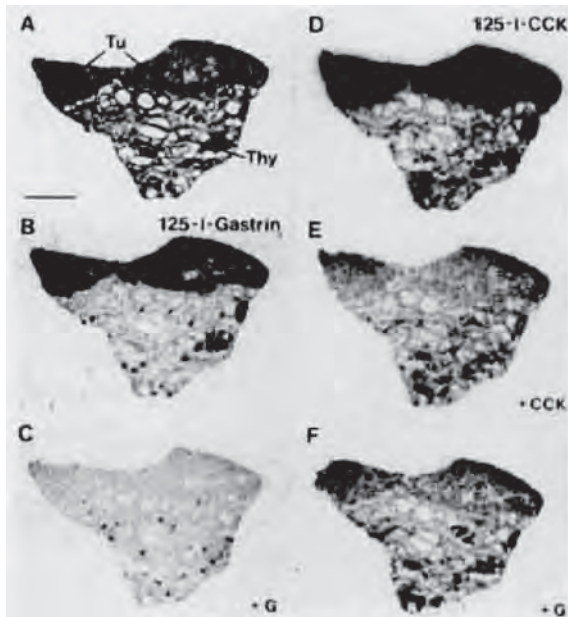


Figure 2 | In vitro identification of CCK2R in a human MTC by autoradiography. A) Hematoxylin-eosin-stained section showing tumor tissue (Tu) and adjacent, normal glandular thyroid tissue (Thy). B) Autoradiogram showing total binding of  $^{125}\text{I}$ -Leu<sup>15</sup>-gastrin I ( $^{125}\text{I}$ -gastrin). The tumor tissue is labeled (black areas), whereas normal thyroid is not. C) Autoradiogram showing non-specific binding of  $^{125}\text{I}$ -gastrin (in presence of 100 nM unlabeled gastrin). D) Autoradiogram showing total binding of  $^{125}\text{I}$ -DTyr-Gly-Asp-Tyr(SO<sub>3</sub>H)-Nle-Gly-Trp-Nle-Asp-Phe-NH<sub>2</sub> ( $^{125}\text{I}$ -CCK). Tumor tissue is massively labeled. E) Autoradiogram showing non-specific binding  $^{125}\text{I}$ -CCK in the presence of 50 nM CCK-8 and F) 50 nM gastrin [5].

## GASTRIN/CCK RADIOPEPTIDES FOR TARGETING CCK2R-POSITIVE TUMORS

Already in the late 90s, Behr et al. conducted preclinical and pilot clinical evaluation studies using the radioiodinated human heptadecapeptide Gastrin I (gastrin= pGlu-Gly-Pro-Trp-Leu-(Glu)<sub>5</sub>-Ala-Tyr-Gly-Trp-Met-Asp-Phe-NH<sub>2</sub>) in mouse models and in an MTC patient. They were able to show promising results for its diagnostic and therapeutic value [40]. This specific peptide was selected mainly due to its high selectivity and affinity for CCK2R, also due to the pyroglutamate moiety on its N-terminus that protects the peptide from aminopeptidases and the non-sulphated Tyr<sup>12</sup> residue allowing for radioiodination. Both preclinical and clinical data showed good receptor targeting in the tumor, as well as in the physiologically CCK2R-expressing stomach and gallbladder, while the main excretory pathway involved the kidneys and the urinary system. Furthermore, pilot therapy studies with [ $^{131}\text{I}$ -Tyr<sup>12</sup>]Gastrin in CCK2R-positive mouse models revealed significant anti-tumor efficacy.

In a following study, the same group developed a variety of CCK- and gastrin-based peptides, which were radioiodinated and tested in vitro as well as in animal models [41]. Significant requirements for high affinity to CCK2R and good uptake in CCK2R-expressing tumors were established, including:



a) the presence of the C-terminal tetrapeptide Trp-Met-Asp-PheNH<sub>2</sub> (where Met can be replaced by Leu or Nle), b) either a sulphated Tyr<sup>12</sup> residue in the case of CCK analogs or c) the highly anionic penta-Glu<sup>6-10</sup> sequence in the case of gastrin analogs. Sulphated CCK derivatives displayed high uptake not only in the CCK2R-positive stomach, but also in the CCK1R-expressing organs, indicating that gastrin analogs may be more favorable for clinical applications, due to their CCK2R selectivity. Therefore, minigastrin (MG, gastrin(5-17)) and its DLeu<sup>1</sup>-counterpart were coupled with the DTPA chelator allowing for labeling with <sup>111</sup>In, which has better physical imaging characteristics than <sup>131</sup>I and is easier to label. The results from this study showed excellent targeting of CCK2R-expressing tissues and tumor sites in animals and a normal human volunteer, as well as in three MTC patients. However, the kidneys were unfavourably strongly visualized as well.

In subsequent studies, Leu<sup>1</sup> was replaced by DGlu in DTPA-MG ([DTPA]MG0) to enhance the stability of radiometal chelation for other potentially therapeutic or diagnostic radionuclides. Whole body scans and SPECT imaging performed in patients with known or occult metastatic MTC revealed tumor lesions in 43 out of 45 patients. Normal organ uptake was limited to stomach and kidneys. Furthermore, an initial therapeutic study with <sup>90</sup>Y-DTPA-DGlu<sup>1</sup>-MG ([<sup>90</sup>Y-DTPA]MG0) in eight patients with advanced metastatic MTC showed promising therapeutic effects, but at the same time induced severe nephrotoxicity. Therefore, studies continued with the Auger electron emitter <sup>111</sup>In instead of the β<sup>-</sup>-emitter <sup>90</sup>Y, resulted in much less nephrotoxicity in preclinical settings [39,42].

At the same time Reubi et al. developed a series of CCK2R-selective non-sulphated CCK-8 analogs coupled at their N-terminus to DTPA or DOTA, with the latter chelator offering higher kinetic inertness and metal chelate stability in vivo [43]. High affinity (in the low nanomolar range) and specificity for CCK2R was reported and also preclinical biodistribution data from healthy rats showed rapid clearance by renal excretion and low uptake in the peripheral tissues, including the kidneys. Furthermore increased stability was documented during in vitro incubation in plasma. It was concluded that non-sulphated CCK analogs are promising as well for human CCK2R scintigraphy [44]. Based on these results, de Jong et al. evaluated in vitro and in vivo the potential of a CCK-8 analog [DAsp<sup>1</sup>,Nle<sup>3,6</sup>]CCK-8 for radionuclide imaging and therapy. The internalization of the [<sup>111</sup>In-DOTA]CCK-8 analog in the rat pancreatic tumor AR42J cells was receptor-specific and time- and temperature-dependent. Biodistribution experiments in a rat tumor model showed modest targeting of the rat pancreatic CA20948 tumor and the CCK2R-expressing stomach. At the same time, much higher tumor-to-blood ratios were observed as compared to a non-sulphated <sup>125</sup>I-labeled CCK-10 peptide. A scan of a human MTC patient with [<sup>111</sup>In-DTPA]CCK-8 visualized the receptor-positive stomach and the tumor metastases even 48 h pi [45]. Clinical diagnostic evaluation of [<sup>111</sup>In-DTPA][Nle<sup>3,6</sup>]CCK-8 was also reported by Kwেকেboom et al. [46]. The scintigraphic images showed high background activity and confirmed MTC lesions in two MTC patients but small lesions could not be detected. In addition, they reported rapid degradation of the radiopeptide in serum.

A few years later Laverman et al. [47] compared a sulphated with a non-sulphated <sup>99m</sup>Tc-labeled CCK-8 analog and showed that the CCK1R and CCK2R expressing tumor uptake of the sulphated [<sup>99m</sup>Tc-HYNIC]CCK-8 was around 15-fold higher than the non-sulphated analog. But also a 90-fold higher uptake in the CCK1R-positive pancreas was documented. In a further study the same group replaced the sulphated tyrosine with a hydrolysis-resistant synthetic isostere, phenylalanine



sulphonate. The affinity of [ $^{111}\text{In}$ -(DOTA)Phe<sup>2</sup>(*p*-CH<sub>2</sub>SO<sub>3</sub>H),Nle<sup>3,6</sup>]CCK-8 was in the low nanomolar range and biodistribution studies in AR42J tumor bearing mice showed comparable tumor uptake with the sulphated [ $^{111}\text{In}$ -DOTA]CCK-8 [48].

Nock et al. [49] developed three DGlu<sup>1</sup>-Gastrin(5-17) (DGlu<sup>1</sup>-MG) analogs coupled at their N-terminus to an open chain tetraamine (N<sub>4</sub>) either directly or via a spacer. This modification allowed efficient labeling with <sup>99m</sup>Tc, which is the label of choice for diagnostic SPECT imaging [50]. During biodistribution studies in AR42J tumor bearing mice, tumor to non-target tissue ratios were especially high for [ $^{99m}\text{Tc}$ ]Demogastrin 2 (with a Gly spacer), but also kidney uptake was unfavourably high. It is interesting to note that significant reduction of renal accumulation was achieved by coinjection of excess DGlu<sup>1</sup>-MG or poly-Glu containing peptides in agreement with previous studies [51]. The first images of [ $^{99m}\text{Tc}$ ]Demogastrin 2 from a metastatic MTC patient revealed all known lesions at 90 min pi and provided high quality images at 4 h pi. Surprisingly, renal uptake was low in these scans in contrast to findings in the animals.

The high renal values of [ $^{99m}\text{Tc}$ ]Demogastrin 2 was in agreement with a study by Good et al. [52], revealing that the deletion of the penta-Glu<sup>6-10</sup> sequence in radiolabeled gastrin results in significant reduction of kidney uptake. They postulated the negative charges of penta-Glu<sup>6-10</sup> may be responsible for tubular reabsorption of the radiolabeled peptides. Subsequently, higher tumor to kidney ratios were observed for the *des*-(Glu)<sub>5</sub> radiopeptide [ $^{111}\text{In}$ -DOTA]MG11 ((DOTA)DGlu<sup>10</sup>)Gastrin(10-17)) as compared to penta-Glu containing [ $^{111}\text{In}$ -DTPA]MG0, although absolute tumor uptake was much lower in the case of [ $^{111}\text{In}$ -DOTA]MG11. Interestingly, during in vitro incubation of [ $^{111}\text{In}$ -DOTA]MG11 and [ $^{111}\text{In}$ -DTPA]MG0 in human serum the *des*-(Glu)<sub>5</sub> radiotracer turned out to be much more vulnerable to proteolytic degradation. Gotthardt et al. determined the clinical performance of [ $^{111}\text{In}$ -DTPA]MG0 reporting a tumor detection rate of 87% by means of gastrin receptor scintigraphy in a group of 26 MTC patients. However, additional tumor lesions in patients with occult disease were found in only one patient [53].

Fröberg et al. compared [ $^{99m}\text{Tc}$ ]Demogastrin 2 with [ $^{111}\text{In}$ -DOTA]nsCCK-8 and the truncated *des*-Glu<sup>6-10</sup> [ $^{111}\text{In}$ -DOTA]MG11 to evaluate their diagnostic potential in six patients with MTC. [ $^{99m}\text{Tc}$ ]Demogastrin 2 visualized all known lesions and also discovered new ones, whereas the other two radiopeptides failed to visualize several known lesions. Once more, the renal uptake of [ $^{99m}\text{Tc}$ ]Demogastrin 2 was low, confirming the findings from the previous study by Nock et al. and was comparable with the other two radiopeptides. Thus, [ $^{99m}\text{Tc}$ ]Demogastrin 2 scintigraphy appeared to be the most promising diagnostic tool for MTC patients [54]. The difference in performance of the three radiotracers can be explained by a combination of several parameters. First of all, <sup>99m</sup>Tc has better imaging properties than <sup>111</sup>In and, in addition, [ $^{99m}\text{Tc}$ ]Demogastrin 2 could be prepared and administered to patients in higher specific activity. Another important factor is the distinct in vivo stability of the radiopeptides compared. HPLC analysis of human blood samples taken 10 min after administration showed that less than 10% of [ $^{111}\text{In}$ -DOTA]MG11 remained intact, while [ $^{99m}\text{Tc}$ ]Demogastrin 2 more than 60% remained intact within the same time period [55]. These in vivo findings were in agreement with conclusions from a previous study by Good et al., correlating the increased number of Glu residues with higher metabolic stability. However, the half-life of 2.4 h determined during in vitro incubation of [ $^{111}\text{In}$ -DOTA]MG11 in serum was considerably longer

compared to that determined in vivo, highlighting the significance of in vivo assays to obtain reliable and representative stability data.

During a more recent study within the frameworks of COST Action (BM0607), the biodistribution of 12  $^{111}\text{In}$ -labeled CCK and gastrin analogs were compared in mice bearing CCK2R-positive tumors. Furthermore, the in vitro and in vivo metabolic stability of the same 12 peptides labeled with  $^{177}\text{Lu}$  were compared in a related study. [ $^{111}\text{In}$ -DOTA]MG0 showed the highest kidney and tumor uptake, while the truncated [ $^{111}\text{In}$ -DOTA]MG11 showed the lowest renal values at the cost, however, of tumor localization. These results correlated with the metabolic stability findings, whereby [ $^{177}\text{Lu}$ -DOTA]MG11 was found to be the least stable radiopeptide, highlighting the importance of metabolic stability for achieving high tumor uptake (*vide infra*). Interestingly, replacement of the natural penta-LGlu residues of [ $^{111}\text{In}$ -DOTA]MG0 by its enantiomeric (DGlu)<sub>5</sub> sequence in [ $^{111}\text{In}$ ]PP-F11 ([ $^{111}\text{In}$ -DOTA, DGlu<sup>5-10</sup>]Gastrin(5-17)) resulted in significantly reduced renal uptake and retention. On the other hand, metabolic stability was much improved and, consequently, tumor uptake was also improved compared with [ $^{111}\text{In}$ -DOTA]MG11 [56,57].

In a study by Brom et al. DOTA-MG0 was labelled with either  $^{111}\text{In}$  or  $^{68}\text{Ga}$  and was preclinically tested in AR42J tumor-bearing mice. Biodistribution experiments showed similarly high tumor uptake for both  $^{111}\text{In}$  and  $^{68}\text{Ga}$  labelled peptide, whereas the kidney accumulation of [ $^{68}\text{Ga}$ -DOTA]MG0 was two times higher than that of [ $^{111}\text{In}$ -DOTA]MG0. Subcutaneous and peritoneal tumors in mice were clearly visualized by PET imaging after intravenous injection of [ $^{68}\text{Ga}$ -DOTA]MG0, despite the close proximity to the kidneys, suggesting that it is a promising tracer for PET imaging of CCK2R-positive human tumors [58].

In a further study of the same group, three different analogs of PP-F11 were developed whereby DOTA was replaced by different chelators (DOTA, NOTA and NODAGA). Each analog was labelled either with  $^{68}\text{Ga}$ ,  $^{64}\text{Cu}$  or  $^{111}\text{In}$  and compared in animal models to evaluate which chelator/radionuclide combination leads to the most favourable characteristics for imaging. All radiotracers were able to visualize the CCK2R-positive tumors in mice by PET or SPECT. However, higher tumor-to-background ratios were achieved by the  $^{68}\text{Ga}$ - and  $^{111}\text{In}$ -labeled analogs during biodistribution studies. The chelator did not seem to influence in vivo behaviour, except in the case of the  $^{64}\text{Cu}$ -labeled analogs which displayed high liver uptake, probably due to in vivo instability of the  $^{64}\text{Cu}$ -chelate. Overall, [ $^{68}\text{Ga}$ -DOTA]PP-F11 showed the best imaging properties and warrants further development into a radiopharmaceutical for PET imaging of CCK2R-expressing human tumors (Tables 2, 3) [59].

Taking into consideration all of the above, the silver lining for the application of radiolabeled gastrin or CCK peptides in the clinic is the high and selective targeting of the radiopeptide in the CCK2R-expressing tumor in combination with low renal accumulation (Table 4). CCK2R-selective tumor targeting is best achieved by gastrin and non-sulphated CCK rather than sulphated CCK radiopeptides, however, radiolabeled non-sulphated CCK analogs show lower CCK2R tumor targeting as compared to their gastrin-based counterparts. Low kidney and poor tumor uptake is obtained by radiogastrins lacking the penta-Glu sequence, while in contrast, radiolabeled metabolically stable gastrins containing the penta-Glu sequence demonstrate high tumor uptake, but are plagued by high kidney retention.

**Table 2 |** Tumor and kidney uptake as %ID/g (mean±SD) of radiolabeled gastrin analogs during biodistribution studies in animal models bearing CCK2R-positive tumors.

Gastrin Radiopeptide	Tumor uptake		Kidney uptake		Animal tumor model
	1 h	4 h	1 h	4 h	
[ <sup>131</sup> I-Tyr <sup>12</sup> ]Gastrin [40]	8.85±2.88		~20		TT-bearing nude mice
[ <sup>111</sup> In-DTPA]MG [41]	5.0±1.2		~45		TT-bearing nude mice
[ <sup>99m</sup> Tc]Demogastrin 2 [49]	5.5±0.85	2.88±0.42	83.92±14.45	42.65±4.8	AR42J-bearing nude mice
[ <sup>111</sup> In-DOTA]MG11 [52]		0.31±0.04		0.36±0.07	AR42J-bearing Lewis rats
[ <sup>111</sup> In-DTPA]MG0 [52]		0.64±0.11		8.66±0.44	AR42J-bearing Lewis rats
[ <sup>111</sup> In-DOTA]MG11 [56]	3.04±1.3	~2.5	0.91±0.14	~0.9	A431-CCK2R-bearing nude mice
[ <sup>111</sup> In-DOTA]MG0 [56]	13.3±4.9	~10	~60	~60	A431-CCK2R-bearing nude mice
[ <sup>111</sup> In-DOTA]PPF11 [56]	9.66±1.78	6.3±2.75	~4.5	~5	A431-CCK2R-bearing nude mice
[ <sup>111</sup> In-DOTA]PPF11 [59]		1.89±0.74		~8	A431-CCK2R-bearing SCID mice
[ <sup>68</sup> Ga-DOTA]PPF11 [59]	5.21±2.19		~5		A431-CCK2R-bearing SCID mice
[ <sup>68</sup> Ga-DOTA]MG0 [58]	4.4±1.3		~90		AR42J-bearing nude mice
[ <sup>111</sup> In-DOTA]MG0 [58]	~5		~55		AR42J-bearing nude mice

**Table 3 |** Tumor and pancreas uptake as %ID/g (mean±SD) of radiolabeled CCK analogs during biodistribution studies in animal models bearing CCK1R and CCK2R-expressing tumors.

CCK Radiopeptide	Tumor uptake			Pancreas uptake		Tumor model
	1 h		2 h	1 h	2 h	
	CCK2R	CCK1R	CCK2R			
[( <sup>111</sup> In-DOTA)DAsp <sup>1</sup> ,Nle <sup>3,6</sup> ]CCK-8 [45]	0.16±0.02			0.04±0.01		CA20948-bearing Lewis rats
Sulphated [ <sup>99m</sup> Tc-HYNIC]CCK-8 [47]	4.15±0.28	2.04±0.65		11.7±0.93		CHO-CCKR-bearing nude mice
Non-sulphated [ <sup>99m</sup> Tc-HYNIC] CCK-8 [47]	0.59±0.06	0.20±0.08		0.13±0.02		CHO-CCKR-bearing nude mice
[ <sup>111</sup> In(DOTA)Phe <sup>2</sup> (p-CH <sub>2</sub> SO <sub>3</sub> H), Nle <sup>3,6</sup> ]CCK-8 [48]			4.54±1.15		~2	AR42J-bearing nude mice
[ <sup>111</sup> In-DOTA]CCK-8 [48]			4.78±0.64		~3	AR42J-bearing nude mice

**Table 4 |** Characteristics of radiolabeled gastrin and CCK-8 analogs considered attractive for clinical translation.

Peptide	CCK2R selectivity	High CCK2R tumor targeting	Low kidney uptake
Gastrin	√	√	×
des-(Glu) <sub>5</sub> Gastrin	√	×	√
Sulphated CCK-8	×	√	√
Non-sulphated CCK-8	√	×	√

## ENZYMES INVOLVED IN THE DEGRADATION OF GASTRIN AND CCK ANALOGS

CCK2R-targeted tumor diagnosis and therapy can only be successful if CCK2R-directed radioligands attain high *in vivo* stability in combination with low renal accumulation. Radiopeptide stability is challenged by proteases, also called peptidases or proteinases. These are enzymes that catalyse the hydrolysis of peptide bonds and are ubiquitously distributed throughout the body of mammals. The human and mouse proteolytic degradome consists of more than 560 and 640 proteases, respectively. Depending on the position of the cleavage site proteases can be roughly divided into exopeptidases (EC 3.4.11-19) and endopeptidases (EC 3.4.21-24) [60]. Exopeptidases specifically cleave either at the C-terminus (carboxy-peptidases) or at the N-terminus (amino-peptidases) of their substrates, while endopeptidases cleave peptide bonds within the molecule. Proteases can be further subdivided on the basis of their catalytic mechanism into aspartic, metallo, serine, threonine and cysteine-proteases [61]. Aspartic and metallo proteases activate a water molecule for peptide bond cleavage. The remaining classes use either the activated side-chain hydroxyl-group of a serine or a threonine residue or the thiolate group of a cysteine located in the active site of the enzyme.

Previous studies have shown that the major enzymes implicated in the catabolism of different length native CCK and gastrin analogs, are aminopeptidase A (APA, glutamyl aminopeptidase, EC 3.4.11.7), neutral endopeptidase (NEP, neprilysin, EC 3.4.24.11) and angiotensin converting enzyme (ACE, EC 3.4.15.1).

APA is a widely distributed membrane-bound type II zinc metalloprotease, which cleaves N-terminal glutamyl and aspartyl residues from peptide substrates. APA plays a role in blood pressure regulation by intrarenal metabolism of the potent vasoconstrictor angiotensin II, but CCK-8 is one of its most preferred substrates [62]. Roques et al. described APA as the key enzyme responsible for the fast *in vivo* inactivation of CCK-8 [63]. However, APA-mediated degradation of CCK-8 could be easily prevented by a N-terminal propionyl group. Consequently, it is reasonable to assume that CCK-8 based radiopeptides with a bulky radiometal chelate covalently attached to Asp<sup>1</sup> will be APA-resistant.

NEP is a Zn-metallopeptidase that cleaves oligopeptides up to 40–50 amino acids in length on the amino side of hydrophobic amino acid residues. The chemotactic peptide formyl-Met-Leu-Phe is the smallest known NEP-substrate, with cleavage occurring at the Met-Leu bond [64]. Neprilysin activity was first detected in renal brush border membranes from rats and subsequently purified to homogeneity from rabbit kidney in 1974 [65,66]. NEP was later rediscovered as a brain membrane bound enzyme inactivating enkephalins, which led to its designation as enkephalinase. Later the elucidation of the complete amino acid sequence of NEP confirmed that the enzyme present in kidney and brain is the same with a leukocyte cell surface antigen, the common acute lymphoblastic antigen (CALLA or CD10) [67]. Finally, neprilysin is also identical with skin fibroblast elastase which plays a role in skin aging [68]. The active site of NEP consists of a large C-terminal domain containing one Glu and two His residues, which are critically involved in the catalytic process [69,70]. Although NEP was originally discovered in the kidneys, it is an ectoenzyme with a wide distribution in the body. In blood it is anchored on the plasma membrane of granulocytes and resides in the endothelial cell surface of the vasculature compartment. It is highly abundant in major organs such as the liver, kidneys and gastrointestinal tract [71-73].

Already in 1985 Pauwels et al. demonstrated that synthetic Gastrin I is converted to both C- and N-terminal fragments after intravenous administration to human volunteers [74]. However, it was in 1987 when Power et al. first demonstrated in pigs that NEP was the enzyme responsible for the metabolism of Gastrin I in vivo [75]. Soon thereafter, Deschodt-Lanckman et al. confirmed that NEP is also involved in the catabolism of Gastrin I in humans [76]. Four cleavage sites of Gastrin I have been identified, i) Gly<sup>13</sup>-Trp<sup>14</sup> occurring rapidly, ii) Asp<sup>16</sup>-Phe<sup>17</sup>, iii) Trp<sup>4</sup>-Leu<sup>5</sup> and iv) Ala<sup>11</sup>-Tyr<sup>12</sup> (Figure 3A). As a result, the N-terminal fragments 1-13, 1-16, 1- 4 and 1-11 and the complementary C-terminal fragments of Gastrin I are formed [76].

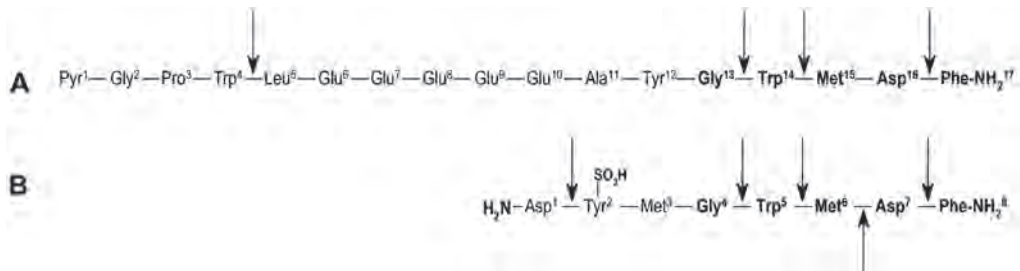


**Figure 3 | A** Major cleavage sites by NEP (descending arrows) in human Gastrin I and **B** additional cleavage sites in sulphated CCK-8 by ACE (ascending arrow) and APA (1<sup>st</sup> descending arrow from left, between H<sub>2</sub>N-Asp<sup>1</sup> and Tyr<sup>2</sup>(SO<sub>3</sub>H)).

In addition, NEP present in different tissue membranes originating from rats, pigs and human metabolizes both sulphated as well as non-sulphated CCK-8 [77-80]. Sulphated CCK-8, which is a better substrate for NEP than its non-sulphated counterpart, is preferentially cleaved between the Asp<sup>6</sup>-Phe<sup>7</sup> bond and has a second minor cleavage site at the Gly<sup>3</sup>-Trp<sup>4</sup> bond. For the non-sulphated CCK-8 analog an additional third cleavage site was detected between Trp<sup>4</sup> and Met<sup>5</sup> [77,79,81].

ACE is classified as peptidyl dipeptidase of the Zn-metallopeptidase superfamily due to its ability to cleave carboxy-terminal dipeptides from active peptides containing a free carboxy-terminus. However, it has also been shown that ACE inactivates C-terminally amidated peptides, thus expressing an endopeptidase activity [82]. It is an enzyme that participates in the body's renin angiotensin system (RAS) by catalyzing the conversion of angiotensin I to angiotensin II, thus controlling the extracellular volume and arterial vasoconstriction [83]. However, ACE has a much wider substrate specificity including many vasoactive peptides, like the vasodilator bradykinin [84]. It was first identified in and isolated from horse plasma by Skeggs et al. in 1956 [85] and consists of two homologous domains. Each domain contains an active site with a conserved HEXXH zinc-binding motif, where the two His and a Glu residue are crucial for enzymatic activity [86]. ACE is widely distributed in the body including the lungs, gastrointestinal tract, vascular endothelium and blood [83].

In the late 80s Dubreuil et al. reported that CCK-8 and gastrin analogs are potential substrates of ACE [87]. Their study was performed in vitro using the purified rabbit lung enzyme. The initial and major site of hydrolysis occurs between the penultimate Met-Asp peptide bond (or Leu-Asp when Met is replaced by Leu) generating the C-terminal amidated dipeptide Asp-Phe-NH<sub>2</sub> (Figure 3B). Secondary cleavage sites were found after the release of the amidated dipeptide and were identified between Gly-Trp and Met-Gly, in the case of CCK-8, or Gly-Trp and Tyr-Gly, in the case of *des*Glu<sub>5</sub> [Leu<sup>15</sup>]gastrin(11-17) analog. Most surprisingly, the deca triapeptide [Leu<sup>15</sup>]minigastrin (5-17) was no substrate for ACE. However, successive shortening of the penta-Glu chain revealed that only gastrin analogs containing two or more Glu residues survived incubation with ACE. Finally, the authors concluded that their study conducted in vitro does not allow any prediction over the role that ACE might play in the catabolism of CCK and gastrin analogs in vivo.

## TOWARD HIGHER IN VIVO STABILITY OF GASTRIN/CCK-RADIOLIGANDS

To improve proteolytic stability of gastrin and CCK peptides, researches have followed a variety of structural modification strategies, such as: shortening of peptide length to the minimum active sequence, introduction of pseudopeptide bonds, changing the stereochemistry (e.g. by replacing the natural L-amino acid by the corresponding D-enantiomer), incorporation of unnatural amino acids (for example of  $\beta$ -amino acids), amino acid deletion(s), capping of N- and/or C-terminii by acylation or amidation, head-to-tail or side-chain cyclization, N-methylation of peptide bonds, pegylation, lipidation, or homo and hetero multimerization and other means [88-91]. However, this approach is highly laborious, resource-intensive and time-demanding. On the other hand, the improvements made on metabolic stability are very often compromised by overall suboptimal pharmacological features, such as partial or total loss of receptor affinity and subtype selectivity, impaired internalization rates, increased toxicity, and unfavourable pharmacokinetics, whereby lower in vivo tumor-targeting is combined with excessive hepatobiliary clearance and/or unfavourably high retention in the kidneys.

The evaluation of radiopeptide stability has been assessed almost entirely by in vitro assays performed in blood, plasma or serum of mice, rat, or human origin. Accordingly, the link between in vitro and in vivo stability of radiopeptides is missing and the action of ectoenzymes anchored in vessel walls and in major organs is completely disregarded. On the other hand, assays that make use of tissue homogenates can be also misleading in predicting radiopeptide in vivo stability. Through tissue homogenization cell walls are disrupted and cell compartmentalization is lost. In this way, all previously intracellularly localized proteases are released into the homogenate and can come in contact and assault the radiopeptide. Consequently, the actual in vivo radiopeptide stability might be erroneously underestimated. It should be considered, that upon intravenous administration, radiopeptides distribute very fast over the hydrophilic body compartments not coming in contact at all with intracellularly localized proteases before reaching and interacting with their cell-surface bound target molecules [92,93].

The significance of *in vivo* studies to estimate actual radiopeptide stability was highlighted in a recent concerted European COST Action on Targeted Radionuclide Therapy (BM0607). In this study, the metabolic stability of twelve  $^{177}\text{Lu}$ -labeled gastrin and CCK analogs was compared by *in vitro* and *in vivo* assays [57]. The two gastrin based radiopeptides  $^{177}\text{Lu}$ PP-F10 ( $^{177}\text{Lu}$ -DOTA)DGLn $^{5-10}$  Gastrin(5-17)) and  $^{177}\text{Lu}$ -DOTA]MG11 presented the highest and lowest half-lives in human serum of 198 h and 4.5 h, respectively. It would be reasonable to assume that even the 4.5 h half-life in serum would suffice for successful *in vivo* targeting – a process known to occur within few minutes in the case of fast localizing peptidic radiotracers. On the other hand, when incubated with liver homogenates both radiopeptides showed dramatically lower half-life ( $\approx 10$  min). During incubation with kidney homogenates half-lives were even shorter, less than 5 min for  $^{177}\text{Lu}$ PP-F10 and less than 1 min for  $^{177}\text{Lu}$ -DOTA]MG11.

In contrast, during assessment of *in vivo* stability of these radiopeptides in healthy mice using HPLC-analysis of peripheral blood withdrawn 10 min after *iv* injection, both radiopeptides were found completely degraded. These comparative stability studies performed *in vitro* and *in vivo* impressively demonstrate that only studies in the “living organism” can provide accurate information on degradation rates and patterns. Still, interspecies differences should be always taken into account when extrapolating animal findings to the human situation. Interestingly, in a recent study Breeman et al. reported only marginally slower degradation rates for  $^{111}\text{In}$ -DOTA]MG11 in peripheral blood of MTC patients compared to those determined in mice [55].

## THE CONCEPT OF IN SITU ENZYME INHIBITION

Recently, we have introduced a new strategy to enhance the *in vivo* stability of radiopeptides by *in situ* inhibition of enzyme(s) involved in their catabolism. The success of this concept largely relies on the identification of the peptidase(s) actually responsible for the proteolytic degradation of the radiopeptide entering the circulation after intravenous injection in the living organism, impairing delivery to tumor-sites and compromising tumor uptake.

Proteinase databases accessible to all, like MEROPS (<http://merops.sanger.ac.uk/>) or BRENDA (<http://www.brenda-enzymes.org/>), provide information on enzymes and their substrates. This information on the substrate repertoire of a specific peptidase is usually acquired from *in vitro* assays with the purified enzyme. As a result, competition across proteases for the catabolism of a specific substrate, expected to occur *in vivo*, is not taken into account. Nevertheless, kinetic data on hydrolysis of the same substrate (e.g. gastrin/CCK) by different peptidases is often available as well and may assist in pinpointing the most aggressive predator. Further information on the presence, concentration, tissue distribution and subcellular localization of peptidase candidates may further assist in narrowing the spectrum of candidates to a few or even one enzyme. Inhibition of the most prominent peptidase by a suitable inhibitor, however, cannot exclude eventual *in vivo* catabolism of the radiopeptide of interest by a second one.

It is clear, that improvement of radiopeptide tumor uptake by short-term stabilization of the radiopeptide in peripheral blood via *in situ* protease-inhibition will depend on the number

and identification of peptidases that need to be inhibited. The unique chemical structure of radiometallated peptides turns out to be very positive in this respect, because their N-terminal capping by the radiometal-chelate rules out degradation by N-terminal exopeptidases, or else aminopeptidases. It should be noted, that aminopeptidases, such as APA, leucyl-aminopeptidase, aminopeptidase M, are the most active enzymes in terminating the activity of a wide array of regulatory peptides. Combining all above information with previous reports on the enzymes involved in the degradation of gastrin and CCK, we came upon NEP.

Accordingly, we postulated that a NEP inhibitor coinjected intravenously together with biodegradable truncated gastrin radioligands could potentially increase metabolic half-life. Such inhibitor would escort and protect the radiopeptide immediately after its entry into circulation and until it reaches the target, hence optimizing the supply to and uptake in the tumor [7].

There is a wide range of NEP inhibitors that have been developed for various purposes by pharmaceutical industry over the years [94]. For our studies we have selected phosphoramidon (PA), which is a hydrophilic, potent, competitive and reversible inhibitor of NEP [95]. PA is a natural product first isolated from extracts of *Streptomyces tanashiensis* by Umezawa et al. in 1972 [96], but can be also chemically synthesized [97]. It consists of a leucyl-tryptophan dipeptide coupled to  $\alpha$ -L-rhamnose via a phosphoramidate linkage (Figure 4). The structure of PA at the active center of NEP has been elucidated by X-ray crystallography, showing PA bound to one side of a large central cavity of NEP that contains the active site [98]. Because of its high water solubility, PA can be co-injected as a bolus together with the radiopeptide in doses sufficient for full in vivo NEP inhibition [99,100].

We have hypothesized that co-administration of PA with radiolabeled gastrin analogs can enhance uptake in the CCK2R-expressing tumors and as a result may improve diagnostic sensitivity and therapeutic efficacy of radiolabeled gastrin based peptide drugs in the clinic.

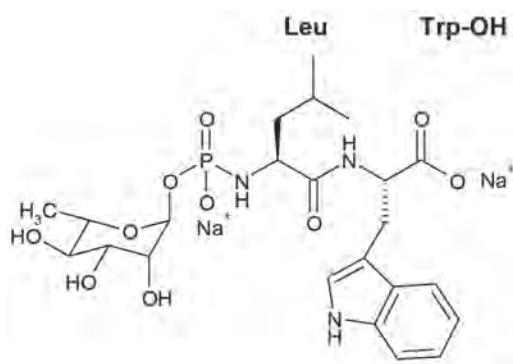


Figure 4 | Chemical structure of phosphoramidon (PA, N- $\alpha$ -Rhamnopyranosyloxy-hydroxyphosphinyl)-Leu-Trp  $\times$  2Na).



## NEP INHIBITION BY PA CO-ADMINISTRATION WITH [<sup>111</sup>In-DOTA]MG11

The concept of in situ enzyme inhibition by PA co-injection was assessed using the truncated <sup>111</sup>In-labeled gastrin analog [DOTA]MG11 [7]. The choice of this particular *des*(Glu)<sub>5</sub>-analog was based on previous findings reporting that [<sup>111</sup>In-DOTA]MG11 is prone to fast in vivo degradation, resulting in poor targeting of CCK2R-expressing tumors. At the same time, however, [<sup>111</sup>In-DOTA]MG11 shows advantageously low kidney accumulation compared with other full chain and more stable gastrin analogs [52,56].

The effect of PA co-injection on the in vivo stability of [<sup>111</sup>In-DOTA]MG11 was studied first in healthy mice 5 min after intravenous injection of the radioligand with vehicle (control group) or with PA (PA-treated group). Blood collected directly from the heart of mice 5 min pi was analyzed by HPLC to assess potential radioligand degradation and radiometabolite formation in the bloodstream. [<sup>111</sup>In-DOTA]MG11 was very unstable in blood circulation with less than 5% of the radiopeptide remaining intact, confirming previous studies in rodents and in man [55,57].

Treatment with PA remarkably increased the percentage of circulating intact [<sup>111</sup>In-DOTA]MG11 to more than 70%. The formation of metabolites present in the corresponding blood radiochromatogram was suppressed by PA co-injection, highlighting the prominent role of NEP in its degradation during this period. Consequently, any significant contribution by ACE, or any other of the more than 600 proteases present in mice can be ruled out. This finding is in agreement with previous work by Dubreuil et al. showing that the (Glu)<sub>2</sub>-gastrin analog [Leu<sup>15</sup>]Gastrin(9-17) is virtually ACE-resistant [87]. [<sup>111</sup>In-DOTA]MG11 is a [DOTA,DGlu<sup>10</sup>]Gastrin(10-17) analog with a DGlu residue at position 10 and the highly polar and sterically bulky <sup>111</sup>In-DOTA-chelate at position 9. These two amino acids are expected to have similar effects in preventing the action of ACE with the two N-terminal Glu<sup>9,10</sup>-residues of the ACE-stabilized analog [Leu<sup>15</sup>]Gastrin(9-17).

The extent by which the positive impact of PA treatment on stability of [<sup>111</sup>In-DOTA]MG11 was translated into tumor uptake was studied in SCID mice at 4 h pi. The first animal model comprised two tumors, with the first transfected to stably express the human CCK2R (A431-CCK2R(+)) and the second tumor devoid of CCK2R expression (A431-CCK2R(-)). An additional model comprised AR42J tumors xenografted in mice and endogenously expressing the rat CCK2R. Co-administration of PA induced an impressive increase in the uptake of [<sup>111</sup>In-DOTA]MG11 in the A431-CCK2R(+) tumors from 2 %ID/g to more than 15 %ID/g, while in the A431-CCK2R(-) tumors tumor uptake (<0.5 %ID/g) remained unchanged. Likewise, treatment with PA resulted in an 8-fold enhancement of [<sup>111</sup>In-DOTA]MG11 uptake in the AR42J tumors from <2 %ID/g to >16 %ID/g, while coinjection of PA and excess DG2 (CCK2R-blocker) confirmed CCK2R-mediated accumulation (uptake remained <0.3%ID/g). Of great importance is the fact that renal uptake remained low and unaffected by PA treatment. Consequently, tumor-to-kidney ratios significantly improved (Figure 5A, B). The impact of PA-treatment on tumor uptake was reproduced by SPECT/CT imaging of [<sup>111</sup>In-DOTA]MG11 in AR42J tumor bearing mice. The signal on the tumor was impressively enhanced, without any visualization of the kidneys, verifying the benefits of this concept on diagnostic sensitivity.

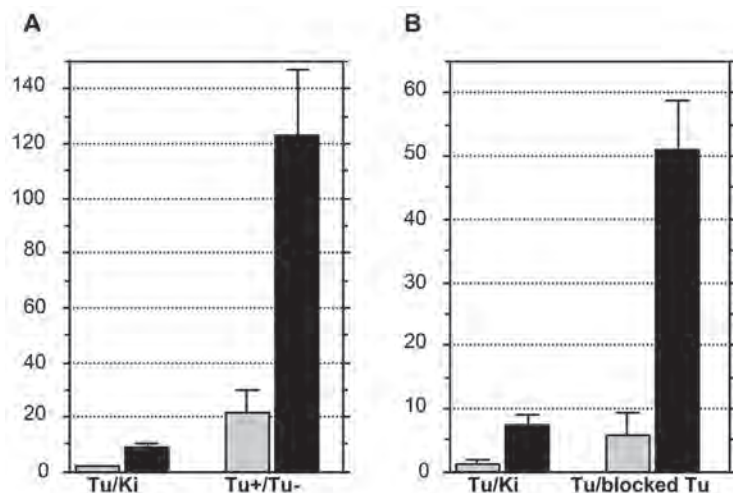


Figure 5 | Ratios of tumor-to-kidney (Tu/Ki) and tumor-to-non-specific tumor uptake 4 h after injection of [<sup>111</sup>In-DOTA]MG11 with vehicle (gray bars) or with PA (black bars) in tumor-bearing SCID mice. **A**) Mice with double A431-CCK2R(+) (Tu+) and naïve A431-CCK2R(-) (Tu-) xenografts (Tu+/Tu- ratios), and **B**) Mice with AR42J tumors (Tu/blocked Tu ratios; in vivo CCK2R blockade after coinjection of excess Demogastatin 2) [49].

## CONCLUSIONS – FUTURE PERSPECTIVES

The application of radiolabeled gastrin or CCK analogs in the clinic has been restricted to date by poor metabolic stability (CCK and truncated gastrin radioligands) or by high accumulation in the kidneys (penta-Glu containing gastrin radioligands). The development of radiolabeled in vivo robust gastrin or CCK peptide radiotracers with favorably low renal retention has been directed to structural modifications of gastrin and CCK motifs. First promising results have been obtained by cyclic *des*(Glu)<sub>5</sub> minigastrin analogs, showing improved in vivo stability, or by full-chain minigastrin analogs after key amino acid substitutions in the penta-Glu chain, showing lower kidney retention. These modifications, however, resulted in lower tumor uptake in animal models.

We have recently proposed a new approach to resolve the problem of in vivo degradation of peptide radioligands, based on the central role of a single protease, NEP, in initiating the fast catabolism of a wide array of such radiotracers after their entry in the blood stream. Thus, by single coinjection of a NEP-inhibitor together with the radiopeptide of interest, we were able to prolong in vivo stability, improve supply to tumor-associated targets and eventually enhance tumor localization. By adopting this innovative concept in the case of the truncated and rapidly biodegradable [<sup>111</sup>In-DOTA]MG11, we were able to induce remarkable improvements in the pharmacokinetic profile of the radiotracer in animal models. In particular, after co-administration of the potent, competitive and reversible NEP-inhibitor PA a striking increase of [<sup>111</sup>In-DOTA]MG11 stability in the blood stream of mice was achieved. Most interestingly, the PA-induced stabilization of [<sup>111</sup>In-DOTA]MG11

translated into impressive increase of radiotracer uptake in CCK2R-positive tumors in mice without affecting the favourably low kidney uptake. As a result, unprecedented tumor-to-kidney ratios could be accomplished, very attractive not only for diagnostic imaging but also for radionuclide therapy.

This approach is currently evaluated further in a broader panel of CCK and gastrin radioligands of various peptide chain lengths, whereby other proteases like ACE may also be involved. Besides  $^{111}\text{In}$ -labeled analogs, this approach may turn out to be also very interesting for SPECT radiotracers labeled with  $^{99\text{m}}\text{Tc}$  or for PET agents labeled with  $^{68}\text{Ga}$ ,  $^{64}\text{Cu}$  and several other radionuclides. While DOTA is a universal chelator allowing binding of several bi- and trivalent radiometals of clinical interest, modifications with different chelator types would allow or improve labeling with such radiometals. Furthermore, labeling with therapeutic beta emitters, such as  $^{177}\text{Lu}$  or  $^{90}\text{Y}$ , needs to be established and the potential of the new concept of in situ NEP-inhibition needs to be evaluated by therapy studies in animal models. For such purposes, substitution of Met<sup>15</sup> in [ $^{111}\text{In}$ -DOTA]MG11 by oxidation-resistant amino acids, like Leu, Nle and others, will facilitate radiopeptide handling and is currently pursued.

Eventually, translation of this concept warrants investigation in MTC and other CCK2R-positive cancer patients. Firstly potential improvements in diagnostic sensitivity in SPECT and PET imaging should be established. Eventually, the impact of the new promising strategy on therapeutic efficacy therapy should be carefully validated. To achieve such ambitious goals several parameters should be taken into account and systematically investigated, such as biosafety issues related with the use of NEP inhibitors in human. Extensive toxicology studies with PA are not currently available and represent one route to follow for clinical translation. On the other hand, several other NEP-inhibitors have been developed by pharmaceutical industry with a few tested already in human.

Hydrophilicity, inhibition potency, inhibition kinetics, in vivo stability, duration of action, biosafety and potential administration route are only few of the issues that need to be rigorously addressed when selecting the most suitable NEP-inhibitor for clinical translation. Dose escalation studies in animals will be instrumental to plan optimized and safe radiopeptide and inhibitor combination regimens in a first proof-of-principle study.

First clinical evidence on the validity of this concept in increasing the diagnostic sensitivity of radiolabeled gastrin analogs in MTC patients is expected to exert a strong impact in radionuclide therapy of MTC patients with disseminated disease, currently left with no effective therapeutic options. Furthermore, different type of gastrin-related therapy may benefit by this approach as well, as for example image-guided surgery of CCK2R-positive tumors using fluorescent dye-coupled gastrin analogs, or targeted chemotherapy with gastrin-coupled cytotoxic drugs. Eventually, this concept may expand to include several other classes of peptide-conjugates, hitherto excluded from further development into drugs for clinical use due to their poor metabolic stability.

## REFERENCES

1. Lee S, Xie J, Chen X. Peptides and peptide hormones for molecular imaging and disease diagnosis. *Chem Rev* 2010;110:3087-111.
2. Volkert WA, Hoffman TJ. Therapeutic radiopharmaceuticals. *Chem Rev* 1999;99:2269-92.
3. Heppeler A, Froidevaux S, Eberle AN, Maecke HR. Receptor targeting for tumor localisation and therapy with radiopeptides. *Curr Med Chem* 2000;7:971-94.
4. Breeman WA, de Jong M, Kwekkeboom DJ, Valkema R, Bakker WH, Kooij PP, et al. Somatostatin receptor-mediated imaging and therapy: basic science, current knowledge, limitations and future perspectives. *Eur J Nucl Med* 2001;28:1421-9.
5. Reubi JC, Waser B. Unexpected high incidence of cholecystokinin-B/gastrin receptors in human medullary thyroid carcinomas. *Int J Cancer* 1996;67:644-7.
6. Adessi C, Soto C. Converting a peptide into a drug: strategies to improve stability and bioavailability. *Curr Med Chem* 2002;9:963-78.
7. Nock BA, Maina T, Krenning EP, de Jong M. "To serve and protect": enzyme inhibitors as radiopeptide escorts promote tumor targeting. *J Nucl Med* 2014;55:121-7.
8. Edkins JS. The chemical mechanism of gastric secretion. *J Physiol* 1906;34:133-44.
9. Ferrand A, Wang TC. Gastrin and cancer: a review. *Cancer Lett* 2006;238:15-29.
10. Rehfeld JF, Johnsen AH. Identification of gastrin component I as gastrin-71. *European Journal of Biochemistry* 1994;223:765-773.
11. Gregory RA, Tracy HJ. The constitution and properties of two gastrins extracted from hog antral mucosa: Part I The isolation of two gastrins from hog antral mucosa. *Gut* 1964;5:103-7.
12. Rehfeld JF. The new biology of gastrointestinal hormones. *Physiol Rev* 1998;78:1087-108.
13. Jensen S, Borch K, Hilsted L, Rehfeld JF. Progastrin processing during antral G-cell hypersecretion in humans. *Gastroenterology* 1989;96:1063-70.
14. Ivy AC, Oldberg E. A hormone mechanism for gall-bladder contraction and evacuation. *Am J Physiol* 1928;86:599-613.
15. Buffa R, Solcia E, Go VL. Immunohistochemical identification of the cholecystokinin cell in the intestinal mucosa. *Gastroenterology* 1976;70:528-32.
16. Rehfeld JF, Sun G, Christensen T, Hillingsø JG. The predominant cholecystokinin in human plasma and intestine is cholecystokinin-33. *J Clin Endocrinol Metab* 2001;86:251-8.
17. Larsson LI, Rehfeld JF. Localization and molecular heterogeneity of cholecystokinin in the central and peripheral nervous system. *Brain Res* 1979;165:201-18.
18. Dufresne M, Seva C, Fourmy D. Cholecystokinin and gastrin receptors. *Physiol Rev* 2006;86:805-47.
19. Vanhoutte PM, Humphrey PP, Spedding M. X. International Union of Pharmacology recommendations for nomenclature of new receptor subtypes. *Pharmacol Rev* 1996;48:1-2.
20. Hellmich MR, Rui XL, Hellmich HL, Fleming RY, Evers BM, Townsend CM, Jr. Human colorectal cancers express a constitutively active cholecystokinin-B/gastrin receptor that stimulates cell growth. *J Biol Chem* 2000;275:32122-8.
21. Reeve JR, Jr., McVey DC, Bunnett NW, Solomon TE, Keire DA, Ho FJ, et al. Differences in receptor binding and stability to enzymatic digestion between CCK-8 and CCK-58. *Pancreas* 2002;25:e50-5.
22. Solomon TE, Yamada T, Elashoff J, Wood J, Beglinger C. Bioactivity of cholecystokinin analogues: CCK-8 is not more potent than CCK-33. *Am J Physiol* 1984;247:G105-11.
23. Silvente-Poirot S, Wank SA. A segment of five amino acids in the second extracellular loop of the cholecystokinin-B receptor is essential for selectivity of the peptide agonist gastrin. *J Biol Chem* 1996;271:14698-706.
24. Silvente-Poirot S, Escrieut C, Gales C, Fehrentz JA, Escherich A, Wank SA, et al. Evidence for a direct interaction between the penultimate aspartic acid of cholecystokinin and histidine 207, located in the second extracellular loop of the cholecystokinin B receptor. *J Biol Chem* 1999;274:23191-7.

25. Gigoux V, Escrieut C, Silvente-Poirot S, Maigret B, Gouilleux L, Fehrentz JA, et al. Met-195 of the cholecystokinin-A receptor interacts with the sulfated tyrosine of cholecystokinin and is crucial for receptor transition to high affinity state. *J Biol Chem* 1998;273:14380-6.
26. Gigoux V, Maigret B, Escrieut C, Silvente-Poirot S, Bouisson M, Fehrentz JA, et al. Arginine 197 of the cholecystokinin-A receptor binding site interacts with the sulfate of the peptide agonist cholecystokinin. *Protein Sci* 1999;8:2347-54.
27. Gales C, Poirot M, Taillefer J, Maigret B, Martinez J, Moroder L, et al. Identification of tyrosine 189 and asparagine 358 of the cholecystokinin 2 receptor in direct interaction with the crucial C-terminal amide of cholecystokinin by molecular modeling, site-directed mutagenesis, and structure/affinity studies. *Mol Pharmacol* 2003;63:973-82.
28. Reubi JC. Peptide receptors as molecular targets for cancer diagnosis and therapy. *Endocr Rev* 2003;24:389-427.
29. Reubi JC, Schaer JC, Waser B. Cholecystokinin(CCK)-A and CCK-B/gastrin receptors in human tumors. *Cancer Res* 1997;57:1377-86.
30. Upp JR, Jr., Singh P, Townsend CM, Jr., Thompson JC. Clinical significance of gastrin receptors in human colon cancers. *Cancer Res* 1989;49:488-92.
31. Reubi JC, Korner M, Waser B, Mazzucchelli L, Guillou L. High expression of peptide receptors as a novel target in gastrointestinal stromal tumours. *Eur J Nucl Med Mol Imaging* 2004;31:803-10.
32. Sethi T, Herget T, Wu SV, Walsh JH, Rozengurt E. CCKA and CCKB receptors are expressed in small cell lung cancer lines and mediate Ca<sup>2+</sup> mobilization and clonal growth. *Cancer Res* 1993;53:5208-13.
33. Matsumori Y, Katakami N, Ito M, Taniguchi T, Iwata N, Takaishi T, et al. Cholecystokinin-B/gastrin receptor: a novel molecular probe for human small cell lung cancer. *Cancer Res* 1995;55:276-9.
34. Goetze JP, Nielsen FC, Burchard F, Rehfeld JF. Closing the gastrin loop in pancreatic carcinoma: coexpression of gastrin and its receptor in solid human pancreatic adenocarcinoma. *Cancer* 2000;88:2487-94.
35. Weinberg DS, Ruggeri B, Barber MT, Biswas S, Miknyocki S, Waldman SA. Cholecystokinin A and B receptors are differentially expressed in normal pancreas and pancreatic adenocarcinoma. *J Clin Invest* 1997;100:597-603.
36. Hazard JB, Hawk WA, Crile G, Jr. Medullary (solid) carcinoma of the thyroid; a clinicopathologic entity. *J Clin Endocrinol Metab* 1959;19:152-61.
37. Behr TM, Gratz S, Markus PM, Dunn RM, Hufner M, Schauer A, et al. Anti-carcinoembryonic antigen antibodies versus somatostatin analogs in the detection of metastatic medullary thyroid carcinoma: are carcinoembryonic antigen and somatostatin receptor expression prognostic factors? *Cancer* 1997;80:2436-57.
38. Seregni E, Chiti A, Bombardieri E. Radionuclide imaging of neuroendocrine tumours: biological basis and diagnostic results. *Eur J Nucl Med* 1998;25:639-58.
39. Behr TM, Béhé MP. Cholecystokinin-B/Gastrin receptor-targeting peptides for staging and therapy of medullary thyroid cancer and other cholecystokinin-B receptor-expressing malignancies. *Semin Nucl Med* 2002;32:97-109.
40. Behr TM, Jenner N, Radetzky S, Béhé M, Gratz S, Yucekent S, et al. Targeting of cholecystokinin-B/gastrin receptors in vivo: preclinical and initial clinical evaluation of the diagnostic and therapeutic potential of radiolabelled gastrin. *Eur J Nucl Med* 1998;25:424-30.
41. Behr TM, Jenner N, Béhé M, Angerstein C, Gratz S, Raue F, et al. Radiolabeled peptides for targeting cholecystokinin-B/gastrin receptor-expressing tumors. *J Nucl Med* 1999;40:1029-44.
42. Béhé M, Becker W, Gotthardt M, Angerstein C, Behr TM. Improved kinetic stability of DTPA- dGlu as compared with conventional monofunctional DTPA in chelating indium and yttrium: preclinical and initial clinical evaluation of radiometal labelled minigastrin derivatives. *Eur J Nucl Med Mol Imaging* 2003;30:1140-6.
43. Reubi JC. Use of labelled cck-b receptor ligands for the detection and localization of malignant human tumors: Google Patents, 1997.
44. Reubi JC, Waser B, Schaer JC, Laederach U, Erion J, Srinivasan A, et al. Unsulfated DTPA- and DOTA-CCK analogs as specific high-affinity ligands for CCK-B receptor-expressing human and rat tissues in vitro and in vivo. *Eur J Nucl Med* 1998;25:481-90.

45. de Jong M, Bakker WH, Bernard BF, Valkema R, Kwekkeboom DJ, Reubi JC, et al. Preclinical and initial clinical evaluation of <sup>111</sup>In-labeled nonsulfated CCK8 analog: a peptide for CCK-B receptor-targeted scintigraphy and radionuclide therapy. *J Nucl Med* 1999;40:2081-7.
46. Kwekkeboom DJ, Bakker WH, Kooij PP, Erion J, Srinivasan A, de Jong M, et al. Cholecystokinin receptor imaging using an octapeptide DTPA-CCK analogue in patients with medullary thyroid carcinoma. *Eur J Nucl Med* 2000;27:1312-7.
47. Laverman P, Béhé M, Oyen WJ, Willems PH, Corstens FH, Behr TM, et al. Two technetium-99m-labeled cholecystokinin-8 (CCK8) peptides for scintigraphic imaging of CCK receptors. *Bioconjug Chem* 2004;15:561-8.
48. Roosenburg S, Laverman P, Joosten L, Eek A, Oyen WJ, de Jong M, et al. Stabilized <sup>111</sup>In-labeled sCCK8 analogues for targeting CCK2-receptor positive tumors: synthesis and evaluation. *Bioconjug Chem* 2010;21:663-70.
49. Nock BA, Maina T, Béhé M, Nikolopoulou A, Gotthardt M, Schmitt JS, et al. CCK-2/gastrin receptor-targeted tumor imaging with <sup>99m</sup>Tc-labeled minigastrin analogs. *J Nucl Med* 2005;46:1727-36.
50. Nock B, Maina T. Tetraamine-coupled peptides and resulting <sup>99m</sup>Tc-radioligands: an effective route for receptor-targeted diagnostic imaging of human tumors. *Curr Top Med Chem* 2012;12:2655-67.
51. Béhé M, Kluge G, Becker W, Gotthardt M, Behr TM. Use of polyglutamic acids to reduce uptake of radiometal-labeled minigastrin in the kidneys. *J Nucl Med* 2005;46:1012-5.
52. Good S, Walter MA, Waser B, Wang X, Muller-Brand J, Béhé MP, et al. Macrocyclic chelator-coupled gastrin-based radiopharmaceuticals for targeting of gastrin receptor-expressing tumours. *Eur J Nucl Med Mol Imaging* 2008;35:1868-77.
53. Gotthardt M, Béhé MP, Beuter D, Battmann A, Bauhofer A, Schurrat T, et al. Improved tumour detection by gastrin receptor scintigraphy in patients with metastasised medullary thyroid carcinoma. *Eur J Nucl Med Mol Imaging* 2006;33:1273-9.
54. Froberg AC, de Jong M, Nock BA, Breeman WA, Erion JL, Maina T, et al. Comparison of three radiolabelled peptide analogues for CCK-2 receptor scintigraphy in medullary thyroid carcinoma. *Eur J Nucl Med Mol Imaging* 2009;36:1265-72.
55. Breeman WA, Froberg AC, de Blois E, van Gameren A, Melis M, de Jong M, et al. Optimised labeling, preclinical and initial clinical aspects of CCK-2 receptor-targeting with 3 radiolabeled peptides. *Nucl Med Biol* 2008;35:839-49.
56. Laverman P, Joosten L, Eek A, Roosenburg S, Peitl PK, Maina T, et al. Comparative biodistribution of 12 <sup>111</sup>In-labelled gastrin/CCK2 receptor-targeting peptides. *Eur J Nucl Med Mol Imaging* 2011;38:1410-6.
57. Ocak M, Helbok A, Rangger C, Peitl PK, Nock BA, Morelli G, et al. Comparison of biological stability and metabolism of CCK2 receptor targeting peptides, a collaborative project under COST BM0607. *Eur J Nucl Med Mol Imaging* 2011;38:1426-35.
58. Brom M, Joosten L, Laverman P, Oyen WJ, Béhé M, Gotthardt M, et al. Preclinical evaluation of <sup>68</sup>Ga-DOTA-minigastrin for the detection of cholecystokinin-2/gastrin receptor-positive tumors. *Mol Imaging* 2011;10:144-52.
59. Roosenburg S, Laverman P, Joosten L, Cooper MS, Kolenc-Peitl PK, Foster JM, et al. PET and SPECT imaging of a radiolabeled minigastrin analogue conjugated with DOTA, NOTA, and NODAGA and labeled with <sup>64</sup>Cu, <sup>68</sup>Ga, and <sup>111</sup>In. *Mol Pharm* 2014;11:3930-7.
60. Puente XS, Sanchez LM, Overall CM, Lopez-Otin C. Human and mouse proteases: a comparative genomic approach. *Nat Rev Genet* 2003;4:544-58.
61. Webb EC. Enzyme nomenclature 1992. Recommendations of the Nomenclature Committee of the International Union of Biochemistry and Molecular Biology on the Nomenclature and Classification of Enzymes: Academic Press; 1992.
62. Wolf G, Mentzel S, Assmann KJ. Aminopeptidase A: a key enzyme in the intrarenal degradation of angiotensin II. *Exp Nephrol* 1997;5:364-9.
63. Migaud M, Durieux C, Viereck J, Soroca-Lucas E, Fournie-Zaluski MC, Roques BP. The in vivo metabolism of cholecystokinin (CCK-8) is essentially ensured by aminopeptidase A. *Peptides* 1996;17:601-7.
64. Connelly JC, Skidgel RA, Schulz WW, Johnson AR, Erdos EG. Neutral endopeptidase 24.11 in human neutrophils: cleavage of chemotactic peptide. *Proc Natl Acad Sci U S A* 1985;82:8737-41.

65. Wong-Leung YL, Kenny AJ. Some properties of a microsomal peptidase in rat kidney. *Biochem J* 1968;110:5p.
66. George SG, Kenny J. Studies on the enzymology of purified preparations of brush border from rabbit kidney. *Biochem J* 1973;134:43-57.
67. Letarte M, Vera S, Tran R, Addis JB, Onizuka RJ, Quackenbush EJ, et al. Common acute lymphocytic leukemia antigen is identical to neutral endopeptidase. *J Exp Med* 1988;168:1247-53.
68. Morisaki N, Moriwaki S, Sugiyama-Nakagiri Y, Haketa K, Takema Y, Imokawa G. Neprilysin is identical to skin fibroblast elastase: its role in skin aging and UV responses. *J Biol Chem* 2010;285:39819-27.
69. Devault A, Nault C, Zollinger M, Fournie-Zaluski MC, Roques BP, Crine P, et al. Expression of neutral endopeptidase (enkephalinase) in heterologous COS-1 cells. Characterization of the recombinant enzyme and evidence for a glutamic acid residue at the active site. *J Biol Chem* 1988;263:4033-40.
70. Devault A, Sales V, Nault C, Beaumont A, Roques B, Crine P, et al. Exploration of the catalytic site of endopeptidase 24.11 by site-directed mutagenesis. Histidine residues 583 and 587 are essential for catalysis. *FEBS Lett* 1988;231:54-8.
71. Sales N, Dutriez I, Maziere B, Ottaviani M, Roques BP. Neutral endopeptidase 24.11 in rat peripheral tissues: comparative localization by 'ex vivo' and 'in vitro' autoradiography. *Regul Pept* 1991;33:209-22.
72. Erdős EG, Skidgel RA. Neutral endopeptidase 24.11 (enkephalinase) and related regulators of peptide hormones. *Faseb J* 1989;3:145-51.
73. Llorens-Cortes C, Huang H, Vicart P, Gasc JM, Paulin D, Corvol P. Identification and characterization of neutral endopeptidase in endothelial cells from venous or arterial origins. *J Biol Chem* 1992;267:14012-8.
74. Pauwels S, Dockray GJ, Walker R, Marcus S. Metabolism of heptadecapeptide gastrin in humans studied by region-specific antisera. *J Clin Invest* 1985;75:2006-13.
75. Power DM, Bunnett N, Turner AJ, Dimaline R. Degradation of endogenous heptadecapeptide gastrin by endopeptidase 24.11 in the pig. *Am J Physiol* 1987;253:G33-9.
76. Deschodt-Lanckman M, Pauwels S, Najdovski T, Dimaline R, Dockray GJ. In vitro and in vivo degradation of human gastrin by endopeptidase 24.11. *Gastroenterology* 1988;94:712-21.
77. Matsas R, Turner AJ, Kenny AJ. Endopeptidase-24.11 and aminopeptidase activity in brain synaptic membranes are jointly responsible for the hydrolysis of cholecystokinin octapeptide (CCK-8). *FEBS Lett* 1984;175:124-8.
78. Deschodt-Lanckman M, Strosberg AD. In vitro degradation of the C-terminal octapeptide of cholecystokinin by 'enkephalinase A'. *FEBS Lett* 1983;152:109-13.
79. Najdovski T, Collette N, Deschodt-Lanckman M. Hydrolysis of the C-terminal octapeptide of cholecystokinin by rat kidney membranes: characterization of the cleavage by solubilized endopeptidase-24.11. *Life Sci* 1985;37:827-34.
80. Pauwels S, Najdovski T, Dimaline R, Lee CM, Deschodt-Lanckman M. Degradation of human gastrin and CCK by endopeptidase 24.11: differential behaviour of the sulphated and unsulphated peptides. *Biochim Biophys Acta* 1989;996:82-8.
81. Durieux C, Charpentier B, Fellion E, Gacel G, Pelaprat D, Roques BP. Multiple cleavage sites of cholecystokinin heptapeptide by "enkephalinase". *Peptides* 1985;6:495-501.
82. Skidgel RA, Erdos EG. Novel activity of human angiotensin I converting enzyme: release of the NH<sub>2</sub>- and COOH-terminal tripeptides from the luteinizing hormone-releasing hormone. *Proc Natl Acad Sci U S A* 1985;82:1025-9.
83. Studdy PR, Lapworth R, Bird R. Angiotensin-converting enzyme and its clinical significance--a review. *J Clin Pathol* 1983;36:938-47.
84. Skidgel RA, Erdos EG. The broad substrate specificity of human angiotensin I converting enzyme. *Clin Exp Hypertens A* 1987;9:243-59.
85. Skeggs LT, Jr., Kahn JR, Shumway NP. The preparation and function of the hypertensin-converting enzyme. *J Exp Med* 1956;103:295-9.
86. Williams TA, Corvol P, Soubrier F. Identification of two active site residues in human angiotensin I-converting enzyme. *J Biol Chem* 1994;269:29430-4.
87. Dubreuil P, Fulcrand P, Rodriguez M, Fulcrand H, Laur J, Martinez J. Novel activity of angiotensin-converting enzyme. Hydrolysis of cholecystokinin and gastrin analogues with release of the amidated C-terminal dipeptide. *Biochem J* 1989;262:125-30.



88. Mather SJ, McKenzie AJ, Sosabowski JK, Morris TM, Ellison D, Watson SA. Selection of radiolabeled gastrin analogs for peptide receptor-targeted radionuclide therapy. *J Nucl Med* 2007;48:615-22.
89. von Guggenberg E, Sallegger W, Helbok A, Ocak M, King R, Mather SJ, et al. Cyclic minigastrin analogues for gastrin receptor scintigraphy with technetium-99m: preclinical evaluation. *J Med Chem* 2009;52:4786-93.
90. Sosabowski JK, Matzow T, Foster JM, Finucane C, Ellison D, Watson SA, et al. Targeting of CCK-2 receptor-expressing tumors using a radiolabeled divalent gastrin peptide. *J Nucl Med* 2009;50:2082-9.
91. Kolenc-Peitzl P, Mansi R, Tamma M, Gmeiner-Stopar T, Sollner-Dolenc M, Waser B, et al. Highly improved metabolic stability and pharmacokinetics of indium-111-DOTA-gastrin conjugates for targeting of the gastrin receptor. *J Med Chem* 2011;54:2602-9.
92. Kim YG, Lone AM, Saghatelian A. Analysis of the proteolysis of bioactive peptides using a peptidomics approach. *Nat Protoc* 2013;8:1730-42.
93. Lone AM, Kim YG, Saghatelian A. Peptidomics methods for the identification of peptidase-substrate interactions. *Curr Opin Chem Biol* 2013;17:83-9.
94. Rawlings ND, Barrett AJ, Bateman A. MEROPS: the database of proteolytic enzymes, their substrates and inhibitors. *Nucleic Acids Res* 2012;40:D343-50.
95. Kukkola PJ, Savage P, Sakane Y, Berry JC, Bilci NA, Ghai RD, et al. Differential structure-activity relationships of phosphoramidon analogues for inhibition of three metalloproteases: endothelin-converting enzyme, neutral endopeptidase, and angiotensin-converting enzyme. *J Cardiovasc Pharmacol* 1995;26 Suppl 3:S65-8.
96. Umezawa S, Tatsuta K, Izawa O, Tsuchiya T, Umezawa H. A new microbial metabolite phosphoramidon (Isolation and structure). *Tetrahedron Letters* 1972;13:97-100.
97. Donahue MG, Johnston JN. Preparation of a protected phosphoramidon precursor via an H-phosphonate coupling strategy. *Bioorg Med Chem Lett* 2006;16:5602-4.
98. Oefner C, D'Arcy A, Hennig M, Winkler FK, Dale GE. Structure of human neutral endopeptidase (Nepilysin) complexed with phosphoramidon. *J Mol Biol* 2000;296:341-9.
99. Roques BP, Noble F, Dauge V, Fournie-Zaluski MC, Beaumont A. Neutral endopeptidase 24.11: structure, inhibition, and experimental and clinical pharmacology. *Pharmacol Rev* 1993;45:87-146.
100. Suda H, Aoyagi T, Takeuchi T, Umezawa H. Letter: A thermolysin inhibitor produced by Actinomycetes: phosphoramidon. *J Antibiot (Tokyo)* 1973;26:621-3.



# CHAPTER

# 3

## In Vivo Inhibition of Neutral Endopeptidase Enhances the Diagnostic Potential of Truncated Gastrin $^{111}\text{In}$ -Radioligands

Aikaterini Kaloudi<sup>1</sup>, Berthold A. Nock<sup>1</sup>, Emmanouil Lymperis<sup>1</sup>,  
Werner Sallegger<sup>2</sup>, Eric P. Krenning<sup>3</sup>, Marion de Jong<sup>3,4</sup>,  
Theodosia Maina<sup>1</sup>

<sup>1</sup>Molecular Radiopharmacy, INRASTES, National Center for Scientific Research  
"Demokritos", GR-153 10 Athens, Greece

<sup>2</sup>piCHEM, A-8045 Graz, Austria

<sup>3</sup>Department of Nuclear Medicine, Erasmus MC, 3015 CE Rotterdam,  
The Netherlands

<sup>4</sup>Department of Radiology, Erasmus MC, 3015 CE Rotterdam,  
The Netherlands

*Nucl. Med. Biol.* 42(11):824-32, 2015

## ABSTRACT

**Introduction:** Radiolabeled gastrin analogs represent attractive candidates for diagnosis and therapy of cholecystokinin subtype-2 receptor (CCK2R)-expressing tumors. Radiolabeled *des*(Glu)<sub>5</sub>-gastrins show favourably low renal accumulation, but localize poorly in CCK2R-positive lesions. We introduce herein three truncated [DOTA-DGlu<sup>10</sup>]gastrin(10-17) analogs, with oxidation-susceptible Met<sup>15</sup> replaced by: Ahp<sup>15</sup> (1), Nle<sup>15</sup> (2), or Leu<sup>15</sup> (3), and study the profile of [<sup>111</sup>In]1/2/3 during in vivo inhibition of neutral endopeptidase (NEP) in comparison to the non-truncated [<sup>111</sup>In-DOTA,DGlu<sup>5</sup>]gastrin(5-17) ([<sup>111</sup>In]4) reference.

**Methods:** Blood samples collected from mice 5 min postinjection (pi) of [<sup>111</sup>In]1/2/3/4 without or with phosphoramidon (PA) coinjection were analyzed by RP-HPLC. Biodistribution was conducted in SCID mice bearing A431-CCK2R(+) or AR42J xenografts 4 h after administration of [<sup>111</sup>In]1/2/3/4 without or with PA coinjection.

**Results:** Firstly, we observed remarkable increases in the amount of radiopeptides detected intact in the blood of PA-treated mice at 5 min pi compared to controls. Secondly, we noted impressive enhancement of [<sup>111</sup>In]1/2/3 localization in AR42J and A431-CCK2R(+) tumors in mice after PA coinjection. Specifically, the uptake of [<sup>111</sup>In]1 at 4 h pi increased from 2.6±0.3%ID/g to 13.3±3.5%ID/g in the AR42J tumors and from 4.3±0.6%ID/g to 20.4±3.6%ID/g in the A431-CCK2R(+) xenografts, with comparable improvements noted for [<sup>111</sup>In]2 and [<sup>111</sup>In]3 as well. Thirdly, renal uptake remained favourably low and unaffected by PA (<2.5%ID/g). Conversely, although the stability and tumor targeting of [<sup>111</sup>In]4 improved, its high renal uptake (>85%ID/g) increased even further by PA (>140%ID/g).

**Conclusions:** In situ inhibition of NEP represents a promising new tool to enhance the diagnostic efficacy of biodegradable gastrin radioligands in the visualization of CCK2R-positive lesions in man.

**Key words:** tumor imaging, cholecystokinin subtype 2-receptor, truncated gastrin, radiolabeled gastrin, neutral endopeptidase inhibition, phosphoramidon

## INTRODUCTION

Cholecystokinin subtype 2-receptors (CCK2Rs) represent molecular targets of considerable clinical interest due to their high level of expression in various human tumors, particularly in medullary thyroid cancer (MTC) [1-3]. Hence, a significant number of CCK2R-directed radiopeptide probes based on gastrin or cholecystokinin (CCK) have been proposed for diagnosis and therapy of primary and metastatic MTC as well as of other CCK2R-related cancers [4-13].

Native gastrin is a linear 17peptide characterized by the presence of a multi-negatively charged penta-Glu chain occupying positions 6 to 10 and, unlike CCK, shows preference for the CCK2R [14-16]. The Glu<sup>6-10</sup>-chain of human gastrin affects several pharmacological features of gastrin and its radiolabeled analogs, including receptor affinity, metabolic stability and pharmacokinetics. A number of recent studies have revealed the higher metabolic stability of human gastrin and minigastrin (MG, gastrin(5-17)) radioligands both in animals and in human as compared to their truncated *des*Glu<sup>6-10</sup>-counterparts [9,11,17,18]. As a result, full-length gastrin and MG analogs show higher efficacy to target CCK2R-positive lesions in vivo, whereas radiolabeled gastrins lacking the Glu<sup>6-10</sup>-sequence poorly localize in CCK2R-sites. On the other hand however, the above attractive qualities of Glu<sup>6-10</sup>-containing gastrin radioligands are severely compromised by their unfavorably high and prolonged renal retention [9,11,19]. This drawback practically precludes their application in the therapy of CCK2R-positive tumors after labeling with particle-emitters due to the expected nephrotoxicity. The exact mechanism for this behavior is still under investigation, but kidney protection regimens could suppress renal accumulation only to a certain extent [20]. Alternatively, structural modifications on the Glu<sup>6-10</sup>-chain, such as substitution of selected or of all five Glu-residues by Gln, Asp or DGLu, have been attempted thus far, leading to improvements in pharmacokinetics [10,11,13,21-23].

We have recently introduced a different and effective strategy to enhance the bioavailability and thereby the tumor uptake of fast biodegradable peptide radioligands. By single co-injection of the neutral endopeptidase (NEP, EC 3.4.24.11, neprilysin, CD10)-inhibitor phosphoramidon (PA) [24-26] we were able to induce impressive stabilization of radiopeptides originating from the somatostatin, bombesin and gastrin families in mouse circulation. As a result, the uptake of such radiopeptides in tumors xenografted in mice remarkably increased [27].

The above promising findings have prompted us to further investigate the effects of in situ NEP-inhibition by PA on three *des*Glu<sup>6-10</sup>-gastrin radioligands derived from [<sup>111</sup>In-DOTA-DGLu<sup>10</sup>]gastrin(10-17) ([DOTA]MG11) by single substitutions of oxidation-susceptible Met<sup>15</sup> by: Ahp<sup>15</sup> (1), Nle<sup>15</sup> (2), or Leu<sup>15</sup> (3) [28-30]. We were first interested to explore the effects of these modifications on CCK2R-affinity. After labeling with <sup>111</sup>In, we have compared the uptake of [<sup>111</sup>In]1/2/3 in CCK2R-positive cells. The stabilities of [<sup>111</sup>In]1/2/3 in mouse circulation were compared to the non-truncated minigastrin reference [<sup>111</sup>In-DOTA,DGLu<sup>5</sup>]gastrin(5-17) ([<sup>111</sup>In-DOTA]MG0, [<sup>111</sup>In]4) [11] without or with PA-coinjection. Eventually, the pharmacokinetics of [<sup>111</sup>In]1/2/3 with emphasis on tumor and kidney uptake were thoroughly studied in mice bearing CCK2R-positive tumors without or during in situ NEP-inhibition and compared to the non-truncated [<sup>111</sup>In]4 reference. This comparative study is expected to outline potential strengths or limitations of the NEP-inhibition strategy applied in gastrin radioligands and to highlight specific advantages for translation in the visualization of CCK2R-positive tumors in man.

## MATERIALS AND METHODS

### Materials and instrumentation

#### Compounds and radionuclides

Unless otherwise stated, all chemicals were reagent grade and were used without further purification. [Leu<sup>15</sup>]gastrin was purchased from Bachem (Bubendorf, Switzerland) and **4** from piCHEM (Graz, Austria), while DG2 was synthesized as previously described [8]. Phosphoramidon disodium dihydrate (N-( $\alpha$ -rhamnopyranosyloxyhydroxyphosphinyl)-L-leucyl-L-tryptophan $\times$ 2Na $\times$ 2H<sub>2</sub>O) was provided by PeptaNova GmbH (Sandhausen, Germany). Indium-111 was obtained in the form of <sup>111</sup>InCl<sub>3</sub> in a solution of 0.05 M HCl (0.5 mL) from Mallinckrodt Medical B.V. (Petten, The Netherlands) and <sup>125</sup>I was purchased from MDS Nordion, SA (Canada) in the form of Na<sup>125</sup>I in a solution of 10<sup>-5</sup> M NaOH (10  $\mu$ L).

#### Analysis-radiochemistry

For analysis RP-HPLC was performed on a Waters Chromatograph (Waters, Vienna, Austria) based on a 600 solvent delivery system coupled to a Waters 996 photodiode array UV detector and a Gabi gamma detector (Raytest, RSM Analytische Instrumente GmbH, Germany) employing a 2-mL injection loop. The Millennium Software (Waters, USA) was used for data processing and chromatographic control and an XTerra RP-18 (5  $\mu$ m, 4.6 mm  $\times$  150 mm) cartridge column (Waters, Germany) was eluted at 1 mL/min flow rate with a linear gradient system 1 starting from 0% B and advancing to 40% B within 20 min (solvent A= 0.1% aqueous TFA and B= MeCN). For metabolism studies HPLC analysis was performed on a Waters Chromatograph (Waters, Vienna, Austria) with 600E multisolvent delivery system coupled to a Gabi gamma-detector (Raytest, Germany) employing a 0.5-mL injection loop. Data processing and chromatography were controlled with Empower Software and a Symmetry Shield RP18 (5  $\mu$ m, 3.9 mm  $\times$  20 mm) column (Waters, Germany) was eluted adopting linear gradient system 2 starting from 0% B and advancing to 40% B within 40 min (solvent A= 0.1% aqueous TFA and B= MeCN) with a flow rate of 1 mL/min. Radioactivity measurements were conducted in an automated well-type gamma counter [NaI(Tl) crystal, Canberra Packard Auto-Gamma 5000 series instrument] calibrated for <sup>111</sup>In or <sup>125</sup>I.

#### Synthesis of 1/2/3 on the solid support

The three peptide conjugates: *i*) DOTA-DGlu-Ala-Tyr-Gly-Trp-Ahp-Asp-Phe-NH<sub>2</sub>, **1**, *ii*) DOTA-DGlu-Ala-Tyr-Gly-Trp-Nle-Asp-Phe-NH<sub>2</sub>, **2**, and *iii*) DOTA-DGlu-Ala-Tyr-Gly-Trp-Leu-Asp-Phe-NH<sub>2</sub>, **3** (Figure 1), were prepared by the SPPS method using a Tenta Gel S Ram resin (substitution 0.25 mmol/g). Anchoring of each amino acid onto the resin as well as coupling reactions were performed using a 10-fold excess of the Fmoc amino acid derivative in the presence of *N,N'*-diisopropylcarbodiimide (DIC), 1-hydroxybenzotriazole (HOBt) and diisopropylamine (DIPEA) in a 90:10 v/v mixture of *N,N*-dimethylformamide (DMF) and dichloromethane (DCM) as solvent. Fmoc-deprotection was carried out with 30% piperidine in DMF. Coupling of DOTA to the assembled amino acid sequences was done by addition of a 3-fold excess of 1-(acetic acid)-4,7,10-tris(*tert*-butoxycarbonylmethyl)-1,4,7,10-tetraazacyclododecane (DOTA-tris(*t*-Bu-ester)), benzotriazol-1-yloxy-tris(pyrrolidino)phosphonium

hexafluorophosphate (PyBOP) and DIPEA in DMF on the resin. Cleavage of the conjugates from the solid support was conducted by treatment of the fully protected peptide chains with a mixture of trifluoroacetic acid (TFA), 1,2-ethanedithiol (EDT), thioanisol (TA) and H<sub>2</sub>O in a ratio of 90:4:4:2 v/v/v/v. The resin was removed from the cleavage mixture by filtration and each crude conjugate was collected by precipitation with ice-cooled diethyl ether. Finally, the crude 1/2/3 were purified by RP-HPLC on a C18 Semi/Prep AKZO Nobel Kromasil column (250 mm × 20 mm) and characterized by mass spectrometric and chromatographic methods. For HPLC analysis a Nucleosil-100 C18 column (5 μm, 150 mm × 4 mm) was eluted at a flow rate of 1 mL/min with a linear gradient: 0.1 % TFA in MeCN (10% to 90% in 30 min) and 0.1 % aqueous TFA as complementary phase; runs were monitored by UV detection at 215 nm (system 3). Analytical data from RP-HPLC (systems 1 and 3) as well as from MALDI TOF MS are shown in Table 1.

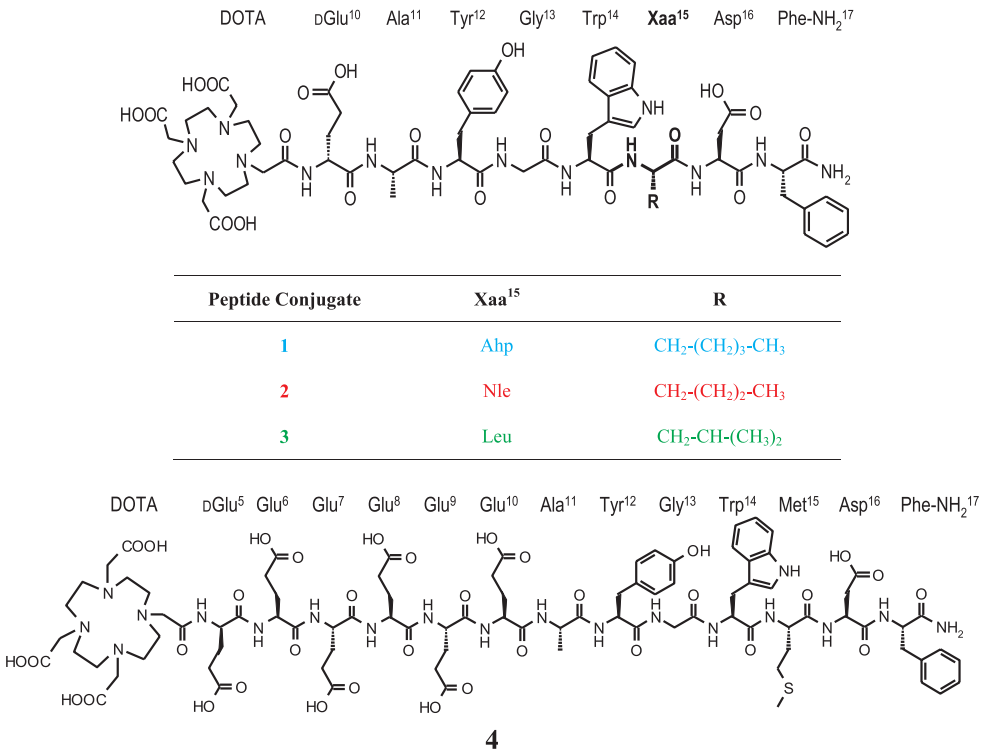


Figure 1 | Chemical structure of 1 (Ahp<sup>15</sup>), 2 (Nle<sup>15</sup>), 3 (Leu<sup>15</sup>) and 4 (reference).

## Radiolabeling

The lyophilized peptide analogs were dissolved in water to a final concentration of 1 mM and 50 μL-aliquots were stored at -20°C. Labeling with <sup>111</sup>In was conducted in an Eppendorf vial containing 0.1 M sodium acetate buffer pH 4.6. Freshly prepared sodium ascorbate buffer (10 mM)

was added in the vial, followed by  $^{111}\text{InCl}_3$  solution (37-74 MBq) and the peptide analog (10 nmol). The mixture was left to react at 80 °C for 20 min. Prior to performing quality control by HPLC, EDTA in 0.1 M acetate buffer (pH 4.6) was added to a final concentration of 1 mM to the labeling reaction mixture to capture free  $^{111}\text{In}^{3+}$  [17].

Radioiodination of [Leu $^{15}$ ]gastrin was performed by using chloramine-T method and [ $^{125}\text{I}$ -Tyr $^{12}$ ,Leu $^{15}$ ]gastrin was isolated in high purity by HPLC. Aliquots of the stock solution in 0.1% BSA-PBS buffer were kept at -20°C and were used for competition binding experiments (specific activity of 74 GBq/ $\mu\text{mol}$ ).

All manipulations with gamma emitting radionuclides and their solutions were performed behind suitable shielding in dedicated laboratories in compliance to national and international radiation safety guidelines.

Table 1 | Analytical Data for 1/2/3.

compound	sequence	%	MW <sup>b</sup>	MW <sup>b</sup> found,	HPLC $t_R$ (min), UV trace	
					calcd	m/z
1	[DOTA,DGlu $^{10}$ ,Ahp $^{15}$ ]gastrin(10-17)	≥ 98.8	1399.5	1399.6 [M + H] <sup>+</sup>	20.8	12.6
2	[DOTA,DGlu $^{10}$ ,Nle $^{15}$ ]gastrin(10-17)	≥ 98.9	1385.5	1386.6 [M + H] <sup>+</sup>	22.8	11.9
3	[DOTA,DGlu $^{10}$ ,Leu $^{15}$ ]gastrin(10-17)	≥ 99	1385.5	1386.9 [M + H] <sup>+</sup>	19.5	11.8

<sup>a</sup>Purity was determined by HPLC system 3. <sup>b</sup>Average mass. <sup>c</sup>system 1: RP-HPLC with UV detection at 220 nm; An Xterra RP18 column (5  $\mu\text{m}$ , 4.6 mm  $\times$  150 mm) was eluted at a flow rate of 1 mL/min with linear gradient: 15% B to 30% B in 30 min, with A= 0.1% TFA in H $_2$ O (v/v) and B= MeCN. <sup>d</sup>system 3: A Nucleosil-100 C18 column (5  $\mu\text{m}$ , 150 mm  $\times$  4 mm) was eluted at a flow rate of 1 mL/min with a linear gradient: 0.1% TFA in MeCN (10% to 90% in 30 min) and 0.1% aqueous TFA as complementary phase; runs were monitored by UV detection at 215 nm.

## Cell culture

The rat pancreatic tumor cell line AR42J, endogenously expressing the CCK2R [31] was kindly provided by Prof. C. Decristoforo (University Clinic Innsbruck, Austria) and the human A431 cell line transfected to stably express the CCK2R (A431-CCK2R(+)) [32] or devoid of CCK2R expression (A431-CCK2R(-)) was a gift from Prof. O. Boerman (Department of Nuclear Medicine, Radboud University Nijmegen Medical Centre, Nijmegen, The Netherlands) and Prof. L. Aloj (Istituto di Biostrutture e Bioimmagini, Consiglio Nazionale delle Ricerche, Naples, Italy).

All culture media were purchased from Gibco BRL, Life Technologies (Grand Island, NY, USA) and supplements were supplied by Biochrom KG Seromed (Berlin, Germany). AR42J cells were cultured in F-12K Nutrient Mixture (Kaighn's Modification), supplemented with 10% (v/v) fetal bovine serum, 100 U/mL penicillin, 100  $\mu\text{g}/\text{mL}$  streptomycin and 1 mM L-glutamine. A431-CCK2R(+) cells were grown in Dulbecco's Modified Eagle medium with GlutaMAX-I supplemented with 10% (v/v) fetal bovine serum, 100 U/mL penicillin, 100  $\mu\text{g}/\text{mL}$  streptomycin, 4,500 mg/L D-glucose and 250  $\mu\text{g}/\text{mL}$  G418. Cells were kept in a controlled humidified air containing 5% CO $_2$  at 37°C. Splitting of cells with a ratio of 1:2 to 1:5 was performed when approaching confluency using a trypsin/EDTA solution (0.05%/0.02% w/v).

## In vitro assays

### **Competition binding assays with 1/2/3 in A431-CCK2R(+) cell membranes**

Competition binding experiments were performed in freshly harvested A431-CCK2R(+) cell membranes. [ $^{125}\text{I}$ -Tyr $^{12}$ ,Leu $^{15}$ ]gastrin served as radioligand [1] and [Leu $^{15}$ ]gastrin as reference compound [28]. In each assay tube 50 pM radioligand (corresponding to  $\sim 30,000$  cpm) was mixed with 25  $\mu\text{g}$  protein and increasing concentrations of tested peptide ( $10^{-5}$ - $10^{-13}$  M) in a total volume of 300  $\mu\text{L}$  of binding buffer (pH 7.4, 50 mM HEPES, 1% BSA, 5.5 mM  $\text{MgCl}_2$ , 35  $\mu\text{M}$  bacitracin). Triplicates of each concentration point were incubated for 60 min at 22°C in an Incubator-Orbital Shaker unit (MPM Instr. Srl, Italy). Ice-cold washing buffer (10 mM HEPES pH 7.4, 150 mM NaCl) was added to interrupt the incubation, followed by rapid filtration over glass fiber filters (Whatman GF/B, presoaked in binding buffer) on a Brandel Cell Harvester (Adi Hassel Ingenieur Büro, Munich, Germany) and filters were washed with cold washing buffer. Filters were counted for their radioactivity content in the  $\gamma$ -counter and  $\text{IC}_{50}$  values were calculated by nonlinear regression according to a one-site model applying the PRISM 2 program (Graph Pad Software, San Diego, CA). Results are the mean  $\pm$  SD of three independent experiments performed in triplicate.

### **Cell-association/internalization of [ $^{111}\text{In}$ ]1/2/3 in CCK2R-positive cells**

A431-CCK2R(+) cells were grown for 24 h to confluency (100%) in six-well plates. Experiments in AR42J cells were conducted 48 h after seeding the cells in six-well plates (80% confluency). At the day of the experiment, cells were rinsed twice with ice-cold internalization medium (DMEM Glutamax-I or F-12K, respectively, supplemented by 1% (v/v) FBS). Fresh medium was added (1.2 mL) at 37°C, followed by [ $^{111}\text{In}$ ]1/2/3 (250 fmol total peptide in 150  $\mu\text{L}$  0.5% BSA-PBS, 50,000-90,000 cpm). Non-specific internalization was determined by a parallel triplicate series containing 1  $\mu\text{M}$  DG2 [8]. Cells were incubated for 60 min at 37°C and then placed on ice. The medium was removed and cells were washed with 0.5% BSA-PBS. Membrane-bound radioactivity was collected by incubating the cells 2  $\times$  5 min in acid-wash solution (50 mM glycine buffer pH 2.8, 0.1 M NaCl) at room temperature. Cells were rinsed with 0.5% BSA-PBS and then lysed with 1 N NaOH. Radioactivity of membrane-bound and internalized fractions was measured using a gamma counter and the percentage of specific and non-specific internalized and membrane-bound fractions were calculated with Microsoft Excel.

## Metabolic studies in mice

In-house male Swiss albino mice (NCSR "Demokritos" Animal House) received a 100  $\mu\text{L}$  bolus containing [ $^{111}\text{In}$ ]1/2/3/4 (11-22 MBq, 3 nmol of total peptide in saline/EtOH 9/1 v/v) through the tail vein, coinjected either with vehicle (100  $\mu\text{L}$ ; control group) or with PA (100  $\mu\text{L}$  of vehicle containing 300  $\mu\text{g}$  PA; PA-group). Animals were euthanized and blood directly collected from the heart at 5 min pi was transferred in a pre-chilled EDTA-containing Eppendorf tube on ice. Samples were centrifuged for 10 min at 2,000 g/4°C and the plasma was collected. After addition of an equal volume of MeCN the mixture was centrifuged for 10 min at 15,000 g/4°C. The supernatant was concentrated under a  $\text{N}_2$ -flux at 40°C, redissolved in saline ( $\sim 400$   $\mu\text{L}$ ), filtered through a 0.22  $\mu\text{m}$  Millex GV filter (Millipore, Milford, USA) and analyzed by RP-HPLC (system 2). The elution time ( $t_R$ ) of parent radioligands was determined by coinjection of blood samples with [ $^{111}\text{In}$ ]1/2/3/4.



### **Biodistribution in SCID mice bearing CCK2R-positive xenografts**

In-house male SCID mice (NCSR "Demokritos" Animal House) of 6-weeks of age at the time of arrival ( $18 \pm 2$  g body weight) were inoculated subcutaneously in their flanks with a  $\sim 150$   $\mu\text{L}$  suspension of freshly harvested AR42J ( $1 \times 10^7$ ) or A431-CCK2R(+/-) ( $1.6 \times 10^7/1.4 \times 10^7$ ) cells in saline. Animals were kept in aseptic conditions until well-palpable tumors developed at the inoculation sites; this period ranged from 8 days for A431-CCK2R(+/-) tumors ( $0.26 \pm 0.08$  g) to 14 days for AR42J tumors ( $0.31 \pm 0.17$  g). At the day of the experiment animals received a 100  $\mu\text{L}$  bolus of [ $^{111}\text{In}$ ]1/2/3 (37-74 kBq, 10 pmol total peptide, in saline/EtOH 9/1 v/v) through the tail vein, coinjected either with vehicle (100  $\mu\text{L}$ ; control group) or PA (300  $\mu\text{g}$  PA dissolved in 100  $\mu\text{L}$  vehicle; PA-group). [ $^{111}\text{In}$ ]4 was included, as a reference in the AR42J tumor model study. In this study, separate mice groups received 40 nmol DG2 [8] dissolved in 100  $\mu\text{L}$  vehicle for in vivo CCK2R-blockade. Animals had access to drinking water *ad libitum* until they were euthanized at 4 h pi. Blood samples, organs of interest and tumors were collected immediately after dissection, weighed and measured for radioactivity in the gamma counter. Stomachs were emptied of their contents. Biodistribution data were calculated as percent of injected dose per gram tissue (%ID/g) with the aid of suitable standards of the injected dose, using the GraphPad Prism Software (San Diego, CA).

### **Statistical analysis**

The unpaired two tailed Student's *t* test of GraphPad Prism Software (San Diego, CA) was applied to evaluate statistically significant differences. *P* values of  $< 0.05$  were considered to be statistically significant.

All animal experiments were approved by national authorities and were carried out in compliance with national and European guidelines.

## **RESULTS**

### **Ligands and radioligands**

#### ***Synthesis of 1/2/3***

The peptide sequences [DGlu<sup>10</sup>,Xaa<sup>15</sup>]gastrin(10-17) (Xaa<sup>15</sup>: Ahp, Nle or Leu) were assembled on the solid support following typical Fmoc-protection methodology and DOTA-tris('Bu-ester) was attached to their N-terminus in the last cycle. After release from the resin and removal of lateral protecting groups with TFA treatment, 1/2/3 (Figure 1) were isolated by chromatographic methods in  $\geq 95\%$  purity, as shown by analytical HPLC; MALDI-TOF spectra of the products were consistent with the expected formulae (Table 1).

#### ***Radiolabeling and quality control of [ $^{111}\text{In}$ ]1/2/3/4***

The respective [ $^{111}\text{In}$ ]1/2/3/4 were easily prepared by 20 min heating of 1/2/3/4 with  $^{111}\text{InCl}_3$  in acidic medium. Complete incorporation of  $^{111}\text{In}$  by DOTA was verified by RP-HPLC; all four radioligands formed in  $> 98\%$  yield and  $> 96\%$  radiochemical purity in typical specific activities of 3.7-7.4 MBq/nmol peptide and were used as such without subsequent purification in all further experiments [17].



## In vitro studies

### CCK2R-affinity of 1/2/3

The receptor affinity of peptide-conjugates was determined during competition binding assays against  $^{125}\text{I}$ -Tyr $^{12}$ ,Leu $^{15}$ gastrin in cell membrane preparations originating from A431-CCK2R(+) cells [32]. As shown in Figure 2, 1/2/3 effectively displaced the radioligand from CCK2R-sites in a monophasic and dose-dependent way. The resulting  $\text{IC}_{50}$  values were in the sub-nM range (1,  $0.73\pm 0.08$  nM; 2,  $0.73\pm 0.07$  nM; 3,  $0.26\pm 0.01$  nM; [Leu $^{15}$ ]gastrin (reference) [28],  $0.86\pm 0.05$  nM). Interestingly, the structural modifications performed, such as truncation at position 10, coupling of DOTA, or substitution of Met $^{15}$  by Ahp $^{15}$ , Nle $^{15}$  or Leu $^{15}$  were all well tolerated by the CCK2R.

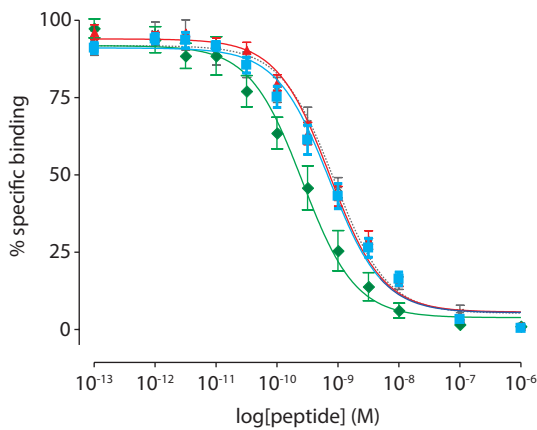


Figure 2 | Displacement of  $^{125}\text{I}$ -Tyr $^{12}$ ,Leu $^{15}$ gastrin from human CCK2R sites in A431-CCK2R(+) cell membranes by increasing concentrations of 1 (■,  $\text{IC}_{50}=0.73\pm 0.08$  nM), 2 (▲,  $\text{IC}_{50}=0.73\pm 0.07$  nM), 3 (◆,  $\text{IC}_{50}=0.26\pm 0.01$  nM) and [Leu $^{15}$ ]gastrin (×,  $\text{IC}_{50}=0.86\pm 0.05$  nM, reference); results are expressed as mean  $\text{IC}_{50}\pm\text{SD}$ ,  $n\geq 3$ .

### Cell-Association and Internalization of $^{111}\text{In}$ 1/2/3

#### In A431-CCK2R(+) Cells

The cell association and internalization properties of  $^{111}\text{In}$ 1/2/3 were first tested by 1 h incubation at 37°C in A431-CCK2R(+) cells (Figure 3A). All radiopeptides bound to the cells and subsequently internalized by a CCK2R mediated process, as demonstrated by the minimal values (<1%) obtained in the presence of 1  $\mu\text{M}$  DG2 [8]. The predominant portion of cell-bound activity corresponded to the internalized fraction, as consistent with an agonist profile. Furthermore,  $^{111}\text{In}$ 1 ( $16.5\pm 0.9\%$ ) and  $^{111}\text{In}$ 3 ( $14.0\pm 1.2\%$ ) internalized significantly faster ( $P<0.01$ ) than  $^{111}\text{In}$ 2 ( $10.0\pm 0.6\%$ ).

#### In AR42J Cells

Cell-association and internalization experiments were additionally performed by 1 h incubation at 37°C in AR42J cells (Figure 3B) [31]. Both processes were likewise repressed in the presence of 1  $\mu\text{M}$  DG2 [8], revealing CCK2R-specificity. Cell-associated activity was mainly located within cells, as consistent for radioagonists. As in the case of A431-CCK2R(+) cells,  $^{111}\text{In}$ 1 ( $11.0\pm 1.4\%$ ) showed the highest internalization capacity also in AR42J cells, followed by  $^{111}\text{In}$ 3 ( $8.0\pm 0.5\%$ ) and  $^{111}\text{In}$ 2 ( $4.3\pm 0.6\%$ ).

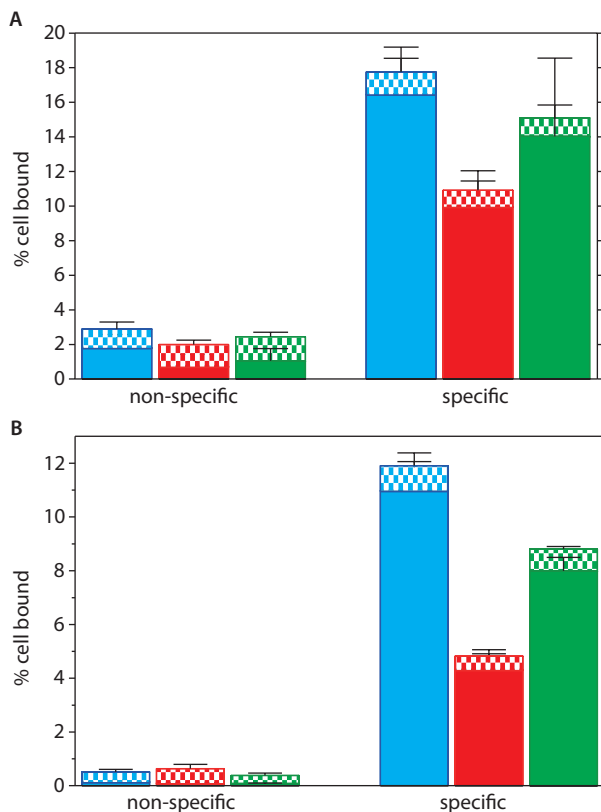


**Figure 3** | Percentage of cell association of  $[^{111}\text{In}]1$  (■, ▨),  $[^{111}\text{In}]2$  (■, ▨) and  $[^{111}\text{In}]3$  (■, ▨) in **A**) A431-CCK2R(+) or **B**) AR42J cells after 1 h incubation at 37°C; solid bars represent internalized fractions and patterned ones membrane-bound fractions. Non-specific values were determined in the presence of 1  $\mu\text{M}$  DG2.

### Metabolic studies in mice

Blood collected 5 min after injection of  $[^{111}\text{In}]1/2/3$  in mice was analyzed by HPLC to assess potential radioligand degradation and radiometabolite formation in the bloodstream. For comparison purposes  $[^{111}\text{In}]4$  was also included in this study as a non-truncated minigastrin reference. Interestingly, the Leu<sup>15</sup>-substituted  $[^{111}\text{In}]3$  turned out to be the most stable member in the *des*(Glu)<sub>5</sub>-gastrin series (27% intact; Figure 4A), while  $[^{111}\text{In}]1$  and  $[^{111}\text{In}]2$  degraded faster in mouse circulation (13% and 10% intact radiopeptide, respectively). On the other hand, the non-truncated  $[^{111}\text{In}]4$  reference substantially surpassed all three  $[^{111}\text{In}]1/2/3$  in stability (70% intact; Figure 4G) [18]. Remarkable stabilization effects were induced by PA treatment for all radiotracers with the levels of circulating  $[^{111}\text{In}]1/2/3$  rising as high as 80-88% (Figure 4B, D, F). Interestingly, even  $[^{111}\text{In}]4$  could profit from PA (84% intact; Figure 4H).

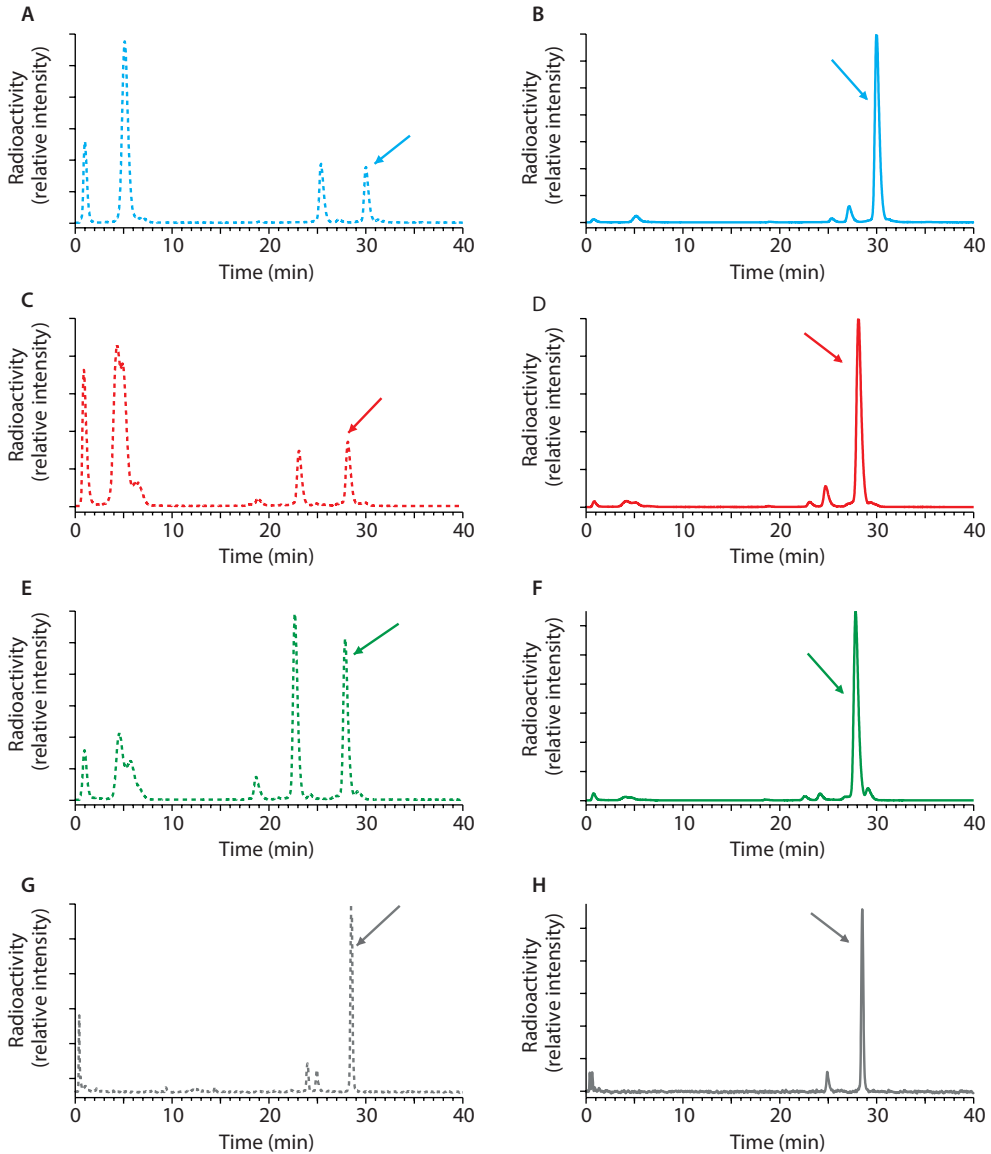


**Figure 4** | Radiochromatograms of HPLC analysis (system 2) of mouse blood samples collected 5 min pi of **A**) [ $^{111}\text{In}$ ]1 (10% intact), **C**) [ $^{111}\text{In}$ ]2 (13% intact), **E**) [ $^{111}\text{In}$ ]3 (27% intact), or **G**) [ $^{111}\text{In}$ ]4 (70% intact) in healthy mice [39]; co-injection of PA significantly raised *in vivo* stability, **B**) [ $^{111}\text{In}$ ]1 (88% intact), **D**) [ $^{111}\text{In}$ ]2 (80% intact), **F**) [ $^{111}\text{In}$ ]3 (85% intact) and **H**) [ $^{111}\text{In}$ ]4 (84% intact). The  $t_r$  of each parent radiopeptide is indicated by the arrow; in **G**) and **H**) a 2-mL injection loop was used.

## Biodistribution of [<sup>111</sup>In]1/2/3 in tumor bearing SCID mice

### *Double human A431-CCK2R(+/-) tumor model*

The biodistribution of [<sup>111</sup>In]1/2/3 was tested in SCID mice bearing a double tumor model: In the right flank animals carried human A431-CCK2R(+) xenografts (CCK2R-positive) and in their left flanks A431-CCK2R(-) tumors devoid of CCK2R expression (negative controls) [11]. Mice received the radioligand alone or with PA (PA-group) and the respective biodistribution results as %ID/g±SD, n≥4, at 4 h pi are summarized in Table 1. The three radiopeptides cleared fast from blood and background tissues via the kidneys rapidly into urine. The uptake in the A431-CCK2R(+) xenografts in the control mice groups was very comparable across compounds ([<sup>111</sup>In]1, 4.32±0.56%ID/g; [<sup>111</sup>In]2, 3.63±0.30%ID/g; [<sup>111</sup>In]3, 4.30±0.86%ID/g). Treatment with PA remarkably enhanced these values ([<sup>111</sup>In]1, 20.41±3.65%ID/g; [<sup>111</sup>In]2, 16.74±2.75%ID/g; [<sup>111</sup>In]3, 19.74±4.71%ID/g; *P*<0.001), presumably as a result of their stabilization by PA in mouse circulation. In contrast, uptake in the negative control tumors remained low and unaffected by PA (<0.4% ID/g), demonstrating CCK2R-specificity. Increase in the uptake was also observed in the CCK2R-positive stomach [33] in the PA animal group (*P*<0.001). Of great importance is the fact, that renal values remained low and unaffected by PA (<2.5%ID/g) for all three <sup>111</sup>In-radiopeptides.

**Table 2 | Biodistribution data of [<sup>111</sup>In]1, [<sup>111</sup>In]2 and [<sup>111</sup>In]3 at 4 h pi in control or PA-treated mice bearing twin A431-CCK2R(+) and naïve A431-CCK2R(-) human xenografts.**

Organs	%ID/g tissue ± SD, n≥4					
	[ <sup>111</sup> In]1		[ <sup>111</sup> In]2		[ <sup>111</sup> In]3	
	Control	PA <sup>a</sup>	Control	PA <sup>a</sup>	Control	PA <sup>a</sup>
Blood	0.02±0.01	0.07±0.01	0.02±0.01	0.03±0.01	0.03±0.01	0.05±0.03
Liver	0.18±0.01	0.37±0.07	0.15±0.01	0.20±0.03	0.20±0.03	0.23±0.03
Heart	0.03±0.01	0.06±0.01	0.04±0.01	0.04±0.01	0.15±0.06	0.11±0.08
Kidneys	<b>2.36±0.40</b>	<b>2.85±0.46</b>	<b>2.39±0.43</b>	<b>2.45±0.32</b>	<b>2.07±0.39</b>	<b>2.46±0.30</b>
Stomach	<b>1.82±0.22</b>	<b>6.48±0.86<sup>b</sup></b>	<b>1.36±0.22</b>	<b>4.23±0.63<sup>b</sup></b>	<b>1.85±0.24</b>	<b>4.99±0.52<sup>b</sup></b>
Intestines	0.26±0.12	0.55±0.13	0.47±0.05	0.04±0.11	0.35±0.11	0.47±0.15
Spleen	0.11±0.04	0.15±0.02	0.09±0.01	0.13±0.02	0.40±0.19	0.27±0.20
Muscle	0.02±0.01	0.03±0.01	0.02±0.01	0.03±0.01	0.11±0.07	0.08±0.05
Lung	0.07±0.03	0.12±0.02	0.06±0.01	0.09±0.01	0.10±0.04	0.15±0.05
Femur	0.05±0.03	0.08±0.01	0.04±0.01	0.06±0.01	0.05±0.01	0.08±0.02
Pancreas	0.10±0.03	0.34±0.03	0.09±0.02	0.25±0.03	0.17±0.05	0.24±0.07
CCK2R(+) Tumor	<b>4.32±0.56</b>	<b>20.41±3.65<sup>b</sup></b>	<b>3.63±0.30</b>	<b>16.74±2.75<sup>b</sup></b>	<b>4.30±0.86</b>	<b>19.74±4.71<sup>b</sup></b>
CCK2R(-) Tumor	<b>0.17±0.01</b>	<b>0.37±0.19</b>	<b>0.19±0.05</b>	<b>0.20±0.03</b>	<b>0.26±0.07</b>	<b>0.25±0.09</b>

<sup>a</sup>Coinjection of PA (300 µg); <sup>b</sup>highly significant (*P*<0.001) difference between the control and the PA-treated groups of animals (unpaired two-tailed Student's *t* test).

Table 3 | Biodistribution data of [<sup>111</sup>In]1, [<sup>111</sup>In]2 and [<sup>111</sup>In]3 in DG2-treated (block), control and PA-treated (PA) mice groups bearing AR42J tumors at 4 h pi.

Organs	%ID/g tissue ± SD, n≥4									
	[ <sup>111</sup> In]1			[ <sup>111</sup> In]2			[ <sup>111</sup> In]3			PA <sup>b</sup>
	Block <sup>a</sup>	Control	PA <sup>b</sup>	Block <sup>a</sup> + PA <sup>b</sup>	Control	PA <sup>b</sup>	Block <sup>a</sup>	Control	PA <sup>b</sup>	
Blood	0.12±0.01	0.07±0.01	0.17±0.06	0.02±0.01	0.05±0.02	0.11±0.08	0.36±0.18	0.24±0.01	0.27±0.05	
Liver	0.26±0.08	0.14±0.02	0.3±0.04	0.15±0.03	0.16±0.05	0.26±0.1	0.31±0.02	0.46±0.07	0.41±0.13	
Heart	0.12±0.03	0.12±0.07	0.13±0.02	0.04±0.01	0.04±0.00	0.09±0.04	0.26±0.13	0.54±0.21	0.42±0.22	
Kidneys	<b>2.1±0.21</b>	<b>2.02±0.21</b>	<b>2.53±0.14</b>	<b>1.22±0.09</b>	<b>1.8±0.22</b>	<b>2.12±0.26</b>	<b>1.5±0.15</b>	<b>2.3±0.52</b>	<b>2.36±0.28</b>	
Stomach	<b>0.2±0.11<sup>c</sup></b>	<b>1.9±0.31</b>	<b>6.66±0.9<sup>c</sup></b>	<b>0.09±0.01<sup>c</sup></b>	<b>1.47±0.47</b>	<b>4.57±1.15<sup>c</sup></b>	<b>0.56±0.19<sup>c</sup></b>	<b>1.81±0.08</b>	<b>3.84±0.51<sup>c</sup></b>	
Intestines	1.1±0.32	1.8±0.06	1.12±0.6	0.39±0.06	1.98±1.38	2.37±1.37	1.13±0.49	1.19±0.71	0.89±0.09	
Spleen	0.36±0.06	0.29±0.1	0.35±0.05	0.1±0.01	0.13±0.04	0.17±0.04	1.2±0.46	1.59±0.05	0.89±0.39	
Muscle	0.06±0.02	0.06±0.01	0.08±0.01	0.02±0.01	0.02±0.00	0.05±0.02	0.2±0.02	0.42±0.21	0.35±0.25	
Lung	0.12±0.02	0.1±0.02	0.17±0.01	0.08±0.01	0.07±0.01	0.15±0.06	0.31±0.08	0.84±0.26	0.4±0.13	
Femur	0.15±0.02	0.21±0.05	0.16±0.02	0.06±0.0	0.06±0.00	0.14±0.04	0.61±0.21	0.22±0.05	0.28±0.09	
Pancreas	0.14±0.02	0.15±0.03	0.34±0.06	0.14±0.01	0.1±0.02	0.69±0.19	0.38±0.09	0.82±0.49	0.49±0.28	
Tumor	<b>0.24±0.05<sup>c</sup></b>	<b>2.6±0.27</b>	<b>13.34±3.49<sup>c</sup></b>	<b>0.4±0.08<sup>c</sup></b>	<b>1.98±0.37</b>	<b>11.9±3.55<sup>c</sup></b>	<b>0.42±0.2<sup>c</sup></b>	<b>3.94±0.46</b>	<b>15.5±2.09<sup>c</sup></b>	

<sup>a</sup>Co-injection of DG2 (40 nmol) for CCK2R-blockade; <sup>b</sup>co-injection of PA (300 µg); <sup>c</sup>highly significant ( $P < 0.001$ ) difference between the control and each of the other groups of animals (unpaired two-tailed Student's *t* test).

### AR42J tumor model

The biodistribution of [<sup>111</sup>In]1/2/3 at 4 h pi was additionally studied in AR42J tumor-bearing SCID mice (Table 3). For comparison purposes, the biodistribution of the non-truncated [<sup>111</sup>In]4 reference was investigated as well in the same model (Table 4). A comparable pharmacokinetic profile is retained across truncated [<sup>111</sup>In]1/2/3 with regards to blood and whole body clearance (Table 3), matching the results obtained in the previous A431-CCK2R(+/-) model (Table 2). Regarding tumor uptake, [<sup>111</sup>In]3 exhibited the highest tumor uptake in the truncated analogs (3.94±0.46%ID/g), followed by [<sup>111</sup>In]1 (2.6±0.27%ID/g) and [<sup>111</sup>In]2 (1.98±0.37%ID/g), whereas the non-truncated [<sup>111</sup>In]4 reference displayed superior tumor values (4.65±1.49%ID/g, Table 4). Treatment with PA impressively enhanced the uptake of all radiopeptides in the AR42J tumors, critically affecting values not only of the three truncated analogs (15.5±2.09%ID/g, [<sup>111</sup>In]3; 11.9±3.55%ID/g, [<sup>111</sup>In]2; 13.34±3.49%ID/g, [<sup>111</sup>In]1; Table 3), but also of the penta-Glu containing [<sup>111</sup>In]4 reference (11.33±3.11%ID/g, Table 4). In all cases tumor uptake was receptor-mediated, as suggested by the significant reduction ( $P<0.001$ ) of tumor values during in vivo CCK2R-blockade. Of great significance is the fact that renal accumulation of [<sup>111</sup>In]1/2/3 remained low and unaffected by PA. In contrast, the unfavorably high kidney uptake of penta-Glu containing [<sup>111</sup>In]4 reference in the control mice (85.62±9.9%ID/g) was further increased during PA treatment (141.69±11.22%ID/g). It is interesting to note the reduction of kidney uptake of [<sup>111</sup>In]4 to 23.95±5.53%ID/g at 4 h pi (Table 4) induced by coinjection of excess DG2 in combination with PA. This effect can be assigned to the presence of the penta-Glu chain both in [<sup>111</sup>In]4 and in DG2, as previously reported [8].

**Table 4 |** Biodistribution data of [<sup>111</sup>In]4 in blocked, control or PA-treated (PA) mice groups bearing AR42J tumors at 4 h pi.

Organs	%ID/g tissue ± SD, n≥4		
	Block <sup>a</sup> + PA <sup>b</sup>	Control	PA <sup>b</sup>
Blood	0.03±0.02	0.04±0.02	0.04±0.02
Liver	0.17±0.03	0.17±0.02	0.16±0.03
Heart	0.03±0.02	0.05±0.01	0.05±0.02
Kidneys	<b>23.95±5.53<sup>c</sup></b>	<b>85.62±9.9</b>	<b>141.69±11.22<sup>c</sup></b>
Stomach	<b>0.05±0.03<sup>c</sup></b>	<b>1.95±0.43</b>	<b>2.22±0.17</b>
Intestines	0.29±0.18	0.84±0.2	0.84±0.37
Spleen	0.08±0.02	0.11±0.03	0.14±0.04
Muscle	0.01±0.01	0.03±0.01	0.02±0.01
Lung	0.06±0.01	0.05±0.01	0.07±0.02
Femur	0.07±0.02	0.08±0.01	0.07±0.02
Pancreas	0.05±0.02	0.13±0.02	0.16±0.02
Tumor	<b>0.32±0.13<sup>c</sup></b>	<b>4.65±1.49</b>	<b>11.33±3.11<sup>c</sup></b>

<sup>a</sup>Coinjection of DG2 (40 nmol) for CCK2R-blockade; <sup>b</sup>coinjection of PA (300 µg); <sup>c</sup>highly significant ( $P<0.001$ ) difference between the control and each of the other groups of animals (unpaired two-tailed Student's t test).

## DISCUSSION

We have recently proposed the coinjection of vulnerable peptide-radioligands with a suitable enzyme-inhibitor as an effective means to improve metabolic stability and consequently tumor targeting [27]. Successful application of this concept largely relies on the identification and in situ inhibition of enzymes truly implicated in the catabolism of intravenously (iv) administered radiopeptides by smart selection of the relevant inhibitor(s). During our stability studies performed in vivo we became increasingly aware of the central role of NEP [24,34] in the enzymatic degradation of radiopeptides from the somatostatin, bombesin and gastrin peptide families. The leading role of NEP in the degradation of radiopeptides has long evaded attention of researchers in the field, primarily because stability tests have been typically performed in plasma or serum. On the other hand, NEP, despite its broad substrate specificity and ubiquitous presence in the body, is a membrane-anchored enzyme found only in low amounts in the blood solute. Exploiting the involvement of NEP in the in vivo degradation of radiopeptides to our benefit, we coinjected the potent NEP-inhibitor PA [25,26]. As a result, we were able not only to increase the stability of radiopeptides in the bloodstream, but most importantly, to markedly enhance their tumor uptake in mice [27].

The catabolism of different length CCK and gastrin analogs involves two enzymes, NEP and angiotensin-converting enzyme (ACE, EC 3.4.15.1) [35-38]. Thus, CCK-8 and *des*-(Glu)<sub>5</sub>-gastrin analogs have been identified as good ACE substrates. However, stepwise addition of Glu-residues at the N-terminus of truncated [Leu<sup>15</sup>]gastrin(11-17) leads to gradual stabilization against ACE, with the Glu<sub>2</sub>-analog becoming virtually ACE-resistant [38]. [<sup>111</sup>In]1/2/3 are [DOTA,DGlu<sup>10</sup>]gastrin(10-17) analogs containing DGlu at position 10 and the highly polar and sterically bulky <sup>111</sup>In-DOTA-chelate at position 9. These two residues are expected to have similar impact on the proteolytic action of ACE as the two N-terminal Glu<sup>9,10</sup>-residues of the ACE-resistant analog [Leu<sup>15</sup>]gastrin(9-17). On the other hand, the effect of Glu-residue introduction at the N-terminus of gastrin analogs on their resistance to NEP has not been investigated thus far. The penta-Glu<sup>6-10</sup>-chain of gastrin radioligands was previously shown to be essential not only for metabolic stability, but also for other important pharmacological parameters, such as CCK2R-affinity, in vivo tumor targeting and renal retention. In general, *des*-(Glu)<sub>5</sub>-gastrin radioligands are prone to fast proteolytic degradation leading to poor tumor targeting, but possess the unique advantage of low kidney accumulation [9,11,17,18].

In the present study, we have compared the in vivo stability of three truncated gastrin <sup>111</sup>In-radioligands, [<sup>111</sup>In]1/2/3, with the full-length minigastrin reference [<sup>111</sup>In]4. In agreement with previous studies, non-truncated minigastrin was much more stable in mouse blood (Figure 4). Interestingly however, during in vivo NEP-inhibition induced by PA, all radioligands were detected >80% intact in mouse bloodstream directly implicating NEP in their in vivo catabolism. As expected, the truncated more degradation-vulnerable [<sup>111</sup>In]1/2/3 profited more by PA. These findings correlated well with biodistribution results in mice bearing CCK2R-expressing xenografts. Concordant to analogous findings from previous studies, renal accumulation of truncated [<sup>111</sup>In]1/2/3 was low, but their tumor uptake was also low. In contrast, the [<sup>111</sup>In]4 reference displayed better tumor uptake, but unfavorably high localization in the kidneys (Figure 5), leading to poor tumor-to-kidney ratios.

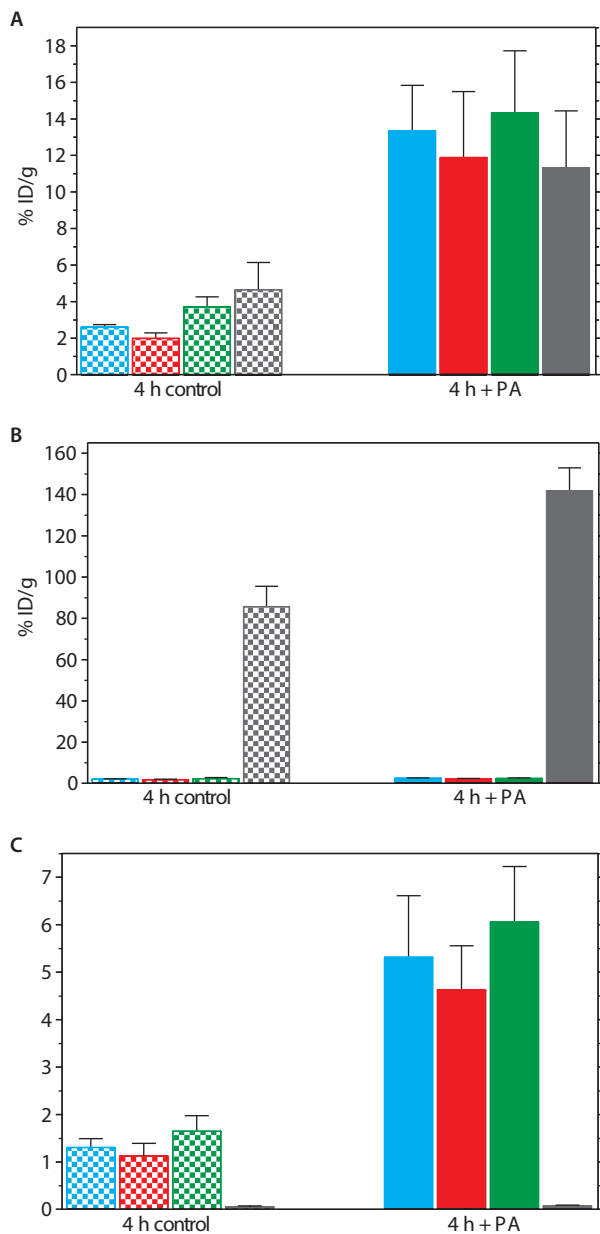


**Figure 5 |** Comparative biodistribution data of [<sup>111</sup>In]1 (■, □), [<sup>111</sup>In]2 (■, □), [<sup>111</sup>In]3 (■, □) and [<sup>111</sup>In]4 (■, □) in SCID mice bearing AR42J tumors at 4 h pi; patterned bars represent control groups (mice coinjecting with vehicle only) and solid bars PA-groups (mice coinjecting with PA). Data expressed as %ID/g±SD (n≥4) are selectively shown for **A**) AR42J tumor, **B**) kidneys and **C**) tumor-to-kidney ratios.

These results were dramatically affected during NEP-inhibition by PA. Tumor uptake of *des*(Glu)<sub>5</sub>-analogs [<sup>111</sup>In]1/2/3 surpassed the tumor values of the [<sup>111</sup>In]4 reference, while renal uptake remained low and unaffected by PA (Figure 5). In contrast, the initially high kidney uptake of [<sup>111</sup>In]4 significantly increased even further by PA. As a result, very favorable for clinical translation tumor-to-kidney values were achieved only by the truncated [<sup>111</sup>In]1/2/3 radiotracers during NEP-inhibition.



## CONCLUSION

In situ NEP-inhibition by single co-injection of PA has proven effective in increasing the in vivo stability and hence the tumor uptake of several biodegradable radiopeptides. In the present study, we have demonstrated the efficacy of in vivo NEP-inhibition in improving the diagnostic profile of a series of truncated gastrin radioligands [<sup>111</sup>In]1/2/3, as compared to a non-truncated [<sup>111</sup>In]4 reference, previously reported for good tumor targeting, but unfavorably high kidney retention. Co-administration of PA induced impressive enhancement of tumor uptake in two separate animal models as a result of higher bioavailability. Thus, during PA-treatment [<sup>111</sup>In]1/2/3 – unlike the pentaGlu-containing [<sup>111</sup>In]4 reference – attained remarkable tumor-to-kidney ratios with clear prospects for improved diagnostic efficacy of CCK2R-positive tumors in man. Furthermore, these findings reveal therapeutic options for 1/2/3 labeled with therapeutic beta emitters, like <sup>90</sup>Y or <sup>177</sup>Lu, during in vivo NEP-inhibition adopting a theranostic approach. Work in this direction is currently pursued.

Eventually, translation of the concept in the clinic needs to be explored, initially via a pilot proof-of-principle study in patients. Accordingly, critical requirements need to be competently addressed first, especially those related to safety and efficacy challenges. To achieve this goal, selection of NEP-inhibitor type, efficacy dose and toxicity limits in human are only some of the parameters, which we are now in the process of thoroughly and systematically investigating.

## Acknowledgments

The Authors wish to thank Mrs. Xanthippi Kotsaka, Aikaterini Tatsi and Mr. Panteleimon J. Marsouvandis for their assistance in the metabolic stability and biodistribution experiments.

## Abbreviations

Gastrin= pGlu-Gly-Pro-Trp-Leu-(Glu)<sub>5</sub>-Ala-Tyr-Gly-Trp-Met-Asp-Phe-NH<sub>2</sub>; DOTA= 1,4,7,10-tetraazacyclododecane-1,4,7,10-tetraacetic acid; Ahp= 2-Aminoheptanoic acid; [<sup>125</sup>I-Tyr<sup>12</sup>,Leu<sup>15</sup>]gastrin= pGlu-Gly-Pro-Trp-Leu-(Glu)<sub>5</sub>-Ala-<sup>125</sup>I-Tyr-Gly-Trp-Leu-Asp-Phe-NH<sub>2</sub>; DG2= Demogastrin 2 (N<sub>4</sub>-Gly-DGlu-(Glu)<sub>5</sub>-Ala-Tyr-Gly-Trp-Met-Asp-Phe-NH<sub>2</sub>, N<sub>4</sub>= 6-(carboxyl)-1,4,8,11-tetraazaundecane); [<sup>111</sup>In-DOTA]MG0= DOTA-Minigastrin 0 (DOTA-DGlu-(Glu)<sub>5</sub>-Ala-Tyr-Gly-Trp-Met-Asp-Phe-NH<sub>2</sub>); [Leu<sup>15</sup>]gastrin= pGlu-Gly-Pro-Trp-Leu-(Glu)<sub>5</sub>-Ala-Tyr-Gly-Trp-Leu-Asp-Phe-NH<sub>2</sub>; SPPS= solid phase peptide synthesis; IC<sub>50</sub>= concentration inhibiting 50% of maximum radioligand binding.

## REFERENCES

1. Reubi JC, Schaer JC, Waser B. Cholecystokinin(CCK)-A and CCK-B/gastrin receptors in human tumors. *Cancer Res.* 1997;57(7):1377-86.
2. Reubi JC. CCK receptors in human neuroendocrine tumors: clinical implications. *Scand J Clin Lab Invest Suppl.* 2001;234:101-4.
3. Reubi JC, Waser B. Unexpected high incidence of cholecystokinin-B/gastrin receptors in human medullary thyroid carcinomas. *Int J Cancer.* 1996;67(5):644-7.
4. Behr TM, Jenner N, Radetzky S, Béhé M, Gratz S, Yucekent S, et al. Targeting of cholecystokinin-B/gastrin receptors in vivo: preclinical and initial clinical evaluation of the diagnostic and therapeutic potential of radiolabelled gastrin. *Eur J Nucl Med.* 1998;25(4):424-30.
5. Behr TM, Béhé M, Angerstein C, Gratz S, Mach R, Hagemann L, et al. Cholecystokinin-B/gastrin receptor binding peptides: preclinical development and evaluation of their diagnostic and therapeutic potential. *Clin Cancer Res.* 1999;5(10 Suppl):3124s-38s.
6. Béhé M, Behr TM. Cholecystokinin-B (CCK-B)/gastrin receptor targeting peptides for staging and therapy of medullary thyroid cancer and other CCK-B receptor expressing malignancies. *Biopolymers.* 2002;66(6):399-418.
7. de Jong M, Bakker WH, Bernard BF, Valkema R, Kwekkeboom DJ, Reubi JC, et al. Preclinical and initial clinical evaluation of <sup>111</sup>In-labeled nonsulfated CCK8 analog: a peptide for CCK-B receptor-targeted scintigraphy and radionuclide therapy. *J Nucl Med.* 1999;40(12):2081-7.
8. Nock BA, Maina T, Béhé M, Nikolopoulou A, Gotthardt M, Schmitt JS, et al. CCK-2/gastrin receptor-targeted tumor imaging with <sup>99m</sup>Tc-labeled minigastrin analogs. *J Nucl Med.* 2005;46(10):1727-36.
9. Fröberg AC, de Jong M, Nock BA, Breeman WA, Erion JL, Maina T, et al. Comparison of three radiolabelled peptide analogues for CCK-2 receptor scintigraphy in medullary thyroid carcinoma. *Eur J Nucl Med Mol Imaging.* 2009;36(8):1265-72.
10. Sosabowski JK, Matzow T, Foster JM, Finucane C, Ellison D, Watson SA, et al. Targeting of CCK-2 receptor-expressing tumors using a radiolabeled divalent gastrin peptide. *J Nucl Med.* 2009;50(12):2082-9.
11. Laverman P, Joosten L, Eek A, Roosenburg S, Peitl PK, Maina T, et al. Comparative biodistribution of 12 <sup>111</sup>In-labelled gastrin/CCK2 receptor-targeting peptides. *Eur J Nucl Med Mol Imaging.* 2011;38(8):1410-6.
12. Roosenburg S, Laverman P, Joosten L, Cooper MS, Kolenc-Peitl PK, Foster JM, et al. PET and SPECT imaging of a radiolabeled minigastrin analogue conjugated with DOTA, NOTA, and NODAGA and labeled with <sup>64</sup>Cu, <sup>68</sup>Ga, and <sup>111</sup>In. *Mol Pharm.* 2014;11(11):3930-7.
13. Mather SJ, McKenzie AJ, Sosabowski JK, Morris TM, Ellison D, Watson SA. Selection of radiolabeled gastrin analogs for peptide receptor-targeted radionuclide therapy. *J Nucl Med.* 2007;48(4):615-22.
14. Dockray GJ, Varro A, Dimaline R, Wang T. The gastrins: their production and biological activities. *Annu Rev Physiol.* 2001;63:119-39.
15. Copps J, Murphy RF, Lovas S. The structure of bioactive analogs of the N-terminal region of gastrin-17. *Peptides.* 2009;30(12):2250-62.
16. Copps J, Murphy RF, Lovas S. The production and role of gastrin-17 and gastrin-17-gly in gastrointestinal cancers. *Protein Pept Lett.* 2009;16(12):1504-18.
17. Breeman WA, Fröberg AC, de Blois E, van Gameren A, Melis M, de Jong M, et al. Optimised labeling, preclinical and initial clinical aspects of CCK-2 receptor-targeting with 3 radiolabeled peptides. *Nucl Med Biol.* 2008;35(8):839-49.
18. Ocak M, Helbok A, Rangger C, Peitl PK, Nock BA, Morelli G, et al. Comparison of biological stability and metabolism of CCK2 receptor targeting peptides, a collaborative project under COST BM0607. *Eur J Nucl Med Mol Imaging.* 2011;38(8):1426-35.
19. Trejtnar F, Laznickova M, Laznickova A, Kopecky M, Petrik M, Béhé M, et al. Biodistribution and elimination characteristics of two <sup>111</sup>In-labeled CCK-2/gastrin receptor-specific peptides in rats. *Anticancer Res.* 2007;27(2):907-12.
20. Gotthardt M, van Eerd-Vismale J, Oyen WJ, de Jong M, Zhang H, Rolleman E, et al. Indication for different mechanisms of kidney uptake of radiolabeled peptides. *J Nucl Med.* 2007;48(4):596-601.

21. von Guggenberg E, Rangger C, Sosabowski J, Laverman P, Reubi JC, Virgolini IJ, et al. Preclinical evaluation of radiolabeled DOTA-derivatized cyclic minigastrin analogs for targeting cholecystokinin receptor expressing malignancies. *Mol Imaging Biol.* 2012;14(3):366-75.
22. Kolenc-Peittl P, Mansi R, Tamma M, Gmeiner-Stopar T, Sollner-Dolenc M, Waser B, et al. Highly improved metabolic stability and pharmacokinetics of indium-111-DOTA-gastrin conjugates for targeting of the gastrin receptor. *J Med Chem.* 2011;54(8):2602-9.
23. von Guggenberg E, Sallegger W, Helbok A, Ocak M, King R, Mather SJ, et al. Cyclic minigastrin analogues for gastrin receptor scintigraphy with technetium-99m: preclinical evaluation. *J Med Chem.* 2009;52(15):4786-93.
24. Roques BP, Noble F, Dauge V, Fournie-Zaluski MC, Beaumont A. Neutral endopeptidase 24.11: structure, inhibition, and experimental and clinical pharmacology. *Pharmacol Rev.* 1993;45(1):87-146.
25. Suda H, Aoyagi T, Takeuchi T, Umezawa H. Letter: A thermolysin inhibitor produced by Actinomycetes: phospholamidin. *J Antibiot (Tokyo).* 1973;26(10):621-3.
26. Oefner C, D'Arcy A, Hennig M, Winkler FK, Dale GE. Structure of human neutral endopeptidase (Nepriylsin) complexed with phosphoramidon. *J Mol Biol.* 2000;296(2):341-9.
27. Nock BA, Maina T, Krenning EP, de Jong M. "To serve and protect": enzyme inhibitors as radiopeptide escorts promote tumor targeting. *J Nucl Med.* 2014;55(1):121-7.
28. Moroder L, Gohring W, Nyfeler R, Scharf R, Thamm P, Wendlberger G. [Syntheses of human little gastrin-I and its leucine-15, norleucine-15 and methoxinine-15 analogs]. *Hoppe Seylers Z Physiol Chem.* 1983;364(2):157-71.
29. Good S, Walter MA, Waser B, Wang X, Muller-Brand J, Béhé MP, et al. Macrocyclic chelator-coupled gastrin-based radiopharmaceuticals for targeting of gastrin receptor-expressing tumours. *Eur J Nucl Med Mol Imaging.* 2008;35(10):1868-77.
30. Horwell DC, Howson W, Rees DC. 'Peptoid' design. *Drug Des Discov.* 1994;12(1):63-75.
31. Scemama JL, De Vries L, Pradayrol L, Seva C, Tronchere H, Vaysse N. Cholecystokinin and gastrin peptides stimulate ODC activity in a rat pancreatic cell line. *Am J Physiol.* 1989;256(5 Pt 1):G846-50.
32. Aloj L, Caracó C, Panico M, Zannetti A, Del Vecchio S, Tesauro D, et al. In vitro and in vivo evaluation of <sup>111</sup>In-DTPAGlu-G-CCK8 for cholecystokinin-B receptor imaging. *J Nucl Med.* 2004;45(3):485-94.
33. Reubi JC, Waser B, Laderach U, Stettler C, Friess H, Halter F, et al. Localization of cholecystokinin A and cholecystokinin B-gastrin receptors in the human stomach. *Gastroenterology.* 1997;112(4):1197-205.
34. Roques BP. Zinc metallopeptidases: active site structure and design of selective and mixed inhibitors: new approaches in the search for analgesics and anti-hypertensives. *Biochem Soc Trans.* 1993;21 ( Pt 3)(3):678-85.
35. Deschodt-Lanckman M, Pauwels S, Najdovski T, Dimaline R, Dockray GJ. In vitro and in vivo degradation of human gastrin by endopeptidase 24.11. *Gastroenterology.* 1988;94(3):712-21.
36. Roques BP, Durieux C, Gacel G, Pelaprat D, Ruiz-Gayo M, Belleney J, et al. Studies on the conformation, enzymatic degradation, pharmacological potency, and binding properties in brain tissue of cholecystokinin-8 and new related peptides. *Ann NY Acad Sci.* 1985;448:61-75.
37. Durieux C, Charpentier B, Fellion E, Gacel G, Pelaprat D, Roques BP. Multiple cleavage sites of cholecystokinin heptapeptide by "enkephalinase". *Peptides.* 1985;6(3):495-501.
38. Dubreuil P, Fulcrand P, Rodriguez M, Fulcrand H, Laur J, Martinez J. Novel activity of angiotensin-converting enzyme. Hydrolysis of cholecystokinin and gastrin analogues with release of the amidated C-terminal dipeptide. *Biochem J.* 1989;262(1):125-30.



# CHAPTER

# 4

## Improving the in Vivo Profile of Minigastrin Radiotracers – A Comparative Study Involving the Neutral Endopeptidase Inhibitor Phosphoramidon

Aikaterini Kaloudi<sup>1</sup>, Berthold A. Nock<sup>1</sup>, Emmanouil Lympers<sup>1</sup>,  
Eric P. Krenning<sup>2</sup>, Marion de Jong<sup>2,3</sup>, Theodosia Maina<sup>1</sup>

<sup>1</sup>Molecular Radiopharmacy, INRASTES, National Center for Scientific Research  
“Demokritos”, GR-153 10 Athens, Greece

<sup>2</sup>Department of Nuclear Medicine, Erasmus MC, 3015 CE Rotterdam,  
The Netherlands

<sup>3</sup>Department of Radiology, Erasmus MC, 3015 CE Rotterdam,  
The Netherlands

*Cancer Biother. Radiopharm.* 31(1):20-8, 2016

## ABSTRACT

Minigastrin radiotracers, like [ $^{111}\text{In}$ -DOTA]MG0 ([ $^{111}\text{In}$ -DOTA-DGlu<sup>1</sup>]minigastrin), have been considered for diagnostic imaging and radionuclide therapy of CCK2R-positive human tumors, such as medullary thyroid carcinoma. However, the high kidney retention assigned to the pentaGlu<sup>2-6</sup>-repeat in the peptide sequence has compromised their clinical applicability. On the other hand, truncated *des*(Glu)<sup>2-6</sup>-analogs, like [ $^{111}\text{In}$ -DOTA]MG11 ([ $^{111}\text{In}$ -DOTA-DGlu<sup>10</sup>,*des*Glu<sup>2-6</sup>]minigastrin), despite their low renal uptake show poor bioavailability and tumor targeting. [ $^{111}\text{In}$ ]CP04 ([ $^{111}\text{In}$ -DOTA-DGlu<sup>1-6</sup>]minigastrin) acquired by Glu<sup>2-6</sup>/DGlu<sup>2-6</sup> substitution showed promising tumor-to-kidney ratios in rodents. In the present study, we compare the biological profiles of [ $^{111}\text{In}$ ]CP04, [ $^{111}\text{In}$ -DOTA]MG11 and [ $^{111}\text{In}$ -DOTA]MG0 during in situ neutral endopeptidase (NEP)-inhibition, recently shown to improve the bioavailability of several peptide radiotracers. After coinjection of the NEP-inhibitor phosphoramidon (PA), the stability of [ $^{111}\text{In}$ ]CP04 and [ $^{111}\text{In}$ -DOTA]MG0 in peripheral mouse blood increased, with an exceptional >14-fold improvement monitored for [ $^{111}\text{In}$ -DOTA]MG11. In line with these findings, PA treatment increased the uptake of [ $^{111}\text{In}$ ]CP04 (8.5±0.4%ID/g to 16.0±2.3%ID/g) and [ $^{111}\text{In}$ -DOTA]MG0 (11.9±2.2%ID/g to 17.2±0.9%ID/g) in A431-CCK2R(+) tumors at 4 h postinjection, whereas the respective increase for [ $^{111}\text{In}$ -DOTA]MG11 was >6-fold (2.5±0.9%ID/g to 15.1±1.7%ID/g). Interestingly, kidney uptake remained lowest for [ $^{111}\text{In}$ -DOTA]MG11, but unfavourably increased by PA treatment for [ $^{111}\text{In}$ -DOTA]MG0. Thus, overall the most favourable in vivo profile was displayed by [ $^{111}\text{In}$ -DOTA]MG11 during NEP-inhibition, highlighting the need to validate this promising concept in the clinic.

**Key words:** cholecystokinin subtype 2-receptor, Glu<sup>2-6</sup>-modified minigastrin, minigastrin radioligand, tumor targeting, kidney retention, neutral endopeptidase, phosphoramidon

## INTRODUCTION

The overexpression of cholecystokinin subtype 2 receptors (CCK2R) has been demonstrated in several human tumors, including medullary thyroid carcinoma (MTC), small cell lung cancer, astrocytomas and stromal ovarian cancers [1-3]. This finding combined with the lack of CCK2R-expression in healthy surrounding tissues provides promising opportunities for high contrast diagnostic imaging and radionuclide therapy of tumors with CCK2R-seeking radioligands [4-11]. Minigastrin (MG, Leu-(Glu)<sub>5</sub>-Ala-Tyr-Gly-Trp-Met-Asp-Phe-NH<sub>2</sub>) based radioligands developed for such purposes, such as [<sup>111</sup>In-DOTA]MG0 ([<sup>111</sup>In-DOTA-DGlu<sup>1</sup>]MG), showed high CCK2R-affinity and good metabolic stability, resulting in high targeting of CCK2R-positive lesions in animals and in man. However, their clinical applicability has been largely restrained by unfavorably high retention in the kidneys [12,13,14].

One approach to suppress renal accumulation has been the full truncation of the implicated pentaGlu<sup>2-6</sup>-chain in the minigastrin sequence [15]. Yet, this modification has inadvertently led to poor metabolic stability and suboptimal tumor localization of the corresponding radioligands, such as [<sup>111</sup>In-DOTA]MG11 ([<sup>111</sup>In-DOTA-DGlu<sup>1</sup>,*des*Glu<sup>2-6</sup>]MG) [10,11,16,17]. Alternatively, a number of structural modifications have been directed to the critical pentaGlu<sup>2-6</sup>-repeat of the minigastrin motif, including substitution of selected or all five Glu-residues by Gln, or DGlu, to modulate charge, charge distribution and stereochemistry in this part of the molecule [18,19]. The radiotracer [<sup>111</sup>In]CP04 ([<sup>111</sup>In-DOTA-DGlu<sup>1-6</sup>]MG) was accordingly developed by complete Glu<sup>2-6</sup>/DGlu<sup>2-6</sup> substitution within the frameworks of a concerted European COST Action (BM0607 Targeted Radionuclide Therapy). Owing to attractive tumor-to-kidney ratios achieved in animal models [<sup>111</sup>In]CP04 was selected among 12 other CCK2R-targeting radiopeptide candidates for further clinical validation in MTC patients [16].

We have recently proposed an innovative approach to enhance the bioavailability and thereby the tumor localization of a wide array of peptide radioligands, including those based on minigastrin [20]. This strategy exploits the prominent role of neutral endopeptidase (NEP) in the *in vivo* catabolism of peptide radiotracers, relying both on its ubiquitous and abundant expression in various tissues and organs of the body as well as on its broad substrate specificity [21]. The impact of NEP on metabolic stability has been often overseen in the field of nuclear medicine, primarily because NEP is an ectoenzyme anchored on vasculature walls and on the surface of tissue cells, but absent in serum or plasma typically used for measuring radiopeptide stability. Coinjection of a potent NEP inhibitor, like phosphoramidon (PA) [22, 23], together with a radiopeptide allows high supply of intact radioligand to receptor-expressing tumor sites, thereby inducing significant enhancement of tumor uptake.

In the present work, we have been interested to assess the efficacy of this strategy in three distinct minigastrin radiotracers differing in the pentaGlu<sup>2-6</sup>-chain, which is critical for radiopeptide metabolic stability, tumor localization and renal retention. For this purpose, we have conducted a head-to-head comparison of [<sup>111</sup>In-DOTA]MG0, its DGlu<sup>2-6</sup> counterpart [<sup>111</sup>In]CP04 and the truncated *des*(Glu)<sup>2-6</sup>-analog [<sup>111</sup>In-DOTA]MG11 during *in vivo* NEP-inhibition by phosphoramidon. Emphasis has been given on the assessment of potential benefits in overall pharmacokinetics of the three structurally different radiotracers induced by PA, especially regarding tumor-to-kidney ratio enhancement.

## MATERIALS AND METHODS

### Compounds and Instrumentation

All chemicals used were reagent grade. CP04, DOTA-MG0 and DOTA-MG11 (Figure 1) as well as DG2 (Demogastrin 2,  $N_4$ -Gly-DGlu-(Glu)<sub>5</sub>-Ala-Tyr-Gly-Trp-Met-Asp-Phe-NH<sub>2</sub>;  $N_4$ , 6-(carboxyl)-1,4,8,11-tetraazaundecane)<sup>9</sup> used for CCK2R-blockade were purchased from piCHEM (Graz, Austria). [<sup>15</sup>Leu]gastrin (pGlu-Gly-Pro-Trp-Leu-(Glu)<sub>5</sub>-Ala-Tyr-Gly-Trp-Leu-Asp-Phe-NH<sub>2</sub>) was obtained from Bachem (Bubendorf, Switzerland). PA (N-( $\alpha$ -rhamnopyranosyloxyhydroxyphosphinyl)-L-leucyl-L-tryptophan $\times$ 2Na $\times$ 2H<sub>2</sub>O) was provided by PeptaNova GmbH (Sandhausen, Germany). For <sup>111</sup>In labeling, <sup>111</sup>InCl<sub>3</sub> was purchased from Mallinckrodt Medical B.V. (Petten, The Netherlands) in a solution of 0.05 M HCl (0.5 mL); for <sup>125</sup>I-labeling, Na<sup>125</sup>I was purchased from MDS Nordion, SA (Fleurus, Belgium) in a solution of 10<sup>-5</sup> M NaOH (10  $\mu$ L).

HPLC analyses were conducted on a Symmetry shield RP18 column (3.9  $\times$  20 mm, 5  $\mu$ m) using Waters Chromatograph with a 600 solvent delivery system coupled to a 996 photodiode array UV detector and a Gabi gamma detector (Raytest RSM Analytische Instrumente GmbH). The Millennium Software was used for data processing and for controlling the HPLC system. For radioactivity measurements an automated well-type gamma counter [NaI(Tl) crystal, Canberra Packard Auto-Gamma 5000 series instrument] calibrated for <sup>111</sup>In or <sup>125</sup>I was used.

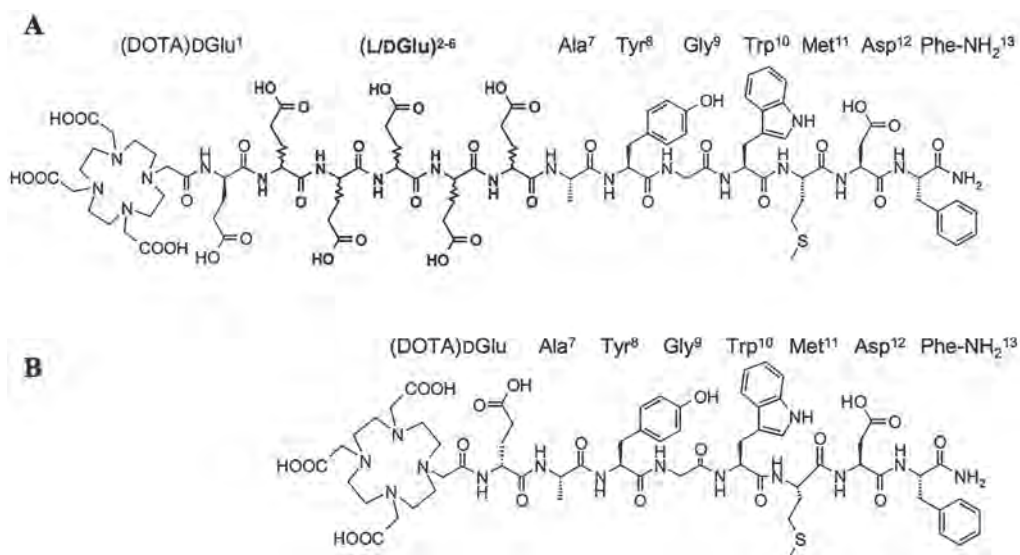


Figure 1 | Chemical structure of DOTA-MG0 ([DOTA-DGlu<sup>1</sup>,LGLu<sup>2-6</sup>]MG), CP04 ([DOTA,DGLu<sup>1-6</sup>]MG) **A** and DOTA-MG11 ([DOTA-DGlu<sup>1</sup>,desGlu<sup>2-6</sup>]MG) **B**.



## Radiolabeling and Quality Control

The lyophilized peptides were dissolved in water to a final concentration of 1 mM and 50  $\mu$ L-aliquots were stored at  $-20^{\circ}\text{C}$ . Labeling with  $^{111}\text{In}$  was conducted by adding 10 nmol peptide per 37–74 MBq of  $^{111}\text{InCl}_3$  in 0.1 M sodium acetate buffer and 0.1 M D,L-Met. Typical end pH was 4.6. Labeling was completed after incubation at  $90^{\circ}\text{C}$  for 10–15 min. Prior to HPLC quality control EDTA in 0.1 M acetate buffer was added to a final concentration of 1 mM to the labeling reaction mixture as a free  $^{111}\text{In}^{3+}$  scavenger. Radiochemical yield and purity were evaluated by HPLC analysis, applying gradient system 1 at 1 mL/min flow rate (100% A / 0% B to 60% A / 40% B in 40 min; A= 0.1% TFA in  $\text{H}_2\text{O}$  and B= MeCN). Radiotracers were used after labeling without further purification. For all subsequent biological experiments solutions containing Met and EDTA were used.

Radioiodination of [Leu $^{15}$ ]gastrin was performed following the chloramine-T methodology and [ $^{125}\text{I}$ -Tyr $^{12}$ ,Leu $^{15}$ ]gastrin was isolated in high purity by HPLC. A stock solution in 0.5% BSA-PBS buffer was kept at  $-20^{\circ}\text{C}$  and aliquots thereof were used for competition binding assays (specific activity 2 Ci/ $\mu\text{mol}$ ).

All manipulations with gamma emitting radionuclides and their solutions were performed behind suitable shielding in dedicated laboratories in compliance to national and international radiation safety guidelines.

## Preparation of [ $^{nat}\text{In}$ ]CP04

Metalation of CP04 with  $^{nat}\text{In}$  was conducted by adding 70 nmol peptide per 350 nmol  $^{nat}\text{In}(\text{NO}_3)_3$  in 0.1 M sodium acetate buffer (pH 3–5). To prevent oxidation of Met-residue to the corresponding sulfoxides 0.2 M D,L-Met solution was added in the labeling reaction mixture to a final concentration of 13 mM. The reaction mixture was incubated for 20 min at  $90^{\circ}\text{C}$ . As described above, EDTA was added as a free  $^{nat}\text{In}^{3+}$  scavenger and [ $^{nat}\text{In}$ ]CP04 was isolated pure by HPLC adopting gradient system 2 (linear gradient elution at a flow rate of 1 mL/min with: 100% A / 0% B to 85% A / 15% B within 5 min, to 80% A / 20% B in the next 10 min, then to 78% A / 22% B for another 8 min and then holding isocratic; A= 0.1% TFA in  $\text{H}_2\text{O}$  and B= MeCN).

## Cell Culture

Human epidermoid carcinoma A431 cell lines transfected to stably express the human CCK2R (A431-CCK2R(+) cells) or mock-transfected with an empty vector (A431-CCK2R(-) cells) were a generous gift from Prof. O. Boerman (Department of Nuclear Medicine, Radboud University Nijmegen Medical Centre, Nijmegen, The Netherlands) and Prof. L. Aloj (Istituto di Biostrutture e Bioimmagini, Consiglio Nazionale delle Ricerche, Naples, Italy) [24]. Cells were kept in a controlled humidified air containing 5%  $\text{CO}_2$  at  $37^{\circ}\text{C}$  and were cultured in Dulbecco's Modified Eagle medium with GlutaMAX-I supplemented with 10% (v/v) fetal bovine serum, 100 U/mL penicillin, 100  $\mu\text{g}/\text{mL}$  streptomycin and 4,500 mg/L D-glucose and 250  $\mu\text{g}/\text{mL}$  G418. Splitting of cells with a ratio of 1:3 to 1:5 was performed when approaching confluency using a trypsin/EDTA solution (0.05%/0.02% w/v). All culture reagents were provided from Gibco BRL, Life Technologies or from Biochrom KG Seromed.

### Competition Binding Assays in A431-CCK2R(+) Cell Membranes

The binding affinity of CP04 and [<sup>125</sup>I]CP04 for the human CCK2R was determined by competition binding experiments in A431-CCK2R(+) cell membranes harvested as previously described [25]. [<sup>125</sup>I-Tyr<sup>12</sup>,Leu<sup>15</sup>]gastrin served as competitive radioligand and [Leu<sup>15</sup>]gastrin as reference. Increasing concentrations of test peptide ( $10^{-5}$ - $10^{-13}$  M) were incubated for 1 h at 22°C with the radioligand (50 pM, ~30,000 cpm) and the membrane homogenate in a total volume of 300 µL binding buffer (BB, 50 mM HEPES pH 7.4, 1% BSA, 5.5 mM MgCl<sub>2</sub>, 35 µM bacitracin). Binding was interrupted by addition of ice-cold washing buffer (WB, 10 mM HEPES pH 7.4, 150 mM NaCl) and rapid filtration (Whatman GF/B filters presoaked in BB) on a Brandel Cell Harvester (Adi Hassel Ing. Büro, Munich, Germany). Filters were washed with ice-cold WB and were measured for radioactivity in the gamma counter. IC<sub>50</sub> values were calculated by nonlinear regression according to a one-site model applying the PRISM 2 program (Graph Pad Software, San Diego, CA). Results are expressed as mean±SD of four experiments performed in triplicate.

### Cell-Association and Internalization in A431-CCK2R(+) Cells

Radioligand cell-association and internalization experiments were performed in A431-CCK2R(+) cells grown for 24 h to confluency in six-well plates. On the day of the experiment, cells were washed twice with ice-cold internalization medium (DMEM Glutamax-I with 1% FBS). Fresh medium (1.2 mL) was added to the cells, followed by [<sup>111</sup>In]CP04, [<sup>111</sup>In-DOTA]MG0 or [<sup>111</sup>In-DOTA]MG11 (150 µL, 250 fmol total peptide in 150 µL 0.5% BSA-PBS, 50,000–90,000 cpm); non-specific values were determined by a parallel triplicate series containing 1 µM DG2 [9]. Cells were incubated at 37°C for 60 min and incubation was interrupted by removal of the medium and rapid rinsing with ice-cold 0.5% BSA-PBS. Membrane-bound and internalized fractions were separated by 2×5 min treatment in acid wash buffer (50 mM glycine in 0.1 M NaCl, pH 2.8). Cells were rinsed with 0.5% BSA-PBS, lysed with 1 N NaOH and lysates were collected. Samples were measured for their radioactivity content in the γ-counter and the percentage of internalized and membrane bound fractions were calculated using the Microsoft Excel program. Results represent average values±SD from 4 ([<sup>111</sup>In]CP04) or 3 ([<sup>111</sup>In-DOTA]MG0 and [<sup>111</sup>In-DOTA]MG11) experiments performed in triplicate.

### Metabolic Studies in Mice

A bolus of [<sup>111</sup>In]CP04, [<sup>111</sup>In-DOTA]MG0 or [<sup>111</sup>In-DOTA]MG11 (100 µL, 11–22 MBq, 3 nmol total peptide in vehicle: saline/EtOH 9/1 v/v) was injected together with vehicle (100 µL; control group) or with PA (100 µL of vehicle containing 300 µg PA; PA group) in the tail vein of healthy Swiss albino mice (NCSR “Demokritos” Animal House Facility). Blood was withdrawn 5 min post injection (pi) and directly placed in pre-chilled polypropylene tubes containing EDTA and D,L-Met. Blood samples were centrifuged (10 min, 2,000×g / 4°C, in a Hettich, Universal 320R, centrifuge, Tuttlingen, Germany). The plasma was collected, mixed with chilled MeCN in a 1/1 v/v ratio and centrifuged again (10 min, 15,000×g / 4°C). Supernatants were concentrated to a small volume under a gentle N<sub>2</sub>-flux at 40°C, diluted with physiological saline (≈400 µL) and filtered through a Millex GV filter (0.22 µm). HPLC analyses were conducted adopting gradient system 3: flow rate of 1 mL/min with a linear gradient 100% A / 0% B to 60% A / 40% B within 40 min; A= 0.1% aqueous TFA and B= MeCN.

The elution times ( $t_R$ ) of intact radiopeptides were determined by coinjection of blood samples with the respective  $^{111}\text{In}$ -labeled peptide. Experiments were conducted twice except for [ $^{111}\text{In}$ -DOTA]MG11 controls performed 3 times.

### **Biodistribution in SCID Mice Bearing A431-CCK2R(+/-) Xenografts**

Inocula (~150  $\mu\text{L}$ ) containing a suspension of freshly harvested A431-CCK2R(+) cells ( $1.6 \times 10^7$ ) or A431-CCK2R(-) cells ( $1.4 \times 10^7$ ) in sterile physiological saline were subcutaneously injected in the flanks of 6 weeks-old male SCID mice (NCSR "Demokritos" Animal House Facility). After 6-8 days well palpable tumors ( $190 \pm 80$  mg) were grown at the inoculation sites and biodistribution was performed. A bolus of [ $^{111}\text{In}$ ]CP04, [ $^{111}\text{In}$ -DOTA]MG0 or [ $^{111}\text{In}$ -DOTA]MG11 (100  $\mu\text{L}$ , 37-74 MBq, 10 pmol total peptide in saline/EtOH 9/1 v/v) was intravenously injected in the tail of mice together with vehicle (100  $\mu\text{L}$ ; control group) or with PA (100  $\mu\text{L}$  of vehicle containing 300  $\mu\text{g}$  PA; PA group). Animals were sacrificed in groups of 5 at 4 h pi. Blood samples were collected and organs of interest as well as tumors were dissected, weighted and counted in the gamma counter; stomachs were emptied of their contents. Results were calculated as percent injected dose per gram tissue (%ID/g) with the aid of suitable standards of the injected dose using the Microsoft Excel program and are reported as mean  $\pm$  SD.

All animal experiments were carried out in compliance with European and national regulations and after approval of protocols by national Authorities.

### **Statistical Analysis**

The unpaired two-tailed student's *t* test of Graph Pad Prism Software (San Diego, SA) was used for statistical analysis; *P* values of less than 0.05 were considered statistically significant.

## **RESULTS**

### **Radioligand Preparation**

Radiolabeling of CP04, DOTA-MG0 and DOTA-MG11 with  $^{111}\text{InCl}_3$  was completed by 10–15 min incubation in acidic medium at 90°C in the presence of excess methionine to suppress sulfoxide formation and EDTA to bind any free  $^{111}\text{In}$ . More than 97% of radiometal was incorporated in the DOTA chelator of the peptides at specific activity of 3.7–7.4 MBq/nmol and >95% radiochemical purity was achieved while recovery from the column was quantitative. These results allowed the use of the forming radioligands without purification in all subsequent experiments in EDTA and Met-containing solutions. Quality control before and after biodistribution experiments revealed the preservation of high radiotracer purity in the injectates till completion of the study.

### **Affinity of CP04 and [ $^{nat}\text{In}$ ]CP04 for CCK2R**

The affinity of CP04 and [ $^{nat}\text{In}$ ]CP04 for the human CCK2R was determined by competition binding experiments in A431-CCK2R(+) cell membranes. As shown in Figure 2, both unmetalated and  $^{nat}\text{In}$ -metalated CP04 displaced [ $^{125}\text{I}$ -Tyr $^{12}$ ,Leu $^{15}$ ]gastrin from the human CCK2R binding sites in a

monophasic and dose dependent manner. The binding affinity of CP04 to CCK2R ( $IC_{50} = 1.28 \pm 0.09$  nM,  $n=4$ ) was found comparable to [ $Leu^{15}$ ]gastrin ( $IC_{50} = 0.86 \pm 0.05$  nM,  $n=4$ ), while incorporation of  $^{nat}In$  led to a minor drop of receptor affinity ( $IC_{50} = 3.17 \pm 0.21$  nM,  $n=4$ ).

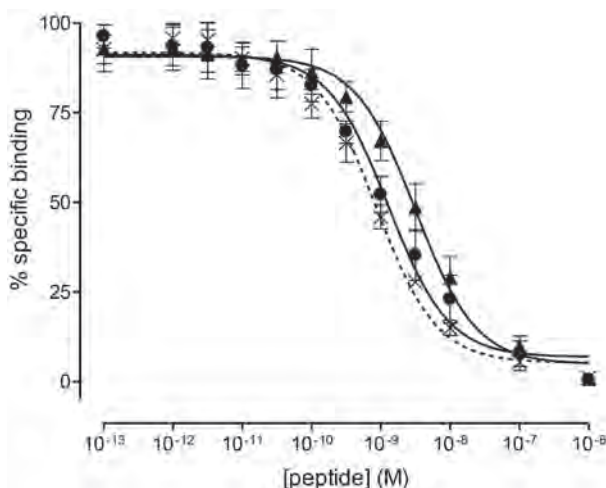


Figure 2 | Displacement of [ $^{125}I$ -Tyr $^{12}$ ,Leu $^{15}$ ] Gastrin from CCK2R binding sites in A431-CCK2R(+) cell membrane homogenates by increasing concentrations of CP04 ( $\bullet$ ,  $IC_{50} = 1.28 \pm 0.09$  nM), [ $^{nat}In$ ]CP04 ( $\blacktriangle$ ,  $IC_{50} = 3.17 \pm 0.21$  nM) or [ $Leu^{15}$ ]Gastrin ( $\times$ ,  $IC_{50} = 0.86 \pm 0.05$  nM, reference); results are presented as mean  $\pm$  SD of 4 experiments performed in triplicate.

### Radioligand Internalization in A431-CCK2R(+) Cells

As shown in Figure 3, [ $^{111}In$ ]CP04, [ $^{111}In$ -DOTA]MG0 and [ $^{111}In$ -DOTA]MG11 efficiently internalized in A431-CCK2R(+) cells after 1 h incubation at 37°C showing a minor portion bound on the cell-membrane, as expected for receptor radioagonists. This process was receptor specific, as suggested by the low internalization and overall suppressed cell-association values acquired in the presence of excess DG2 [9]. Substitution of Glu $^{2-6}$  by DGLu $^{2-6}$  had no impact on internalization rates, as shown after comparison of the respective values between [ $^{111}In$ ]CP04 (Figure 3A) and [ $^{111}In$ -DOTA]MG0 (Figure 3B) ( $P > 0.05$ ). On the other hand, truncation of the pentaGlu $^{2-6}$ -repeat in [ $^{111}In$ -DOTA]MG11 caused a significant drop ( $P < 0.001$ ) in internalization rates (Figure 3C).

### Radioligand Stability in Mice

The in vivo stability of [ $^{111}In$ ]CP04, [ $^{111}In$ -DOTA]MG0 and [ $^{111}In$ -DOTA]MG11 was studied in peripheral mouse blood 5 min pi using HPLC analysis. Within this period  $\approx 70\%$  of [ $^{111}In$ -DOTA]MG0 and its DGLu $^{2-6}$ -equivalent [ $^{111}In$ ]CP04 were detected intact in the blood samples (Figure 4; A and C, respectively). In contrast, truncated [ $^{111}In$ -DOTA]MG11 rapidly degraded, with less than 5% detected intact in blood as previously reported (Figure 3E) [20]. Impressively, treatment with PA increased the levels of circulating [ $^{111}In$ -DOTA]MG11 to 70% (Figure 4F), while even the more stable [ $^{111}In$ ]CP04 and [ $^{111}In$ -DOTA]MG0 profited as well by PA coinjection with the amount of parent radiopeptide detected intact raised to  $\approx 85\%$  (Figure 4; B and D, respectively).

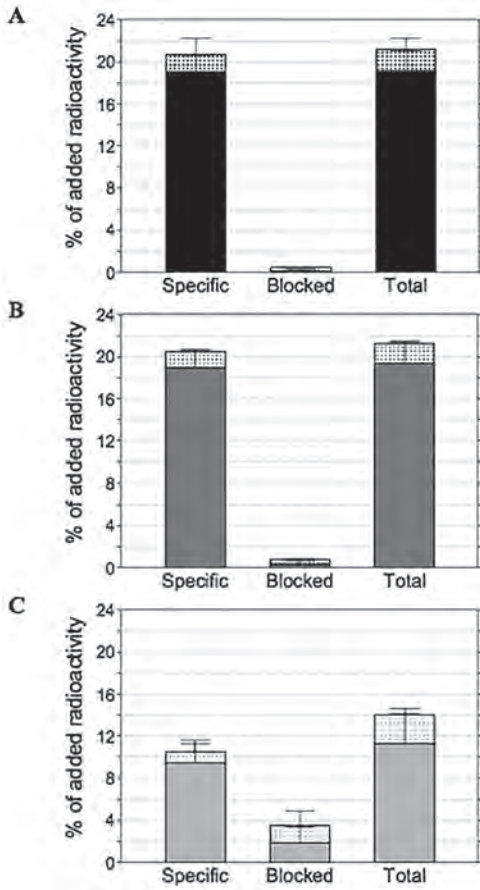


Figure 3 | Internalization and cell-association of [ $^{111}\text{In}$ ]CP04 (■,■, n=4) A), [ $^{111}\text{In}$ -DOTA]MG0 (■,■, n=3) B) and [ $^{111}\text{In}$ -DOTA]MG11 (■,■, n=3) C) in A431-CCK2R(+) cells after 1 h incubation at 37°C. Results represent the mean $\pm$ SD of experiments (n) performed in triplicate. Cell-association comprises the internalized (solid bars) and the membrane-bound (checkered bars) fractions; non-specific or blocked values have been determined from triplicates in the presence of 1  $\mu\text{M}$  DG2 [30].

### Radioligand Biodistribution in SCID Mice Bearing A431-CCK2R(+/-) Xenografts

The biodistribution of [ $^{111}\text{In}$ ]CP04, [ $^{111}\text{In}$ -DOTA]MG0 and [ $^{111}\text{In}$ -DOTA]MG11 was compared in SCID mice bearing a double tumor model: in their right flank animals carried A431-CCK2R(+) xenografts and in their left flank A431-CCK2R(-) tumors devoid of CCK2R expression and thus serving as negative controls [24]. Biodistribution at 4 h pi involved two separate groups per radioligand, the first comprising mice coinjected with vehicle (control) and the second with PA, as shown in Table 1; data in the table is expressed as mean %ID/g $\pm$ SD, n=5. All three radioligands displayed a rapid clearance from blood and background tissues. While the predominant excretion pathway was via the kidneys and the urinary tract, kidney retention significantly differed across analogs. Specifically, [ $^{111}\text{In}$ -DOTA]MG0 exhibited by far the highest renal uptake (127.04 $\pm$ 21.86%ID/g), while these values notably dropped in its DGlu<sup>2-6</sup>-counterpart [ $^{111}\text{In}$ ]CP04 (6.52 $\pm$ 0.63%ID/g) and were minimal in truncated [ $^{111}\text{In}$ -DOTA]MG11 (1.30 $\pm$ 0.29%ID/g). On the other hand, in line with stability findings [ $^{111}\text{In}$ -DOTA]MG0 displayed the highest tumor uptake (11.91 $\pm$ 2.21%ID/g), followed by [ $^{111}\text{In}$ ]CP04 (8.49 $\pm$ 0.39%ID/g), while truncated [ $^{111}\text{In}$ -DOTA]MG11 exhibited the lowest tumor uptake (2.49 $\pm$ 0.92%ID/g). In all cases,

the uptake in the A431-CCK2R(-) tumors remained very low ( $<0.20\%ID/g$ ) suggesting a CCK2R-mediated localization process.

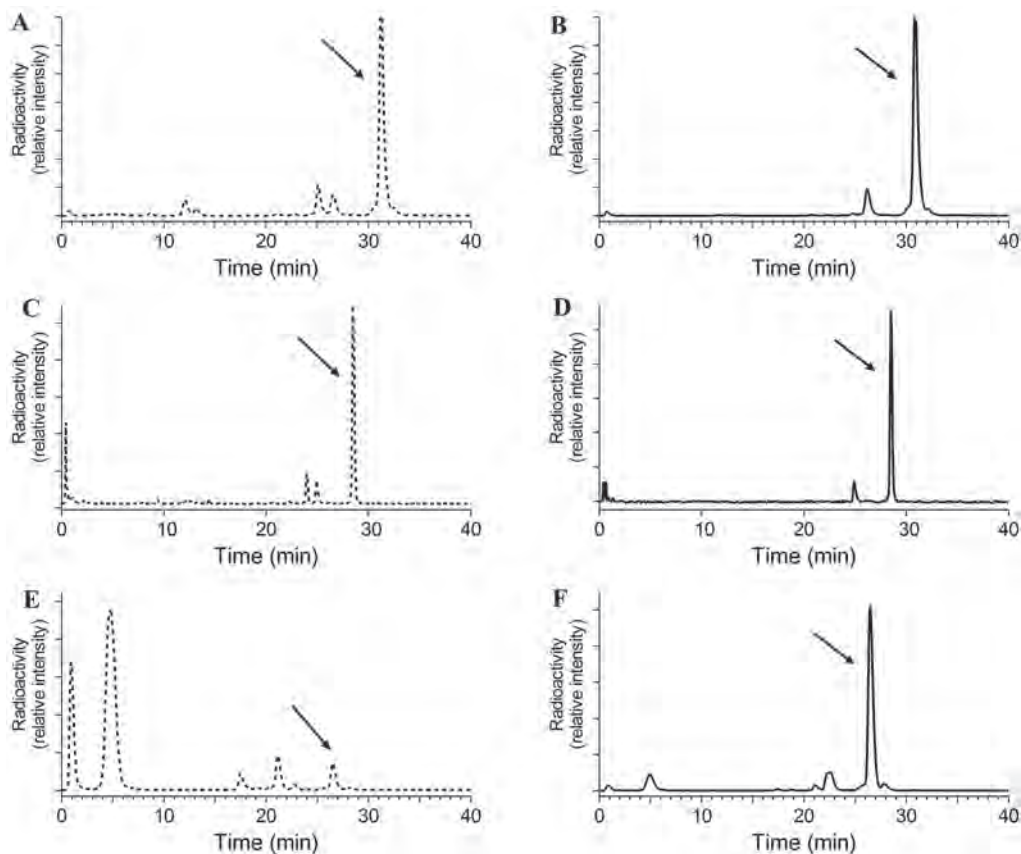


Figure 4 | HPLC analysis (system 3) of blood collected 5 min pi of  $[^{111}\text{In}]\text{CP04}$  (~70% intact) **A**),  $[^{111}\text{In}]\text{-DOTA}]\text{MG0}$  (~70% intact) **C**) and  $[^{111}\text{In}]\text{-DOTA}]\text{MG11}$  (~5% intact) **E**) in healthy mice with vehicle coinjection (control), or 5 min pi of  $[^{111}\text{In}]\text{CP04}$  (~85% intact) **B**),  $[^{111}\text{In}]\text{-DOTA}]\text{MG0}$  (~85% intact) **D**) and  $[^{111}\text{In}]\text{-DOTA}]\text{MG11}$  (70% intact) **F**) with PA coinjection; the  $t_R$  of intact radiopeptides is indicated by the arrows.

Treatment with PA had a prominent impact in almost all above values, presumably as a direct result of their stabilization in the circulation. As expected,  $[^{111}\text{In}]\text{-DOTA}]\text{MG11}$  was the most critically PA-affected radiotracer, showing an impressive increase in the CCK2R(+) tumor uptake ( $15.05 \pm 1.65\%ID/g$ ,  $P < 0.001$ ). At the same time the uptake of  $[^{111}\text{In}]\text{-DOTA}]\text{MG11}$  in the kidneys and the CCK2R(-) tumors remained low and unaffected by PA treatment ( $P > 0.05$ ), resulting in the most favorable tumor-to-kidney ratios (Figure 5). Similar levels of uptake were displayed in the CCK2R(+) tumors after PA coinjection also by  $[^{111}\text{In}]\text{CP04}$  ( $16.01 \pm 2.31\%ID/g$ ) and  $[^{111}\text{In}]\text{-DOTA}]\text{MG0}$

(17.18±0.93%ID/g). Of particular interest is the effect of PA treatment on the kidney accumulation of these analogs. Interestingly, [<sup>111</sup>In]CP04 remained unaffected by PA treatment (7.86±1.61%ID/g,  $P>0.05$ ), whereas the unfavorably high renal values of [<sup>111</sup>In-DOTA]MG0 were significantly elevated even further by PA coinjection (194.71±13.24%ID/g;  $P<0.001$ ).

**Table 1** | Biodistribution of [<sup>111</sup>In]CP04, [<sup>111</sup>In-DOTA]MG0 and [<sup>111</sup>In-DOTA]MG11 in mice bearing twin CCK2R(+) and CCK2R(-) tumors at 4 h pi; data are expressed as %ID/g tissue for control and PA groups and values represent mean±SD, n=5.

Organs	%ID/g tissue ± SD, n=5					
	[ <sup>111</sup> In]CP04		[ <sup>111</sup> In-DOTA]MG0		[ <sup>111</sup> In-DOTA]MG11 <sup>a</sup>	
	Control	PA <sup>b</sup>	Control	PA <sup>b</sup>	Control	PA <sup>b</sup>
Blood	0.04±0.21	0.04±0.02	0.02±0.01	0.03±0.01	0.01±0.01	0.02±0.01
Liver	0.12±0.02	0.15±0.03	0.16±0.05	0.12±0.02	0.11±0.02	0.12±0.01
Heart	0.03±0.01	0.03±0.01	0.04±0.02	0.02±0.01	0.02±0.01	0.02±0.01
Kidneys	<b>6.52±0.63</b>	<b>7.86±1.61</b>	<b>127.04±21.86</b>	<b>194.71±13.24<sup>c</sup></b>	<b>1.30±0.29</b>	<b>1.57±0.15</b>
Stomach	<b>1.63±0.20</b>	<b>1.86±0.28</b>	<b>2.57±0.28</b>	<b>2.79±0.28</b>	<b>1.32±0.26</b>	<b>5.37±0.49<sup>c</sup></b>
Intestines	0.29±0.18	0.26±0.11	0.62±0.37	0.33±0.05	0.83±0.53	0.57±0.20
Spleen	0.06±0.02	0.07±0.01	0.09±0.04	0.07±0.02	0.06±0.01	0.08±0.17
Muscle	0.02±0.01	0.03±0.01	0.02±0.01	0.02±0.01	0.02±0.01	0.03±0.01
Lung	0.04±0.01	0.07±0.01	0.05±0.01	0.05±0.01	0.03±0.01	0.08±0.04
Femur	0.39±0.08	0.19±0.06	0.13±0.03	0.09±0.03	0.02±0.01	0.06±0.02
Pancreas	0.07±0.01	0.08±0.01	0.10±0.03	0.12±0.02	0.05±0.02	0.20±0.04
CCK2R(+) Tumor	<b>8.49±0.39</b>	<b>16.01±2.31<sup>c</sup></b>	<b>11.91±2.21</b>	<b>17.18±0.93<sup>d</sup></b>	<b>2.49±0.92</b>	<b>15.05±1.65<sup>c</sup></b>
CCK2R(-) Tumor	<b>0.14±0.02</b>	<b>0.14±0.03</b>	<b>0.14±0.05</b>	<b>0.19±0.04</b>	<b>0.12±0.02</b>	<b>0.14±0.03</b>

<sup>a</sup>In agreement to results previously reported; [20] <sup>b</sup>coinjection of PA; <sup>c</sup>highly significant ( $P<0.001$ ) or <sup>d</sup>significant ( $P<0.01$ ) difference between control and PA animal groups (unpaired two-tailed Student's *t* test).

## DISCUSSION

Previous studies have indicated a significant role for radiolabeled minigastrin analogs in the management of patients with CCK2R-positive tumors, and especially in the diagnostic imaging and radionuclide therapy of primary and metastatic MTC [4-6,8,11,26]. Coupling of a suitable metal chelator at the N-terminus of minigastrin and its analogs has allowed labeling with diagnostic radiometals for SPECT and PET imaging as well as with therapeutic beta-emitters [9,15,16,27-31]. Studies at the preclinical and the clinical level have shown that the Glu<sup>2-6</sup>-repeat in the minigastrin chain is associated to higher metabolic stability and better localization in CCK2R-positive tumor lesions, but also to unfavourable accumulation in the kidneys [10,12,15,17]. On the other hand, truncation of the Glu<sup>2-6</sup>-chain, while resolving the problem of high renal accumulation, has led to poor metabolic stability and, consequently, to weak tumor targeting [10,11,15,17]. To tackle this



problem, modifications of the Glu<sup>2-6</sup>-part of the molecule have been attempted [18, 19]. Thus, by switching the stereochemistry from L to D in the Glu<sup>2-6</sup>-chain [<sup>111</sup>In]CP04 was developed within the frameworks of COST Action BM6070 [16]. [<sup>111</sup>In]CP04 was selected among 12 CCK2R-directed radioligand candidates for further clinical evaluation due to its most favourable tumor to kidney ratios.

We have recently proposed an effective new strategy to increase the in vivo tumor targeting of peptide radioligands through their stabilization in peripheral blood by coinjection of a suitable peptidase inhibitor [20]. More specifically, by coinjection of the NEP-inhibitor PA together with somatostatin, bombesin and gastrin radioligands we were able to induce impressive amplification of tumor uptake in animal models. This strategy has resulted in higher diagnostic sensitivity and recently also in enhanced therapeutic efficacy of peptide radioligands at the preclinical level [20, 32-34]. By adopting this concept in the case of [<sup>111</sup>In-DOTA]MG11 and other fast biodegradable *des*Glu<sup>2-6</sup> minigastrin radiotracers obtained by Met<sup>11</sup>-substitution, we have consistently achieved unprecedented tumor-to-kidney ratios in mice [32,35].

In the present work we have been interested to compare the efficacy of this approach across the three aforementioned minigastrin radiotracers [<sup>111</sup>In-DOTA]MG0, [<sup>111</sup>In]CP04 and [<sup>111</sup>In-DOTA]MG11 which differ in the critical Glu<sup>2-6</sup>-part of the molecule. As expected, assessment of metabolic stability after injection in mice revealed Glu<sup>2-6</sup>-related differences, with [<sup>111</sup>In-DOTA]MG0 and its D<sup>6</sup>-congener [<sup>111</sup>In]CP04 being significantly more robust in vivo compared to their *des*Glu<sup>2-6</sup>-counterpart [<sup>111</sup>In-DOTA]MG11 (Figure 4). This situation dramatically changed after coinjection of PA, which strengthened the resistance of all three radiotracers to in vivo degradation by NEP. As expected, the most metabolically vulnerable [<sup>111</sup>In-DOTA]MG11 profited most by PA (>14-fold increase in stability).

Regarding biodistribution (Table 1, Figure 5), the radiotracer rank of tumor-targeting efficacy was found to be [<sup>111</sup>In-DOTA]MG0 > [<sup>111</sup>In]CP04 >> [<sup>111</sup>In-DOTA]MG11 in controls, showing that D<sup>6</sup>-substitution only marginally affected tumor uptake. This finding is in line to the combination of in vitro internalization (Figure 3) and in vivo stability results (Figure 4). Furthermore, the radiotracers could be ranked according to renal retention as [<sup>111</sup>In-DOTA]MG0 >> [<sup>111</sup>In]CP04 > [<sup>111</sup>In-DOTA]MG11, revealing favorable tumor-to-kidney ratios for [<sup>111</sup>In]CP04 and especially for [<sup>111</sup>In-DOTA]MG11. This discrepancy may be assigned to the distinct features of each radiotracer and its individual interaction with the mouse renal system. For example, in previous studies [<sup>111</sup>In-DOTA]MG0 demonstrated high kidney uptake and retention due to reabsorption in the proximal tubules which was associated to the penta-Glu chain. The exact mechanism of the observed renal retention has not been elucidated yet, but the involvement of polyglutamate negative charges has been hypothesized [14,36,37]. Changing the stereochemistry of the implicated multi-negative polyglutamate sequence from L to D ([<sup>111</sup>In]CP04) or its full truncation ([<sup>111</sup>In-DOTA]MG11) have been shown to significantly or fully bypass such processing in the kidneys [16].



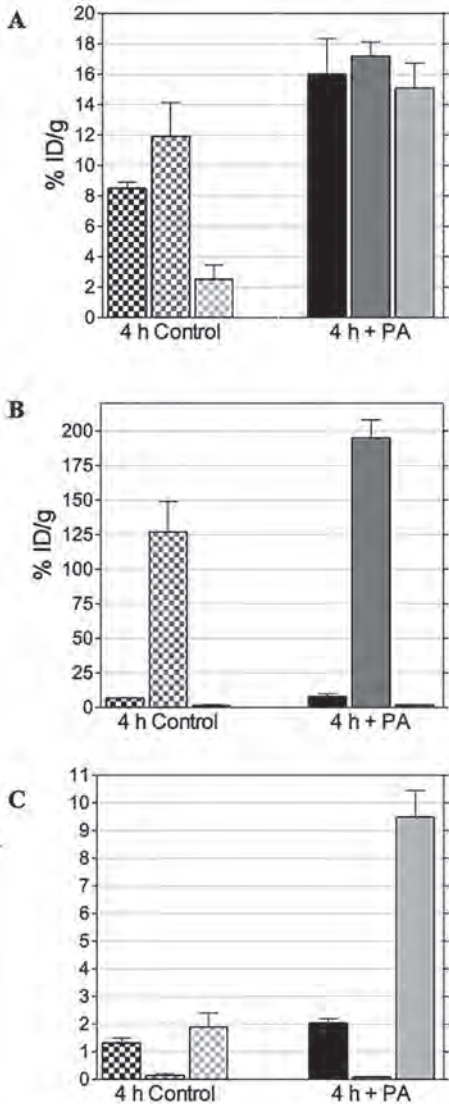


Figure 5 | Comparative biodistribution data of [<sup>111</sup>In]CP04 (■, ■), [<sup>111</sup>In-DOTA]MG0 (■, ■) and [<sup>111</sup>In-DOTA]MG11 (■, ■) in SCID mice bearing twin A431-CCK2R(+) and A431-CCK2R(-) human xenografts at 4 h pi; patterned bars represent control groups (mice coinjecting with vehicle only) and solid bars PA-groups (mice coinjecting with PA). Data expressed as %ID/g±SD (n=5) are selectively shown for A431-CCK2R(+) tumor A), kidneys B) and tumor/kidney ratios C).

It is interesting to compare the impact of in situ NEP-inhibition by PA on the above biodistribution profiles of the three radiotracers, especially focusing on tumor and kidney values. Although the tumor uptake of both [<sup>111</sup>In-DOTA]MG0 and [<sup>111</sup>In]CP04 visibly increased by PA treatment (up to 2-fold), the corresponding value for [<sup>111</sup>In-DOTA]MG11 showed a remarkable >6-fold enhancement. Apparently, the extent of in vivo stabilization induced by PA across analogs determined the respective increase of tumor uptake, being maximum for [<sup>111</sup>In-DOTA]MG11 and less pronounced for the other two more stable analogs (Table 1). Eventually, after treatment with PA all three radiotracers exhibited comparable tumor values and thus similar tumor targeting efficacy.

On the other hand, the renal uptake unfavorably increased even further by PA treatment in the case of [<sup>111</sup>In-DOTA]MG0, while remaining at similar to control levels for both the D<sup>Glu</sup><sup>2-6</sup>-substituted and the *desGlu*<sup>2-6</sup>-truncated analogs. It is reasonable to assume that PA treatment by in situ peptide stabilization in peripheral blood only increased the amount of intact radiotracer reaching the kidneys, but thereafter each analog underwent different processing and was trapped ([<sup>111</sup>In-DOTA]MG0) or not ([<sup>111</sup>In]CP04 and [<sup>111</sup>In-DOTA]MG11) after reabsorption in the proximal tubules. This hypothesis is further supported by the distinct impact of PA treatment on the kidney uptake of other radiopeptides as well. For example, the kidney uptake of the Lys<sup>9</sup>-containing [<sup>111</sup>In-DOTA]SS14 (<sup>111</sup>In-DOTA-Ala-Gly-c[Cys-Lys-Asn-Phe-Phe-Trp-Lys-Thr-Phe-Thr-Ser-Cys]-OH) significantly increased after PA coinjection (from 4.2±0.3%ID/g to 33.1±3.7%ID/g at 4 h pi) [20]. On the other hand, the low kidney uptake of [<sup>111</sup>In]PanSB1 (<sup>111</sup>In-DOTA-PEG<sub>2</sub>-DTyr-Gln-Trp-Ala-Val-βAla-His-Phe-Nle-NH<sub>2</sub>), containing neither positively-charged Lys nor negatively charged polyglutamate residues associated to renal retention, remained unaffected by PA coinjection (from 2.7±0.3%ID/g to 3.4±0.5%ID/g at 4 h pi) [20].

As a result of PA treatment, tumor-to-kidney ratios impressively increased from 1.9±0.5 to 9.6±1.0 only in the case of [<sup>111</sup>In-DOTA]MG11, but remained significantly lower for the other two Glu<sup>2-6</sup>-modified radiotracers (Figure 5C). Accordingly, in vivo NEP-inhibition turned out to be a very powerful tool to improve the pharmacokinetic properties of rapidly biodegradable and not kidney-retained [<sup>111</sup>In-DOTA]MG11, hitherto not considered for clinical application. However, the present study has shown that in situ NEP-inhibition may lead to superior radiotracer pharmacokinetic profiles in preclinical models compared to time- and cost-intensive structural modification approaches [38], as those adopted for the development of [<sup>111</sup>In]CP04. It would be most interesting to establish if and to what extent [<sup>111</sup>In-DOTA]MG11 performs better during in situ NEP-inhibition in human compared with [<sup>111</sup>In]CP04. While [<sup>111</sup>In]CP04 is currently undergoing evaluation in MTC patients in a multi-center European clinical trial, we have been intensively engaged in initiating a “proof-of-principle” study of the new concept in man. Toward this goal, [<sup>111</sup>In-DOTA]MG11 has been selected as a paradigm compound for human application in combination with a suitable NEP-inhibitor. For this purpose, inhibitor type, potency, dose, chemical stability, route of administration and other parameters related to biosafety and efficacy for successful clinical translation are under investigation [39].

## CONCLUSIONS

The efficacy of molecular imaging and radionuclide therapy of tumors with the aid of peptide radioligands largely relies on their stability in the biological milieu, especially for the short period of time needed to reach their tumor-associated targets after entering the circulation. The development of in vivo robust radiotracers derived from native peptide motifs is a lengthy and resource-intensive process, given that the attempted structural modifications may compromise important properties of end-compounds other than metabolic stability, such as receptor affinity and in vivo pharmacokinetics.

Based on the prominent role of NEP in initiating the in vivo degradation of many peptide-radioligands of interest to nuclear oncology, we have proposed the coinjection of a NEP-inhibitor to improve radiopeptide bioavailability, in vivo tumor targeting and overall pharmacokinetics. This approach, has turned out to be particularly successful in the case of [<sup>111</sup>In-DOTA]MG11 and undeniably warrants further validation in human. A first successful application of biodegradable [<sup>111</sup>In-DOTA]MG11 in human after in situ stabilization by a NEP-inhibitor will serve as a paradigm to establish this simple approach in the clinic and will highlight its strength of bypassing the need for extensive and costly development of compound libraries.

### **Acknowledgements**

Partial financial support has been provided by the ERA-NET program GRAN-T-MTC.

### **Disclosure Statement**

The authors declare no potential conflicts of interest.

## REFERENCES

1. Reubi JC, Schaer JC, Waser B. Cholecystokinin(CCK)-A and CCK-B/gastrin receptors in human tumors. *Cancer Res.* 1997;57:1377.
2. Reubi JC, Waser B. Unexpected high incidence of cholecystokinin-B/gastrin receptors in human medullary thyroid carcinomas. *Int J Cancer.* 1996;67:644.
3. Reubi JC. CCK receptors in human neuroendocrine tumors: clinical implications. *Scand J Clin Lab Invest Suppl.* 2001;234:101.
4. Gotthardt M, Béhé MP, Beuter D, et al. Improved tumour detection by gastrin receptor scintigraphy in patients with metastasised medullary thyroid carcinoma. *Eur J Nucl Med Mol Imaging.* 2006;33:1273.
5. Gotthardt M, Béhé MP, Grass J, et al. Added value of gastrin receptor scintigraphy in comparison to somatostatin receptor scintigraphy in patients with carcinoids and other neuroendocrine tumours. *Endocr Relat Cancer.* 2006;13:1203.
6. Behr TM, Jenner N, Radetzky S, et al. Targeting of cholecystokinin-B/gastrin receptors in vivo: preclinical and initial clinical evaluation of the diagnostic and therapeutic potential of radiolabelled gastrin. *Eur J Nucl Med.* 1998;25:424.
7. Behr TM, Béhé M, Angerstein C, et al. Cholecystokinin-B/gastrin receptor binding peptides: preclinical development and evaluation of their diagnostic and therapeutic potential. *Clin Cancer Res.* 1999;5:3124s.
8. Béhé M, Behr TM. Cholecystokinin-B (CCK-B)/gastrin receptor targeting peptides for staging and therapy of medullary thyroid cancer and other CCK-B receptor expressing malignancies. *Biopolymers.* 2002;66:399.
9. Nock BA, Maina T, Béhé M, et al. CCK-2/gastrin receptor-targeted tumor imaging with <sup>99m</sup>Tc-labeled minigastrin analogs. *J Nucl Med.* 2005;46:1727.
10. Breeman WA, Fröberg AC, de Blois E, et al. Optimised labeling, preclinical and initial clinical aspects of CCK-2 receptor-targeting with 3 radiolabeled peptides. *Nucl Med Biol.* 2008;35:839.
11. Fröberg AC, de Jong M, Nock BA, et al. Comparison of three radiolabelled peptide analogues for CCK-2 receptor scintigraphy in medullary thyroid carcinoma. *Eur J Nucl Med Mol Imaging.* 2009;36:1265.
12. Brom M, Joosten L, Laverman P, et al. Preclinical evaluation of <sup>68</sup>Ga-DOTA-minigastrin for the detection of cholecystokinin-2/gastrin receptor-positive tumors. *Mol Imaging.* 2011;10:144.
13. Trejtnar F, Laznickec M, Laznickova A, et al. Biodistribution and elimination characteristics of two <sup>111</sup>In-labeled CCK-2/gastrin receptor-specific peptides in rats. *Anticancer Res.* 2007;27:907.
14. Gotthardt M, van Eerd-Vismale J, Oyen WJ, et al. Indication for different mechanisms of kidney uptake of radiolabeled peptides. *J Nucl Med.* 2007;48:596.
15. Good S, Walter MA, Waser B, et al. Macrocyclic chelator-coupled gastrin-based radiopharmaceuticals for targeting of gastrin receptor-expressing tumours. *Eur J Nucl Med Mol Imaging.* 2008;35:1868.
16. Laverman P, Joosten L, Eek A, et al. Comparative biodistribution of 12 <sup>111</sup>In-labelled gastrin/CCK2 receptor-targeting peptides. *Eur J Nucl Med Mol Imaging.* 2011;38:1410.
17. Oçak M, Helbok A, Rangger C, et al. Comparison of biological stability and metabolism of CCK2 receptor targeting peptides, a collaborative project under COST BM0607. *Eur J Nucl Med Mol Imaging.* 2011;38:1426.
18. Kolenc-Peitzl P, Mansi R, Tamma M, et al. Highly improved metabolic stability and pharmacokinetics of indium-111-DOTA-gastrin conjugates for targeting of the gastrin receptor. *J Med Chem.* 2011;54:2602.
19. Kolenc Peitzl P, Tamma M, Kroselj M, et al. Stereochemistry of amino acid spacers determines the pharmacokinetics of <sup>111</sup>In-DOTA-minigastrin analogues for targeting the CCK2/gastrin receptor. *Bioconjug Chem.* 2015;26:1113.
20. Nock BA, Maina T, Krenning EP, et al. "To serve and protect": enzyme inhibitors as radiopeptide escorts promote tumor targeting. *J Nucl Med.* 2014;55:121.
21. Roques BP, Noble F, Dauge V, et al. Neutral endopeptidase 24.11: structure, inhibition, and experimental and clinical pharmacology. *Pharmacol Rev.* 1993;45:87.
22. Suda H, Aoyagi T, Takeuchi T, et al. Letter: A thermolysin inhibitor produced by Actinomycetes: phosphoramidon. *J Antibiot (Tokyo).* 1973;26:621.

23. Oefner C, D'Arcy A, Hennig M, et al. Structure of human neutral endopeptidase (Nepriylsin) complexed with phosphoramidon. *J Mol Biol.* 2000;296:341.
24. Aloj L, Caracó C, Panico M, et al. In vitro and in vivo evaluation of <sup>111</sup>In-DTPAGlu-G-CCK8 for cholecystokinin-B receptor imaging. *J Nucl Med.* 2004;45:485.
25. Maina T, Nock B, Nikolopoulou A, et al. [<sup>99m</sup>Tc]Demotate, a new <sup>99m</sup>Tc-based [Tyr<sup>3</sup>]octreotate analogue for the detection of somatostatin receptor-positive tumours: synthesis and preclinical results. *Eur J Nucl Med Mol Imaging.* 2002;29:742.
26. Behr TM, Jenner N, Béhé M, et al. Radiolabeled peptides for targeting cholecystokinin-B/gastrin receptor-expressing tumors. *J Nucl Med.* 1999;40:1029.
27. Reubi JC, Waser B, Schaer JC, et al. Unsulfated DTPA- and DOTA-CCK analogs as specific high-affinity ligands for CCK-B receptor-expressing human and rat tissues in vitro and in vivo. *Eur J Nucl Med.* 1998;25:481.
28. Mather SJ, McKenzie AJ, Sosabowski JK, et al. Selection of radiolabeled gastrin analogs for peptide receptor-targeted radionuclide therapy. *J Nucl Med.* 2007;48:615.
29. von Guggenberg E, Rangger C, Sosabowski J, et al. Preclinical evaluation of radiolabeled DOTA-derivatized cyclic minigastrin analogs for targeting cholecystokinin receptor expressing malignancies. *Mol Imaging Biol.* 2012;14:366.
30. Roosenburg S, Laverman P, Joosten L, et al. PET and SPECT imaging of a radiolabeled minigastrin analogue conjugated with DOTA, NOTA, and NODAGA and labeled with <sup>64</sup>Cu, <sup>68</sup>Ga, and <sup>111</sup>In. *Mol Pharm.* 2014;11:3930.
31. Tornesello AL, Aurilio M, Accardo A, et al. Gastrin and cholecystokinin peptide-based radiopharmaceuticals: an in vivo and in vitro comparison. *J Pept Sci.* 2011;17:405.
32. Kaloudi A, Nock BA, Krenning EP, et al. Radiolabeled gastrin/CCK analogs in tumor diagnosis - towards higher stability and improved tumor targeting. *Q J Nucl Med Mol Imaging.* 2015;59(3):287.
33. Marsouvanidis PJ, Melis M, de Blois E, et al. In vivo enzyme inhibition improves the targeting of [<sup>177</sup>Lu]DOTA-GRP(13-27) in GRPR-positive tumors in mice. *Cancer Biother Radiopharm.* 2014;29:359.
34. Chatalic KLS, Konijneberg M, Nonnekens J, et al. In Vivo Stabilization of Gastrin-Releasing Peptide Receptor Antagonist enhances PET Imaging and Radionuclide Therapy of Prostate Cancer in Preclinical Studies. *Theranostics.* 2016;6(1):104.
35. Kaloudi A, Nock BA, Lymperis E, et al. In vivo inhibition of neutral endopeptidase enhances the diagnostic potential of truncated gastrin In-radioligands. *Nucl Med Biol.* 2015;42(11):824.
36. Melis M, Krenning EP, Bernard BF, et al. Renal uptake and retention of radiolabeled somatostatin, bombesin, neurotensin, minigastrin and CCK analogues: species and gender differences. *Nucl Med Biol.* 2007;34:633.
37. Béhé M, Kluge G, Becker W, et al. Use of polyglutamic acids to reduce uptake of radiometal-labeled minigastrin in the kidneys. *J Nucl Med.* 2005;46:1012.
38. Vlieghe P, Lisowski V, Martinez J, et al. Synthetic therapeutic peptides: science and market. *Drug Discov Today.* 2010;15:40.
39. Roques BP. Zinc metallopeptidases: active site structure and design of selective and mixed inhibitors: new approaches in the search for analgesics and anti-hypertensives. *Biochem Soc Trans.* 1993;21 ( Pt 3):678.



# CHAPTER

# 5

## Impact of Clinically Tested NEP/ACE Inhibitors on Tumor Uptake of [<sup>111</sup>In-DOTA]MG11 – First Estimates for Clinical Translation

Aikaterini Kaloudi<sup>1</sup>, Berthold A. Nock<sup>1</sup>, Emmanouil Lympers<sup>1</sup>,  
Roelf Valkema<sup>2</sup>, Eric P. Krenning<sup>2</sup>, Marion de Jong<sup>2,3</sup>, and Theodosia Maina<sup>1</sup>

<sup>1</sup>Molecular Radiopharmacy, INRASTES, NCSR “Demokritos”,  
Ag. Paraskevi Attikis, GR-153 10 Athens, Greece

<sup>2</sup>Department of Nuclear Medicine and <sup>3</sup>Radiology, Erasmus MC,  
3015 GD Rotterdam, The Netherlands

*EJNMMI Res. 6(1):15, 2016*

## ABSTRACT

**Background:** We have recently shown that treatment of mice with the neutral endopeptidase (NEP)-inhibitor phosphoramidon (PA) improves the bioavailability and tumor uptake of biodegradable radiopeptides. For the truncated gastrin radiotracer [ $^{111}\text{In}$ -DOTA]MG11 ( $[(\text{DOTA})\text{DGlu}^{10}]$ gastrin(10-17)) this method led to impressively high tumor-to-kidney ratios. Translation of this concept in the clinic requires the use of certified NEP inhibitors, such as thiorphan (TO) and its orally administered prodrug racecadotril (Race). Besides NEP, angiotensin converting enzyme (ACE) has also been implicated in the catabolism of gastrin analogs. In the present study, we first compared the effects induced by NEP inhibition (using PA, TO or Race) and/or by ACE-inhibition (using lisinopril, Lis) on the biodistribution profile of [ $^{111}\text{In}$ -DOTA]MG11 in mice. In addition, we compared the efficacy of PA and TO at different administered doses to enhance tumor uptake.

**Methods:** [ $^{111}\text{In}$ -DOTA]MG11 was co-injected with: a) vehicle, b) PA (300  $\mu\text{g}$ ), c) TO (150  $\mu\text{g}$ ), d) Lis (100  $\mu\text{g}$ ), e) PA (300  $\mu\text{g}$ ) plus Lis (100  $\mu\text{g}$ ), or f) 30-40 min after intraperitoneal (ip) injection of Race (3 mg) in SCID mice bearing AR42J xenografts. In addition, [ $^{111}\text{In}$ -DOTA]MG11 was co-injected with vehicle, or with progressively increasing amounts of PA (3  $\mu\text{g}$ , 30  $\mu\text{g}$  or 300  $\mu\text{g}$ ) or TO (1.5  $\mu\text{g}$ , 15  $\mu\text{g}$  and 150  $\mu\text{g}$ ) in SCID mice bearing twin A431-CCK2R(+/-) tumors. In all above cases, biodistribution was conducted at 4 h postinjection (pi).

**Results:** During NEP-inhibition, the uptake of [ $^{111}\text{In}$ -DOTA]MG11 in the AR42J tumors impressively increased from  $1.8 \pm 1.0\% \text{ID/g}$  (controls) to  $15.3 \pm 4.7\% \text{ID/g}$  (PA) and  $12.3 \pm 3.6\% \text{ID/g}$  (TO), while with Race tumor values reached  $6.8 \pm 2.8\% \text{ID/g}$ . Conversely, Lis had no effect on tumor uptake and no additive effect when co-injected with PA. During the dose-dependence study in mice, PA turned out to be more efficacious in enhancing tumor uptake of [ $^{111}\text{In}$ -DOTA]MG11 in the CCK2R-positive tumors compared to equimolar amounts of TO. In all cases, renal accumulation remained low, resulting in notable increases of tumor-to-kidney ratios.

**Conclusion:** This study has confirmed NEP as the predominant degrading enzyme of [ $^{111}\text{In}$ -DOTA]MG11 and ruled out the involvement of ACE in the in vivo catabolism of the radiotracer. NEP inhibition with the clinically tested NEP-inhibitors TO and Race resulted in significant enhancement of tumor-to-kidney ratios versus controls. However, compared with PA, TO and its prodrug Race induced less potent increases of tumor uptake, highlighting the significance of inhibitor type, administration route and dose for implementing a first proof-of-principle study in human.

**Key Words:** NEP inhibition, ACE inhibition, in situ radioligand stabilization, tumor targeting, enhancement of tumor uptake, [ $^{111}\text{In}$ -DOTA]MG11



## INTRODUCTION

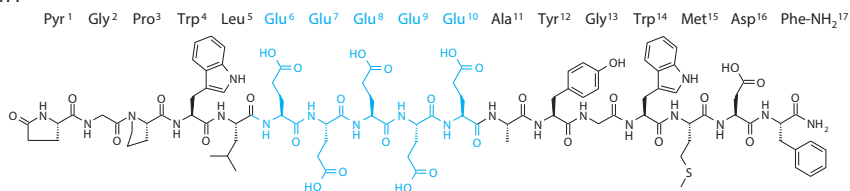
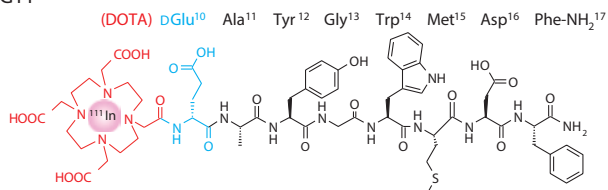
Cholecystokinin subtype 2 receptors (CCK2Rs) have attracted much attention in nuclear oncology due to their overexpression in various human tumors, including medullary thyroid carcinoma (MTC), small cell lung cancer, astrocytomas and stromal ovarian cancers [1-4]. Accordingly, peptide-radioligands based on gastrin or on cholecystokinin (CCK) have been proposed for diagnostic imaging and radionuclide therapy of CCK2R-positive tumors [5,6].

Human gastrin I is a C-terminally amidated heptadecapeptide characterized by a pentaGlu repeat in positions 6 through 10 (pGlu-Gly-Pro-Trp-Leu-(Glu)<sub>5</sub>-Ala-Tyr-Gly-Trp-Met-Asp-Phe-NH<sub>2</sub>; Figure 1) [7]. This highly polar and negatively charged amino acid sequence determines important biological properties of gastrin and its radiolabeled analogs. Thus, Glu<sup>6-10</sup>-containing radioligands show high receptor affinity and are metabolically robust. As a result, they efficiently localize in CCK2R-rich lesions in rodents and in patients, but their application in the clinic has been hitherto restricted by their unfavorably high renal retention. Conversely, truncated *des*Glu<sup>6-10</sup> gastrin analogs, as for example [<sup>111</sup>In-DOTA]MG11 ((DOTA)DGlu<sup>10</sup>)gastrin(10-17); Figure 1), display favorably low renal uptake, but also severely impaired ability to target CCK2R-positive tumors in vivo, owing to their poor metabolic stability [6,8].

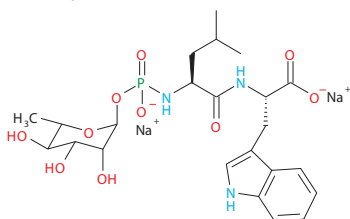
According to previous reports, proteases that might be implicated in the degradation of CCK and gastrin analogs include: a) aminopeptidases [9], b) angiotensin converting enzyme (ACE, EC 3.4.15.1) [10] and c) neutral endopeptidase (NEP, neprilysin, EC 3.4.24.11) [11,12]. Given that N-terminal capping is an effective means to prevent peptide degradation by aminopeptidases [9,13], it is reasonable to assume that [<sup>111</sup>In-DOTA]MG11 with a bulky radiometal-chelate attached at the N-terminus becomes aminopeptidase-resistant. The role of ACE in the degradation of CCK and different-length gastrin analogs has been previously investigated in vitro [10]. Interestingly, minigastrin (MG, gastrin(5-17)) was shown to be resistant to ACE, whereas successive shortening of the penta-Glu chain to truncated gastrin analogs with less than two Glu residues led to in vitro degradation by ACE. Accordingly, [<sup>111</sup>In-DOTA]MG11 is expected to be resistant to ACE by virtue of the polar <sup>111</sup>In-DOTA<sup>9</sup>-DGlu<sup>10</sup> sequence, mimicking the Glu<sup>9-10</sup> construct of ACE-resistant gastrin(9-17). However, the role of ACE on the in vivo fate of gastrin analogs, including [<sup>111</sup>In-DOTA]MG11, has not been elucidated yet. The third protease implicated in the metabolism of gastrin is NEP, an ectoenzyme with broad substrate-specificity and a wide distribution in the body. While scarcely found in plasma, NEP is abundantly expressed in most tissues, anchored on the endothelial cell surface of the vasculature compartment, and in major organs, such as kidneys, liver, lungs and gastrointestinal tract [14]. The involvement of NEP in the in vitro and in vivo degradation of gastrin has been well-described in previous reports [11,12].

We have recently proposed an effective strategy to improve the bioavailability and tumor uptake of biodegradable radiopeptides, involving in situ inhibition of the degrading protease(s) (e.g. NEP) by coinjection of a suitable inhibitor (e.g. the NEP-inhibitor phosphoramidon, PA) [15-17]. For the truncated gastrin radiotracer [<sup>111</sup>In-DOTA]MG11, this method led to impressive in vivo stabilization, which translated into remarkably increased uptake in CCK2R-positive tumors in mice and into high tumor-to-kidney ratios [15,18].

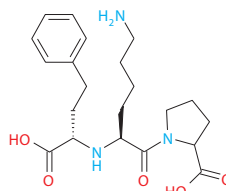
## Gastrin I

[<sup>111</sup>In-DOTA]MG11

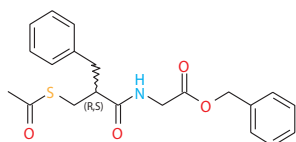
## Phosphoramidon



## Lisinopril



## Racecadotril



## Thiorphan

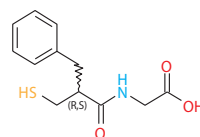


Figure 1 | Human gastrin I, [<sup>111</sup>In-DOTA]MG11, the NEP inhibitors PA, TO and its prodrug Race, and the ACE inhibitor Lis.

The above promising results have prompted further research toward clinical translation of the proposed concept in a first “proof-of-principle” study in man, using [<sup>111</sup>In-DOTA]MG11 as a paradigm. The success of this step largely relies on the identification of the peptidase(s) actually responsible for the proteolytic degradation of [<sup>111</sup>In-DOTA]MG11 after its entry in the circulation by intravenous injection. Rapid *in vivo* degradation deteriorates the radiotracer supply to target-sites and eventually compromises its localization on tumor CCK2R-positive lesions. Therefore, we were first interested to study the potential involvement of ACE on the tumor uptake of [<sup>111</sup>In-DOTA]MG11. For this purpose, the effect of *in situ* ACE-inhibition by lisinopril (Lis) [19] alone vs. controls was compared in mice bearing AR42J tumors. Furthermore, the combination of dual ACE/NEP-inhibition after injection of a Lis and PA mixture vs. single NEP-inhibition by PA was compared in the same mouse model.

Another important step toward clinical translation is the assessment of biosafety and efficacy of the NEP-inhibitor intended for human application. It should be noted that so far no extensive toxicity studies have been reported for PA. This bacterial-origin and potent NEP-inhibitor has been administered in human only in homoeopathic amounts [16,20]. Consequently, we decided to compare the *in vivo* efficacy of the clinically certified NEP-inhibitor thiorphan (TO) [21,22] vs. PA to enhance the tumor uptake of [<sup>111</sup>In-DOTA]MG11 in the same mouse model. Racecadotril (Race) is a prodrug of TO administered orally and a registered anti-diarrheal drug (Figure 1) [23,24], which has also been included in our study. Race was administered intraperitoneally (ip) due to its poor water solubility prior to [<sup>111</sup>In-DOTA]MG11 iv injection.

In the last part of the present study, we have directly compared the efficacy of TO and PA iv-injected in equimolar and progressively increasing doses to enhance the uptake of [<sup>111</sup>In-DOTA]MG11 in a double A431-CCK2R(+/-) tumor mouse model.

## MATERIALS AND METHODS

### Chemistry and Radiochemistry

#### *Chemicals and Radionuclides*

All chemicals were reagent grade and used without further purification. DOTA-MG11 (DOTA-Minigastrin 11, DOTA-DGlu-Ala-Tyr-Gly-Trp-Met-Asp-Phe-NH<sub>2</sub>) and DG2 (Demogastrin 2, N<sub>4</sub>-Gly-DGlu-(Glu)<sub>5</sub>-Ala-Tyr-Gly-Trp-Met-Asp-Phe-NH<sub>2</sub>) [25] were purchased from PiChem (Graz, Austria). PA (Phosphoramidon disodium dehydrate, N-(α-rhamnopyranosyloxyhydroxyphosphinyl)-L-leucyl-L-tryptophan×2Na×2H<sub>2</sub>O) was provided by PeptaNova GmbH (Sandhausen, Germany). TO (DL-Thiorphan, DL-3-Mercapto-2-benzylpropanoylglycine) was a kind gift of Prof. B. Roques (Université René Descartes, Paris, France). Lis (lisinopril dehydrate, ((S)1-1-[N2-(1-carboxy-3-phenylpropyl)-lysylproline dehydrate, MK 521) and Race (Racecadotril, (RS)-benzyl N-[3-(acetylthio)-2-benzylpropanoyl] glycinate) were purchased from Sigma-Aldrich (Figure 1).

Indium-111 used for labelling was purchased in the form of <sup>111</sup>InCl<sub>3</sub> in a solution of 0.05 M HCl (0.5 mL) from Mallinckrodt Medical B.V. (Petten, The Netherlands).

#### *Preparation of [<sup>111</sup>In-DOTA]MG11*

Lyophilized DOTA-MG11 was dissolved in water to a final concentration of 1 mM and 50 μL-aliquots were stored at -20°C. Labeling with <sup>111</sup>In was conducted in an Eppendorf vial containing 0.1 M sodium acetate buffer pH 4.6 in the presence of excess methionine (Met) to prevent oxidation of Met<sup>15</sup> in DOTA-MG11 [26]. Freshly prepared sodium ascorbate buffer (10 mM) was added in the vial, followed by <sup>111</sup>InCl<sub>3</sub> solution (37-74 MBq), Met (1,000 nmol) and DOTA-MG11 (10 nmol). The mixture was left to react at 80°C for 20 min. Prior to performing quality control by HPLC, EDTA in 0.1 M acetate buffer (pH 4.6) was added to a final concentration of 1 mM to the labeling reaction mixture as a “free” <sup>111</sup>In<sup>3+</sup> scavenger.

### **Quality Control of [<sup>111</sup>In-DOTA]MG11**

For quality control of the labeled reaction mixture RP-HPLC was performed using system 1: A Waters Chromatograph (Waters, Vienna, Austria) based on a 600 solvent delivery system coupled to a Waters 996 photodiode array UV detector and a Gabi gamma detector (Raytest, RSM Analytische Instrumente GmbH, Germany) employing a 20 µL injection loop was applied. The Millennium Software (Waters, USA) was used for data processing and chromatographic control and an XTerra RP-18 (5 µm, 4.6 mm × 150 mm) cartridge column (Waters, Germany) was eluted at 1 mL/min flow rate with a linear gradient starting from 0% B and advancing to 40% B within 40 min (solvent A= 0.1% aqueous TFA and B= MeCN). For metabolism studies HPLC analysis was performed using system 2: A Waters Chromatograph (Waters, Vienna, Austria) with 600E multisolvent delivery system coupled to a Gabi gamma-detector (Raytest, Germany) employing a 0.5-mL injection loop was applied. Data processing and chromatography run were controlled with Empower Software and a Symmetry Shield RP18 (5 µm, 3.9 mm × 20 mm) column (Waters, Germany) was eluted adopting linear gradient starting from 0% B and advancing to 40% B within 40 min (solvent A= 0.1% aqueous TFA and B= MeCN) with a flow rate of 1 mL/min. Radioactivity measurements were conducted in an automated well-type gamma counter [NaI(Tl) crystal, Canberra Packard Auto-Gamma 5000 series instrument] calibrated for <sup>111</sup>In.

## **Biology**

### **Cell Lines and Cell Culture**

The rat pancreatic tumor cell line AR42J, endogenously expressing the CCK2R [27] was kindly provided by Prof. C. Decristoforo (University Clinic Innsbruck, Austria). The human epidermoid carcinoma A431 cell line transfected to stably express the CCK2R (A431-CCK2R(+)) or devoid of CCK2R expression (A431-CCK2R(-)) was a gift from Prof. O. Boerman (Department of Nuclear Medicine, Radboud University Nijmegen Medical Centre, Nijmegen, The Netherlands) and Prof. L. Aloj (Istituto di Biostrutture e Bioimmagini, Consiglio Nazionale delle Ricerche, Naples, Italy) [28].

All culture media were purchased from Gibco BRL, Life Technologies (Grand Island, NY, USA) and supplements were supplied by Biochrom KG Seromed (Berlin, Germany). AR42J cells were cultured in F-12K Nutrient Mixture (Kaighn's Modification), supplemented with 10% (v/v) fetal bovine serum, 100 U/mL penicillin, 100 µg/mL streptomycin and 1 mM L-glutamine. A431-CCK2R(+/-) cells were grown in Dulbecco's Modified Eagle medium with GlutaMAX-I supplemented with 10% (v/v) fetal bovine serum, 100 U/mL penicillin, 100 µg/mL streptomycin, 4,500 mg/L D-glucose and 250 µg/mL G418. Cells were kept in a controlled humidified air containing 5% CO<sub>2</sub> at 37°C. Splitting of cells with a ratio of 1:2 to 1:5 was performed when approaching confluency using a trypsin/EDTA solution (0.05%/0.02% w/v) [29].

### **Metabolism in Blood**

Animal experiments were carried out in compliance with European and national regulations and were approved by national authorities. For metabolic studies, in-house male Swiss albino mice (30±5g) were used. A bolus containing [<sup>111</sup>In-DOTA]MG11 (100 µL, 11-22 MBq, 3 nmol of total peptide, normal saline/EtOH v/v 9/1) was injected in the tail vein of healthy male Swiss Albino mice, together with: a) vehicle (100 µL; control), b) PA (100 µL of vehicle containing 300 µg PA; PA), or c) (100 µL of

vehicle containing 150 µg TO; TO). Additional animals intraperitoneally (ip) received a fine dispersed suspension of Race (3 mg Race dissolved in 0.025 mL DMSO and freshly mixed with 0.375 mL saline) 30–40 min prior to radioligand injection. The animals were kept for 5 min in cages with free access to water. They were sacrificed by cardiac puncture under ether anesthesia and blood was withdrawn with a syringe and immediately placed in a pre-chilled polypropylene vial on ice containing EDTA and Met. Blood samples were centrifuged at 2,000 g at 4°C for 10 min. The plasma was collected, an equal volume of MeCN was added and the mixture was centrifuged for 10 min at 15,000 g at 4°C. The supernatant was collected and concentrated under a gentle N<sub>2</sub>-flux at 40°C to a volume of ≈0.1 mL; the concentrate was diluted with physiological saline (0.4 mL) and passed through a Millex-GV syringe-driven filter unit (0.22 µm/13 mm; Millipore, Milford/USA). Suitable aliquots of the filtrate were analyzed by RP-HPLC [15,29]. The t<sub>r</sub> of the parent radiopeptide in the applied chromatographic conditions (system 2) was established by coinjection of samples with [<sup>111</sup>In-DOTA]MG11.

### ***Biodistribution in AR42J Tumor-Bearing SCID Mice***

In-house male SCID mice (NCSR “Demokritos” Animal House) of 6-weeks of age at the time of arrival (18±2 g body weight) were inoculated subcutaneously (sc) in their flanks with a suspension of freshly harvested AR42J cells (1×10<sup>7</sup> cells in ~150 µL saline). Animals were kept in aseptic conditions for 14 days when well-palpable tumors developed at the inoculation sites (0.31±0.17 g) [29]. At the day of biodistribution animals received a bolus of [<sup>111</sup>In-DOTA]MG11 (100 µL, 37–74 kBq, 10 pmol total peptide, in saline/EtOH 9/1 v/v) through the tail vein, coinjected with: a) vehicle (100 µL; control group, n=10), b) PA (100 µL vehicle containing 300 µg PA; PA-group, n=10), c) TO (100 µL of vehicle containing 150 µg TO; TO-group, n=4), d) Lis (100 µL of vehicle containing 100 µg Lis; Lis-group, n=4), e) PA plus Lis (100 µL vehicle containing 300 µg PA and 100 µg Lis; PA+Lis-group, n=5), or f) 30–40 min after ip injection of Race (3 mg Race dissolved in 0.025 mL DMSO and freshly mixed with 0.375 mL saline, Race-group, n=4). In a separate animal group, mice were coinjected with 100 µL vehicle containing both 300 µg PA and 100 µg DG2 [25] to assess non-specific tumor uptake during in situ NEP-inhibition (in vivo CCK2R-blockade; block-group, n=4).

Mice had access to drinking water *ad libitum* until they were euthanized at 4 h pi. Blood samples, organs of interest and tumors were collected immediately after dissection, weighted and measured for radioactivity in the gamma counter; only stomachs were emptied of their contents prior to measurements. Biodistribution data were calculated as percent of injected dose per gram tissue (%ID/g) with the aid of suitable standards of the injected dose, using the GraphPad Prism Software (San Diego, CA).

### ***PA and TO Dose-Dependence Study in SCID Mice Bearing Twin A431-CCK2R(+/-) Tumors***

Inocula of freshly harvested A431-CCK2R(+/-) cells (1.6×10<sup>7</sup>/1.4×10<sup>7</sup> cell suspensions in 150 µL saline) were sc-injected in the right and left flanks of SCID mice (male SCID mice, 6-weeks of age and of 18±2 g body weight on arrival day; NCSR “Demokritos” Animal House). Animals were kept in aseptic conditions for 8 days till well-palpable tumors (0.26±0.08 g) developed at the inoculation sites [29]. At the day of the experiment mice received a bolus of [<sup>111</sup>In-DOTA]MG11 (100 µL, 37–74 kBq, 10 pmol total peptide, in saline/EtOH 9/1 v/v) through the tail vein, coinjected with: a) vehicle (100 µL; control

group, n=5), b) three different doses of PA (3  $\mu\text{g}$  – n=5, 30  $\mu\text{g}$  – n=4, or 300  $\mu\text{g}$  PA – n=10 – dissolved in 100  $\mu\text{L}$  vehicle) and c) three different doses of TO (1.5  $\mu\text{g}$ , 15  $\mu\text{g}$ , or 150  $\mu\text{g}$  TO dissolved in 100  $\mu\text{L}$  vehicle, all groups of n=4). Mice had free access to drinking water until they were sacrificed at 4 h pi and biodistribution was conducted as described above.

### **Statistical Analysis**

The in vivo data were statistically analyzed with the Student's *t* test (Prism™ 2.01, GraphPad Software, San Diego, CA). Analyses were 2-tailed and a *P* value <0.05 was considered statistically significant.

## **RESULTS**

### **Radiolabeling**

The radiolabeling of DOTA-MG11 with  $^{111}\text{In}$  was straightforward following published methods and involved 20-min incubation of the peptide-conjugate in acidic medium at 90°C in the presence of  $^{111}\text{InCl}_3$  [26]. A >96% radiometal incorporation was typically demonstrated by RP-HPLC analysis (system 1). The radiochemical purity was >97%, verifying that the addition of Met in the labeling reaction mixture prevented the oxidation of Met<sup>15</sup> in the peptide chain.

### **Metabolism in Blood**

As shown by HPLC analysis of mouse blood collected 5 min pi, [ $^{111}\text{In}$ -DOTA]MG11 was very rapidly degraded in vivo in agreement with previous findings (Figure 2A) [8,15,26]. Treatment of mice with PA, TO and its ip-preadministered prodrug Race notably increased the amount of intact radiotracer in peripheral blood from <5% to >70% (Figure 2; B, C and D, respectively). Conversely, coinjection of [ $^{111}\text{In}$ -DOTA]MG11 with the ACE-inhibitor Lis produced no change on radiotracer stability in mouse circulation up to 5 min pi (results not shown), in support of the assumption that [ $^{111}\text{In}$ -DOTA]MG11 is resistant to ACE [18].

### **Biodistribution in AR42J Tumor-Bearing Mice – Impact of NEP/ACE Inhibitors**

Results of [ $^{111}\text{In}$ -DOTA]MG11 biodistribution in SCID mice bearing AR42J tumors at 4 h pi are summarized in Table 1 and in Figure 3, as %ID/g (n≥4). In addition to the values obtained by coinjection of the radiotracer with vehicle (controls), Table 1 includes values obtained during treatment of mice with one of the NEP-inhibitors (PA, TO and Race) and/or the ACE-inhibitor Lis. In all cases, the radiotracer rapidly cleared from background tissues via the kidneys and the urinary tract with consistently low renal values. Uptake in the AR42J tumors remarkably increased from  $1.82\pm 1.25\%$ ID/g in controls to  $15.32\pm 4.71\%$ ID/g in the PA group ( $P<0.001$ ). Most importantly, this increase was shown to be receptor-specific, as suggested by the significantly reduced tumor values determined during coinjection of excess DG2 [25] and PA ( $0.34\pm 0.04\%$ ID/g,  $P<0.001$ ). In contrast, coinjection of the ACE-inhibitor Lis did not provoke any raise in tumor values ( $1.80\pm 0.74\%$ ID/g) vs. controls ( $P>0.05$ ), whereas coinjection of both peptidase inhibitors PA and Lis did not provoke any additional increase in the PA-group values ( $14.51\pm 4.73\%$ ID/g,  $P>0.05$ ). This finding is a strong indication that ACE is not involved in the in vivo catabolism of [ $^{111}\text{In}$ -DOTA]MG11.

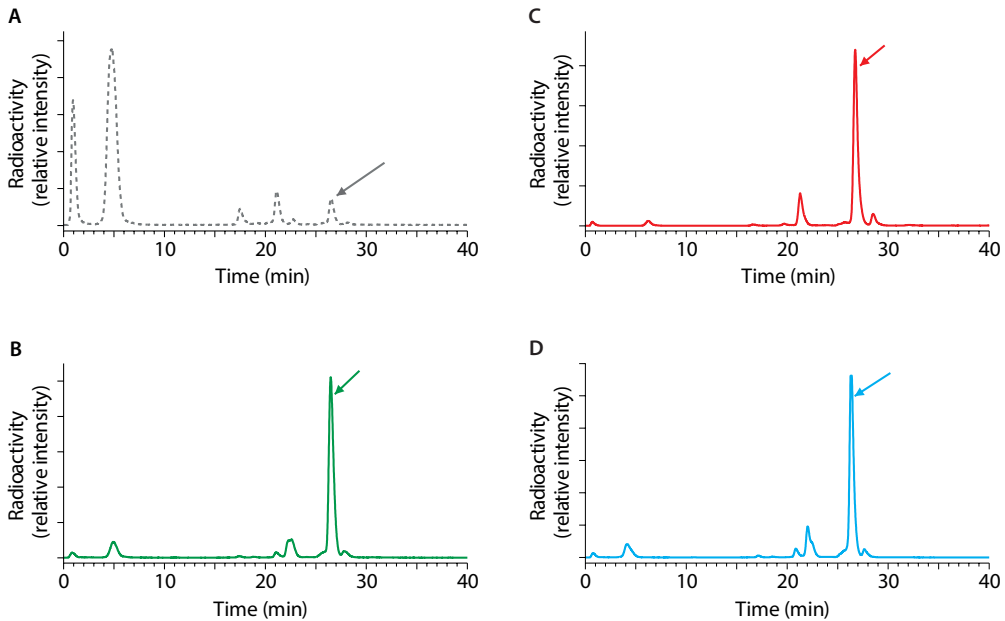


**Figure 2** | Stability of [<sup>111</sup>In-DOTA]MG11 in peripheral mouse blood at 5 min pi. Analysis by HPLC (system 2) of murine blood collected 5 min after injection of [<sup>111</sup>In-DOTA]MG11 with **A**) vehicle (<4% intact radiotracer), **B**) PA (300 µg; >70% intact radiopeptide), **C**) TO (150 µg; >70% intact radiopeptide), or 30–40 min after ip-injection of Race (2 mg; >70% intact radiopeptide). The  $t_r$  of [<sup>111</sup>In-DOTA]MG11 is indicated by the arrow.

On the other hand, coinjection of TO, at a dose equimolar to PA, produced similar albeit slightly less potent increase of AR42J tumor uptake ( $12.32 \pm 3.66\% \text{ID/g}$ ,  $P > 0.05$ ). Interestingly, the TO prodrug Race although administered at a ten times higher dose than TO induced half as high an increase on the tumor uptake of [<sup>111</sup>In-DOTA]MG11 ( $6.81 \pm 2.79\% \text{ID/g}$ ,  $P < 0.001$ ).

### Biodistribution in A431-CCK2R(+/-) Tumor-Bearing Mice – Impact of PA and TO Dose

The efficacy of the two NEP-inhibitors PA and TO in improving the in vivo targeting of [<sup>111</sup>In-DOTA]MG11 was compared at 4 h pi in SCID mice bearing double A431-CCK2R(+/-) tumors. Three gradually increasing inhibitor doses and equimolar for PA (3 µg, 30 µg and 300 µg) and TO (1.5 µg, 15 µg and 150 µg), were tested and the respective results are summarized in Table 2 and Figure 4. It is interesting to note that in all cases a significant and receptor-specific increase was recorded in the uptake of the radiotracer in the CCK2R-expressing tumors ( $P < 0.001$ ), whereas no change was observed in the tumors devoid of CCK2R-expression. Stepwise increase of TO dose resulted in significant and gradual increase of tumor uptake vs. controls. In the case of PA, however, increasing the dose from 30 µg to 300 µg did not further improve tumor uptake. Overall, PA clearly exerted a more potent tumor enhancement effect compared to the respective equimolar doses of TO ( $P < 0.001$ ).

**Table 1** | Cumulative biodistribution data of [<sup>111</sup>In-DOTA]MG11 in AR42J tumor bearing SCID mice including controls and animals treated with NEP and/or ACE inhibitors.

Organs	[ <sup>111</sup> In-DOTA]MG11 (%ID/g tissue ± SD at 4 h pi, n≥4)						
	+DG2 +PA <sup>a</sup>	control	+Lis <sup>b</sup>	+PA <sup>c</sup>	+PA +Lis <sup>d</sup>	+TO <sup>e</sup>	+Race <sup>f</sup>
Blood	0.02±0.01	0.04±0.01	0.05±0.02	0.06±0.04	0.05±0.02	0.02±0.01	0.20±0.08
Liver	0.14±0.02	0.13±0.03	0.13±0.01	0.15±0.04	0.17±0.09	0.17±0.05	1.19±0.03
Heart	0.02±0.01	0.05±0.02	0.05±0.01	0.07±0.03	0.07±0.03	0.03±0.02	0.13±0.03
Kidneys	<b>1.31±0.03</b>	<b>1.86±0.25</b>	<b>1.85±0.30</b>	<b>2.26±0.33</b>	<b>1.82±0.06</b>	<b>2.95±0.80</b>	<b>1.93±0.46</b>
Stomach	0.08±0.01	1.53±0.65	2.83±0.68	5.13±2.29	6.21±2.73	2.90±0.51	4.60±1.09
Intestines	0.48±0.08	0.89±0.76	0.65±0.25	0.69±0.13	0.82±0.26	2.16±0.88	0.83±0.12
Spleen	0.09±0.02	0.17±0.07	0.34±0.30	0.20±0.08	0.30±0.13	0.14±0.04	0.30±0.06
Muscle	0.01±0.01	0.04±0.01	0.04±0.01	0.09±0.17	0.07±0.04	0.02±0.01	0.10±0.03
Lung	0.05±0.01	0.07±0.02	0.07±0.01	0.10±0.01	0.28±0.19	0.12±0.05	0.12±0.03
Femur	0.04±0.01	0.09±0.05	0.08±0.01	0.12±0.06	0.15±0.04	0.05±0.01	0.26±0.22
Pancreas	0.08±0.01	0.11±0.03	0.18±0.09	0.36±0.17	0.53±0.24	0.30±0.16	0.30±0.061
Tumor	<b>0.34±0.04</b>	<b>1.82±1.25</b>	<b>1.80±0.74</b>	<b>15.32±4.71</b>	<b>14.51±4.73</b>	<b>12.32±3.66</b>	<b>6.81±2.79</b>

<sup>a</sup>Coinjection of 50 nmol DG2 [25] and 300 µg PA to assess non-specific tumor uptake; <sup>b</sup>coinjection of 100 µg Lis; <sup>c</sup>coinjection with 300 µg PA; <sup>d</sup>coinjection with 300 µg PA and 100 µg Lis; <sup>e</sup>coinjection with 150 µg TO; <sup>f</sup>radiotracer injection 30–40 min after ip-injection of 3 mg Race.

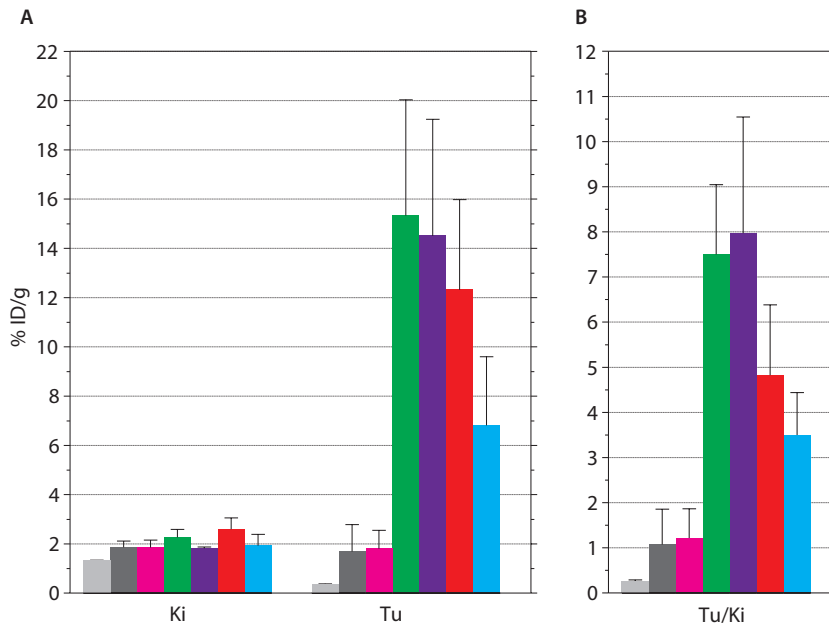


**Figure 3** | **A**) Uptake of [<sup>111</sup>In-DOTA]MG11 in kidneys and AR42J tumors at 4 h pi in SCID mice. Data are given for kidneys and tumors as mean of %ID/g±sd, n≥ 4; [<sup>111</sup>In-DOTA]MG11 iv-coinjection with vehicle (■), with 100 µg Lis (■), with 300 µg PA (■), with a mixture of 100 µg Lis and 300 µg PA (■), with 150 µg TO (■), or 30–40 min after ip injection of 3 mg Race (■); for CCK2R-blockade 40 nmol DG2 [25] was iv-coinjected along with 300 µg PA (■). **B**) Corresponding tumor-to-kidney ratios. (Tu/Ki).



**Table 2** | Comparative biodistribution data of [<sup>111</sup>In-DOTA]MG11 in SCID mice bearing double A431-CCK2R(+/-) tumors at 4 h pi, including controls and animals coinjected with gradually increasing amounts of TO and PA; TO and PA injected doses were equimolar.

Organs	[ <sup>111</sup> In-DOTA]MG11 (%ID/g tissue ± SD at 4 h pi, n≥4)						
	control	+TO			+PA		
		1.5 µg	15 µg	150 µg	3 µg	30 µg	300 µg
Blood	0.01±0.01	0.02±0.01	0.03±0.02	0.02±0.01	0.02±0.01	0.04±0.01	0.02±0.01
Liver	0.11±0.02	0.16±0.02	0.15±0.02	0.16±0.01	0.13±0.03	0.13±0.02	0.12±0.01
Heart	0.02±0.01	0.03±0.00	0.03±0.00	0.03±0.01	0.02±0.01	0.04±0.01	0.03±0.01
Kidneys	<b>1.30±0.29</b>	<b>2.67±0.30</b>	<b>2.28±0.21</b>	<b>2.22±0.19</b>	<b>2.11±0.45</b>	<b>2.81±1.03</b>	<b>1.78±0.37</b>
Stomach	1.32±0.26	2.59±0.40	3.38±0.20	4.01±0.20	2.68±0.67	3.19±0.12	4.56±1.16
Intestines	0.83±0.53	0.43±0.10	0.47±0.04	0.48±0.02	0.40±0.17	0.32±0.09	0.47±0.20
Spleen	0.06±0.01	0.12±0.02	0.10±0.01	0.14±0.04	0.09±0.04	0.10±0.02	0.07±0.01
Muscle	0.02±0.01	0.03±0.01	0.02±0.01	0.03±0.02	0.03±0.01	0.04±0.01	0.02±0.01
Lung	0.03±0.01	0.05±0.00	0.05±0.00	0.62±0.02	0.07±0.05	0.07±0.01	0.07±0.03
Femur	0.02±0.01	0.05±0.00	0.06±0.00	0.09±0.07	0.04±0.03	0.05±0.01	0.06±0.01
Pancreas	0.05±0.02	0.14±0.03	0.12±0.03	0.22±0.04	0.14±0.07	0.17±0.02	0.20±0.03
Tumor(-)	0.12±0.02	0.18±0.03	0.13±0.01	0.17±0.04	0.17±0.013	0.18±0.07	0.13±0.02
Tumor(+)	<b>2.50±0.92</b>	<b>4.98±0.58</b>	<b>6.10±1.26</b>	<b>7.99±1.12</b>	<b>10.55±1.77</b>	<b>15.41±2.28</b>	<b>16.05±2.37</b>

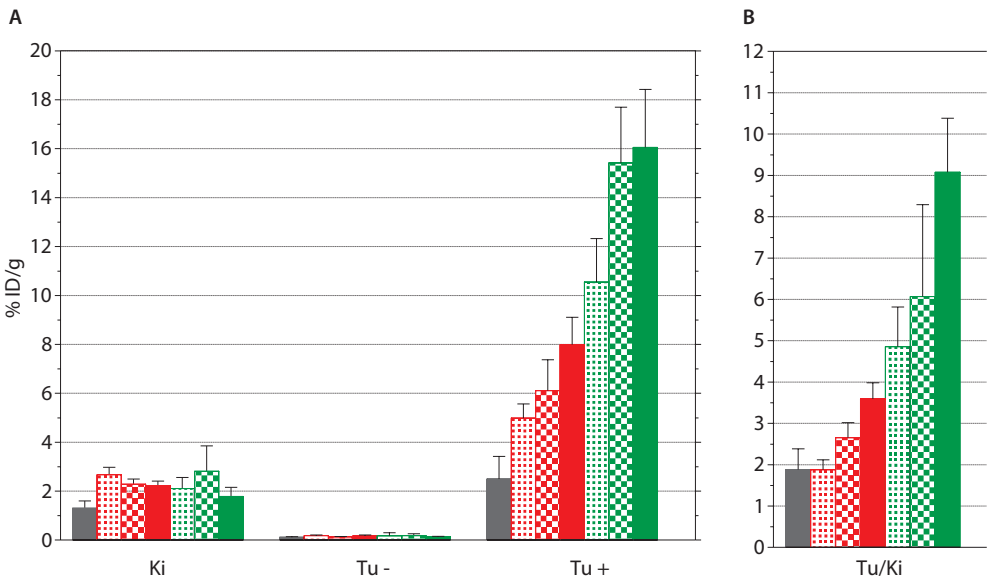


**Figure 4** | **A**) Uptake of [<sup>111</sup>In-DOTA]MG11 in kidneys and A431-CCK2R(+) and A431-CCK2R(-) tumors at 4 h pi in SCID mice for controls, and increasing amounts of the NEP inhibitors TO and PA. Data are given as mean of %ID/g±sd, n≥ 4. [<sup>111</sup>In-DOTA]MG11 iv-coinjection with vehicle (■), with 1.5 µg TO (⊞), with 15 µg TO (■), with 150 µg TO (■), with 3 µg PA (⊞), with 30 µg PA (■), or 300 µg PA (■) in SCID mice bearing twin A431-CCK2R(+) (Tu+) and naïve A431-CCK2R(-) (Tu-) human xenografts. **B**) Corresponding tumor-to-kidney ratios (Tu/Ki).

## DISCUSSION

The advent of radiolabeled somatostatin analogs, like OctreoScan® ( $[^{111}\text{In-DTPA}]$ octreotide) and Lutathera® ( $[^{177}\text{Lu-DOTA}]$ Tate), in the management of  $\text{sst}_2$ -expressing neuroendocrine tumors [30], has established the application of peptide-radioligands for molecular imaging and radionuclide therapy of tumors. This success has largely depended on the metabolic robustness of the cyclic-octapeptide analogs applied. The evolution of peptide-receptor targeted diagnosis and therapy beyond the boundaries of  $\text{sst}_2$ -positive neuroendocrine tumors is valid based on the overexpression of other peptide-receptors in a variety of human tumors [31]. However, progress in this direction has been greatly restricted by the sub-optimal metabolic stability of peptide-radioligands. Structural interventions to improve metabolic stability often deteriorate other important biological features of radiopeptides, as for example receptor-affinity or pharmacokinetics [9].

We have recently proposed the in situ stabilization of biodegradable radiopeptides by coinjection of a suitable protease inhibitor, leading to significant improvement of tumor-uptake [15]. This concept has indeed led to impressive diagnostic signal amplification on tumor-lesions in preclinical models and was recently shown to improve the outcome of radionuclide therapy as well [32]. Especially in the case of  $[^{111}\text{In-DOTA}]$ MG11 and other radiolabeled gastrins, high enhancement of tumor uptake combined with a preserved low kidney retention were observed, resulting in particularly appealing tumor-to-kidney ratios [18,29]. These preclinical results, obtained after coinjection of  $[^{111}\text{In-DOTA}]$ MG11 with the NEP-inhibitor PA, warrant further validation in a “proof-of-principle” study in patients.

It should be noted, that our studies on in situ radiopeptide stabilization and enhancement of tumor uptake have primarily been focused on NEP-inhibition by PA. Remarkably, a great variety of radioligands originating from different peptide families, including somatostatin, bombesin and gastrin, have profited by application of this simple methodology, revealing a central role of NEP in initiating the in vivo degradation of these analogs [15]. The impact of in situ NEP-inhibition relies on the abundant and ubiquitous presence of this ectoenzyme in the body combined with its broad substrate specificity [14]. However, NEP may not always exclusively determine the in vivo fate of radiopeptides. For example, ACE has often been implicated in the degradation of peptide ligands and its role on the in vitro degradation of different-length gastrin analogs has been previously reported [10]. It should be stressed that the impact of in situ ACE-inhibition on the bioavailability and tumor localization of  $[^{111}\text{In-DOTA}]$ MG11 in vivo has not been thus far investigated.

For this purpose, in our study we have coinjected  $[^{111}\text{In-DOTA}]$ MG11 together with the potent ACE-inhibitor Lis, a registered antihypertensive drug [19]. As a result, we were not able to observe any change in the radioligand uptake in AR42J tumors in mice treated with Lis vs. controls at 4 h pi. In addition, dual NEP/ACE-inhibition by combined coinjection of both Lis and PA inhibitors with  $[^{111}\text{In-DOTA}]$ MG11 induced no additive effect vs. single NEP-inhibition by PA (Table 1, Figure 3;  $P>0.05$ ). These findings strongly suggest that ACE does not contribute to the in vivo processing of  $[^{111}\text{In-DOTA}]$ MG11 and verify NEP as the major degrading protease.

Owing to the fast kinetics of radiopeptide localization to target-sites upon entry in the bloodstream, only rapidly occurring degradation events – as those related to NEP – are relevant for tumor-targeting efficacy. Hence, the onset of NEP-inhibition should occur and reach its maximum

quite rapidly, but not last longer than the time needed for the radioactivity to clear from blood and access the target. In this respect, the inhibitor should preferably induce rapid, complete and transient NEP-inhibition. In addition, it should be potent, water-soluble, chemically stable and available at a reasonable cost. PA combines most of the above desirable properties however it has not been thoroughly investigated in terms of biosafety [17]. Only very low amounts of PA have been iv-injected in human, not sufficient for in vivo effective inhibition of NEP [20].

Aiming at clinical translation our interest has been attracted by two clinically certified NEP-inhibitors, TO and its prodrug Race. TO is a potent, reversible NEP-inhibitor with a relative rapid onset of action [21], but its water solubility is not ideal for iv injection as a bolus together with the radiopeptide. It has been previously tested in high doses in human, as for example by iv-infusion of 150 mg in 250 mL of isotonic glucose in 42 patients showing excellent hemodynamic tolerance [22]. The impact of TO on the bioavailability and tumor uptake of our paradigm compound [<sup>111</sup>In-DOTA]MG11 was compared vs. PA 4 h after coinjection of the radiotracer with equimolar amounts of either inhibitor in AR42J tumor-bearing mice. As a result, we observed comparable and impressive enhancement of tumor values (Table 1, Figure 3). On the other hand, Race is a registered antidiarrheal drug for oral use and a prodrug for TO [23,24]. Due to its poor water-solubility it cannot be iv-administered in mice and was instead ip-injected in high molar excess (10-fold than the TO dose) 30–40 min prior to the iv-injection of [<sup>111</sup>In-DOTA]MG11. As a result, tumor values significantly increased compared to controls, but half as efficiently compared to the iv-injected hydrophilic inhibitors PA and TO. This finding highlights the significance of administration route and actual concentration of the inhibitor in the blood at the time of the radiotracer injection to achieve maximum enhancement of uptake on tumor-lesions.

In the last part of this study, the efficacy of TO to enhance the uptake of [<sup>111</sup>In-DOTA]MG11 specifically in human CCK2R(+)-expressing tumors was compared vs. PA at progressively increasing administered doses in mice bearing double A431-CCK2R(+/-) tumors (Table 2, Figure 4). While both NEP-inhibitors induced significant and CCK2R-specific tumor uptake enhancement even at the lowest administered doses (1.5 µg TO and 3 µg PA), PA showed consistently superior efficacy at all tested dose-levels compared to TO ( $P < 0.001$ ). Remarkably, PA reached maximum tumor uptake-enhancement at the 30 µg dose already, whereas TO reached half as high tumor values at the corresponding 10-fold molar dose of 150 µg. These intriguing findings may be tentatively assigned to the free thiol functionality of TO (Figure 1). This strong nucleophile is prone to interact in vivo with electrophiles and hence the effective dose of TO might be much lower than originally anticipated. In fact, previous reports have demonstrated the fast in vivo inactivation of thiol-based NEP-inhibitors, including TO [33,34]. Another practical disadvantage of thiols is their propensity to oxidize in aqueous solutions to the respective disulphides and hence their storage for longer time-periods in ready to use formulations for clinical application becomes challenging.

## CONCLUSIONS

In summary, translation of the concept of in situ stabilization of biodegradable peptide-radioligands to improve tumor-targeting and hence diagnostic sensitivity and therapeutic efficacy, from the preclinical setting into patients, poses certain challenges that need to be competently addressed. Promising data thus far obtained from mouse models for our paradigm radiotracer [<sup>111</sup>In-DOTA] MG11 and the NEP-inhibitor PA have been directly compared herein with results retrieved after treatment of mice with the ACE-inhibitor Lis and the NEP-inhibitors TO and Race, all of which are clinically tested. This study has shown that only NEP-inhibition is relevant for clinical translation. It has also shown that significant enhancement of the radiotracer tumor uptake is indeed feasible by both TO and Race. However, for maximum efficacy, matching that of PA, further studies need to be performed to optimise dose, administration route and time of inhibitor injection in respect to radiotracer injection, and are currently actively pursued.

### Glossary

SPECT: Single photon emission computed tomography; PET: Positron Emission Tomography; DOTA: 1,4,7,10-tetraazacyclododecane-1,4,7,10-tetraacetic acid; N<sub>4</sub> = 6-(carboxyl)-1,4,8,11-tetraazaundecane; DTPA: diethylenetriamine-pentaacetic acid; octreotide: H<sub>2</sub>N-DPhe-c[Cys-Phe-DTrp-Lys-Thr-Cys]-Thr(ol); Tate: H<sub>2</sub>N-DPhe-c[Cys-Tyr-DTrp-Lys-Thr-Cys]-Thr-OH; sst<sub>2</sub>: somatostatin subtype 2 receptor.

### Competing Interests

The authors declare that they have no competing interests.

### Contributions of Authors

AK was actively engaged in the biological studies and assisted in the writing of this manuscript (ms). BAN designed the overall study, supervised radiochemical work as well as the generation and final editing of the ms. EL performed radiolabeling and radioanalytical work. RV contributed in the selection of the inhibitors and in editing the ms. MdJ and EPK participated in the design of the study and editing of the ms. TM performed animal studies and drafted most parts of the ms.

### Acknowledgments

This work has been partially supported by the Greek General Secretariat for Research and Technology and the European Regional Development Fund under the Action “Development Grants For Research Institutions-KRIPIS” of OPCE II.

## REFERENCES

1. Reubi JC, Schaer JC, Waser B. Cholecystokinin(CCK)-A and CCK-B/gastrin receptors in human tumors. *Cancer Res* 1997, 57(7):1377-1386.
2. Reubi JC, Waser B. Unexpected high incidence of cholecystokinin-B/gastrin receptors in human medullary thyroid carcinomas. *Int J Cancer* 1996, 67(5):644-647.
3. Reubi JC. CCK receptors in human neuroendocrine tumors: clinical implications. *Scand J Clin Lab Invest Suppl* 2001, 234:101-104.
4. Ferrand A, Wang TC. Gastrin and cancer: a review. *Cancer Lett* 2006, 238(1):15-29.
5. Béhé M, Behr TM. Cholecystokinin-B (CCK-B)/gastrin receptor targeting peptides for staging and therapy of medullary thyroid cancer and other CCK-B receptor expressing malignancies. *Biopolymers* 2002, 66(6):399-418.
6. Laverman P, Joosten L, Eek A, Roosenburg S, Peitl PK, Maina T, Macke H, Aloj L, von Guggenberg E, Sosabowski JK, de Jong M, Reubi JC, Oyen WJ, Boerman OC. Comparative biodistribution of 12 <sup>111</sup>In-labelled gastrin/CCK2 receptor-targeting peptides. *Eur J Nucl Med Mol Imaging* 2011, 38(8):1410-1416.
7. Dufresne M, Seva C, Fourmy D. Cholecystokinin and gastrin receptors. *Physiol Rev* 2006, 86(3):805-847.
8. Ocak M, Helbok A, Rangger C, Peitl PK, Nock BA, Morelli G, Eek A, Sosabowski JK, Breeman WA, Reubi JC, Decristoforo C. Comparison of biological stability and metabolism of CCK2 receptor targeting peptides, a collaborative project under COST BM0607. *Eur J Nucl Med Mol Imaging* 2011, 38(8):1426-1435.
9. Vlieghe P, Lisowski V, Martinez J, Khrestchatsky M. Synthetic therapeutic peptides: science and market. *Drug Discov Today* 2010, 15(1-2):40-56.
10. Dubreuil P, Fulcrand P, Rodriguez M, Fulcrand H, Laur J, Martinez J. Novel activity of angiotensin-converting enzyme. Hydrolysis of cholecystokinin and gastrin analogues with release of the amidated C-terminal dipeptide. *Biochem J* 1989, 262(1):125-130.
11. Deschodt-Lanckman M, Pauwels S, Najdovski T, Dimaline R, Dockray GJ. In vitro and in vivo degradation of human gastrin by endopeptidase 24.11. *Gastroenterology* 1988, 94(3):712-721.
12. Power DM, Bunnett N, Turner AJ, Dimaline R. Degradation of endogenous heptadecapeptide gastrin by endopeptidase 24.11 in the pig. *Am J Physiol* 1987, 253(1 Pt 1):G33-39.
13. Migaud M, Durieux C, Viereck J, Soroca-Lucas E, Fournie-Zaluski MC, Roques BP. The in vivo metabolism of cholecystokinin (CCK-8) is essentially ensured by aminopeptidase A. *Peptides* 1996, 17(4):601-607.
14. Roques BP, Noble F, Dauge V, Fournie-Zaluski MC, Beaumont A. Neutral endopeptidase 24.11: structure, inhibition, and experimental and clinical pharmacology. *Pharmacol Rev* 1993, 45(1):87-146.
15. Nock BA, Maina T, Krenning EP, de Jong M. "To serve and protect": enzyme inhibitors as radiopeptide escorts promote tumor targeting. *J Nucl Med* 2014, 55(1):121-127.
16. Suda H, Aoyagi T, Takeuchi T, Umezawa H. Letter: A thermolysin inhibitor produced by Actinomycetes: phosphoramidon. *J Antibiot (Tokyo)* 1973, 26(10):621-623.
17. Oefner C, D'Arcy A, Hennig M, Winkler FK, Dale GE. Structure of human neutral endopeptidase (Nepriylsin) complexed with phosphoramidon. *J Mol Biol* 2000, 296(2):341-349.
18. Kaloudi A, Nock BA, Krenning EP, Maina T, De Jong M. Radiolabeled gastrin/CCK analogs in tumor diagnosis: towards higher stability and improved tumor targeting. *Q J Nucl Med Mol Imaging* 2015, 59(3):287-302.
19. Brunner DB, Desponds G, Biollaz J, Keller I, Ferber F, Gavras H, Brunner HR, Schelling JL. Effect of a new angiotensin converting enzyme inhibitor MK 421 and its lysine analogue on the components of the renin system in healthy subjects. *Br J Clin Pharmacol* 1981, 11(5):461-467.
20. Polosa R, Santonocito G, Magri S, Paolino G, Armato F, Pagano C, Crimi N. Neutral endopeptidase inhibition with inhaled phosphoramidon: no effect on bronchial responsiveness to adenosine 5'-monophosphate (AMP) in asthma. *Eur Respir J* 1997, 10(11):2460-2464.
21. Roques BP, Fournie-Zaluski MC, Soroca E, Lecomte JM, Malfroy B, Llorens C, Schwartz JC. The enkephalinase inhibitor thiorphan shows antinociceptive activity in mice. *Nature* 1980, 288(5788):286-288.
22. Floras P, Bidabe AM, Caille JM, Simonnet G, Lecomte JM, Sabathie M. Double-blind study of effects of enkephalinase inhibitor on adverse reactions to myelography. *AJNR Am J Neuroradiol* 1983, 4(3):653-655.

23. Lecomte JM, Costentin J, Vlaiculescu A, Chaillet P, Marcais-Collado H, Llorens-Cortes C, Leboyer M, Schwartz JC. Pharmacological properties of acetorphan, a parenterally active "enkephalinase" inhibitor. *J Pharmacol Exp Ther* 1986, 237(3):937-944.
24. Salazar-Lindo E, Santisteban-Ponce J, Chea-Woo E, Gutierrez M. Racecadotril in the treatment of acute watery diarrhea in children. *N Engl J Med* 2000, 343(7):463-467.
25. Nock BA, Maina T, Behe M, Nikolopoulou A, Gotthardt M, Schmitt JS, Behr TM, Macke HR. CCK-2/gastrin receptor-targeted tumor imaging with <sup>99m</sup>Tc-labeled minigastrin analogs. *J Nucl Med* 2005, 46(10):1727-1736.
26. Breeman WA, Froberg AC, de Blois E, van Gameren A, Melis M, de Jong M, Maina T, Nock BA, Erion JL, Macke HR, Krenning EP. Optimised labeling, preclinical and initial clinical aspects of CCK-2 receptor-targeting with 3 radiolabeled peptides. *Nucl Med Biol* 2008, 35(8):839-849.
27. Scemama JL, De Vries L, Pradayrol L, Seva C, Tronchere H, Vaysse N. Cholecystokinin and gastrin peptides stimulate ODC activity in a rat pancreatic cell line. *Am J Physiol* 1989, 256(5 Pt 1):G846-850.
28. Aloj L, Caracó C, Panico M, Zannetti A, Del Vecchio S, Tesaro D, De Luca S, Arra C, Pedone C, Morelli G, Salvatore M. In vitro and in vivo evaluation of <sup>111</sup>In-DTPAGlu-G-CCK8 for cholecystokinin-B receptor imaging. *J Nucl Med* 2004, 45(3):485-494.
29. Kaloudi A, Nock BA, Lymperis E, Sallegger W, Krenning EP, de Jong M, Maina T. In vivo inhibition of neutral endopeptidase enhances the diagnostic potential of truncated gastrin <sup>111</sup>In-radioligands. *Nucl Med Biol* 2015, 42(11):824-832.
30. de Jong M, Breeman WA, Kwekkeboom DJ, Valkema R, Krenning EP. Tumor imaging and therapy using radiolabeled somatostatin analogues. *Acc Chem Res* 2009, 42(7):873-880.
31. Reubi JC. Peptide receptors as molecular targets for cancer diagnosis and therapy. *Endocr Rev* 2003, 24(4):389-427.
32. Chatalic KL, Konijnenberg M, Nonnekens J, de Blois E, Hoeben S, de Ridder C, Brunel L, Fehrentz JA, Martinez J, van Gent DC, Nock BA, Maina T, van Weerden WM, de Jong M. In vivo stabilization of gastrin-releasing peptide receptor antagonist enhances PET imaging and radionuclide therapy of prostate cancer in preclinical studies. *Theranostics* 2016, 6(1):104-117.
33. Iyer RA, Mitroka J, Malhotra B, Bonacorsi S, Jr., Waller SC, Rinehart JK, Roongta VA, Kripalani K. Metabolism of [(14)C]omapatrilat, a sulfhydryl-containing vasopeptidase inhibitor in humans. *Drug Metab Dispos* 2001, 29(1):60-69.
34. Poras H, Bonnard E, Dange E, Fournie-Zaluski MC, Roques BP. New orally active dual enkephalinase inhibitors (DENKIs) for central and peripheral pain treatment. *J Med Chem* 2014, 57(13):5748-5763.

# CHAPTER

# 6

## <sup>99m</sup>Tc-Labeled Gastrins of Varying Peptide Chain Length: Distinct Impact of NEP/ACE-Inhibition on Stability and Tumor Uptake in Mice

Aikaterini Kaloudi<sup>a</sup>, Berthold A. Nock<sup>a</sup>, Emmanouil Lympersis<sup>a</sup>,  
Eric P. Krenning<sup>b</sup>, Marion de Jong<sup>b,c</sup>, Theodosia Maina<sup>a</sup>

<sup>a</sup>Molecular Radiopharmacy, INRASTES, National Center for Scientific Research "Demokritos", GR-153 10 Athens, Greece

<sup>b</sup>Department of Nuclear Medicine, Erasmus MC,  
3015 CE Rotterdam, The Netherlands

<sup>c</sup>Department of Radiology, Erasmus MC,  
3015 CE Rotterdam, The Netherlands

*Nucl. Med. Biol.* 43:347-354,2016

## ABSTRACT

**Introduction:** In situ inhibition of neutral endopeptidase (NEP) has been recently shown to impressively increase the bioavailability and tumor uptake of biodegradable gastrin radioligands. Furthermore, angiotensin converting enzyme (ACE) has been previously shown to cleave gastrin analogs in vitro. In the present study, we have assessed the effects induced by single or dual NEP/ACE-inhibition on the pharmacokinetic profile of three  $^{99m}\text{Tc}$ -labeled gastrins of varying peptide chain length: [ $^{99m}\text{Tc}$ ]SG6 ([ $^{99m}\text{Tc}$ -N<sub>4</sub>-Gln<sup>1</sup>]gastrin(1-17)), [ $^{99m}\text{Tc}$ ]DG2 ([ $^{99m}\text{Tc}$ -N<sub>4</sub>-Gly<sup>4</sup>,DGLu<sup>5</sup>]gastrin(4-17)) and [ $^{99m}\text{Tc}$ ]DG4 ([ $^{99m}\text{Tc}$ -N<sub>4</sub>-DGLu<sup>10</sup>]gastrin(10-17)).

**Methods:** Mouse blood samples were collected 5 min after injection of each of [ $^{99m}\text{Tc}$ ]SG6/DG2/DG4 together with: a) vehicle, b) the NEP-inhibitor phosphoramidon (PA), c) the ACE-inhibitor lisinopril (Lis), or d) PA plus Lis and were analyzed by RP-HPLC for radiometabolite detection. Biodistribution was studied in SCID mice bearing A431-CCK2R(+/-) xenografts at 4 h postinjection (pi). [ $^{99m}\text{Tc}$ ]SG6 or [ $^{99m}\text{Tc}$ ]DG4 was coinjected with either vehicle or the above described NEP/ACE-inhibitor regimens; for [ $^{99m}\text{Tc}$ ]DG2 control and PA animal groups were only included.

**Results:** Treatment of mice with PA induced significant stabilization of  $^{99m}\text{Tc}$ -radiotracers in peripheral blood, while treatment with Lis or Lis+PA affected the stability of *des*(Glu)<sub>5</sub> [ $^{99m}\text{Tc}$ ]DG4 only. In line with these findings, PA coinjection led to notable amplification of tumor uptake of radiopeptides compared to controls ( $P < 0.01$ ). Only [ $^{99m}\text{Tc}$ ]DG4 profited by single Lis ( $2.06 \pm 0.39\% \text{ID/g}$  vs.  $0.99 \pm 0.13\% \text{ID/g}$  in controls) or combined Lis+PA coinjection ( $8.91 \pm 1.61\% \text{ID/g}$  vs.  $4.89 \pm 1.33\% \text{ID/g}$  in PA-group). Furthermore, kidney uptake remained favourably low and unaffected by PA and/or Lis coinjection only in the case of [ $^{99m}\text{Tc}$ ]DG4 ( $< 1.9\% \text{ID/g}$ ) resulting in the most optimal tumor-to-kidney ratios.

**Conclusions:** In situ NEP/ACE-inhibition diversely affected the in vivo profile of  $^{99m}\text{Tc}$ -radioligands based on different-length gastrins. Truncated [ $^{99m}\text{Tc}$ ]DG4 exhibited overall the most attractive profile during combined NEP/ACE-inhibition in mouse models, providing new opportunities for CCK2R-expressing tumor imaging in man with SPECT.

**Key words:** Gastrin-based  $^{99m}\text{Tc}$ -radiotracers, NEP-inhibition, ACE-inhibition, radioligand stabilization, tumor targeting, kidney retention



## INTRODUCTION

Cholecystokinin subtype 2 receptors (CCK2R) can serve as molecular targets for diagnostic imaging and radionuclide therapy of CCK2R-expressing human tumors, such as medullary thyroid carcinoma (MTC), with the aid of gastrin radioligands [1-5]. Native gastrin I (gastrin, pGlu-Gly-Pro-Trp-Leu-(Glu)<sub>5</sub>-Ala-Tyr-Gly-Trp-Met-Asp-Phe-NH<sub>2</sub>) and its analogs modified with various chelators have allowed labeling with radiometals relevant for SPECT or PET imaging as well as for internal radiotherapy. For SPECT applications in particular,  $^{99m}\text{Tc}$  remains the label of choice, combining optimal nuclear characteristics with easy availability in high purity and high specific activity at a low cost by means of commercial  $^{99}\text{Mo}/^{99m}\text{Tc}$  generators [6].

Development of gastrin  $^{99m}\text{Tc}$ -radiotracers has likewise involved coupling of a suitable chelator at the peptide N-terminus enabling facile incorporation of the radiometal in high yields and high specific activities. Thus, the [ $^{99m}\text{Tc}(\text{CO})_3$ ]<sup>+</sup>-synthon, or the hydrazinonicotinic acid (HYNIC)-derived [ $^{99m}\text{Tc}^{\text{V}}=\text{N}=\text{N}-\text{R}$ ]-unit have been employed for such purposes, with suitable co-chelators completing the metal coordination sphere while at the same time introducing the peptide vector and/or “fine-tuning” in vivo pharmacokinetics [7-9]. In our previous work, we have instead reported on gastrin analogs coupled to open chain tetraamines (N<sub>4</sub>) to produce radiotracers carrying the hydrophilic and monocationic [ $^{99m}\text{Tc}(\text{O})_2\text{N}_4$ ]<sup>+</sup>-chelate and displaying high CCK2R-affinity and excellent tumor targeting properties in animal models and in man [6, 10]. In particular, the minigastrin radiotracer [ $^{99m}\text{Tc}$ ]Demogastrin 2 ([ $^{99m}\text{Tc}-\text{N}_4-\text{Gly}^4,\text{DGlu}^5$ ]gastrin(4-17)); [ $^{99m}\text{Tc}$ ]DG2) was able to successfully visualize all known lesions in a group of MTC patients, displaying superior pharmacokinetics and higher in vivo stability compared to other [ $^{111}\text{In}-\text{DOTA}$ ]-derivatized CCK and truncated gastrin(5-17) analogs [11,12].

A relationship has been previously revealed between peptide chain length, especially the penta-Glu unit occupying positions 6 through 10 in native gastrin, and important biological features of gastrin radioligands, such as receptor-affinity, metabolic stability, tumor targeting efficacy, and kidney accumulation. Evidently, truncated *des*(Glu)<sub>5</sub> radiogastrins are rapidly degraded and poorly localize in CCK2R-expressing tumors, but their renal uptake is favorably low. Conversely, radiogastrins containing the multi-negatively charged penta-Glu<sup>6-10</sup>-chain are metabolically more robust showing good in vivo tumor uptake, which is compromised however by unfavorably high kidney accumulation [13-15].

We have recently shown that stabilization of fast biodegradable gastrin radioligands in peripheral blood of mice is feasible by in situ inhibition of neutral endopeptidase (NEP) [16,17]. Stabilization was achieved by coinjection of a suitable NEP-inhibitor, such as phosphoramidon (PA), and in the case of *des*(Glu)<sub>5</sub>-gastrin radioligands led to impressive improvements of tumor uptake without undesirably raising kidney accumulation [18-21]. As a result, unprecedentedly high tumor-to-kidney ratios were achieved, very attractive for clinical translation. Although NEP plays a major role in initiating the in vivo catabolism of gastrin and its analogs [22], angiotensin converting enzyme (ACE) has been implicated in the in vitro degradation of truncated gastrins with less than two Glu-residues [23]. The two negatively charged Glu<sup>9-10</sup> in gastrin(9-17) were postulated to provide resistance to ACE. In line

with this hypothesis, we have recently shown that the in vivo degradation of truncated [ $^{111}\text{In}$ -DOTA $^9$ -D $\text{Glu}^{10}$ ]gastrin(9-17) does not involve ACE [21].

In the present study, we have been interested to investigate first the effect of gastrin chain-length on the in vitro and in vivo profile of three different  $\text{N}_4$ -derivatized and  $^{99\text{m}}\text{Tc}$ -labeled analogs: a) novel full length [ $^{99\text{m}}\text{Tc}$ - $\text{N}_4$ -Gln $^1$ ]gastrin ([ $^{99\text{m}}\text{Tc}$ ]SG6), b) minigastrin-based [ $^{99\text{m}}\text{Tc}$ ]DG2 [10], and c) truncated [ $^{99\text{m}}\text{Tc}$ - $\text{N}_4$ -D $\text{Glu}^{10}$ ]gastrin(10-17) ([ $^{99\text{m}}\text{Tc}$ ]DG4) [24] (Figure 1). Special attention has been given on peptide chain-related differences on in vivo stability, CCK2R-positive tumor uptake and kidney retention in mice models. Furthermore, we have investigated the impact of single NEP or ACE, or dual NEP/ACE-inhibition on the in vivo profile of the aforementioned radiotracers. Focus has been directed on different responses induced across radiotracers on stability, pharmacokinetics and tumor targeting in CCK2R-positive mice models.

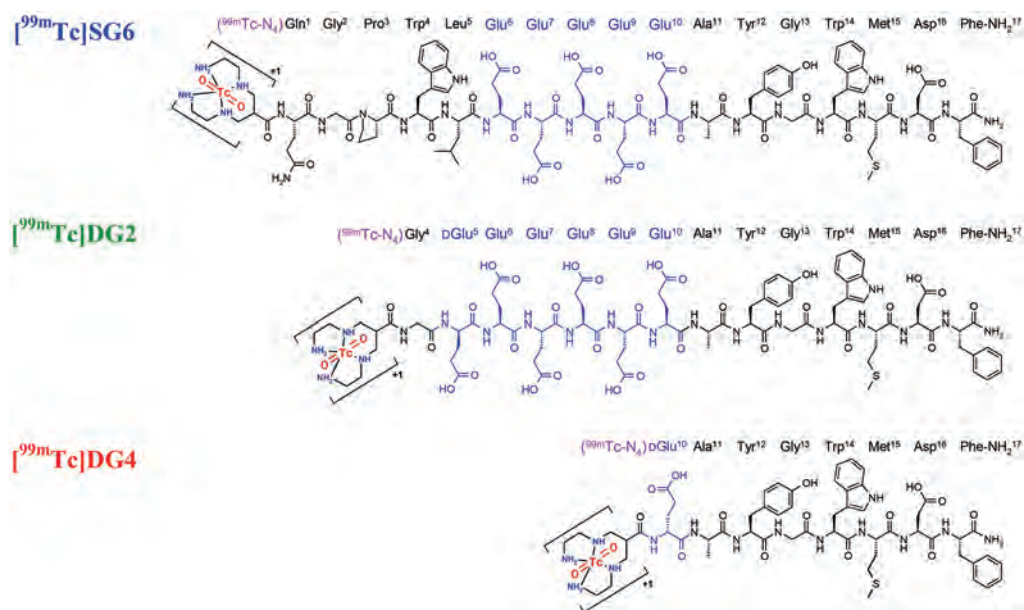


Figure 1 | Chemical structure of [ $^{99\text{m}}\text{Tc}$ ]SG6, [ $^{99\text{m}}\text{Tc}$ ]DG2 and [ $^{99\text{m}}\text{Tc}$ ]DG4.

## MATERIALS AND METHODS

### Chemicals and Radionuclides

All chemicals were reagent grade and were used as such without additional purification. The peptide-conjugates DG2 and DG4 were synthesized on the solid support as previously described [10, 24]. SG6 was purchased from PiChem (Graz, Austria) and [ $\text{Leu}^{15}$ ]gastrin from Bachem (Bubendorf, Switzerland). PA (phosphoramidon disodium dehydrate,  $\text{N}$ -( $\alpha$ -rhamnopyranosyloxyhydroxyphosphinyl)- $\text{L}$ -leucyl- $\text{L}$ -tryptophan $\times 2\text{Na}\times 2\text{H}_2\text{O}$ ) was provided by PeptaNova GmbH (Sandhausen, Germany)

and Lis (lisinopril dehydrate, ((S)1-1-[N2-(1-carboxy-3-phenylpropyl)-lysyl-proline dehydrate, MK 521) by Sigma-Aldrich (St. Louis, USA).

Technetium-99m in the form of  $^{99m}\text{Tc}[\text{NaTcO}_4]$  was obtained by elution of a  $^{99}\text{Mo}/^{99m}\text{Tc}$  generator (DRYTEC, GE Healthcare, Little Chalfont, UK), while  $^{125}\text{I}$  in the form of  $\text{Na}^{125}\text{I}$  in a solution of  $10^{-5}\text{ M}$  NaOH (10  $\mu\text{L}$ ) was purchased from MDS Nordion, SA (Canada).

### Radiolabeling

The lyophilized peptide analogs were dissolved in water to a final concentration of 1 mM and 50  $\mu\text{L}$ -aliquots were stored at  $-20^\circ\text{C}$ . Labeling with  $^{99m}\text{Tc}$  was performed in an Eppendorf vial containing 0.5 M phosphate buffer (pH 11.5) in the presence of excess methionine (Met) to prevent oxidation of Met.  $^{99m}\text{Tc}[\text{NaTcO}_4]$  eluate (370-740 MBq) was added to the vial followed by 0.1 M sodium citrate, the peptide stock solution (15 nmol) and a freshly prepared  $\text{SnCl}_2$  solution in ethanol (30  $\mu\text{g}$ ). The mixture was left to react for 30 min at  $40^\circ\text{C}$  and the pH was neutralised with the addition of 1 M HCl.

Radioiodination of  $[\text{Leu}^{15}]\text{gastrin}$  was performed following the chloramine-T method and  $^{125}\text{I}\text{-Tyr}^{12}, [\text{Leu}^{15}]\text{gastrin}$  was isolated in high purity by HPLC. Aliquots of the radioligand stock solution in 0.1% BSA-PBS buffer were kept at  $-20^\circ\text{C}$  and were used in competition binding experiments (specific activity of 74 GBq/ $\mu\text{mol}$ ).

### Quality Control

For quality control of radiolabeled products RP-HPLC was performed on a Waters Chromatograph (Waters, Vienna, Austria) based on a 600E multisolvent delivery system coupled to a Gabi gamma-detector (Raytest, RSM Analytische Instrumente GmbH, Germany). Data processing and chromatography were controlled with the Empower Software (Waters, USA) and an XTerra RP-18 (5  $\mu\text{m}$ , 4.6 mm  $\times$  150 mm) cartridge column (Waters, Germany) was eluted at 1 mL/min flow rate with a linear gradient system 1 starting from 0% B and advancing to 40% B within 20 min (solvent A= 0.1% aqueous TFA and B= MeCN). For the detection of reduced hydrolyzed technetium traces ( $^{99m}\text{TcO}_2 \times \text{H}_2\text{O}$ ) instant thin layer chromatography (ITLC) was conducted on ITLC silica gel strips, as previously described [17].

### Cell Culture

The human epidermoid carcinoma A431 cell line transfected to stably express the human CCK2R (A431-CCK2R(+)) or devoid of CCK2R expression (A431-CCK2R(-)) was a kind gift of Prof. O. Boerman (Department of Nuclear Medicine, Radboud University Nijmegen Medical Centre, Nijmegen, The Netherlands) and Prof. L. Aloj (Istituto di Biostrutture e Bioimmagini, Consiglio Nazionale delle Ricerche, Naples, Italy). Cells were grown in Dulbecco's Modified Eagle medium with GlutaMAX-I supplemented with 10% fetal bovine serum, 100 U/mL penicillin, 100  $\mu\text{g}/\text{mL}$  streptomycin, 4500 mg/L D-glucose, and 250  $\mu\text{g}/\text{mL}$  G418 and kept in a controlled humidified air containing 5%  $\text{CO}_2$  at  $37^\circ\text{C}$ , as previously described [25]. Splitting of cells with a ratio of 1:3 to 1:5 was performed when approaching confluency using a trypsin/EDTA solution (0.05%/0.02% w/v). All culture reagents were

obtained from Gibco BRL, Life Technologies (Grand Island, NY, USA) or from Biochrom KG Seromed (Berlin, Germany).

### **In vitro assays**

#### ***Competition Binding Assays in A431-CCK2R(+) Cell Membranes***

Competition binding experiments of SG6, DG2 and DG4 against [<sup>125</sup>I-Tyr<sup>12</sup>,Leu<sup>15</sup>]gastrin were conducted in A431-CCK2R(+) cell membranes, harvested as previously described [26]; [Leu<sup>15</sup>]gastrin served as reference compound. Increasing concentrations of the tested peptide ( $10^{-5}$ - $10^{-13}$  M) were mixed with the radioligand (50 pM, ~30,000 cpm) and the membrane homogenate in a total volume of 300  $\mu$ L binding buffer (pH 7.4, 50 mM HEPES, 1% BSA, 5.5 mM MgCl<sub>2</sub>, 35  $\mu$ M bacitracin). Triplicates of each concentration point were incubated for 60 min at 22°C in an Incubator-Orbital Shaker unit (MPM Instr. Srl, Italy). The incubation was interrupted by adding ice-cold washing buffer (10 mM HEPES pH 7.4, 150 mM NaCl), followed by rapid filtration over glass fiber filters (Whatman GF/B, presoaked in binding buffer) on a Brandel Cell Harvester (Adi Hassel Ingenieur Büro, Munich, Germany). Filters were washed with cold washing buffer and were counted for their radioactivity content in an automated well-type gamma counter [NaI(Tl) crystal, Canberra Packard Auto-Gamma 5000 series instrument]. The 50% inhibitory concentration (IC<sub>50</sub>) values were calculated by nonlinear regression according to a one-site model applying the PRISM 2 program (Graph Pad Software, San Diego, CA) and are expressed as mean $\pm$ SD of three experiments performed in triplicate.

#### ***Internalization of Radiotracers in A431-CCK2R(+) Cells***

For time-dependent internalization studies with [<sup>99m</sup>Tc]SG6, [<sup>99m</sup>Tc]DG2 and [<sup>99m</sup>Tc]DG4, A431-CCK2R(+) cells were seeded in six-well plates 24 h before the experiment. Cells were rinsed twice with ice-cold internalization medium (DMEM Glutamax-I, supplemented by 1% (v/v) FBS) and then fresh medium was added (1.2 mL) at 37°C, followed by test radiopeptide (200 fmol total peptide in 150  $\mu$ L 0.5% BSA-PBS, 100,000-200,000 cpm). Non-specific internalization was determined by a parallel triplicate series containing 1  $\mu$ M DG2. Radiotracer incubation in A431-CCK2R(+) cells at 37°C was interrupted at 15 min, 30 min, 60 min, or 120 min by placing the plates on ice, removal of the medium and washing with 0.5% BSA-PBS. Membrane-bound fractions were collected by incubating the cells 2  $\times$  5 min in acid-wash solution (50 mM glycine buffer pH 2.8, 0.1 M NaCl) at room temperature, while internalized fractions by adding 1 N NaOH after rinsing the cells with 0.5% BSA-PBS. Samples were measured for radioactivity using a gamma counter and the percentage of specific internalized and membrane-bound fractions were calculated with Microsoft Excel. Results represent specific internalized $\pm$ SD of total added radioactivity per well from 5 ([<sup>99m</sup>Tc]DG2) or 4 experiments ([<sup>99m</sup>Tc]SG6 and [<sup>99m</sup>Tc]DG4) performed in triplicate.

### **Metabolic studies in mice**

A bolus containing [<sup>99m</sup>Tc]SG6, [<sup>99m</sup>Tc]DG2 or [<sup>99m</sup>Tc]DG4 (100  $\mu$ L, 55.5-111 MBq, 3 nmol of total peptide in vehicle: saline/EtOH 9/1 v/v) was injected in the tail vein of healthy male Swiss Albino mice, together with: a) vehicle (100  $\mu$ L; control-group), b) PA (100  $\mu$ L of vehicle containing 300  $\mu$ g PA; PA-group), c) PA plus Lis (100  $\mu$ L vehicle containing 300  $\mu$ g PA and 100  $\mu$ g Lis; PA+Lis-group), or

d) Lis (100  $\mu$ L of vehicle containing 100  $\mu$ g Lis; Lis-group: for [<sup>99m</sup>Tc]DG4). Animals were euthanized 5 min post-injection (pi) and blood was collected and immediately placed on ice, in pre-chilled polypropylene vials containing EDTA and Met. Samples were centrifuged at 2,000 g at 4°C for 10 min, the plasma was collected and mixed with an equal volume of MeCN and centrifuged again for 10 min at 15,000 g at 4°C. The supernatant was collected and concentrated to a small volume under a gentle N<sub>2</sub>-flux at 40°C, diluted with physiological saline ( $\approx$ 400  $\mu$ L) and filtered through a Millex GV filter (0.22  $\mu$ m). Suitable aliquots of the filtrate were analyzed by RP-HPLC on a Symmetry Shield RP18 (5  $\mu$ m, 3.9 mm  $\times$  20 mm) column (Waters, Germany) eluted at a flow rate of 1 mL/min and adopting gradient system 2: 100% A / 0% B to 50% A / 50% B in 50 min; A= 0.1% TFA in H<sub>2</sub>O and B= MeCN. The elution time ( $t_R$ ) of intact radioligand was determined by coinjection with a sample of the labeling reaction solution. Experiments were repeated twice.

### Biodistribution in SCID mice bearing CCK2R-positive xenografts

A  $\sim$ 150  $\mu$ L bolus containing a suspension of freshly harvested A431-CCK2R(+/-) ( $1.6 \times 10^7/1.4 \times 10^7$ ) cells in normal saline was subcutaneously inoculated in the flanks of 6-weeks old male SCID mice (NCSR "Demokritos" Animal House,  $18 \pm 2$  g body weight). After approximately 8 days well palpable A431-CCK2R(+/-) tumors ( $190 \pm 80$  mg) were developed at the inoculation sites and biodistribution was performed. At the day of the experiment, a bolus of [<sup>99m</sup>Tc]SG6, [<sup>99m</sup>Tc]DG2 or [<sup>99m</sup>Tc]DG4 (148-185 kBq, 10 pmol total peptide, in vehicle: saline/EtOH 9/1 v/v) was intravenously injected in the tail of mice together with either vehicle (100  $\mu$ L; control group), or Lis (100  $\mu$ g Lis dissolved in 100  $\mu$ L vehicle; Lis-group: for [<sup>99m</sup>Tc]SG6 and [<sup>99m</sup>Tc]DG4), or PA (300  $\mu$ g PA dissolved in 100  $\mu$ L vehicle; PA-group), or PA plus Lis (300  $\mu$ g PA + 100  $\mu$ g Lis dissolved in 100  $\mu$ L vehicle; PA+Lis-group: for [<sup>99m</sup>Tc]SG6 and [<sup>99m</sup>Tc]DG4). Animals were euthanized at 4 h pi in groups of at least 4 and blood samples, organs of interest and tumors were dissected, weighted and counted in the gamma counter; stomachs were emptied of their contents. Biodistribution data were calculated as percent of injected dose per gram tissue (%ID/g) with the aid of suitable standards of the injected dose, using the Microsoft Excel program. Results represent average values  $\pm$ SD,  $n=4$ ; for [<sup>99m</sup>Tc]SG6 PA- and PA+Lis-groups and for all [<sup>99m</sup>Tc]DG2-groups  $n=5$ .

All animal experiments were carried out in compliance with European and national regulations and after approval of protocols by national Authorities.

### Statistical analysis

The unpaired two tailed Student's *t* test of GraphPad Prism Software (San Diego, CA) was used for statistical analysis. *P* values of  $<0.05$  were considered to be statistically significant.

## RESULTS

### Radiolabeling and quality control

Radiolabeling of SG6, DG2 and DG4 with <sup>99m</sup>Tc was accomplished after 30 min incubation at 40°C in alkaline aqueous medium containing citrate anions, SnCl<sub>2</sub> and excess Met to suppress sulfoxide

formation. A >96% radiometal incorporation in the open chain tetraamine chelator was verified by RP-HPLC analysis. Radiopeptides were obtained in >98% radiochemical purity demonstrating that the addition of Met in the labeling solution prevented the oxidation of Met in the peptide chain.

## In Vitro Studies

### CCK2R-Affinity of Peptide-Conjugates

Competition binding assays for SG6, DG2 and DG4 were performed in A431-CCK2R(+) cell membranes. As shown in Figure 2, all peptides were able to displace [<sup>125</sup>I-Tyr<sup>12</sup>,Leu<sup>15</sup>]gastrin from CCK2R binding sites of the membranes in a monophasic and dose-dependent manner. The receptor binding affinity of truncated DG4 ( $IC_{50} = 0.9 \pm 0.1$  nM) was comparable to the [Leu<sup>15</sup>]gastrin reference ( $IC_{50} = 0.9 \pm 0.1$  nM), with the longer chain analogs SG6 ( $IC_{50} = 9.3 \pm 0.9$  nM) and DG2 ( $IC_{50} = 10.7 \pm 1.3$  nM) exhibiting less affinity for the CCK2R.

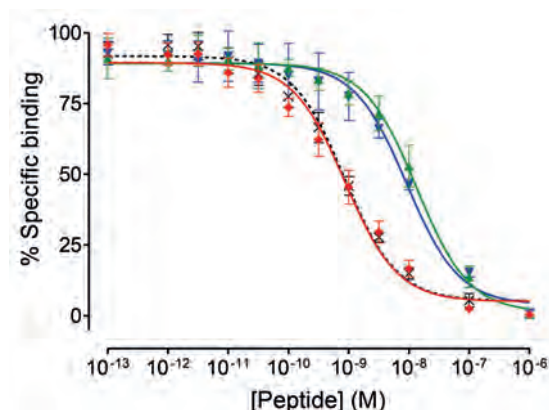


Figure 2 | Displacement of [<sup>125</sup>I-Tyr<sup>12</sup>,Leu<sup>15</sup>]gastrin from CCK2R binding sites in A431-CCK2R(+) cell membranes by increasing concentrations of SG6 ( $\nabla$ ,  $IC_{50} = 9.3 \pm 0.9$  nM), DG2 ( $\blacktriangle$ ,  $IC_{50} = 10.7 \pm 1.3$  nM), DG4 ( $\blacklozenge$ ,  $IC_{50} = 0.9 \pm 0.1$  nM) and [Leu<sup>15</sup>]gastrin (\*,  $IC_{50} = 0.9 \pm 0.1$  nM, reference); values represent mean  $IC_{50} \pm SD$ ,  $n = 3$ .

### Radiotracer Internalization in A431-CCK2R(+) Cells

Time-dependent internalization curves of [<sup>99m</sup>Tc]SG6, [<sup>99m</sup>Tc]DG2 and [<sup>99m</sup>Tc]DG4 in A431-CCK2R(+) cells are included in Figure 3. The internalization efficacy of [<sup>99m</sup>Tc]SG6 (19.0 ± 0.4% specific internalized of total-added radioactivity at 1 h incubation) was found comparable to that of [<sup>99m</sup>Tc]DG2 (20.4 ± 0.4% at 1 h incubation,  $P > 0.05$ ). Conversely, truncated [<sup>99m</sup>Tc]DG4 internalized much slower ( $P < 0.001$ ) at all time points (e.g. 2.3 ± 0.1% at 1 h incubation). A ~70-85% of cell-associated radioactivity was internalized at all time points, revealing a fast endocytosis process at 37°C and consistent with a receptor radioagonist profile (results not shown). In all cases internalization was banned (<0.2% at all time points) in the presence of 1 μM DG2, suggesting a CCK2R-mediated process.

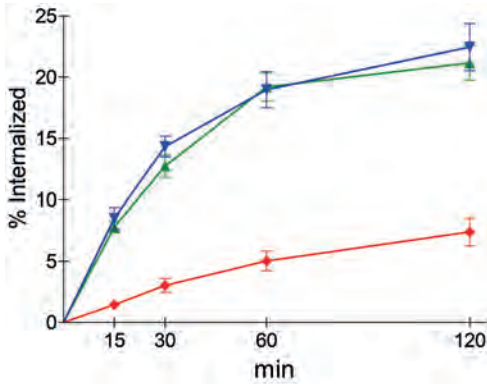


Figure 3 | Specific time-dependent internalization of [ $^{99m}\text{Tc}$ ]SG6 ( $\blacktriangledown$ ,  $n=4$ ), [ $^{99m}\text{Tc}$ ]DG2 ( $\blacktriangle$ ,  $n=5$ ) and [ $^{99m}\text{Tc}$ ]DG4 ( $\blacklozenge$ ,  $n=4$ ) in A431-CCK2R(+) cells at 37°C; results represent the mean $\pm$ SD of  $n$  experiments performed in triplicate.

### Metabolic Studies in Mice

The stability of [ $^{99m}\text{Tc}$ ]SG6, [ $^{99m}\text{Tc}$ ]DG2 and [ $^{99m}\text{Tc}$ ]DG4 in peripheral mouse blood was studied by HPLC analysis of blood samples collected 5 min pi. Based on in vivo stability (radiochromatograms in Figure 4A), the three radiotracers could be ranked as follows: [ $^{99m}\text{Tc}$ ]DG2 (60% intact) > [ $^{99m}\text{Tc}$ ]SG6 (40% intact) >> [ $^{99m}\text{Tc}$ ]DG4 (10% intact). Treatment with the NEP inhibitor PA led to notably enhanced radiotracer stability (Figure 4B), namely: [ $^{99m}\text{Tc}$ ]DG2: to 85% intact; [ $^{99m}\text{Tc}$ ]SG6: to 70% intact; and [ $^{99m}\text{Tc}$ ]DG4: to 60% intact. Coinjection of both PA and Lis affected the stability of truncated [ $^{99m}\text{Tc}$ ]DG4 only, with the respective radiotracer stabilities shown in Figure 4C to be: [ $^{99m}\text{Tc}$ ]DG2: 85% intact; [ $^{99m}\text{Tc}$ ]SG6: 70% intact; and [ $^{99m}\text{Tc}$ ]DG4: 80% intact. These results implicating not only NEP, but also ACE, in the in vivo degradation of truncated [ $^{99m}\text{Tc}$ ]DG4, were corroborated by the increase of radiotracer stability after coinjection of Lis (40% intact [ $^{99m}\text{Tc}$ ]DG4,  $P<0.001$ ; Figure 4D) vs. control (10% intact; Figure 4A).

### Biodistribution in A431-CCK2R(+/-) Tumor-Bearing Mice

Cumulative biodistribution data of [ $^{99m}\text{Tc}$ ]SG6, [ $^{99m}\text{Tc}$ ]DG2 and [ $^{99m}\text{Tc}$ ]DG4 in SCID mice bearing a double A431-CCK2R(+/-) tumor model at 4 h pi are summarized in Table 1 and Figure 5, as %ID/g $\pm$ SD. All radioligands showed a fast blood and background clearance via the kidneys, but renal retention significantly differed across analogs. While the *des*(Glu)<sub>5</sub>-radiotracer [ $^{99m}\text{Tc}$ ]DG4 showed favourably low kidney uptake (1.16 $\pm$ 0.13%ID/g), [ $^{99m}\text{Tc}$ ]DG2 exhibited the highest kidney uptake (58.62 $\pm$ 8.98%ID/g,  $P<0.001$ ), followed by the gastrin-17 analog [ $^{99m}\text{Tc}$ ]SG6 (26.07 $\pm$ 3.28%ID/g,  $P<0.001$ ). The uptake of the three radiotracers in A431-CCK2R(+) xenografts also differed, resulting in the following rank of tumor uptake: [ $^{99m}\text{Tc}$ ]DG2: 12.89 $\pm$ 4.69%ID/g ( $n=5$ )  $\geq$  [ $^{99m}\text{Tc}$ ]SG6: 10.25 $\pm$ 3.51%ID/g ( $n=4$ ) >> [ $^{99m}\text{Tc}$ ]DG4 0.99 $\pm$ 0.13%ID/g ( $n=4$ ,  $P<0.001$ ). The radiotracer uptake in the A431-CCK2R(-) xenografts was minimal, indicating CCK2R-specificity.



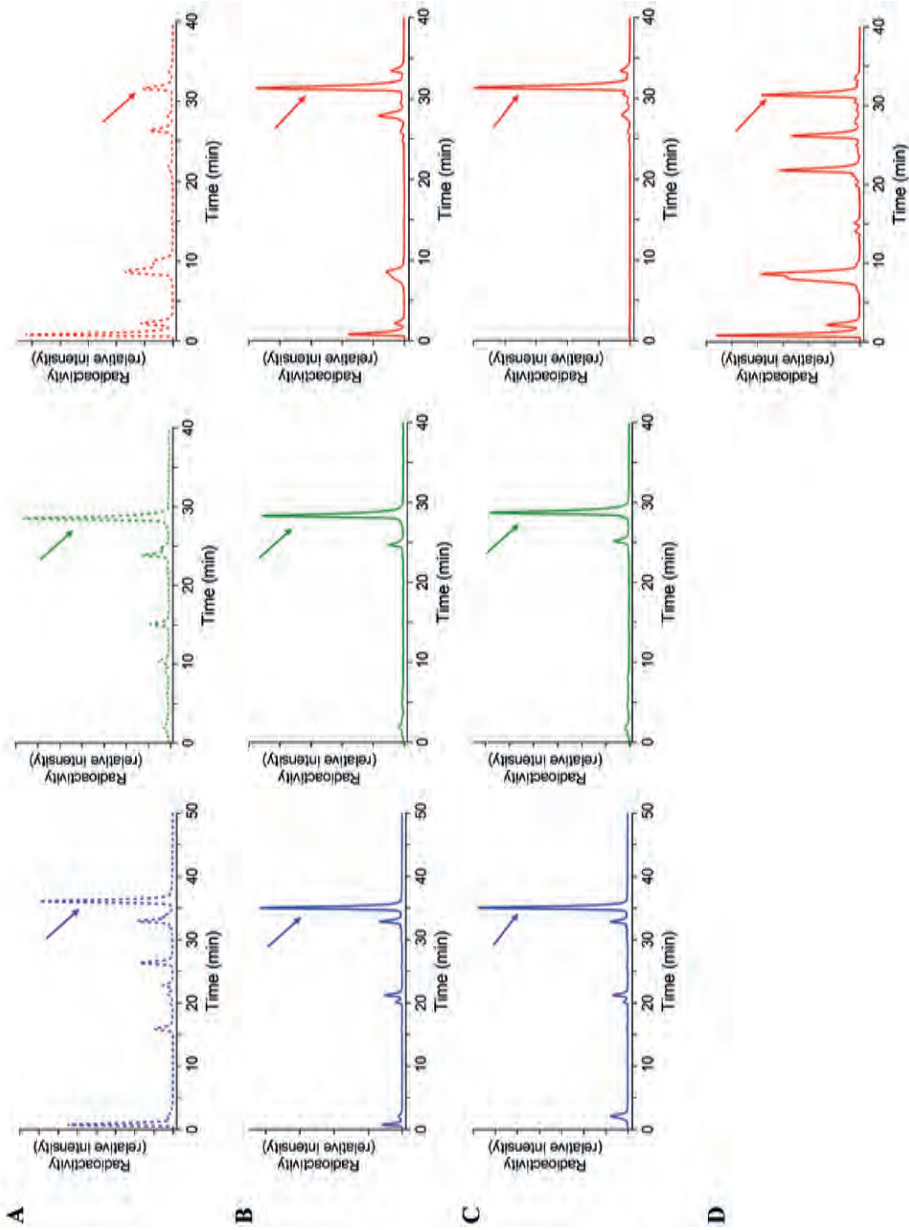


Figure 4 | HPLC radiochromatograms (system 2) of mouse blood collected 5 min after iv injection of [ $^{99m}\text{Tc}$ ]SG6 (1<sup>st</sup> column; blue line), [ $^{99m}\text{Tc}$ ]DG2 (2<sup>nd</sup> column; green line) and [ $^{99m}\text{Tc}$ ]DG4 (3<sup>rd</sup> column; red line) co-injected with A) vehicle, B) PA (300 µg), C) PA plus Lis (300 µg PA and 100 µg Lis) or D) Lis (100 µg); the  $t_R$  of intact radiotracer is indicated by the arrow.



Table 1 | Biodistribution of [<sup>99m</sup>Tc]SG6, [<sup>99m</sup>Tc]DG2 and [<sup>99m</sup>Tc]DG4 in A431-CCK2R(+/-) tumor-bearing mice at 4 h pi.

Organs	%ID/g ± SD, n≥4											
	<sup>99m</sup> Tc]SG6				<sup>99m</sup> Tc]DG2				<sup>99m</sup> Tc]DG4			
	Control	+Lis <sup>b</sup>	+PA <sup>a</sup>	+PA +Lis <sup>c</sup>	Control	+PA <sup>a</sup>	Control	+Lis <sup>b</sup>	+PA <sup>a</sup>	Control	+Lis <sup>b</sup>	+PA +Lis <sup>c</sup>
Blood	0.03±0.01	0.07±0.02	0.05±0.01	0.06±0.03	0.10±0.05	0.13±0.03	0.06±0.01	0.07±0.02	0.09±0.01	0.06±0.01	0.07±0.02	0.12±0.01
Liver	0.20±0.04	0.25±0.04	0.21±0.03	0.27±0.05	0.28±0.05	0.31±0.05	0.32±0.08	0.39±0.20	0.44±0.03	0.32±0.08	0.39±0.20	0.52±0.10
Heart	0.03±0.00	0.05±0.01	0.04±0.01	0.06±0.02	0.06±0.02	0.08±0.02	0.04±0.00	0.05±0.02	0.06±0.01	0.04±0.00	0.05±0.02	0.07±0.01
Kidneys	<b>26.07±3.28</b>	<b>26.54±4.93</b>	<b>58.51±7.77</b>	<b>58.18±9.89</b>	<b>58.62±8.98</b>	<b>134.24±23.04</b>	<b>1.16±0.13</b>	<b>0.97±0.14</b>	<b>1.33±0.19</b>	<b>1.16±0.13</b>	<b>0.97±0.14</b>	<b>1.34±0.27</b>
Stomach	<b>1.66±0.19</b>	<b>2.04±0.26</b>	<b>2.28±0.48</b>	<b>2.48±0.60</b>	<b>2.58±0.74</b>	<b>2.98±0.67</b>	<b>0.70±0.27</b>	<b>0.79±0.16</b>	<b>1.14±0.15</b>	<b>0.70±0.27</b>	<b>0.79±0.16</b>	<b>2.48±0.28</b>
Intestines	0.99±0.64	1.72±0.41	0.44±0.10	0.47±0.13	0.96±0.48	0.90±0.50	0.44±0.12	1.28±0.68	0.94±0.29	0.44±0.12	1.28±0.68	2.08±0.92
Spleen	0.11±0.03	0.15±0.04	0.09±0.04	0.19±0.06	0.09±0.02	0.13±0.04	0.16±0.02	0.14±0.02	0.19±0.02	0.16±0.02	0.14±0.02	0.36±0.18
Muscle	0.01±0.00	0.04±0.05	0.02±0.00	0.04±0.02	0.04±0.02	0.04±0.01	0.03±0.01	0.03±0.01	0.04±0.01	0.03±0.01	0.03±0.01	0.05±0.01
Lung	0.06±0.01	0.10±0.02	0.09±0.01	0.15±0.05	0.10±0.03	0.15±0.04	0.10±0.02	0.09±0.01	0.14±0.01	0.10±0.02	0.09±0.01	0.20±0.03
Pancreas	0.10±0.03	0.15±0.03	0.11±0.02	0.15±0.04	0.14±0.02	0.20±0.03	0.10±0.01	0.16±0.04	0.18±0.03	0.10±0.01	0.16±0.04	0.33±0.08
Tumor(+)	<b>10.25±3.51</b>	<b>11.50±4.07</b>	<b>17.78±3.76</b>	<b>18.46±3.56</b>	<b>12.89±4.69</b>	<b>18.21±5.97</b>	<b>0.99±0.13</b>	<b>2.06±0.39</b>	<b>4.89±1.33</b>	<b>0.99±0.13</b>	<b>2.06±0.39</b>	<b>8.91±1.61</b>
Tumor(-)	<b>0.15±0.04</b>	<b>0.15±0.03</b>	<b>0.18±0.05</b>	<b>0.19±0.07</b>	<b>0.15±0.04</b>	<b>0.18±0.03</b>	<b>0.19±0.04</b>	<b>0.23±0.07</b>	<b>0.33±0.06</b>	<b>0.19±0.04</b>	<b>0.23±0.07</b>	<b>0.42±0.11</b>

<sup>a</sup>Coinjection with 300 µg PA; <sup>b</sup>coinjection with 100 µg Lis; <sup>c</sup>coinjection with 300 µg PA and 100 µg Lis.

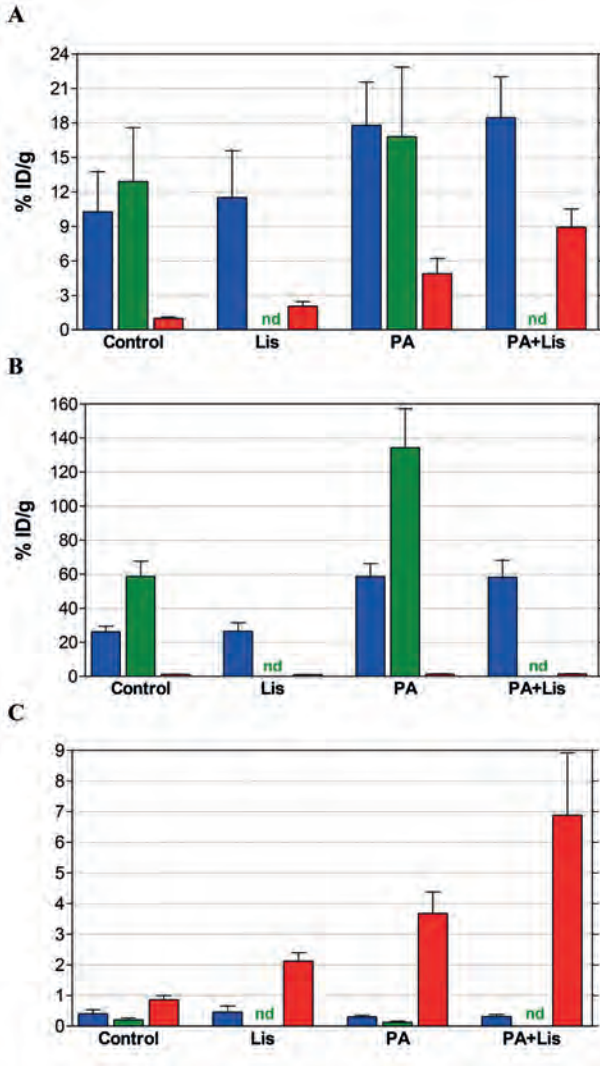


Figure 5 | Biodistribution of [<sup>99m</sup>Tc]SG6 (■), [<sup>99m</sup>Tc]DG2 (■) and [<sup>99m</sup>Tc]DG4 (■) in A431-CCK2R(+) tumor bearing SCID mice at 4 h pi. Results expressed as mean %ID/g±SD are selectively shown for comparison for A) tumor, B) kidneys and C) tumor-to-kidney ratios. Animals were coinjected with vehicle (control), Lis (100 µg), PA (300 µg), or PA plus Lis (300 µg PA and 100 µg Lis); nd= not done.

NEP-inhibition resulted in markedly enhanced uptake of the three radiotracers in the A431-CCK2R(+), but not in the A431-CCK2R(-) tumors, revealing CCK2R-specificity also during treatment of mice with PA. The A431-CCK2R(+) tumor values thus obtained were: [<sup>99m</sup>Tc]SG6: 17.78±3.76%ID/g (n=5,  $P<0.001$ ); [<sup>99m</sup>Tc]DG2: 18.21±5.97%ID/g (n=5,  $P<0.01$ ); [<sup>99m</sup>Tc]DG4: 4.89±1.33%ID/g (n=4,  $P<0.01$ ). Interestingly, dual NEP and ACE inhibition by combined treatment with PA and Lis, did not lead to further increase of tumor uptake of [<sup>99m</sup>Tc]SG6 (18.46±3.56%ID/g, n=5,  $P>0.05$ ) when compared with single NEP-inhibition by PA only, consistent with in vivo stability findings. In contrast, such dual NEP and ACE inhibition led to significant increase of [<sup>99m</sup>Tc]DG4 uptake in the A431-CCK2R(+) tumors (8.91±1.61%ID/g, n=4;  $P<0.01$ ) vs. single PA-treatment. These findings, linking the in vivo profile of [<sup>99m</sup>Tc]DG4 not only to NEP but also to ACE, were corroborated by results obtained during

single ACE-inhibition by Lis. During Lis-coinjection, enhancement of tumor uptake vs. controls was observed only for [<sup>99m</sup>Tc]DG4 ( $2.06 \pm 0.39\% \text{ID/g}$ ,  $n=4$ ;  $P < 0.01$ ), but not for [<sup>99m</sup>Tc]SG6 serving as a negative control ( $11.50 \pm 4.07\% \text{ID/g}$ ,  $n=4$ ,  $P > 0.05$ ).

Of great significance is the observation, that the originally high kidney uptake of the longer chain analogs, [<sup>99m</sup>Tc]SG6 and [<sup>99m</sup>Tc]DG2, doubled by PA-treatment ( $P < 0.001$ ). Conversely, the initially low renal uptake of [<sup>99m</sup>Tc]DG4 remained low and unaffected by single PA- or combined PA+Lis-treatment ( $< 1.4\% \text{ID/g}$ ). Accordingly, the truncated [<sup>99m</sup>Tc]DG4 radiotracer displayed the highest tumor-to-kidney ratios in mice during dual NEP/ACE-inhibition (Figure 5C).

## DISCUSSION

Diagnostic imaging and radionuclide therapy of CCK2R-positive tumors, such as MTC, have been attempted with a variety of radiolabeled gastrin and CCK derived probes [17]. However, successful implementation of this approach in clinical practice, as shown in the management of neuroendocrine tumors with radiolabeled somatostatin analogs [27], has not been yet achieved [28]. One of the problems delaying progress in this direction has been the suboptimal metabolic stability of CCK2R-targeted radiotracers, impairing the in vivo performance [15,17].

We have recently proposed the concept of in situ stabilization of peptide radioligands in the circulation applying key-protease inhibitors [16]. Based on the leading role of NEP in the degradation of gastrin and its analogs [22], we have coinjected the potent NEP-inhibitor PA [29,30] together with several DOTA-coupled gastrin peptides radiolabeled with trivalent metals [17-20]. As a result, the tumor uptake in mice was notably enhanced. This effect was assigned to the increased supply of intact radioligand to tumor-associated CCK2R-targets following their stabilization in peripheral blood. During these studies, the length of gastrin radiotracers played an important role in end-pharmacokinetics, especially in the tumor-to-kidney ratios reached after PA-coinjection.

In the present work we first report on the biological profile of three different-length gastrins coupled to acyclic tetraamines and labeled with <sup>99m</sup>Tc (Figure 1). As expected, the length of the gastrin chain had a strong influence on <sup>99m</sup>Tc-radiotracer stability and biodistribution in A431-CCK2R(+/-) tumor-bearing mice. Interestingly, results followed a similar trend to that previously observed for the corresponding DOTA-derivatized radioligands. Specifically, the uptake of the minigastrin [<sup>99m</sup>Tc]DG2 and the full-length gastrin-17 [<sup>99m</sup>Tc]SG6 analogs in the A431-CCK2R(+) tumors reached the highest values (Table 1). These were very comparable to [<sup>111</sup>In-DOTA]MG0 ( $11.91 \pm 2.21\% \text{ID/g}$ ) [20] and [<sup>111</sup>In]SG1 ( $9.83 \pm 4.3\% \text{ID/g}$  at 4 h pi) [14] and can be attributed to the higher in vivo stability of the longer-chain analogs (Figure 4A). However, the kidney accumulation of [<sup>99m</sup>Tc]DG2 and [<sup>99m</sup>Tc]SG6 were quite high as well. In contrast, the tumor uptake of the rapidly biodegradable *des*-Glu<sup>6-10</sup> tracer [<sup>99m</sup>Tc]DG4 was notably lower, even lower than the previously reported for [<sup>111</sup>In-DOTA]MG11 ( $2.49 \pm 0.92\% \text{ID/g}$  at 4 h pi) [20], directly linking radiopeptide in vivo stability with observed tumor uptake. On the other hand, the kidney accumulation was favourably low for both <sup>99m</sup>Tc- and <sup>111</sup>In-labeled *des*-Glu<sup>6-10</sup> analogs.

Coinjection of PA exerted a strong impact on the in vivo performance of all three  $^{99m}\text{Tc}$ -radiogastrins, dependent again upon the length of the peptide chain. In all cases, the observed enhancement of tumor uptake induced by PA was consonant with the radiotracer stability in peripheral blood. Accordingly, the longer-chain  $^{99m}\text{Tc}$ ]SG6 and  $^{99m}\text{Tc}$ ]DG2, showing high stability in blood after PA-treatment, reached remarkably high tumor values compared to  $^{99m}\text{Tc}$ ]DG4 (Table 1, Figure 5). However, their kidney accumulation unfavourably doubled leading to poor tumor-to-kidney ratios. On the other hand, PA treatment only partially stabilized truncated  $^{99m}\text{Tc}$ ]DG4, consequently leading to lower uptake in the A431-CCKR(+) xenografts, whereas the originally low renal uptake remained unchanged. Although these findings were in agreement to those obtained with the corresponding  $^{111}\text{In}$ -DOTA-gastrins, intriguing discrepancies were revealed in the efficacy of PA to enhance the bioavailability and hence the tumor uptake of the truncated analogs  $^{99m}\text{Tc}$ ]DG4 and  $^{111}\text{In}$ -DOTA]MG11 [20].

It should be noted that the positive charge of the forming  $^{99m}\text{Tc}$ -complex of  $^{99m}\text{Tc}$ ]DG4 may have led to different interaction patterns with attacking proteases in the biological milieu than to those reported for  $^{111}\text{In}$ -DOTA]MG11. Therefore, it is reasonable to assume that the susceptibility of  $^{99m}\text{Tc}$ ]DG4 and  $^{111}\text{In}$ -DOTA]MG11 to peptidases other than NEP, as for example to ACE, could be different. According to previous in vitro studies, at least two negatively charged Glu residues at the N-terminus of truncated gastrin are needed for full resistance to ACE [23]. In line with this hypothesis, we have recently shown that ACE was not involved in the in vivo catabolism of  $^{111}\text{In}$ -DOTA]MG11 [21]. The latter with its polar  $^{111}\text{In}$ -DOTA<sup>9</sup>-DGLu<sup>10</sup> sequence seems to better mimic the Glu<sup>9-10</sup> construct of ACE-resistant gastrin(9-17). This no longer holds true for  $^{99m}\text{Tc}$ ]DG4, having the monocationic  $^{99m}\text{Tc}$ -tetraamine chelate at the critical for ACE-resistance position 9.

To test this hypothesis, we have investigated the effects of dual NEP/ACE- and single ACE-inhibition on the in vivo behaviour of  $^{99m}\text{Tc}$ ]DG4, using  $^{99m}\text{Tc}$ ]SG6 as ACE-resistant negative control. Interestingly, only  $^{99m}\text{Tc}$ ]DG4 profited in in vivo stability by combined PA+Lis treatment or by single Lis coinjection, for the first time implicating ACE in the in vivo degradation of a gastrin-based radiotracer (Figure 4). In line with these results, treatment of mice with Lis+PA or Lis only led to tumor uptake enhancements only in the case of the truncated analog  $^{99m}\text{Tc}$ ]DG4, while the corresponding values of the ACE-resistant  $^{99m}\text{Tc}$ ]SG6 reference remained unaffected (Table 1). Neither PA nor Lis (or their combination) had any effect on the kidney accumulation of  $^{99m}\text{Tc}$ ]DG4, albeit synergistically increasing tumor uptake. As a result, tumor-to-kidney ratios attractively increased only for  $^{99m}\text{Tc}$ ]DG4 during dual NEP/ACE inhibition (Figure 5).

It is difficult to predict the value of above findings for translation in human in view of reported interspecies differences. Previous studies with  $^{99m}\text{Tc}$ ]DG2 in a small number of MTC patients have shown very rapid renal clearance of radioactivity from human kidneys [11]. In mice however  $^{99m}\text{Tc}$ ]DG2 displayed high and persistent accumulation in the kidneys [10]. Such contrasting kidney clearance patterns between mice and men have not been reported for the respective DOTA-derivatized analogs. Therefore, further translational studies in mice and men are warranted to evaluate the impact of the new peptidase-inhibition approach in the case of  $^{99m}\text{Tc}$ -radiolabeled gastrins. Such studies will also contribute to our better understanding the renal processing of gastrin radiotracers [31], and radiopeptides in general, in man.

## CONCLUSION

The present work has provided new data demonstrating the importance of in vivo stability of gastrin radiotracers for successful targeting of CCK2R-expressing tumors. Identification of implicated proteases is essential to better understand the biological milieu and to adopt rationale approaches toward improved in vivo profiles. For the first time the involvement of both NEP and ACE in the in vivo catabolism of a gastrin <sup>99m</sup>Tc-based radiotracer could be shown in the case of the *des*-Glu<sup>6-10</sup> analog [<sup>99m</sup>Tc]DG4. Most importantly, combined PA and Lis treatment of mice synergistically enhanced metabolic stability in mouse blood. As a result, tumor-to-kidney ratios very attractive for clinical translation could be achieved for [<sup>99m</sup>Tc]DG4. Nevertheless, the impact of key-protease inhibition on the performance of <sup>99m</sup>Tc-labeled gastrins in man needs to be established by appropriate clinical studies.

## Acknowledgments

Partial financial support by the Greek General Secretariat for Research and Technology and the European Regional Development Fund under the Action "Development Grants for Research Institutions – KRIPIS" of OPCE II is gratefully acknowledged.

## Abbreviations

SPECT= single photon emission computed tomography; PET= positron emission tomography; N<sub>4</sub>= 6-(carboxyl)-1,4,8,11-tetraazaundecane; DOTA= 1,4,7,10-tetraazacyclododecane-1,4,7,10-tetraacetic acid; [Leu<sup>15</sup>]gastrin= pGlu-Gly-Pro-Trp-Leu-(Glu)<sub>5</sub>-Ala-Tyr-Gly-Trp-Leu-Asp-Phe-NH<sub>2</sub>; [<sup>125</sup>I-Tyr<sup>12</sup>,Leu<sup>15</sup>] gastrin= pGlu-Gly-Pro-Trp-Leu-(Glu)<sub>5</sub>-Ala-<sup>125</sup>I-Tyr-Gly-Trp-Leu-Asp-Phe-NH<sub>2</sub>; [<sup>111</sup>In-DOTA]MG11= <sup>111</sup>In-DOTA-DGlu-Ala-Tyr-Gly-Trp-Met-Asp-Phe-NH<sub>2</sub>; [<sup>111</sup>In-DOTA]MG0= <sup>111</sup>In-DOTA-DGlu-(Glu)<sub>5</sub>-Ala-Tyr-Gly-Trp-Met-Asp-Phe-NH<sub>2</sub>; [<sup>111</sup>In-DOTA]SG1= <sup>111</sup>In-DOTA-DGlu-Gln-Gly-Pro-Trp-Leu-(Glu)<sub>5</sub>-Ala-Tyr-Gly-Trp-Leu-Asp-Phe-NH<sub>2</sub>.

## REFERENCES

1. Reubi JC, Schaer JC, Waser B. Cholecystokinin(CCK)-A and CCK-B/gastrin receptors in human tumors. *Cancer Res.* 1997;57(7):1377-86.
2. Reubi JC, Waser B. Unexpected high incidence of cholecystokinin-B/gastrin receptors in human medullary thyroid carcinomas. *Int J Cancer.* 1996;67(5):644-7.
3. Behr TM, Jenner N, Radetzky S, Béhé M, Gratz S, Yucekent S, et al. Targeting of cholecystokinin-B/gastrin receptors in vivo: preclinical and initial clinical evaluation of the diagnostic and therapeutic potential of radiolabelled gastrin. *Eur J Nucl Med.* 1998;25(4):424-30.
4. Behr TM, Béhé M, Angerstein C, Gratz S, Mach R, Hagemann L, et al. Cholecystokinin-B/gastrin receptor binding peptides: preclinical development and evaluation of their diagnostic and therapeutic potential. *Clin Cancer Res.* 1999;5(10 Suppl):3124s-38s.
5. Béhé M, Behr TM. Cholecystokinin-B (CCK-B)/gastrin receptor targeting peptides for staging and therapy of medullary thyroid cancer and other CCK-B receptor expressing malignancies. *Biopolymers.* 2002;66(6):399-418.
6. Nock B, Maina T. Tetraamine-coupled peptides and resulting <sup>99m</sup>Tc-radioligands: an effective route for receptor-targeted diagnostic imaging of human tumors. *Curr Top Med Chem.* 2012;12(23):2655-67.
7. von Guggenberg E, Béhé M, Behr TM, Saurer M, Seppi T, Decristoforo C. <sup>99m</sup>Tc-labeling and in vitro and in vivo evaluation of HYNIC- and (Nalpha-His)acetic acid-modified [D-Glu<sup>1</sup>]-minigastrin. *Bioconjug Chem.* 2004;15(4):864-71.
8. von Guggenberg E, Dietrich H, Skvortsova I, Gabriel M, Virgolini IJ, Decristoforo C. <sup>99m</sup>Tc-labelled HYNIC-minigastrin with reduced kidney uptake for targeting of CCK-2 receptor-positive tumours. *Eur J Nucl Med Mol Imaging.* 2007;34(8):1209-18.
9. von Guggenberg E, Sallegger W, Helbok A, Ocak M, King R, Mather SJ, et al. Cyclic minigastrin analogues for gastrin receptor scintigraphy with technetium-99m: preclinical evaluation. *J Med Chem.* 2009;52(15):4786-93.
10. Nock BA, Maina T, Béhé M, Nikolopoulou A, Gotthardt M, Schmitt JS, et al. CCK-2/gastrin receptor-targeted tumor imaging with <sup>99m</sup>Tc-labeled minigastrin analogs. *J Nucl Med.* 2005;46(10):1727-36.
11. Fröberg AC, de Jong M, Nock BA, Breeman WA, Erion JL, Maina T, et al. Comparison of three radiolabelled peptide analogues for CCK-2 receptor scintigraphy in medullary thyroid carcinoma. *Eur J Nucl Med Mol Imaging.* 2009;36(8):1265-72.
12. Breeman WA, Fröberg AC, de Blois E, van Gameren A, Melis M, de Jong M, et al. Optimised labeling, preclinical and initial clinical aspects of CCK-2 receptor-targeting with 3 radiolabeled peptides. *Nucl Med Biol.* 2008;35(8):839-49.
13. Good S, Walter MA, Waser B, Wang X, Muller-Brand J, Béhé MP, et al. Macrocyclic chelator-coupled gastrin-based radiopharmaceuticals for targeting of gastrin receptor-expressing tumours. *Eur J Nucl Med Mol Imaging.* 2008;35(10):1868-77.
14. Laverman P, Joosten L, Eek A, Roosenburg S, Peitl PK, Maina T, et al. Comparative biodistribution of 12 <sup>111</sup>In-labelled gastrin/CCK2 receptor-targeting peptides. *Eur J Nucl Med Mol Imaging.* 2011;38(8):1410-6.
15. Oçak M, Helbok A, Rangger C, Peitl PK, Nock BA, Morelli G, et al. Comparison of biological stability and metabolism of CCK2 receptor targeting peptides, a collaborative project under COST BM0607. *Eur J Nucl Med Mol Imaging.* 2011;38(8):1426-35.
16. Nock BA, Maina T, Krenning EP, de Jong M. "To serve and protect": enzyme inhibitors as radiopeptide escorts promote tumor targeting. *J Nucl Med.* 2014;55(1):121-7.
17. Kaloudi A, Nock BA, Krenning EP, Maina T, de Jong M. Radiolabeled gastrin/CCK analogs in tumor diagnosis: towards higher stability and improved tumor targeting. *Q J Nucl Med Mol Imaging.* 2015;59(3):287-302.
18. Kaloudi A, Nock BA, Lymperis E, Sallegger W, Krenning EP, de Jong M, et al. In vivo inhibition of neutral endopeptidase enhances the diagnostic potential of truncated gastrin <sup>111</sup>In-radioligands. *Nucl Med Biol.* 2015;42(11):824-32.
19. Kaloudi A, Nock BA, Lymperis E, Marsouvanidis PJ, Krenning EP, de Jong M, Maina T. A new route toward enhancing the uptake of [<sup>111</sup>In/<sup>177</sup>Lu-DOTA,Leu<sup>15</sup>]MG11 in CCK2R-positive xenografts in mice *Eur J Nucl Med Mol Imaging.* 2013;40(Suppl. 2):S119.

20. Kaloudi A, Nock BA, Lymperis E, Krenning EP, de Jong M, Maina T. Improving the In Vivo Profile of Minigastrin Radiotracers: A Comparative Study Involving the Neutral Endopeptidase Inhibitor Phosphoramidon. *Cancer Biother Radiopharm.* 2016;31(1):20-8.
21. Kaloudi A, Nock BA, Lymperis E, Valkema R, Krenning EP, de Jong M, et al. Impact of clinically tested NEP/ACE inhibitors on tumor uptake of [<sup>111</sup>In-DOTA]MG11-first estimates for clinical translation. *EJNMMI Res.* 2016;6(1):15.
22. Deschodt-Lanckman M, Pauwels S, Najdovski T, Dimaline R, Dockray GJ. In vitro and in vivo degradation of human gastrin by endopeptidase 24.11. *Gastroenterology.* 1988;94(3):712-21.
23. Dubreuil P, Fulcrand P, Rodriguez M, Fulcrand H, Laur J, Martinez J. Novel activity of angiotensin-converting enzyme. Hydrolysis of cholecystokinin and gastrin analogues with release of the amidated C-terminal dipeptide. *Biochem J.* 1989;262(1):125-30.
24. Nikolopoulou A, Nock BA, Petrou C, Ketani E, Cordopatis P, Maina T. In vivo targeting of CCK-2/gastrin-R and reduction of renal accumulation with truncated [<sup>99m</sup>Tc]Demogastrin 4 – 6. In: *Technetium, Rhenium and other Metals in Chemistry and Nuclear Medicine*; vol. 7: pg:325-326; 2006; U. Mazzi (Editor); SGEEditoriali, Padova.
25. Aloj L, Caracó C, Panico M, Zannetti A, Del Vecchio S, Tesauro D, et al. In vitro and in vivo evaluation of <sup>111</sup>In-DTPAGlu-G-CCK8 for cholecystokinin-B receptor imaging. *J Nucl Med.* 2004;45(3):485-94.
26. Maina T, Nock B, Nikolopoulou A, Sotiriou P, Loudos G, Maintas D, et al. [<sup>99m</sup>Tc]Demotate, a new <sup>99m</sup>Tc-based [Tyr<sup>3</sup>]octreotate analogue for the detection of somatostatin receptor-positive tumours: synthesis and preclinical results. *Eur J Nucl Med Mol Imaging.* 2002;29(6):742-53.
27. de Jong M, Breeman WA, Kwekkeboom DJ, Valkema R, Krenning EP. Tumor imaging and therapy using radiolabeled somatostatin analogues. *Acc Chem Res.* 2009;42(7):873-80.
28. Pawlak D, Rangger C, Kolenc Peitl P, Garnuszek P, Maurin M, Ihli L, et al. From preclinical development to clinical application: Kit formulation for radiolabelling the minigastrin analogue CP04 with In-111 for a first-in-human clinical trial. *Eur J Pharm Sci.* 2016;85:1-9.
29. Suda H, Aoyagi T, Takeuchi T, Umezawa H. Letter: A thermolysin inhibitor produced by Actinomycetes: phosphoramidon. *J Antibiot (Tokyo).* 1973;26(10):621-3.
30. Oefner C, D'Arcy A, Hennig M, Winkler FK, Dale GE. Structure of human neutral endopeptidase (Nepilysin) complexed with phosphoramidon. *J Mol Biol.* 2000;296(2):341-9.
31. Gotthardt M, van Eerd-Vismale J, Oyen WJ, de Jong M, Zhang H, Rolleman E, et al. Indication for different mechanisms of kidney uptake of radiolabeled peptides. *J Nucl Med.* 2007;48(4):596-601.





# CHAPTER

# 7

## Summary and Concluding Remarks

## Samenvatting

## Acknowledgements

## Curriculum Vitae

## List of Publications

## PhD Portfolio



# Summary

Radiolabeled peptides have become valuable tools for peptide receptor imaging and radionuclide therapy of tumors over the last 25 years. The overexpression of peptide receptors on tumors in comparison to normal tissues is one of the main reasons for the increasing interest in developing peptide radiopharmaceuticals [1,2]. Radiolabeled somatostatin analogs, like [ $^{111}\text{In}$ -DTPA]octreotide (OctreoScan), have been developed for diagnostic imaging and radionuclide therapy of tumors overexpressing the somatostatin subtype 2 receptor ( $\text{sst}_2$ ) [3]. These analogs have paved the way for the development of more peptide radioligands targeting a wide spectrum of cancer types. Cholecystokinin subtype 2 receptors (CCK2R) can serve as molecular targets for diagnostic imaging and radionuclide therapy of CCK2R-expressing human tumors, such as medullary thyroid carcinoma (MTC), with the aid of gastrin radioligands [4,5].

The clinical application of radiolabeled gastrin analogs has been largely restricted by their fast in vivo catabolism that eventually compromises tumor uptake [6]. This challenge has been mainly addressed by structural modifications, which, however, often led to suboptimal pharmacological features [7]. The major enzyme implicated in the degradation of gastrin-based peptides is neutral endopeptidase (NEP), which is widely distributed in the body [8-10]. A promising new concept to increase bioavailability and ultimately tumor localization of radiopeptides recently introduced, involves coinjection of the NEP inhibitor phosphoramidon (PA) with radiolabeled gastrin analogs. The first results of this approach showed a remarkable increase of the bioavailability of the rapidly biodegradable [ $^{111}\text{In}$ -DOTA]MG11 after PA coinjection in mice, which led to an 8-fold enhancement of CCK2R-positive tumor uptake (**Chapter 2**) [11].

In this thesis, several novel radiolabeled gastrin analogs were developed and evaluated preclinically in vitro as well as in vivo in animal models. In addition, the effect of in situ enzyme inhibition on metabolic stability and tumor uptake of the same gastrin radioligands was investigated (Table 1).

The evaluation of a series of  $^{111}\text{In}$ -labeled analogs based on the truncated [DOTA]MG11, in which the oxidation-susceptible  $\text{Met}^{15}$  was replaced by  $\text{Ahp}^{15}$ ,  $\text{Nle}^{15}$  or  $\text{Leu}^{15}$  is described in **Chapter 3**. The in vitro profile of the radiopeptides was evaluated as well as the stability in mouse circulation and biodistribution in CCK2R-positive tumor bearing mice during in situ NEP inhibition by PA. For comparison reasons the minigastrin radiotracer [ $^{111}\text{In}$ -DOTA]MG0, previously reported for good tumor localization but unfavourably high renal accumulation, was included in the studies [12]. Co-administration of PA induced impressive enhancement of tumor uptake of all radiotracers, as a result of higher bioavailability. However, only the three truncated radiogastrins attained remarkably high tumor-to-kidney ratios with clear prospects for improved diagnostic efficacy of CCK2R-positive tumors in man.

In **Chapter 4** the efficacy of in situ NEP inhibition by PA coinjection was evaluated in three  $^{111}\text{In}$ -labeled gastrin radiotracers differing in their  $(\text{Glu})^{6-10}$  sequence. Previous studies have shown that the penta(Glu)-sequence in native gastrin is crucial for metabolic stability, kidney retention, and tumor uptake of radiogastrins [13,14]. Thus, D(Glu) $^{6-10}$ -containing [ $^{111}\text{In}$ ]CP04, which has been selected as the best candidate among 12 gastrin-based radiotracers in a previous study [12], was directly compared with its LGlu-counterpart [ $^{111}\text{In}$ -DOTA]MG0 and the truncated *des*(Glu) $^{6-10}$  analog [ $^{111}\text{In}$ -DOTA]MG11.

The new peptide-stabilizing approach has turned out to be particularly successful in the case of [<sup>111</sup>In-DOTA]MG11, as tumor-to-kidney ratios impressively increased ~5fold after PA coinjection, while for the other two radiotracers tumor-to-kidney ratios remained significantly lower. Thus this concept is promising for further validation in human.

Aiming toward clinical translation of this concept, the in vivo efficacy of PA was compared vs. the clinically tested NEP inhibitor thiorphan (TO) and its orally administered prodrug racecadotril (Race) in **Chapter 5**. In this study [<sup>111</sup>In-DOTA]MG11 was used as a model radiotracer. Comparable and impressive enhancement of tumor values were observed by PA or TO co-administration, while the intraperitoneal injection of Race 30–40 min prior to the intravenous injection of [<sup>111</sup>In-DOTA]MG11 was half as effective. Different administration doses of PA and TO were also tested in mice models, showing that both NEP inhibitors induced significant increase of tumor uptake even at the lowest administered doses, with PA however having consistently superior efficacy at all tested dose levels compared to TO. Nevertheless, PA has not been tested clinically in such high doses. Apart from NEP, another enzyme that was previously associated with the in vitro catabolism of gastrin analogs is angiotensin converting enzyme (ACE) [15]. Therefore, the in vivo stability and biodistribution profile of [<sup>111</sup>In-DOTA]MG11 was also studied in mice models during ACE inhibition by lisinopril (Lis). The findings of the study strongly suggested that ACE does not contribute to the in vivo processing of [<sup>111</sup>In-DOTA]MG11 and verified NEP as the major degrading protease.

<sup>99m</sup>Tc is the most widely used label of choice for SPECT imaging due to its optimal nuclear characteristics and its easy availability at low cost [16]. Thus, a series of <sup>99m</sup>Tc-labeled gastrins with different chain-length were evaluated preclinically in **Chapter 6**, during in situ NEP and/or ACE inhibition. A full length gastrin-17 ([<sup>99m</sup>Tc]SG6), a minigastrin ([<sup>99m</sup>Tc]DG2) and a *des*(Glu)<sup>6-10</sup> minigastrin ([<sup>99m</sup>Tc]DG4) analog were compared in the study. Diverse responses across the radiopeptides were reported during NEP/ACE-inhibition, by PA and/or Lis respectively, and special attention has been given on the tumor-to-kidney ratios attained. In particular, all three radiopeptides clearly profited from PA treatment in terms of metabolic stability and tumor uptake, while combined PA and Lis treatment significantly increased the bioavailability and tumor values of only the truncated [<sup>99m</sup>Tc]DG4. These findings suggest that ACE was involved only in the in vivo degradation of [<sup>99m</sup>Tc]DG4, assigned to the positive charge at position 9 of gastrin. Overall, the truncated [<sup>99m</sup>Tc]DG4 exhibited the most attractive profile during combined NEP/ACE-inhibition in mouse models, with a ~7fold increase in tumor-to-kidney ratios, thus providing new opportunities for CCK2R-expressing tumor imaging in man with SPECT.

Table 1 | Summary of the main findings of the thesis.

Radiopeptides	In vivo stability 5 min pi	Tu/Ki ratio at 4 h pi	Remarks
<p><b>Chapter 3</b></p> <p>[<sup>111</sup>In]SG3 (SG3= [DGLu<sup>10</sup>,Ahp<sup>15</sup>]gastrin(10-17))                      [<sup>111</sup>In]SG4 (SG4= [DGLu<sup>10</sup>,Nle<sup>15</sup>]gastrin(10-17))                      [<sup>111</sup>In]SG5 (SG5= [DGLu<sup>10</sup>,Leu<sup>15</sup>]gastrin(10-17))                      [<sup>111</sup>In-DOTA]MG0 (MG0= [DGLu<sup>5</sup>]gastrin(5-17))</p>	<p>Control: 10%, 13%, 27%, 70%                      +PA: 88%, 80%, 85%, 85%</p>		<p>Only the three truncated des(Glu)<sub>5</sub> radiogastrins have clear prospects for improved diagnostic efficacy of CCK2R-positive tumors in man</p>
<p><b>Chapter 4</b></p> <p>[<sup>111</sup>In]CP04 (CP04= [DOTA,DGLu<sup>5-10</sup>]gastrin(5-17))                      [<sup>111</sup>In-DOTA]MG0 (MG0= [DGLu<sup>5</sup>]gastrin(5-17))                      [<sup>111</sup>In-DOTA]MG11 (MG11= [DGLu<sup>10</sup>]gastrin(10-17))</p>	<p>Control: 70%, 70%, 5%                      +PA: 85%, 85%, 70%</p>		<p>The new peptide-stabilization approach has turned out to be particularly successful for [<sup>111</sup>In-DOTA]MG11 and is promising for further validation in human</p>
<p><b>Chapter 5</b></p> <p>[<sup>111</sup>In-DOTA]MG11 (MG11= [DGLu<sup>10</sup>]gastrin(10-17))</p>	<p>Control: 5%                      +PA: 70%                      +PA+Lis: 70%                      +TO: 70%                      +Racc: 70%</p>		<p>Translation of the concept of peptide-stabilization to the clinic requires optimization of inhibitor type, administration dose and route</p>
<p><b>Chapter 6</b></p> <p>[<sup>99m</sup>Tc]SG6 (SG6= [N<sub>4</sub>-Gln<sup>1</sup>]gastrin)                      [<sup>99m</sup>Tc]DG2 (DG2= [N<sub>4</sub>-Gly<sup>1</sup>,DGLu<sup>5</sup>]gastrin(4-17))                      [<sup>99m</sup>Tc]DG4 (DG4= [N<sub>4</sub>-DGLu<sup>10</sup>]gastrin(10-17))</p>	<p>Control: 40%, 60%, 10%                      +PA: 70%, 85%, 60%                      +PA+Lis: 70%, 85%, 80%                      +Lis: 40%</p>		<p>ACE was involved only in the in vivo degradation of [<sup>99m</sup>Tc]DG4, assigned to the positive charge at position 9</p>

## CONCLUSIONS – FUTURE PERSPECTIVES

Throughout the studies described in this thesis the importance of *in vivo* stability of gastrin radiotracers for successful targeting of CCK2R-expressing tumors has been demonstrated. Identification of proteases involved is vital to better understand the biological environment and to implement rational methods toward optimal *in vivo* profiles of radiolabeled gastrins. The major role of NEP in the *in vivo* catabolism of gastrin radiotracers has prompted the introduction of the concept of *in situ* NEP inhibition by coadministration of an appropriate NEP inhibitor. The preclinical studies described in the thesis highlight that *in situ* stabilization of biodegradable gastrin radioligands represents a promising tool to improve diagnostic sensitivity in CCK2R-expressing cancer patients. However, translation of this concept in the clinic poses many challenges that need to be addressed in further studies.

An important step toward clinical translation is the assessment of biosafety and efficacy of the NEP-inhibitor intended for human application. So far no extensive toxicity studies have been reported for PA. This potent NEP-inhibitor has been administered in human only in very low amounts.<sup>17</sup> Thus, extensive toxicology studies with PA represent one way to follow for clinical translation and hence will be of great value. On the other hand, there are several other NEP-inhibitors that have been already tested in human, such as TO and Race [18,19]. In the study described in Chapter 4 a first step was taken toward clinical translation of the concept by comparing the *in vivo* efficacy of TO and Race versus PA. However, in order to reach the maximum efficacy of PA with these clinically tested NEP inhibitors, further studies need to be performed to optimise dose, administration route and time of inhibitor injection with respect to radiotracer injection.

Recently it was shown that the concept of *in situ* NEP inhibition improves the outcome of radionuclide therapy in animal models, using the <sup>177</sup>Lu-labeled GRPR-antagonist JMV4168 [20]. Therapeutic studies need also to be conducted for promising gastrin analogs labelled with <sup>177</sup>Lu or <sup>90</sup>Y, such as the Met<sup>15</sup>-substituted oxidation resistant analogs described in Chapter 3. First clinical evidence on the therapeutic efficacy of this concept is expected to have a great impact in radionuclide therapy of MTC patients with disseminated disease, currently left with no effective therapeutic options. Moreover, other types of gastrin-related therapy may profit by this approach as well, as for example image-guided surgery of CCK2R-expressing tumors using fluorescent dye-coupled gastrin analogs, or targeted chemotherapy with gastrin-coupled cytotoxic drugs.

Besides <sup>111</sup>In- and <sup>99m</sup>Tc-labeled gastrin analogs, this approach may also turn out to be very appealing for PET imaging agents labeled with <sup>68</sup>Ga, <sup>64</sup>Cu and several other radionuclides. Modifications with different chelator types other than DOTA and N<sub>4</sub>, would allow or improve labeling with such radiometals.

Finally, this concept may eventually expand to include several other classes of peptide-conjugates, such as somatostatin or bombesin, thus far excluded from further development into drugs for clinical applications due to their poor *in vivo* metabolic stability.

## REFERENCES

1. Reubi JC. Peptide receptors as molecular targets for cancer diagnosis and therapy. *Endocr Rev* 2003;24:389-427.
2. Fani M, Maecke HR, Okarvi SM. Radiolabeled peptides: valuable tools for the detection and treatment of cancer. *Theranostics* 2012;2:481-501.
3. Krenning EP, Bakker WH, Kooij PP, Breeman WA, Oei HY, de Jong M, et al. Somatostatin receptor scintigraphy with indium-111-DTPA-D-Phe-1-octreotide in man: metabolism, dosimetry and comparison with iodine-123-Tyr-3-octreotide. *J Nucl Med* 1992;33:652-8.
4. Reubi JC, Schaer JC, Waser B. Cholecystokinin(CCK)-A and CCK-B/gastrin receptors in human tumors. *Cancer Res* 1997;57:1377-86.
5. Reubi JC, Waser B. Unexpected high incidence of cholecystokinin-B/gastrin receptors in human medullary thyroid carcinomas. *Int J Cancer* 1996;67:644-7.
6. Ocak M, Helbok A, Rangger C, Peitl PK, Nock BA, Morelli G, et al. Comparison of biological stability and metabolism of CCK2 receptor targeting peptides, a collaborative project under COST BM0607. *Eur J Nucl Med Mol Imaging* 2011;38:1426-35.
7. Adessi C, Soto C. Converting a peptide into a drug: strategies to improve stability and bioavailability. *Curr Med Chem* 2002;9:963-78.
8. Deschodt-Lanckman M, Pauwels S, Najdovski T, Dimaline R, Dockray GJ. In vitro and in vivo degradation of human gastrin by endopeptidase 24.11. *Gastroenterology* 1988;94:712-21.
9. Erdos EG, Skidgel RA. Neutral endopeptidase 24.11 (enkephalinase) and related regulators of peptide hormones. *Faseb j* 1989;3:145-51.
10. Llorens-Cortes C, Huang H, Vicart P, Gasc JM, Paulin D, Corvol P. Identification and characterization of neutral endopeptidase in endothelial cells from venous or arterial origins. *J Biol Chem* 1992;267:14012-8.
11. Nock BA, Maina T, Krenning EP, de Jong M. "To serve and protect": enzyme inhibitors as radiopeptide escorts promote tumor targeting. *J Nucl Med* 2014;55:121-7.
12. Laverman P, Joosten L, Eek A, Roosenburg S, Peitl PK, Maina T, et al. Comparative biodistribution of <sup>125</sup>I-labelled gastrin/CCK2 receptor-targeting peptides. *Eur J Nucl Med Mol Imaging* 2011;38:1410-6.
13. Good S, Walter MA, Waser B, Wang X, Muller-Brand J, Behe MP, et al. Macrocyclic chelator-coupled gastrin-based radiopharmaceuticals for targeting of gastrin receptor-expressing tumours. *Eur J Nucl Med Mol Imaging* 2008;35:1868-77.
14. Gotthardt M, van Eerd-Vismale J, Oyen WJ, de Jong M, Zhang H, Rolleman E, et al. Indication for different mechanisms of kidney uptake of radiolabeled peptides. *J Nucl Med* 2007;48:596-601.
15. Dubreuil P, Fulcrand P, Rodriguez M, Fulcrand H, Laur J, Martinez J. Novel activity of angiotensin-converting enzyme. Hydrolysis of cholecystokinin and gastrin analogues with release of the amidated C-terminal dipeptide. *Biochem J* 1989;262:125-30.
16. R. Dilworth J, J. Parrott S. The biomedical chemistry of technetium and rhenium. *Chemical Society Reviews* 1998;27:43-55.
17. Polosa R, Santonocito G, Magri S, Paolino G, Armato F, Pagano C, et al. Neutral endopeptidase inhibition with inhaled phosphoramidon: no effect on bronchial responsiveness to adenosine 5'-monophosphate (AMP) in asthma. *Eur Respir J* 1997;10:2460-4.
18. Floras P, Bidabe AM, Caille JM, Simonnet G, Lecomte JM, Sabathie M. Double-blind study of effects of enkephalinase inhibitor on adverse reactions to myelography. *AJNR Am J Neuroradiol* 1983;4:653-5.
19. Salazar-Lindo E, Santisteban-Ponce J, Chea-Woo E, Gutierrez M. Racecadotril in the treatment of acute watery diarrhea in children. *N Engl J Med* 2000;343:463-7.
20. Chatalic KL, Konijnenberg M, Nonnekens J, de Blois E, Hoeben S, de Ridder C, et al. In Vivo Stabilization of a Gastrin-Releasing Peptide Receptor Antagonist Enhances PET Imaging and Radionuclide Therapy of Prostate Cancer in Preclinical Studies. *Theranostics* 2016;6:104-17.





# Samenvatting

De afgelopen 25 jaar zijn tracers gebaseerd op radioactief gemaakte peptiden zeer waardevol gebleken voor peptide-receptor-imaging (beeldvorming) en radionuclidentherapie van tumoren. De overexpressie van receptoren voor dergelijke peptiden op tumorcellen en de lagere expressie in normale weefsels is een van de belangrijkste drijfveren geweest voor de ontwikkeling van dergelijke tracer-medicijnen [1,2]. Radioactief gelabelde somatostatine-analogen, zoals [<sup>111</sup>In-DTPA] octreotide (OctreoScan), zijn ontwikkeld voor zowel diagnostiek als voor radionuclidentherapie van tumoren die de somatostatine subtype 2 receptor (sst<sub>2</sub>) tot expressie brengen [3]. Deze succesvolle analogen hebben de weg geëffend voor de ontwikkeling van andere, ook op peptiden gebaseerde, radioliganden voor visualisatie en therapie van vele verschillende soorten tumoren. De cholecystokinin subtype 2 receptor (CCK2R) kan dienen als moleculaire target (doelwit) voor diagnostische imaging and radionuclidentherapie van CCK2R-positieve humane tumoren, zoals medullair schildklier carcinoom (MTC), door toepassing van gastrine-radioliganden [4,5].

De klinische toepassing van radioactief gelabelde gastrine-analogen wordt beperkt door hun zeer snelle afbraak in het lichaam na injectie, hetgeen uiteindelijk de tumoropname negatief beïnvloedt [6]. Om dit probleem op te lossen worden vaak structurele modificaties aangebracht in de peptiden, maar deze aanpak kan ook leiden tot suboptimale eigenschappen van de peptiden, zoals bijvoorbeeld verminderde binding aan de receptor [7]. Het enzym dat de belangrijkste rol speelt in de afbraak van gastrine-analogen is het neutrale endopeptidase (NEP), dat wijd verbreid is in het lichaam [8-10]. Een veelbelovende en nieuwe aanpak om de beschikbaarheid en dus uiteindelijk ook de tumoropname van de peptide-analogen te verhogen is de co-injectie van de NEP-remmer phosphoramidon (PA) tegelijk met de radioactief gelabelde gastrine-analogen. De eerste resultaten voortkomend uit deze nieuwe aanpak lieten een opmerkelijke verbetering zien met betrekking tot de beschikbaarheid van de peptide-tracer [<sup>111</sup>In-DOTA]MG11, dat normaal heel snel wordt afgebroken na injectie, na injectie van de tracer in muizen samen met PA, leidend tot een maar liefst 8x hogere tumoropname van de peptide-tracer (**Hoofdstuk 2**) [11].

In dit proefschrift wordt vervolgens beschreven hoe we verschillende nieuwe radioactief gelabelde gastrine-tracers hebben ontwikkeld en bestudeerd in preklinische in vitro en in vivo studies, de laatste in diersystemen. Tevens hebben we bestudeerd wat het effect is van de remming van de enzymactiviteit in het lichaam op de metabole stabiliteit en de tumoropname van deze nieuwe tracers. De evaluatie van een serie <sup>111</sup>In-gelabelde analogen, gebaseerd op de ons bekende tracer [DOTA]MG11, maar met Ahp<sup>15</sup>, Nle<sup>15</sup> of Leu<sup>15</sup> in plaats van het voor oxidatie gevoelige Met<sup>15</sup>, is beschreven in **Hoofdstuk 3**. Het in vitro profiel van de radiopeptiden is geëvalueerd en ook is gekeken naar de stabiliteit in de muizencirculatie na injectie en naar de biodistributie in CCK2R-positieve tumordragende muizen tijdens remming van NEP door PA. Ter vergelijking is de minigastrine radiotracer [<sup>111</sup>In-DOTA]MG0 ook meegenomen in de studies, deze tracer was bekend vanwege hoge tumoropname, maar tevens zeer ongunstige, hoge nieropname [12]. Het tegelijk toedienen van de enzymremmer PA en de tracers leidde tot zeer indrukwekkende toename van de tumoropname van alle bestudeerde tracers vanwege de betere beschikbaarheid voor binding aan de receptoren op de tumorcellen. Echter, alleen de 3 getrunceerde (ingekorte) radiogastrines

toonden opvallend hoge tumor-nieropname ratio's met goede vooruitzichten voor toepassing in de kliniek, voor verbeterde diagnostiek en therapie van CCK2R-positieve tumoren.

In **Hoofdstuk 4** is beschreven hoe we de effectiviteit van in situ NEP inhibitie door PA hebben geëvalueerd voor 3  $^{111}\text{In}$ -gelabelde gastrine-radiotracers die verschillen in hun (Glu) $^{6-10}$ -sequentie. Eerdere studies hadden al aangetoond dat de penta(Glu)-sequentie die aanwezig is in het natieve gastrine belangrijk is voor metabole stabiliteit en hoge tumoropname, maar ook zorgt voor ongewenst hoge nieropname van tracers afgeleid van gastrine [13,14]. Het D(Glu) $^{6-10}$ -bevattende [ $^{111}\text{In}$ ]CP04, dat eerder geselecteerd was als de meest veelbelovende tracer in een eerdere studie met 12 tracers die alle gebaseerd waren op gastrine [12], werd daarom vergeleken met de LGlu-tegenhanger [ $^{111}\text{In}$ -DOTA]MG0 en het ingekorte *des*(Glu) $^{6-10}$  analoog [ $^{111}\text{In}$ -DOTA]MG11. De nieuwe toepassing (van tracerstabilisatie door enzymremming) bleek met name een succes voor [ $^{111}\text{In}$ -DOTA]MG11, omdat de tumor-nieropname ratio steeg met een factor 5 na PA-injectie, hetgeen klinische validatie van deze tracer-enzymremmercombinatie aantrekkelijk maakt.

Met als uiteindelijk doel de klinische translatie van het nieuwe concept, is de enzymremmende effectiviteit van PA vergeleken met die van de klinisch geteste en toegepaste NEP-remmer thiorphan (TO) en van de prodrug racecadotril (Race) die oraal toegediend wordt (**Hoofdstuk 5**). In deze studie is [ $^{111}\text{In}$ -DOTA]MG11 gebruikt als model-radiotracer. Vergelijkbare en indrukwekkende toenames van tumoropname van de tracer werden gevonden na PA or TO toediening via intraveneuze injectie, terwijl intraperitoneale injectie van Race, 30–40 min voor intraveneuze injectie van [ $^{111}\text{In}$ -DOTA]MG11, maar half zo effectief bleek. Dosis-afhankelijkheidsstudies lieten zien dat PA en TO in muizen al een significante tumoropname bewerkstelligden bij de laagste onderzochte dosis. PA bleek echter steeds superieur t.o.v. TO.

Naast NEP is nog een ander enzym geassocieerd met de afbraak in het lichaam van gastrine-analogen: angiotensin convertend enzyme (ACE) [15]. Daarom hebben we de stabiliteit en het biodistributieprofiel van [ $^{111}\text{In}$ -DOTA]MG11 ook bestudeerd in muizen onder ACE remming door lisinopril (Lis). Onze bevindingen laten zien dat ACE niet bijdraagt aan de afbraak van [ $^{111}\text{In}$ -DOTA]MG11 in het lichaam en wijzen naar NEP als het belangrijkste enzym in dit proces.

$^{99\text{m}}\text{Tc}$  is een veel gebruikt radionuclide voor SPECT imaging vanwege de optimale nucleaire karakteristieken, brede beschikbaarheid en lage kosten [16]. Daarom hebben we een serie nieuwe  $^{99\text{m}}\text{Tc}$ -gelabelde gastrine-analogen met verschillende ketenlengte ontwikkeld en preklinisch geëvalueerd (**Hoofdstuk 6**). De effecten van in situ NEP en/of ACE remming zijn ook onderzocht. Een gastrine-17-analoog ( $^{99\text{m}}\text{Tc}$ ]SG6), een minigastrine-analoog ( $^{99\text{m}}\text{Tc}$ ]DG2) en een *des*(Glu) $^{6-10}$  minigastrine-analoog ( $^{99\text{m}}\text{Tc}$ ]DG4) werden vergeleken in deze studie. Verschillende effecten zijn gezien gedurende NEP/ACE-inhibitie door respectievelijk de remmers PA en/of Lis. Speciale aandacht hebben we gegeven aan de tumor-nieropname ratio's. Alle 3 radiopeptiden profiteerden duidelijk van PA co-injectie met betrekking tot metabole stabiliteit en tumoropname, terwijl gecombineerde PA en Lis co-injectie alleen voor [ $^{99\text{m}}\text{Tc}$ ]DG4 een additief effect liet zien. Deze bevindingen suggereren dat ACE alleen betrokken is bij de afbraak van [ $^{99\text{m}}\text{Tc}$ ]DG4; dit wordt toegeschreven aan de positieve lading op positie 9 van gastrine. [ $^{99\text{m}}\text{Tc}$ ]DG4 is zeer veelbelovend voor imaging van CCK2R-positieve tumoren in mensen, gezien de gunstige biodistributie bij gecombineerde NEP/ACE-inhibitie in muizenmodellen, met een  $\sim 7\text{x}$  toename in tumor-nieropname ratio's.

## REFERENTIES

1. Reubi JC. Peptide receptors as molecular targets for cancer diagnosis and therapy. *Endocr Rev* 2003;24:389-427.
2. Fani M, Maecke HR, Okarvi SM. Radiolabeled peptides: valuable tools for the detection and treatment of cancer. *Theranostics* 2012;2:481-501.
3. Krenning EP, Bakker WH, Kooij PP, Breeman WA, Oei HY, de Jong M, et al. Somatostatin receptor scintigraphy with indium-111-DTPA-D-Phe-1-octreotide in man: metabolism, dosimetry and comparison with iodine-123-Tyr-3-octreotide. *J Nucl Med* 1992;33:652-8.
4. Reubi JC, Schaer JC, Waser B. Cholecystokinin(CCK)-A and CCK-B/gastrin receptors in human tumors. *Cancer Res* 1997;57:1377-86.
5. Reubi JC, Waser B. Unexpected high incidence of cholecystokinin-B/gastrin receptors in human medullary thyroid carcinomas. *Int J Cancer* 1996;67:644-7.
6. Ocak M, Helbok A, Rangger C, Peitl PK, Nock BA, Morelli G, et al. Comparison of biological stability and metabolism of CCK2 receptor targeting peptides, a collaborative project under COST BM0607. *Eur J Nucl Med Mol Imaging* 2011;38:1426-35.
7. Adessi C, Soto C. Converting a peptide into a drug: strategies to improve stability and bioavailability. *Curr Med Chem* 2002;9:963-78.
8. Deschodt-Lanckman M, Pauwels S, Najdovski T, Dimaline R, Dockray GJ. In vitro and in vivo degradation of human gastrin by endopeptidase 24.11. *Gastroenterology* 1988;94:712-21.
9. Erdos EG, Skidgel RA. Neutral endopeptidase 24.11 (enkephalinase) and related regulators of peptide hormones. *Faseb j* 1989;3:145-51.
10. Llorens-Cortes C, Huang H, Vicart P, Gasc JM, Paulin D, Corvol P. Identification and characterization of neutral endopeptidase in endothelial cells from venous or arterial origins. *J Biol Chem* 1992;267:14012-8.
11. Nock BA, Maina T, Krenning EP, de Jong M. "To serve and protect": enzyme inhibitors as radiopeptide escorts promote tumor targeting. *J Nucl Med* 2014;55:121-7.
12. Laverman P, Joosten L, Eek A, Roosenburg S, Peitl PK, Maina T, et al. Comparative biodistribution of <sup>125</sup>I-labelled gastrin/CCK2 receptor-targeting peptides. *Eur J Nucl Med Mol Imaging* 2011;38:1410-6.
13. Good S, Walter MA, Waser B, Wang X, Muller-Brand J, Behe MP, et al. Macrocyclic chelator-coupled gastrin-based radiopharmaceuticals for targeting of gastrin receptor-expressing tumours. *Eur J Nucl Med Mol Imaging* 2008;35:1868-77.
14. Gotthardt M, van Eerd-Vismale J, Oyen WJ, de Jong M, Zhang H, Rolleman E, et al. Indication for different mechanisms of kidney uptake of radiolabeled peptides. *J Nucl Med* 2007;48:596-601.
15. Dubreuil P, Fulcrand P, Rodriguez M, Fulcrand H, Laur J, Martinez J. Novel activity of angiotensin-converting enzyme. Hydrolysis of cholecystokinin and gastrin analogues with release of the amidated C-terminal dipeptide. *Biochem J* 1989;262:125-30.
16. R. Dilworth J, J. Parrott S. The biomedical chemistry of technetium and rhenium. *Chemical Society Reviews* 1998;27:43-55.



# Acknowledgements

Undertaking this PhD has been a challenging and enjoyable experience for me and it would not have been possible to realize without the support and guidance that I received from many people. First and foremost I would like to gratefully thank my co-promotors Dr. Theodosia Maina and Dr. Berthold A. Nock for believing in me and for giving me the opportunity to start a PhD thesis in their lab. Their support and guidance during all these years and their enthusiasm for research motivated and encouraged me to engage in realizing this thesis. I have learned a lot from them and without their advice and their constructive and critical feedback I could not have finished this work successfully.

I would also like to sincerely thank Prof. dr. Marion de Jong and Prof. dr. Eric Krenning for providing me with the opportunity to complete my PhD thesis in Erasmus MC Rotterdam as an external student at NCSR "Demokritos" in Athens. The collaboration between the two centers has been a great success since 2000 and continuous to be fruitful after all these years. I deeply appreciate the support and encouragement of my promoter Prof. dr. Marion de Jong, who has been actively interested in my work and has always been available to advise me and kindly offer her help.

Special thanks to all my colleagues at NCSR "Demokritos"; Manolis, Pantelis, Katerina and Athina for their support, their advise and their hard teamwork. They all have provided valuable contribution towards collecting data for my PhD thesis and they created a great and pleasant working atmosphere in the lab.

I am also thankful for the direction and support of Dr. Marleen Melis during my visit in Erasmus MC. I must also thank all my colleagues in Erasmus MC for their assistance and guidance while I was in Rotterdam and during the preparation of my thesis book.

Special thanks to Costanza Santini for her valuable and much appreciated help in the distribution of the thesis books.

Many thanks to Dr. Werner Sallegger and Dr. Roelf Valkema for their valuable collaboration in some of the projects of this thesis.

I would also like to thank my family for believing in me and encouraging me all these years. Their support, guidance and love have motivated me to work harder and pursuit my goals. At the end I would like to express my heartfelt thanks to my encouraging and patient partner Dimitri whose faithful support during this PhD is so appreciated.



# Curriculum vitae

Katerina Kaloudi was born on April 29<sup>th</sup> 1985 in Athens. She lived her childhood in Chios, where she obtained her secondary school certificate from the 2<sup>nd</sup> General Lyceum in 2003. After that, she studied Biology at the Aristotle University of Thessaloniki, where she specialized in genetic development and molecular biology. During this period she did a two month internship in Elytron Analysis, a molecular biology diagnostic laboratory in Athens, under the supervision of Dr. Alexandros Triantafyllidis. After completing her Bachelor Degree in 2008 she started her Master's Degree in Human Molecular Genetics at Imperial College of London. She graduated in 2009 after completing her dissertation research project with the title "Use of HPRT gene to study endonuclease stimulated gene targeting efficiency", under the supervision of Dr. Andy Porter.

In 2011 she started a PhD study at the Erasmus MC in Rotterdam under the supervision of Prof. Marion de Jong in collaboration with NCSR "Demokritos" in Athens. Co-supervisors in this PhD research study were Dr. Theodosia Maina and Berthold A. Nock from NCSR "Demokritos". Her research focuses on radiolabeled gastrins for targeting CCK2R-expressing tumors and the improvement of diagnostic sensitivity by using enzyme inhibitors. In 2013 she obtained the Marie Curie Award at the 26<sup>th</sup> Annual Meeting of European Association of Nuclear Medicine (EANM) for an oral presentation and the next year her scientific work was amongst the finalist for the same award.





# List of publications

1. **Kaloudi A**, Nock BA, Lympers E, Krenning EP, de Jong M, Maina T. <sup>99m</sup>Tc-Labeled Gastrins of Varying Peptide Chain Length: Distinct Impact of NEP/ACE-Inhibition on Stability and Tumor Uptake in Mice. *Nucl. Med. Biol.* 43:347-354,2016.
2. **Kaloudi A**, Nock BA, Lympers E, Krenning EP, de Jong M, Maina T. Improving the in Vivo Profile of Minigastrin Radiotracers – A Comparative Study Involving the Neutral Endopeptidase Inhibitor Phosphoramidon. *Cancer Biother. Radiopharm.* 31(1):20-8, 2016.
3. **Kaloudi A**, Nock BA, Lympers E, Valkema R, Krenning EP, de Jong M, Maina T. Impact of clinically tested NEP/ACE inhibitors on tumor uptake of [<sup>111</sup>In-DOTA]MG11 - First estimates for clinical translation. *EJNMMI Res.* 6(1):15, 2016.
4. **Kaloudi A**, Nock BA, Lympers E, Sallegger W, Krenning EP, de Jong M, Maina T. In vivo inhibition of neutral endopeptidase enhances the diagnostic potential of truncated gastrin <sup>111</sup>In-radioligands. *Nucl. Med. Biol.* 42(11):824-32, 2015.
5. **Kaloudi A**, Nock BA, Krenning EP, Maina T, de Jong M. Radiolabeled gastrin/CCK analogs in tumor diagnosis - towards higher stability and improved tumor targeting. *Q. J. Nucl. Med. Mol. Imaging* 59 (3):287-302, 2015.
6. Maina T, Cescato R, Waser B, Tatsi A, **Kaloudi A**, Krenning E, de Jong M, Nock B, Reubi JC. [<sup>111</sup>In-DOTA]LTT-SS28, a First Pansomatostatin Radioligand for in Vivo Targeting of Somatostatin Receptor-Positive Tumors. *J. Med. Chem.* 57 (15): 6564-6571, 2014.
7. Gravells P, Ahrabi S, Vangala RK, Tomita K, Brash JT, Brustle LA, Chung C, Hong JM, **Kaloudi A**, Humphrey TC, Porter ACG. Use of the HPRT gene to study nuclease-induced DNA double strand break repair. *Hum. Mol. Gen.* 24 (24): 7097-110, 2015.



# PhD Portfolio

**Name PhD Student:** Aikaterini Kaloudi  
**Erasmus MC Department:** Nuclear Medicine and Radiology  
**Research School:** Molecular Medicine  
**Promotor:** Prof. dr. ir. M. de Jong  
**Co-promotors:** Dr. T. Maina-Nock, Dr. B.A. Nock

Short – Term Scientific Mission (STSM)	Year	ECTS
COST-STSM-TD1004, Rotterdam, The Netherlands “Imaging & Therapy Studies with [ <sup>177</sup> Lu]SG5 in Small Animals”	2013	4,3

International Conferences	Year	ECTS
COST BM0607 Final Action Congress, Sorrento, Italy	2011	1
32 <sup>nd</sup> European Peptide Symposium, Athens, Greece	2012	1.25
5 <sup>th</sup> BBBB International Conference, Athens, Greece	2013	1
Nuclear Technologies for Health Symposium, Nantes, France	2013	1
ECR Annual Congress, Vienna, Austria	2014	1
EANM Annual Congress, Gothenburg, Sweden	2014	1.25
1 <sup>st</sup> International Congress: from drug discovery to drug delivery, Athens, Greece	2014	1
10 <sup>th</sup> European Molecular Imaging Meeting, Tübingen, Germany	2015	1.25

Seminars, symposia, meetings, workshops and training	Year	ECTS
COST TD1004 Action Annual Meeting, Athens, Greece	2013	1
1 <sup>st</sup> Hellenic Workshop on Gallium-68: From Isotope Production to PET Imaging, Athens, Greece	2014	0,3
16 <sup>th</sup> Hellenic Symposium on Medicinal Chemistry, Patras, Greece	2015	1
Animal Handling/ Biodistribution in-depth training	2011-12	10
Research Seminars at Demokritos	2011	1

Teaching activities	Year	ECTS
Supervising trainees (5x)	2012-15	10

---

**Total** **36.65**

---





[The page contains a large, faint watermark that reads "www.ck12.org".]